PROMOTING LIPID PRODUCTIVITY AND FATTY ACID SECRETION IN MICROALGAE

TAN WEI MIN KENNETH

(*B.Sc. (Hons), NUS*)

A THESIS SUBMITTED

FOR THE DEGREE OF DOCTOR OF PHILOSOPHY

DEPARTMENT OF MICROBIOLOGY AND IMMUNOLOGY

NATIONAL UNIVERSITY OF SINGAPORE

2017

Supervisor:
Associate Professor Lee Yuan Kun

Examiners:
Associate Professor Tan May Chin, Theresa
Associate Professor Lehming, Norbert
Professor Choul-Gyun Lee, Inha University

DECLARATION

I hereby declare that the thesis is my original work and it has been written by me in its entirety. I have duly acknowledged all the sources of information which have been used in the thesis.

This thesis has also not been submitted for any degree in any university previously.

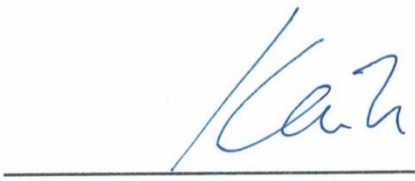

Tan Wei Min Kenneth

1 January 2017

Acknowledgements

I would like to extend my heartfelt gratitude to my supervisor, A/P Lee Yuan Kun, for his guidance throughout my PhD. I have gained much experience and insights into microbiological and applied research under his mentorship. Despite his busy schedule, he would undeniably set aside time for discussion, wherever it might be. He not only taught us about scientific rigor and critical thinking, but was also instrumental in developing us into mature individuals who are able to persevere and prevail through difficulties, whatever they might be. Prof. Lee, thank you for giving me the opportunity to work with you on a very interesting topic in microbiology and biotechnology. Your unwavering support enabled me to pursue and experience diverse interests throughout my PhD, engagements which vary from academic to industry. Your unparalleled trust gave me the chance to learn and feel like an independent scientist, skills which would stay with me wherever I go. By extension, I would also like to thank the National Research Foundation (NRF), Singapore-Peking University Research Centre (SPURc), as well as the Department of Microbiology and Immunology for supporting this project.

My life in the laboratory would not have been as smooth-sailing if it was not for the assistance of very capable people. I would like to thank my research mentors and postdoctoral research fellows, Dr. Shen Hui and Dr. Ng Yi Kai for imparting their knowledge and experience, and for their support and encouragements in PhD journey. I would like to give special thanks to Dr. Ng Yi Kai and my lab mates

Lina Yao and Huixin Lin for their help in developing many of the protocols including Next-Generation Sequencing and Gas-Chromatography Mass Spectrometry platforms. To my lab mates, past and present, Zhao Ran, Daphne Ng, Yao Lina, Huixin Lin, Kelvin Koh, and Radiah Safie, thank you for the unforgettable times of fun and laughter. I will never forget the times we spent together. I would like to thank Mr. Low Chin Seng for his technical expertise and capable management of the lab. His professional experience and assistance has been central to the proper function of the lab. Lastly, I would like to acknowledge the assistance and friendship of the wonderful people of NRF, SPURc, and Department of Microbiology and Immunology, Dr. Alvin Ng, Dorothy Teng, Eileen Lim, and Miao Lian Voong for all the help they have provided through the years.

Finally, I am indebted to my family, especially my parents, for supporting me all along. They knew of my innate curiosity for the natural sciences and love for inquisition since I was young, and never prevented me from pursuing my interests. All this would not have been possible without their support and encouragement.

TABLE OF CONTENTS

Summary

Rising oil prices and concerns over climate change have resulted in more emphasis on research into renewable biofuels from microalgae. Unlike plants, microalgae have higher biomass productivity, will not compete with food and agriculture, and do not require fertile land for cultivation. However, microalgae biofuels currently suffers from high capital and operating costs due to low yields and costly extraction methods. Two main bottlenecks in achieving improved yields and decreased costs are: 1) finding the balance between increasing biomass productivity and lipid accumulation, and 2) reducing the energy costs incurred while extracting lipids from the cells. Microalgae grown under optimal conditions produce large amounts of biomass but with low lipid content, while microalgae grown in nitrogen depleted (N-depletion) conditions accumulate high levels of lipids but are slow growing. Producing lipids while maintaining high growth rates is vital for biofuel production because high biomass productivity increases yield per harvest volume while high lipid content decreases the cost of extraction per unit product. Therefore, there is a need for metabolic engineering of microalgae to constitutively produce high amounts of lipids without sacrificing growth. Substrate availability is a rate-limiting step in balancing growth and fatty acid (FA) production because both biomass and FA synthesis pathways compete for the same substrates, namely acetyl-CoA and NADPH. In this study, we induced N-depletion in microalgae to identify key enzymes which correspond with lipid

accumulation. To this end, we found upregulation of several transcripts encoding for enzymes which catalyze the formation acetyl-CoA and NADPH. Four of these enzymes, malic enzyme, glucose-6-phosphate dehydrogenase, pyruvate dehydrogenase, and fatty acyl-ACP thioesterase (TE), were then overexpressed in the model microalga *Chlamydomonas reinhardtii* to investigate its effects on increasing lipid productivity. We found that one mutant which overexpressed TE demonstrated a 56% increase in lipid content without compromising growth, while the other mutants had slightly lesser improvements in lipids. The second bottleneck is the costly extraction of lipids from microalgae. Generally, the cells need to be dried and lipids are obtained by cell lysis and separation, which is expensive and energy intensive, typically accounting for 70-80% of the total cost of production. A better approach is for the cells to secrete the oil into the culture medium, removing the need for harvesting, drying and extracting lipids from microalgal biomass. In this project, we seek to introduce a codon-optimized plant ATP-binding cassette (ABC) protein, ABCG11, which is known to actively secrete FAs from plant cells, into the model cyanobacteria *Synechococcus elongatus* PCC 7942 and *C. reinhardtii*. We hypothesize that ABCG11 would be able to function similarly in cyanobacteria and microalgae as ABC are a well-conserved family of proteins. However, although we were able to increase FA production in the cells from the knockdown of genes from competing pathways, we did not find evidence of FA secretion in the external culture media, suggesting

that active export of FAs may not be a feasible option for FA secretion. (483 words)

List of Tables

List of Figures

Chapter 1 Literature Review

1.1 Biofuel production from microalgae

Diminishing fossil fuel reserves, rising oil prices and concerns over climate change due to increasing atmospheric CO_2 levels have renewed support for alternative and renewable energy sources (Stephens et al., 2010b). In particular, biofuels derived from photosynthetic microorganisms such as cyanobacteria and microalgae have received considerable interest because compared to plants, they require smaller land area that does not need to be arable and can be cultivated in saltwater systems which will not directly compete with resources necessary for agricultural food production (Wigmosta et al., 2011). Furthermore, microalgae are efficient in converting solar energy and sequestering CO_2 into storage lipids, with several species having higher biomass production rates and containing a higher percentage of oil than terrestrial plants (Gouveia and Oliveira, 2009; Malcata, 2011). Even by conservative standards, microalgae are still predicted to produce 10 times more biodiesel per unit area of land compared to terrestrial oleaginous crops (Halim et al., 2012) (**Table 1.1, Fig. 1.1**). However, microalgal biofuel production based on present yields and extraction methods is unlikely to be economically viable as algae fuel currently cost more per unit mass due to the high capital and operating costs (Stephens et al., 2010a). Although the U.S. Department of Energy's Aquatic Species Program identified around 300 species of microalgae that are desirable for biofuel production (Sheehan et al.,

1998), continued engineering of microalgae is still required to unlock the feasibility of algal strains to serve as a factory for the production of cost-efficient biofuels.

Microalgae utilize solar energy, water and CO_2 which are assimilated into the reserve storage components of carbohydrates, lipids and proteins. Of these three biochemical forms, lipids have the highest energy content (Quintana et al., 2011a) which makes them favorable high-value molecules. Harvested lipids typically undergo transesterification with methanol to be converted into fatty acid methyl esters that can be used as a transportation fuel in the form of biodiesel (Nagle and Lemke, 1990). The remaining biomass may be converted into methane gas or the carbohydrates may be transformed into ethanol by dark fermentation (Stal and Moezelaar, 2006; Sialve et al., 2009). Although microalgae generally use starch as their primary carbon storage compound, some strains accumulate neutral lipids, mainly in the form of triacylglycerols (TAG) under environmental stress conditions such as nitrogen limitation (Radakovits et al., 2010). During logarithmic growth, microalgae do not produce large amounts of storage lipids. However, in response to environmental stress they reduce their proliferation and start producing TAG (Hu et al., 2008). The accumulation of TAG likely occurs as a means of creating an energy deposit that can be readily utilized in response to a more favorable environment allowing for rapid growth (Yu et al., 2011). While an increase in TAG production during nitrogen deprivation is ideal, reduced growth caused by nutrient deficiency hampers the use of this strategy for producing

biofuel as the decrease in biomass productivity would reduce overall yield. Therefore, a new focus in microalgal biofuel research is to genetically engineer an ideal strain which will have high growth rate while possessing high lipid content.

Table 1.1 Oil yields from typical terrestrial crops and microalgae in ascending order. Data source: (Singh and Gu, 2010).

Crop type	Oil yield (liters/hectare/year)
Corn	172
Soybean	446
Jatropha	1,892
Oil palm	5,950
Microalgae (30% oil by weight)	58,700

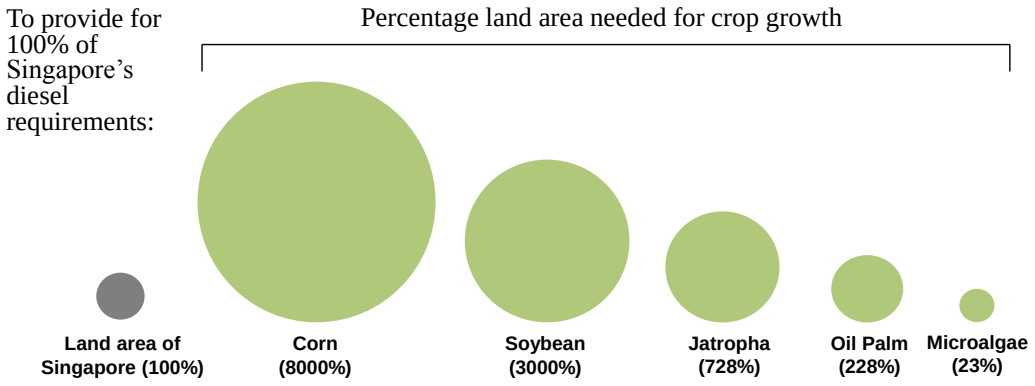

Figure 1.1 Corresponding oil yield and land area needed for potential feedstock for biodiesel production in Singapore. Data source: Lee YK, Wang JY. 2011. Biorenewables Primer 2011. National Climate Change Secretariat, Singapore Prime Minister's Office.

1.2 Strategies targeting the overproduction of lipids

To date, most studies seeking to improve TAG accumulation in photosynthetic organisms focus on the fatty acid (FA) synthesis pathway, which provides the acyl-coenzyme A (CoA) substrates for TAG synthesis. Overexpression of the enzyme acetyl-CoA carboxylase (ACCase), believed to catalyze the important rate-limiting step in FA synthesis, have been performed in diatoms (Dunahay et al., 1995) and plants (Kindle, 1990; Roesler et al., 1997) but only minor (5%), if any, increase in lipid content were observed. Increasing the expression of another enzyme in FA synthesis, 3-ketoacyl-acyl carrier protein synthase (KAS) III, was also not successful in improving lipid content in three species of plants (Dehesh et al., 2001). On the other hand, manipulation of genes involved in TAG assembly has achieved better results. One of the more successful attempts is the overexpression of glycerol-3-phosphate dehydrogenase (G3PDH), an enzyme involved in supplying glycerol-3-phosphate (G3P) required for TAG formation. By overexpressing G3PDH in developing seeds of *Brassica napus*, Vigeolas and colleagues (Vigeolas et al., 2007) observed a three- to four-fold increase in G3P and a 40% increase in final seed oil content, suggesting that genes involved in substrate synthesis are also important for increasing lipid production. The overexpression of diacylglycerol acyltransferase (DGAT), the major enzyme catalyzing the final step of TAG synthesis, in seeds of *Arabidopsis thaliana* (Jako et al., 2001) and soybean (Lardizabal et al., 2008) also resulted in a substantial increase in oil content. Despite the success in plants, overexpression of

three DGAT homologue genes identified in *Chlamydomonas reinhardtii* did not boost intracellular TAG during standard growth or nitrogen depleted conditions (La Russa et al., 2012). Transcriptomic analysis of *C. reinhardtii* subjected to nitrogen depletion showed consistently low levels of DGAT (Miller *et al.*, 2010), while the oleaginous microalga *Neochloris oleoabundans* also presented no changes in DGAT expression between normal growth and nitrogen limited cultures (Rismani-Yazdi et al., 2012). This suggests that increasing DGAT expression may not be effective in increasing lipid content for microalgae. One possibility is that TAG assembly might differ between plants and microalgae (Liu and Benning, 2013), such as the location of TAG synthesis. In plants, the synthesis of TAG occurs at the ER, but in microalgae a large proportion of TAG is synthesized at the plastids in parallel to FA synthesis (Fan et al., 2011; Goodson et al., 2011). This would affect the selection of genes because overexpression of ER-localized enzymes may not have much effect in increasing TAG content. However, all known *Chlamydomonas* DGATs lack plastid targeting sequences, highlighting the possibility that novel enzymes might be involved in the assembly of TAG in *Chlamydomonas* plastids (Liu and Benning, 2013). Researchers have found plastidial isoforms of G3PDH in *Dunaliella* (Ghoshal et al., 2002; He et al., 2007; He et al., 2009) and recently in *C. reinhardtii* (Herrera-Valencia et al., 2012) which may suggest a specific chloroplast pathway for TAG synthesis in microalgae.

While little information is available regarding the metabolic pathways in microalgae, the *de novo* FA synthesis pathway is consistent with those proposed for higher plants (Rismani-Yazdi et al., 2011; Rismani-Yazdi et al., 2012). FA elongation by long-chain KAS enzymes ends with the production of 16 to 18C fatty acyl groups esterified to acyl carrier protein (ACP), which are used by the cell to synthesize membrane lipids (Chen and Smith, 2012). The buildup of fatty acyl-ACPs can regulate the rate of FA synthesis by feedback inhibition of ACCase (Davis and Cronan, 2001) and KAS (Heath and Rock, 1996a). However, acyl-ACP thioesterases (TEs) can reduce this inhibition by hydrolyzing the acyl-ACP into free FAs, which are converted into acyl-CoA and released from the chloroplast to be incorporated into TAGs (Chen and Smith, 2012). The expression of endogenous TEs such as oleoyl-ACP hydrolase and acyl-ACP thioesterase A were found to be up-regulated in microalgae subjected to nitrogen limiting conditions (Miller et al., 2010; Rismani-Yazdi et al., 2012). In addition, expression of TE showed a linear relationship with FA synthesis in *Haematococcus pluvialis*, indicating that TE could be involved in a key rate-limiting step for FA synthesis (Lei et al., 2012). Based on this principle, increasing the activity of TEs appears to be a good strategy to promote the continuous production of FAs and channeling them to storage lipids rather than membrane lipids. Indeed, the overexpression of TEs has been shown to increase total FAs in *E. coli* (Lu et al., 2008) and cyanobacteria (Liu et al., 2011b), and in microalgae by up to 72% (Gong et al., 2011). As different TEs are specific for

different FA chain lengths, manipulating the type of TE could also result in overproduction of short and medium-chain FAs which are preferred for biodiesel production. For example, overproducing a TE from *Umbellularia californica* in *E. coli* and cyanobacteria increased accumulation of myristate (14:0) and laurate (12:0) (Voelker and Davies, 1994; Liu et al., 2011b), which are beneficial as biofuels because saturated carbon chains have higher octane rating and are more resistant to oxidation during storage. Furthermore, targeted engineering of TEs with KAS enzymes specific for short- or medium-chain length FAs would enable the synthesis of customized biofuel molecules that are industrially relevant (Howard et al., 2013; Torella et al., 2013).

Another possible approach to complement an increase in lipid content is decreasing lipid catabolism. Genes involved in β-oxidation of FAs, as well as the activation of free FAs could be targeted for deletion. Knocking out the acyl-CoA synthetase (ACSL) gene, which targets free FAs for β-oxidation in *Escherichia coli* (Lu et al., 2008) and *Saccharomyces cerevisiae* (Michinaka et al., 2003; Runguphan and Keasling, 2014) resulted in a significant increase in free FA production; knockout of ACSL in *S. cerevisiae* also led to extracellular FA secretion (Michinaka et al., 2003; Scharnewski et al., 2008). In addition, ACSL is also downregulated in *N. oleoabundans* during nitrogen-limited conditions when lipids are accumulated (Rismani-Yazdi et al., 2012), suggesting that this enzyme could be a major factor in controlling the flux of FAs toward their degradation by β-oxidation. A recent screening of small organic molecules on microalgae showed

that antioxidant compounds such as propyl gallate and butylated hydroxyanisole increased lipid productivity up to 67% without compromising growth and biomass production (Franz et al., 2013), suggesting that preventing oxidation could protect intracellular fats and oils from degradation. Enzymes of β-oxidation in microalgae include acyl-CoA dehydrogenase (ACD) and acyl-CoA oxidase (ACOX) which are responsible for the breakdown of FAs in the mitochondria and peroxisomes respectively, and could be promising targets for microRNA silencing. Transcript levels of ACOX decreased in *C. reinhardtii* under nitrogen depletion (Miller et al., 2010), but ACD levels were upregulated in N-depleted *Nannochloropsis* (Li et al., 2014), indicating the varied roles these pathways might play in lipid accumulation. On one hand, inhibiting β-oxidation would prevent the loss of lipids and result in intracellular buildup of acyl-CoAs, as observed in *A. thaliana* mutants lacking ACOX (Rylott et al., 2003). On the other hand, an increase in β-oxidation could provide for enhanced recycling of carbon skeletons from degraded membrane lipids for TAG synthesis.

The importance of lipid degradation and turnover was recently demonstrated in *A. thaliana* leaves by Fan *et al.* (2014). The study found that while overexpression of phospholipid:diacylglycerol actyltransferase (PDAT) did not substantially increase TAGs relative to wild-type, concurrent disruption of a TAG lipase greatly increased TAG content by up to 14-fold, suggesting that preventing TAG degradation could play a bigger role in lipid accumulation. However, membrane lipid composition was altered in the double mutant, leading

to compromised growth and development. Their results indicate TAG lipases are key regulators of FA turnover by degrading TAGs and redirecting acyl-CoAs for membrane lipid synthesis, thereby maintaining lipid homeostasis. The importance of TAG lipases is made more pronounced when the overexpression of PDAT channels phospholipids away from membrane lipids. In contrast, inhibiting TAG degradation alone without interfering with membrane lipid composition could prove more useful. A recent study by Trentacoste *et al.* found that knocking down a multifunctional lipase/phospholipase/acyltransferase increases lipid content without compromising growth in the diatom *Thalassiosira pseudonana* (Trentacoste et al., 2013). During exponential growth, the mutants showed a 2.4 to 3.3-fold increase in lipid content relative to wild-type, and an even higher 4-fold increase during silicon starvation. As lipases specifically target the release of FAs from TAG and lipid droplets, the authors propose that reducing lipid catabolism would have minimal impact on growth compared to strategies which disrupt carbohydrate pools. For instance, Li *et al.* had previously disrupted the ADP-glucose pyrophosphrylase gene involved in starch synthesis in *C. reinhardtii* (Li et al., 2010). While the microalgae accumulated up to an 8-fold increase in TAGs during nitrogen deprivation, it also resulted in reduced photosynthetic efficiency and growth impairment. Consequently, it was discovered that a major shift in carbon flux from starch to lipid synthesis might compromise cellular growth and biomass productivity as polysaccharides are consumed to support cell division (KaiXian and Borowitzka, 1993; Siaut et al., 2011; Yu et al., 2011;

Bišová and Zachleder, 2014). Hence, manipulation of genes involved in starch synthesis pathways might not be a practical approach due to the shift in balance between lipid accumulation and growth; increasing the efficiency of one pathway without accounting for the other will likely sacrifice overall yield.

1.3 Overproduction without sacrificing growth and productivity

The extent of lipid accumulation in microalgae is influenced by stress factors such as nutrient levels and culture conditions. Under optimal growth conditions, large amounts of algal biomass are produced, but with relatively low lipid content. In nutrient stress conditions, cells have high lipid contents but are typically slow growing. Lipid content alone does not allow for rational species selection as faster growing species may demonstrate lipid productivity greater than those with high lipid content (Griffiths and Harrison, 2009) (**Fig. 1.2**). Producing lipids while also maintaining high growth rates and increasing biomass is therefore vital for algal biofuel production on large economic scales. High biomass productivity increases yield per harvest volume while high lipid content decreases the cost of extraction per unit product (Griffiths and Harrison, 2009). Rapid growth rate also provides a competitive advantage over contaminating algal species in outdoor cultures, and requires less culture space due to a higher cell density per area. Thus, cost-effective production of lipids for commercial use ideally requires deregulated microalgae which constitutively accumulate high amounts of lipids, regardless of environmental conditions that impede growth.

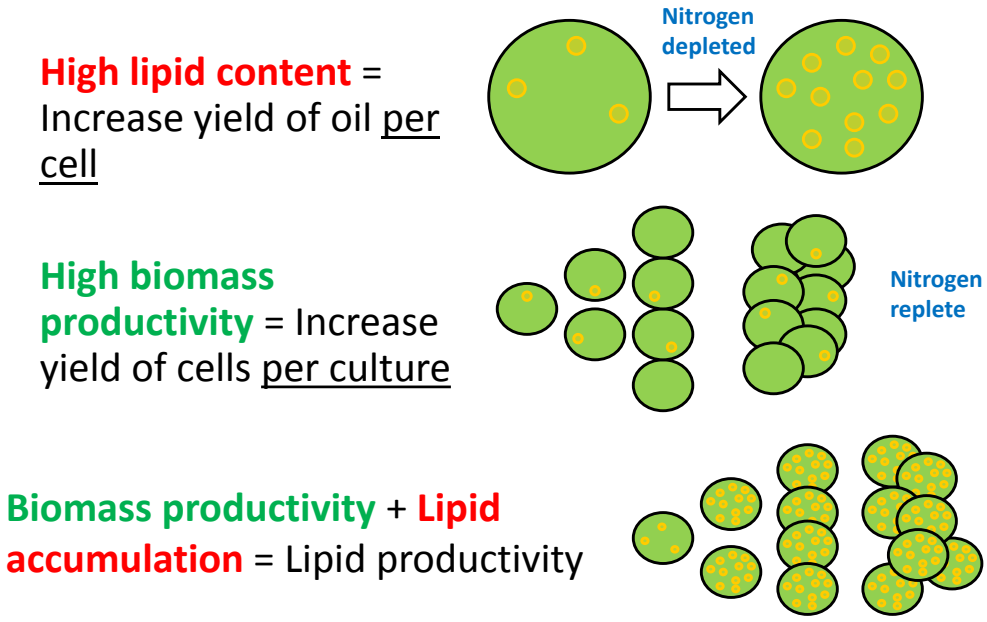

Figure 1.2 The dilemma for lipid productivity in green microalgae. Microalgae grown in nutrient starvation accumulate high levels of neutral lipids but are slow growing. Microalgae grown under optimal conditions produce large amounts of biomass but with low neutral lipid content. Producing lipids while maintaining high growth rates is vital for biofuel production because high biomass productivity increases yield per harvest volume while high lipid content decreases the cost of extraction per unit product.

As it is in plant leaves, green algae have proven to be recalcitrant to oil accumulation as their metabolism favors starch accumulation (Chapman et al., 2013; Johnson and Alric, 2013). However, under stressed conditions they being to accumulate higher amounts of TAGs, akin to plant oil seeds (Johnson and Alric, 2013). This suggests that oleaginicity could be initiated by the diversion of carbon flux from central carbon metabolism towards lipids instead of starch. For example, although the oleaginous green algae *Pseudochlorococcum sp.* uses

starch as a primary storage product, it was found to accumulate up to 52% lipids under nitrogen depletion because it is able to convert starch into lipids (Li et al., 2011). Inhibition of starch synthesis in microalgae may therefore not only reduce growth but also result in decreased lipid content. On the other hand, microalgae species that are capable of heterotrophic growth on sugars were able to enhance lipid accumulation by 900% compared with photoautotrophically grown cells (Liu et al., 2011a). Green algae such as *Chlorella zofingiensis* were able to achieve as much as 79.5% total lipids when fed with glucose and grown in darkness (Liu et al., 2011a), compared to 65% lipids when it is grown photoautotrophically and subjected to nitrogen-deprivation (Feng et al., 2012). The difference in potential for lipid accumulation between these cells suggests that growth conditions and type of carbon source may play a defining role in the carbon flux towards storage of lipids. Taken together, these observations serve to highlight that alterations in central carbon metabolism could influence carbon partitioning towards oil accumulation in microalgae (Johnson and Alric, 2013). For biofuel applications, rather than inhibiting starch synthesis which is detrimental to growth, it might be useful to manipulate the flow of photosynthetic carbon towards the accumulation of lipids – rather than starch – in high biomass-producing microalgae species (Griffiths and Harrison, 2009; Hempel et al., 2012).

Overexpression of genes that increase TAG synthesis alone is likely to reduce microalgae growth rate because TAG synthesis requires the supply of two substrates, acyl-CoA and G3P. G3P is derived from dihydroxyacetone phosphate

(DHAP) produced from the Calvin cycle and glycolysis. Channeling of carbon away from either of these pathways to TAG synthesis would reduce the carbon available for pathways supporting cellular growth, such as the tricarboxylic acid (TCA) cycle. Scientists have overexpressed G3PDH in the diatom *Phaeodactylum tricornutum* leading to a 60% increase in neutral lipids during stationary phase, as a 6.8-fold increase in glycerol content provided the backbone for TAG synthesis (Yao et al., 2014). However, it also resulted in a 20% decrease in cell growth, as overexpressing G3PDH promoted the conversion of DHAP to G3P, shunting carbon away from glycolysis and the TCA cycle to form glycerol. Likewise, overexpression of FA synthesis genes such as ACCase could result in reduced growth as carbon required for acyl-CoA formation is tapped from acetyl-CoA, the key two-carbon metabolite shared between the TCA cycle and FA synthesis. As both of these pathways compete for acetyl-CoA, it is not surprising that overexpression of genes involved in FA synthesis produced only modest increases in lipid content (Courchesne et al., 2009). These evidences highlight substrate availability as a critical bottleneck to lipid synthesis because biomass and lipid production essentially compete for photosynthetic assimilate. Clearly, the solution to balancing growth and lipid accumulation should lie upstream of lipid producing pathways.

Increasing evidence suggest that the "pulling" of carbon from FA and TAG synthesis pathways might not be as crucial as the "pushing" of carbon into FA synthesis. For instance, recent transcriptomic studies on carbon fixation in *P.*

tricornutum (Valenzuela et al., 2012; Yang et al., 2013) found that the build-up of precursors such as acetyl-CoA and NADPH may provide a more significant contribution to TAG accumulation than the activity of ACCase. Following nitrogen deprivation, genes involved in carbon fixation, TCA cycle and glycolysis were enhanced, possibly providing the resources necessary for carbon flux towards neutral lipid synthesis (Yang et al., 2013). In contrast, RNA-seq performed on nitrogen-deprived *C. reinhardtii* showed no change in the transcript levels of genes encoding for FA synthesis (Miller et al., 2010), suggesting that the increased lipid content associated with nitrogen deprivation might be influenced by factors outside the FA synthesis pathway. Transcriptomics performed on oil palm revealed that supply of pyruvate in the plastids, rather than acyl assembly into TAGs, was the major contributing factor responsible for its oleagenicity (Bourgis et al., 2011), as transcript levels of enzymes involved in plastidial carbon metabolism including phosphofructokinase, pyruvate kinase and pyruvate dehydrogenase subunits were more than 50-fold higher compared to date palm, a closely-related species that accumulate almost exclusively sugars rather than oil. Surprisingly, despite a 100-fold difference in flux to lipids, most enzymes involved in TAG synthesis were expressed at similar levels in oil palm and date palm (Bourgis et al., 2011). Notably, transcriptomic comparisons between oleaginous and non-oleaginous microbes revealed no significant changes in genes encoding enzymes directly involved in FA synthesis (Chen et al., 2015a). Rather, the availability of precursors appears to be the key point of transcriptional

regulation contributing to oleagenicity in oil-accumulating microbes. Therefore, increasing the availability of precursors for both primary metabolism and FA synthesis could be a viable approach to simultaneously increase the yield of biomass and lipids in microalgae.

1.4 Provision of substrates: Acetyl-CoA and NADPH

When cerulenin, an inhibitor of *de novo* FA synthesis, was added to *C. reinhardtii* cells, lipid droplet formation was strongly inhibited, indicating that a significant portion of storage lipids (i.e. TAGs) are likely derived from *de novo* FA synthesis (Imamura et al., 2015). High rates of *de novo* FA synthesis require a continuous supply of acetyl-CoA and NADPH (Rawsthorne, 2002). During nitrogen starvation, carbon precursors in the form of acetyl-CoA rapidly rise, preceding TAG accumulation (Avidan et al., 2015). Reactions that provide for these precursor molecules lie outside the FA synthesis pathway which is common to all microorganisms, implying that the difference between non-oleaginous and oleaginous microorganisms might be the latter's ability to direct more substrates to FAs (Ratledge, 2004). Despite possessing the same pathway to synthesize FAs, non-oleaginous microorganisms typically do not accumulate FAs but instead divert carbon into polysaccharides (Ratledge, 2004; Avidan et al., 2015). In high TAG-accumulating microalgae such as *Chlorella desiccata*, the levels of acetyl-CoA far exceeded those seen in moderate TAG accumulators such as *D. tertiolecta* and *C. reinhardtii* (Avidan et al., 2015), suggesting that the availability

of carbon precursors may limit TAG accumulation in green microalgae. Metabolic flux analysis performed in *Chlorella protothecoides* showed that carbon flow from acetyl-CoA to FA pools increased from 58% to 109% of glucose uptake during nitrogen-limited growth (Gopalakrishnan et al., 2015), indicating that algal cells substantially reorganize their metabolism to divert more acetyl-CoA towards lipid production. Increased NADPH pool in a *Chlorella pyrenoidosa* mutant overexpressing an *A. thaliana* NADH kinase (AtNADK3) has also been associated with enhanced lipid content of up to 110% (Fan et al., 2015) (**Table 2**). Oleaginicity is hence attributed to the presence and activity of enzymes responsible for the supply of acetyl-CoA and NADPH to FA synthesis. Enzymes contributing to the intracellular pool of acetyl-CoA include acetyl-CoA synthetase (ACS), ATP:citrate lyase (ACL) and pyruvate dehydrogenase complex (PDC) while those that provide for NADPH include NADP-malic enzyme (ME) and glucose-6-phosphate dehydrogenase (G6PDH).

1.4.1 Acetyl-CoA synthetase

Acetyl-CoA is a central metabolite involved in various physiological pathways linked with anabolism and catabolism, such as FA synthesis and the TCA cycle. Besides being a precursor for biochemical reactions, acetyl-CoA also serves in post-translational modifications, namely acetylation, of proteins including histones and transcription factors (Shtaida et al., 2015). Due to its versatility in functions, its synthesis is suggested to occur in different

compartments under the control of various enzymes. While much of acetyl-CoA production still remains unknown in microalgae, mechanisms that include the three enzymes (ACS, PDC, and ACL) are thought to be involved (Shtaida et al., 2015). ACS carries out the reversible reaction which converts acetate to acetyl-CoA, and was once thought to be the primary source of acetyl-CoA for FA synthesis as it was the first enzyme identified to produce acetyl-CoA in plastids (Lichtenthaler and Golz, 1995). However, subsequent studies have refuted that claim as its expression was not correlated with increased lipids (Ke et al., 2000) and mutants lacking ACS still fix CO_2 into FAs at the same rate as wild-type (Lin and Oliver, 2008). In addition, increased lipid production in microalgae appears to be dependent on exogenously supplied acetate (Goodson et al., 2011; Ramanan et al., 2013), suggesting that the cells themselves do not produce enough physiological acetate required by ACS for it to be a primary source of acetyl-CoA. An exception exists where heterotrophically grown *Schizochytrium* sp. supplemented with glucose produced high amounts of intracellular acetate (Yan et al., 2013). Genetically modified *Schizochytrium* mutants overexpressing ACS can therefore readily convert the available pool of acetate to acetyl-CoA, resulting in increased FA and biomass accumulation (Yan et al., 2013) (**Table 1.2**). Thus, utilizing acetate as the major carbon source for acetyl-CoA can occur only when exogenous acetate is supplied to microalgae for heterotrophic growth and FA production (Spalding, 2009). Nevertheless, ACS have been identified in the proteomes of lipid droplets in *C. reinhardtii* (Moellering and Benning, 2010;

Nguyen et al., 2011) and *Dunaliella bardawil* (Davidi et al., 2012), suggesting a possible role of ACS in providing acetyl-CoA at the early stages of FA synthesis. Indeed, upregulation of ACS has been demonstrated recently to provide an alternative route for acetyl-CoA production in oleaginous *C. desiccata*, by-passing the traditional pathway catalyzed by plastidial pyruvate dehydrogenase (PDH), resulting in a coordinated large increase in acetyl-CoA levels that precedes TAG accumulation (Avidan and Pick, 2015).

Table 1.2 Influence of genes supplying substrates for lipid synthesis in transgenic strains.

Genes	Description	Host species	Method	Effects (relative to control)	Inferred role	Ref.
PDK	Pyruvate dehydrogenase kinase	*Phaeodactylum tricornutum*	Antisense knockdown	33% to 82% more neutral lipids in 2 mutants	PDK deactivates Pyruvate dehydrogenase complex (PDC). Knocking down PDK increases acetyl-CoA production from pyruvate via PDC	(Ma et al., 2014)
NADK3	*Arabidopsis thaliana* NAD(H) kinase (AtNADK3)	*Chlorella pyrenoidosa*	Gene over-expression	Total lipid content increased by 45.3% to 110.4%; NADPH content increased by 39.3% to 79.9%	Heterologous NADH kinase increases NADPH which drives reductive biosynthesis reactions such as FA synthesis	(Fan et al., 2015)
ACS	*E. coli* Acetyl-CoA synthetase (ACS)	*Schizochytrium sp.*	Gene over-expression	Total lipid content increased by 6.4% to 11.4%; Biomass increased by 24.3% to 29.9%	Heterologous ACS overexpression improved utilization of acetate as a carbon resource for growth and lipid synthesis	(Yan et al., 2013)
ACL	*Mus musculus* ATP:citrate lyase	*Yarrowia lipolytica*	Gene over-expression	Total lipid content increased by 50.6% to 215.1%; Citrate content decreased by 32%	Heterologous expression of ACL with a low Km value for citrate increases lipid synthesis by providing more cytosolic acetyl-CoA as substrates	(Zhang et al., 2014)
PDH E1α	E1 alpha subunit of the Pyruvate Dehydrogenase Complex	*Chlamydomonas reinhardtii*	Artificial microRNA knockdown	Total lipid content decreased by 25% to 40%; Lower chlorophyll content, lower photosynthetic yield on PSII, and lower biomass in mutants	PDC serves an essential role in the supply of carbon precursors for FA synthesis under photoautotrophy	(Shtaida et al., 2014)

Genes	Description	Host species	Method	Effects (relative to control)	Inferred role	Ref.
ME	Malic enzyme	*Phaeodactylum tricornutum*	Gene overexpression	2.3- to 2.5-fold more neutral lipids in 2 mutants; growth rate unaffected	ME could increase lipid synthesis without affecting biomass accumulation by providing NADPH	(Xue et al., 2015)
ME	*Phaeodactylum tricornutum* malic enzyme (PtME)	*Chlorella pyrenoidosa*	Gene overexpression	2.4- to 3.2-fold more neutral lipids in 2 mutants; growth rate unaffected	Heterologous ME could increase lipid synthesis without affecting biomass accumulation by providing NADPH	(Xue et al., 2016)
G6PDH	Glucose-6-phosphate dehydrogenase	*Mortierella alpina*	RNAi knockdown	Total lipid content decreased by 50%; NADPH content decreased by 40%	G6PDH is a critical component of the Oxidative Pentose Phosphate Pathway which enables efficient lipid synthesis	(Chen et al., 2015a)
ACL/ME	ATP:citrate lyase and Malic enzyme	*Yarrowia lipolytica*	Five gene modifications including overexpression of ME and ACL subunit 1 and subunit 2	Total lipid content increased to 74%, a 15-fold improvement over wild-type (16.8%)	ACL and ME cooperatively divert carbon precursors and reducing power towards lipid synthesis, and in conjunction with other modifications, lead to enhanced lipid accumulation	(Blazeck et al., 2014)

1.4.2 ATP:citrate lyase

Acetyl-CoA can also be produced from sugars via citrate through ACL which cleaves cytosolic citrate to form acetyl-CoA and oxaloacetate (**Fig. 3**). Compared to acetate, citrate is produced continuously from the TCA cycle, thus representing a more sustained source of acetyl-CoA for FA synthesis. ACL has often been proposed to be a major rate-limiting enzyme in oleaginous heterotrophs (Ratledge, 2004; Kosa and Ragauskas, 2011), and overexpression of ACL and ME in the yeast *Yarrowia lipolytica* reportedly resulted in a 60-fold increase in lipid yields by providing substrates for induction of FA synthesis (Blazeck et al., 2014) (**Table 1.2**). In plants, ACL activity is correlated with lipid accumulation (Ratledge et al., 1997) and its mRNA levels coincide with peak cytosolic ACCase expression (Fatland et al., 2002). In addition, negative regulation of ACL subunit A (ACLA) reduced cuticular wax synthesis in epidermal cells of *Arabidopsis* (Go et al., 2014), leading to the notion that increased acetyl-CoA supply in the cytosol may be to support the synthesis and elongation of long-chain FAs. Two species of microalgae, *Nannochloropsis salina* and *Chlorella sp.*, were found to exhibit ACL activity comparable to those in oleaginous heterotrophs (Bellou and Aggelis, 2012), indicating that microalgae possess ACL required to utilize citrate as a carbon source for generating acetyl-CoA. Gene expression of cytoplasmic ACL was also upregulated prior to TAG accumulation in *C. desiccata*, but not in low TAG accumulators such as *D. tertiolecta* and *C. reinhardtii* (Avidan and Pick, 2015). However, ACL activity

would require an efflux of citrate from the mitochondria to the cytoplasm, effectively draining the TCA cycle of its intermediates. The contribution of cytoplasmic acetyl-CoA to FA synthesis in oleaginous microalgae also requires further validation (Avidan and Pick, 2015). As mitochondria functions in the light to export citrate via the citrate-oxaloacetate shuttle (Gardeström et al., 2002), the exported citrate could thus be exploited to produce acetyl-CoA. However, unlike yeasts where acetyl-CoA can be used directly for fatty acid synthesis in the cytosol (Tang et al., 2013), microalgae may require the import of carbon substrates into the chloroplast where FA synthesis takes place. Targeting ACL to the plastids of tobacco leaves was previously found to increase fatty acid content by 16% (Rangasamy and Ratledge, 2000), but as the source of plastidial citrate was not identified, it is doubtful that ACL can provide acetyl-CoA for FA synthesis in the chloroplast. Subsequent biochemical and bioinformatics studies in *Arabidopsis* did not reveal presence of ACL in chloroplasts (Fatland et al., 2000; Fatland et al., 2002). Hence, its cytosolic nature means that the supply of acetyl-CoA by ACL is likely to be restricted to FA synthesis within the cytosol.

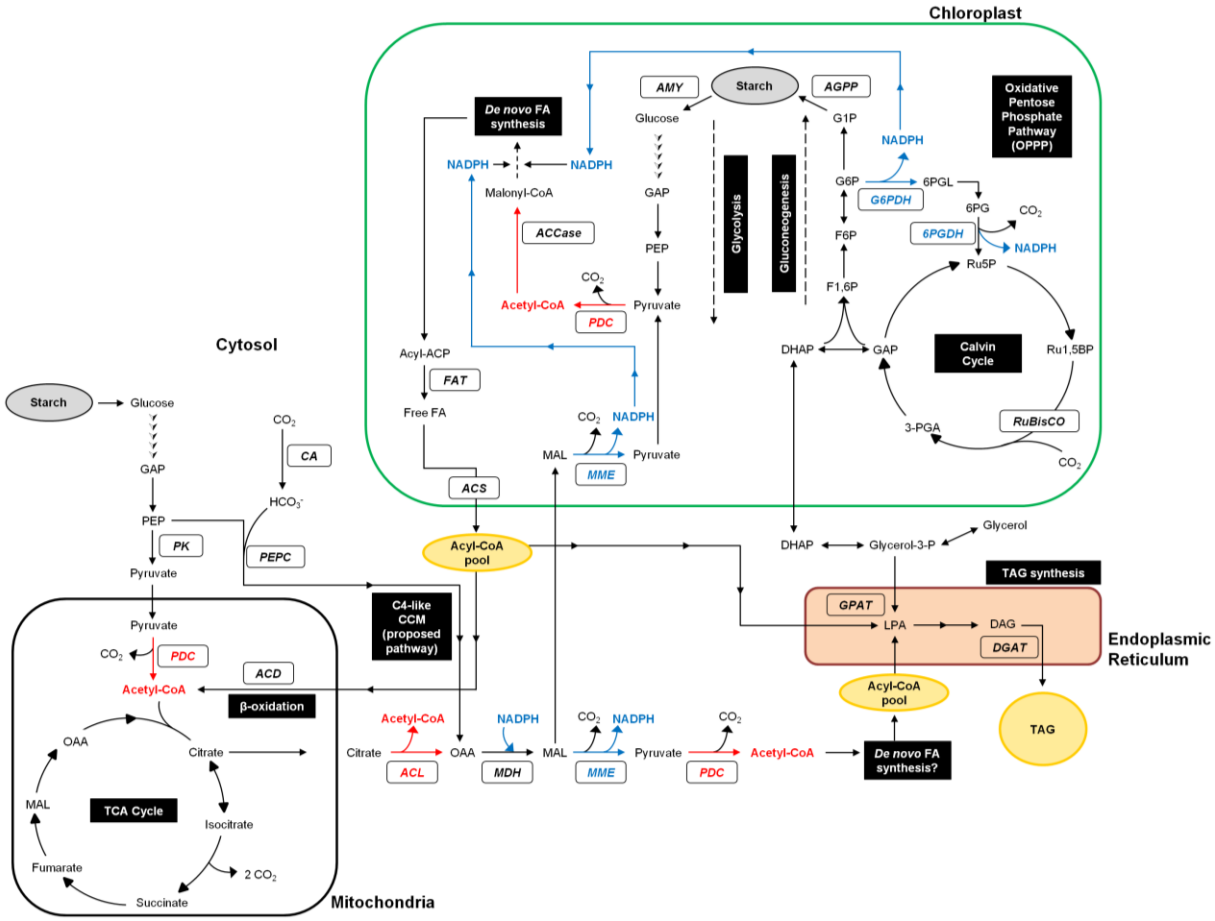

Figure 1.3 Simplified scheme of central carbon metabolism in microalgae. Arrows represent potential carbon fluxes. Enzymes are in bold italics. Blue arrows represent reducing power (NADPH). Red arrows represent acetyl-CoA. Black boxes denote pathway names. Neutral lipid droplets found in microalgae consist mostly of triacylglycerols (TAGs), formed by combining FAs and glycerol. Legend: ACCase, acetyl-CoA carboxylase; ACD, acyl-CoA dehydrogenase; ACL, ATP-citrate lyase; ACS, acyl-CoA synthetase; AGPP, ADP-glucose pyrophosphorylase; AMY, amylase; CA, carbonic anhydrase; DGAT, diacylglycerol acyltransferase; DHAP, dihydroxyacetone phosphate; F1,6P, fructose 1,6-bisphosphate; F6P, fructose 6-phosphate; FAT, fatty acyl-acyl carrier protein (ACP) thioesterase; G1P,

glucose 1-phosphate; G6P, glucose 6-phosphate; G6PDH: G6P dehydrogenase, GAP, glyceraldehyde 3-phosphate; GPAT, glycerol-3-phosphate acyltransferase; MAL, malate; MDH, malate dehydrogenase; MME: NADP-malic enzyme; OAA, oxaloacetate; PDC, pyruvate dehydrogenase complex; PEP, phosphoenolpyruvate; PEPC, PEP carboxylase; PK, pyruvate kinase; Ru5P, ribulose 5-phosphate; Ru1,5BP, ribulose 1,5-bisphosphate; RuBisCO, Ru1,5BP carboxylase/oxygenase; 3-PGA, 3-phosphoglycerate; 6PGDH, 6-phosphogluconate dehydrogenase.

1.4.3 Pyruvate dehydrogenase

Since FA synthesis occurs in the chloroplast, the most efficient way for direct acetyl-CoA synthesis is in the chloroplast itself. Plastidial FA synthesis which rely on acetyl-CoA from ACS or ACL usually applies only to energy-starved or non-green plastids which lack the ability to generate acetyl-CoA locally in the chloroplast (Møller, 2005; Flügge et al., 2011). These plastids therefore require the import of intermediate metabolites such as acetate, phosphoenolpyruvate or pyruvate in order to support synthesis of acetyl-CoA (Møller, 2005). In contrast, chloroplasts are capable of independently generating ATP by photosynthesis, which drives the synthesis of energy-rich metabolites such as G3P. Hence, for the majority of photoautotrophic microalgae used to produce renewable biofuels by sequestration of CO_2, the most common way to produce acetyl-CoA in the plastids is from pyruvate via PDC. The concept that plastidial acetyl-CoA may be derived from pyruvate is substantiated with the isolation of cDNA encoding for subunits of plastidial PDC (Johnston et al., 1997), and organelle fractionation studies demonstrating PDC activity in the plastids (Kang and Rawsthorne, 1994). In addition, carbon labeling experiments demonstrated that ^{14}C-pyruvate was a superior substrate to ^{14}C-acetate for the formation of FAs (Kang and Rawsthorne, 1994), implying that PDC is sufficient for producing acetyl-CoA for FA synthesis. While mRNA levels of ACS did not correlate with lipid formation in developing seeds of *Arabidopsis*, the mRNA levels of plastidial PDC E1β subunit displayed temporal and spatial accumulation

patterns consistent with a predominant role for plastidial PDC in FA synthesis (Ke et al., 2000). A compelling recent study comparing the transcriptomic and metabolic profiles of oil and date palms reaffirmed the importance of plastid carbon precursor supply for FA synthesis by demonstrating a 24-fold increase in abundance of plastidial PDH during fruit ripening (Bourgis et al., 2011) which suggests an indispensable role of plastidial PDH in storage lipid production.

Similarly in microalgae, the most upregulated genes in the transcriptome under nitrogen depletion were consistently associated with nitrate uptake and assimilation, the PDC, and the TCA cycle (Levitan et al., 2015), with multiple studies reporting an upregulation of plastidial PDC correlating with an increase in overall lipid production (Li et al., 2014; Yang et al., 2014). Interestingly, transcript levels of plastidial PDC were 2- to 6-fold higher than those of mitochondrial PDC, supporting the concept that plastid is the primary site of pyruvate conversion to acetyl-CoA (Li et al., 2014). Gene expression of the plastidial PDC E1α subunit was rapidly induced during nitrogen depletion in the high TAG-accumulating microalga *C. desiccata*, in concert with increasing levels of acetyl-CoA (Avidan et al., 2015). This trend was not observed in two other microalgae species, *C. reinhardtii* and *D. tertiolecta*, which produced significantly lower amounts of acetyl-CoA and did not experience an increase in PDC E1α transcript levels (Avidan et al., 2015). Additionally, downregulation of plastidial PDC E1α impaired TAG accumulation and photosynthetic activity in nitrogen-depleted *C. reinhardtii* (Shtaida et al., 2014), signifying the importance

of PDC in supplying carbon precursors for *de novo* lipid synthesis in microalgae (**Table 1.2**). However, the negative effects of its downregulation was not so apparent when acetate is present in the media, suggesting that ACS might have a role in PDH by-pass, incorporating exogenously available acetate into acetyl-CoA (Avidan and Pick, 2015). Furthermore, antisense knockdown of a putative PDC kinase - which deactivates PDC – increased neutral lipid content up to 82% (Ma et al., 2014) (**Table 1.2**). Even under non-nitrogen limiting conditions, PDC subunits were also observed to be upregulated following transition from starch-rich heterotrophy (dark conditions) to lipid-rich photoautotrophy (light conditions) in the oleaginous *C. pyrenoidosa* (Fan et al., 2015). Under elevated doses of CO_2 which improves lipid accumulation in microalgae, genes involved in carbohydrate metabolic pathways, such as the components of the PDC, were found to be upregulated in *Chlorella sorokiniana*, despite a down-regulation of most FA synthesis genes (Sun et al., 2016). This implies that the positive correlation between PDC expression and lipid build-up is not primarily confined to nutrient-depleted conditions. The notion is that PDC transforms pyruvate into acetyl-CoA, which may then be used for FA synthesis or channeled to the TCA cycle for cellular respiration.

The generation of plastidial pyruvate is governed by three reactions: by plastidial pyruvate kinase, by pyruvate import into plastids, or by plastidial ME (Lonien and Schwender, 2009). The glycolytic enzymes phosphoglycerate mutase, enolase and pyruvate kinase, which produce pyruvate from glycolysis, are

notably absent from algal chloroplasts (Terashima et al., 2011), meaning that sources of plastidial pyruvate are likely to be imported into the chloroplast (Chapman et al., 2013; Johnson and Alric, 2013)or partially compensated for by plastidial ME (Lonien and Schwender, 2009). Although pyruvate is relatively small and able to passively permeate lipid bilayers, it is also possible that pyruvate is transported by specialized pyruvate transporters, as evidenced in C4 plants (Furumoto et al., 2011) (**Fig. 1.3**).

1.4.4 Glucose-6-phosphate dehydrogenase

In addition to carbon supply from acetyl-CoA, production of FAs require the provision of reducing power in the form of NADPH. Generation of NADPH for FA synthesis were mainly attributed to the metabolism of glucose-6-phosphate (G6P), pyruvate and malate as these metabolites were found to support high rates of FA synthesis in plant plastids (Smith et al., 1992; Pleite et al., 2005). Multiple routes provide NADPH for plastids, including plastidial glycolysis, photochemical reactions, import of metabolites from cytosol or mitochondria, or the Oxidative Pentose Phosphate Pathway (OPPP) (Nishida, 2004). The OPPP in particular, was found to be enhanced along with the Calvin cycle when algal cells were exposed to higher CO_2 concentrations; their respective enzyme activities and gene expression increased in parallel with photosynthetic performance, growth rate and lipid productivity (Wu et al., 2015).

G6P can be utilized in two pathways: Glycolysis and the OPPP; the latter is a major source of reducing power for biosynthetic processes. Multiple studies show that plastidial G6P flux through the OPPP stimulates the incorporation of carbon from pyruvate into FAs (Kang and Rawsthorne, 1994; Johnson et al., 2000; Pleite et al., 2005), suggesting that there is an interaction between provision of carbon substrates and reducing power to simultaneously increase FA synthesis. The first committed reaction of the OPPP is catalyzed by G6PDH, which metabolizes G6P to produce NADPH (Kruger and von Schaewen, 2003). G6PDH is considered to be an important source of NADPH in heterotrophic plant plastids producing high amounts of FAs, but which are not able to synthesize NADPH by photosynthesis (Hutchings et al., 2005; Møller, 2005). Nevertheless, there is conflicting evidence regarding the dependence on OPPP to sufficiently meet the demands for FA synthesis. *Brassica napus* and maize embryos demonstrated 10% and 36% of carbon influx to OPPP respectively, accounting for only 22% of NADPH required by FA synthesis (Schwender et al., 2003; Alonso et al., 2010). In sunflower embryos, however, NADPH production by OPPP was more than enough to supply for FA synthesis (Alonso et al., 2007). Metabolic flux analysis for the microalga *C. pyrenoidosa* found that culture conditions determine glycolytic flux through the OPPP (Yang et al., 2000). When in an autotrophic state, glucose flux through the OPPP was very small as the synthesis of NADPH is provided by photosynthetic electron transport, but during heterotrophic growth, 90% of glucose proceeds via G6PDH (Yang et al., 2000). Recent reports on *C.*

protothecoides adds further weight to this notion by demonstrating that under nitrogen-limited conditions, [13-C]glucose flux to glycolysis through the OPPP increased from 3% to 20% of the glucose uptake, reflecting increased NADPH requirements for lipid synthesis (Xiong et al., 2010; Gopalakrishnan et al., 2015). On the other hand, halotolerant microalgae such as *Dunaliella salina* may exhibit higher OPPP flux and increased G6PDH proteins under autotrophic growth as the OPPP appears to play a major role in osmoregulation (Chitlaru and Pick, 1991; Liska et al., 2004). When the oleaginous microalgae *N. oleoabundans* was subjected to nitrogen depletion inducing the accumulation of lipids, it displayed an upregulation of genes encoding for the OPPP including G6PDH, suggesting that the OPPP could be activated as a response to supply reductants for FA synthesis and/or inorganic nitrogen assimilation (Rismani-Yazdi et al., 2012). In *P. tricornutum*, high activity and mRNA expression of G6PDH were observed as cells were exposed to increasing levels of CO_2 (Wu et al., 2015), suggesting that NADPH produced through OPPP might play an important role in both growth and lipid synthesis under higher CO_2 concentration. Most intriguingly, recent efforts to identify a critical determinant of FA synthesis have pointed to the OPPP as the NADPH producer responding to lipogenesis (Chen et al., 2015a). While studying global gene expression patterns, Chen *et al.* found that oleaginous microbes such as *C. reinhardtii* and *Mucor circinelloides* showed upregulated expression of 6-phosphogluconate dehydrogenase (6-PGDH) and G6PDH under nitrogen starvation, but they remain unchanged in the non-oleaginous fungi *Aspergillus*

nidulans. G6PDH was identified to be particularly important for FA synthesis as RNAi knock down of G6PDH resulted in a corresponding 40% decrease in both NADPH levels and FA content, while suppression of 6-PGDH and ME had a much lesser effect on NADPH and FA accumulation. G6PDH, and by extension the OPPP, could therefore be an indispensable source of NADPH which enables efficient FA synthesis in oleaginous microbes.

1.4.5 NADP-malic enzyme

That NADPH produced from OPPP only partially fulfills the demand for reducing power by FA synthesis (Schwender et al., 2003; Alonso et al., 2010) indicates that other intraplastidial sources of reducing power may be available to compensate for the need for reductants (Wakao et al., 2008; Baud and Lepiniec, 2010). Malate, when supplied alone, was able to support the highest rates of FA synthesis in plastids (Kang and Rawsthorne, 1996; Pleite et al., 2005). In contrast, G6P and pyruvate must be supplied together to obtain rates of FA synthesis comparable to those supported by malate (Pleite et al., 2005). These observations reveal another potential source of reductants for FA synthesis - utilization of malate by plastidial NADP-dependent malic enzyme (ME). ME produces NADPH by catalyzing the decaboxylation of malate to pyruvate, while PDC subsequently converts pyruvate to acetyl-CoA, thus providing for the two key substrates required for FA synthesis. Import of malate into the plastids relies on the translocation of mitochondrial malate or the refixation of CO_2 into

oxaloacetate (OAA) in the cytosol by phosphoenolpyruvate carboxylase, followed by conversion of OAA into malate catalyzed by malate dehydrogenase (Baud and Lepiniec, 2010; Radakovits et al., 2012) (**Fig. 1.3**). The latter route involves a proposed C4 carbon-concentrating mechanism in microalgae which describes a malate/pyruvate shuttle permitting cytosolic malate into the chloroplast where plastidial ME releases CO_2 and NADPH (Radakovits et al., 2012; Yang et al., 2013). Mitochondrial TCA cycle reactions were found to be accelerated under N-depleted conditions producing OAA and/or malate (Li et al., 2014; Recht et al., 2014), suggesting that these metabolites may be crucial to support increased FA synthesis. Malate can be transported to the chloroplast via malate transporters (Kinoshita et al., 2011) and utilized by plastidial ME producing pyruvate and NADPH, which flows into FA synthesis. Moreover, the CO_2 produced by this reaction could be directly fixed by RuBisCO to increase photosynthetic capacity. This repartitioning route for supplying carbon precursors was supported by a computational hypothesis testing approach, where the authors assign to the TCA cycle a central role for *de novo* FA synthesis by providing excess malate (Recht et al., 2014).

Recent studies have provided evidence to establish the possible role of ME in microalgal lipid synthesis. Expression levels of ME were correlated with an increase in lipid content during nitrogen limitation (Yang et al., 2013; Fan et al., 2014). When sesamol, a known inhibitor of ME, is added to nitrogen-limited cultures of *Nannochloropsis* sp. and *H. pluvialis*, it reduced both growth and fatty

acid accumulation (Recht et al., 2012), suggesting that ME might be important for providing NADPH for essential cellular functions as well as for FA synthesis. Indeed, overexpression of ME in *P. tricornutum* enhanced neutral lipids by 2.5-fold, while maintaining similar growth rates to the wild-type (Xue et al., 2015) thus enabling the increased production of lipids without sacrificing biomass. Introduction of heterologous *P. tricornutum* ME into *C. pyrenoidosa* also increased neutral lipids up to 3.2-fold relative to wild-type, with the mutants achieving lipid contents of between 30% and 40% relative to wild-type strains which exhibited 12.7% lipids (Xue et al., 2016) (**Table 1.2**). However, low ME activity was also detected in some microalgae species (Xiong et al., 2010; Bellou and Aggelis, 2012) which may limit NADPH supply, suggesting that ME could be rate-limiting in the provision of substrates for FA production. Several isoforms of ME exist with distinct localization in the mitochondria, cytosol and plastid (Wheeler et al., 2005; Vongsangnak et al., 2012), possibly carrying out different functions. In oleaginous heterotrophic species, cytosolic ME is proposed to form a lipogenic metabolon with ACL and ACCase, where it supports FA synthesis by continuous NADP reduction (Kosa and Ragauskas, 2011). Overexpression of mitochondrial ME did not result in any significant changes in lipid content (Zhang et al., 2013), while the use of cytosolic ME may only be effective when fatty acid synthesis occurs in the cytosol (Zhang et al., 2007; Meng et al., 2011). Plastidial ME, on the other hand, was found to increase over 7-fold in transcript levels during nitrogen depletion in *P. tricornutum* (Yang et al., 2013), suggesting that it

could provide for essential reducing power for FA synthesis in photoautotrophic cells. In the model microalga *C. reinhardtii*, six isoforms of ME exist, with two predicted plastidial isoforms, but they are associated with anaerobic metabolism and not with FA synthesis (Wheeler et al., 2008; Terashima et al., 2011). Hence, although ME has the potential to supply reductants for increased FA synthesis, like G6PDH and the OPPP, its role within specific cell types relating to lipid accumulation has to be pre-determined.

1.4.6 Multi-gene approach

Individual genes participating in the supply of acetyl-CoA or NADPH are claimed by various studies to be rate-limiting for FA synthesis (Ratledge, 2004; Zhang et al., 2007; Lei et al., 2012). However, it is likely that a multi-gene approach may be required to completely rewire an organism's ability to switch from non-oleaginous to oleaginous, without compromising growth. For example, the claim that NADPH provision by ME was a rate-limiting step in FA synthesis was previously backed by observations that ME overexpression in the fungus *Mucor circinelloides* led to a 2.5-fold increase in FAs (Zhang et al., 2007). This conclusion was challenged by another report revealing that it is actually leucine auxotrophy - which the previous authors used for selection - that decreased FA content by 2.5-fold, and that ME overexpression did not translate into higher lipid levels despite an increase in ME activity (Rodríguez-Frómeta et al., 2013). It was thus proposed that the leucine metabolism pathway, by participating in the

generation of acetyl-CoA substrates, may be critical for FA synthesis in *M. circinelloides*. A subsequent study showed that ME overexpression increased FA content by only 30% relative to control, despite a 2-fold increase in ME activity, suggesting that ME may not be the sole rate-limiting enzyme, but does play a role during FA synthesis in oleaginous fungi (Hao et al., 2014). Recently, a large-scale genomic engineering of *Y. lipolytica* involved the simultaneous overexpression of ACL and ME to increase acetyl-CoA and NADPH supply, while DGAT was also overexpressed to increase carbon flux towards TAG synthesis (Blazeck et al., 2014). In addition, these targets were multiplexed with deletions of genes which serve to reduce FA catabolism by inhibiting the peroxisomal β-oxidation pathway. Consequently, the cells became lipid saturated up to 90% biomass with lipid titres exceeding 25 g/L, which is a 60-fold improvement over the parental strain (Blazeck et al., 2014). Thus, increasing of FA synthesis in microorganisms may not be simply explained by overexpression of a single enzyme, but influenced by a combination of pathways spanning FA synthesis, TAG synthesis and central carbon metabolism, including production of FA precursors like acetyl-CoA and NADPH.

1.5 Free fatty acid secretion and tolerance

As most biofuel molecules, specifically fatty acids are synthesized and stored inside cells, a major technical barrier that hinders successful commercialization of microalgae biofuels is the energy costs incurred while

harvesting and extracting oil from the cells (Mercer and Armenta, 2011). Generally, the cells need to be dried and lipids are obtained by solvent extraction, supercritical fluid extraction or ultrasonic-assisted extraction (Mercer and Armenta, 2011). These methods of oil recovery from microalgae biomass are expensive and energy intensive, typically accounting for 70-80% of the total cost of biofuel production (Molina Grima et al., 2003). Despite efforts to create a sustainable model of biodiesel production by modifying the pathway from cultivation to extraction, these steps were still responsible for an average of 42% of total energy consumption (Delrue et al., 2012; Delrue et al., 2013). A better approach that could potentially improve the economic viability of producing biofuels is the direct secretion of oil from cells into the culture medium, removing the need for harvesting, drying and extracting lipids from microalgal biomass (**Fig. 1.4**). Akin to milking a cow, biofuel secretion from microalgae without killing them allows the cells to replenish their intracellular lipid content, resulting in a sustainable system where biofuel is harvested (Ramachandra et al., 2009). Secreted oil droplets into the surrounding liquid would progressively separate into a different phase, ultimately appearing as a layer above the culture medium, enabling easy and cheap recovery (Ramachandra et al., 2009). Moreover, secretion of lipids may also reduce the toxicity of intracellular accumulation of certain lipids in over-producing strains (Dunlop et al., 2011b).

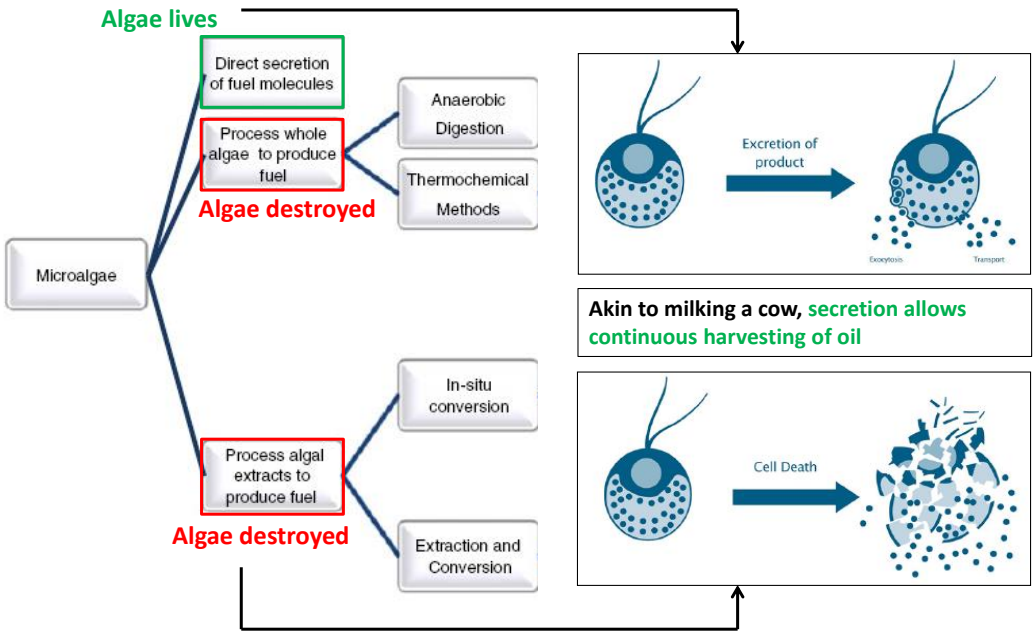

Figure 1.4 Conversion pathways from microalgae to biofuels. Modified from: (de Boer et al., 2012).

The build-up of intracellular FFAs can lead to cellular stress resulting in the generation of ROS and toxic lipid hydroperoxides (Ruffing and Jones, 2012; Ruffing, 2013). Moreover, the amphipathic structure of FFAs enables them to intercalate into membranes, disrupting membrane structure and causing widespread damage (Desbois and Smith, 2010). A potential solution to mitigate FFA toxicity is to effectively remove the FFAs from the cells by overexpressing FFA export pumps or transporters, therefore increasing the cells' tolerance against the buildup of biofuels (Dunlop et al., 2011b; Chen et al., 2013). *Synechococcus elongatus* PCC 7942 mutants engineered to accumulate high amounts of FFAs was shown to generate ROS, leading to increased cell permeability (Ruffing,

2013). Subsequent overexpression of ROS-degrading enzymes in these cells, however, improved growth and reduced cellular damage. These mutants were found to have increased extracellular FFA concentrations compared to those that were not overexpressing ROS-degrading enzymes. Notably, cell viability was correlated with FFA export; mutants showing increased cell concentrations experienced increased extracellular FFA concentrations (Ruffing, 2013). This suggests that secretion of FFAs could also aid in reducing the effects of FFA toxicity. Efflux pumps have been identified in *E. coli* for FFA export that improved tolerance to biofuels (Dunlop et al., 2011b), but these transporters belong to the RND (resistance-nodulation-cell division) family of proteins which have a tripartite structure spanning the inner and outer bacteria cell membrane, limiting its translation to other economically viable hosts such as eukaryotic microalgae.

Attention has now been shifted to the ATP-binding cassette (ABC) family of transporters as they are highly conserved and widely found in all species (Higgins, 1992), potentially allowing for cross-species translation. An interesting characteristic of ABC transporters is their preferential gating properties, as the transmembrane domain determines ligand specificity while the nucleotide-binding domain is homologous and highly conserved throughout the family (Pohl et al., 2005; Linton, 2007; Verrier et al., 2008). Recently, various bacterial ABC transporters have been found to facilitate the export of hydrophobic substances such as zeaxanthin and β-carotene in carotenoid-producing *E. coli*, depicting the

ability of ABC transporters to function across species barriers (Doshi et al., 2013). Expression of MdlB, an ABC transporter identified to be upregulated in *E. coli* during isopentenol exposure, was shown to not only improve growth, but also increase isopentenol production relative to control , suggesting that export pumps could confer increased tolerance to the production of these compounds. ABC transporters have also been implicated as part of a transcriptomic response to the cytotoxic build-up of alkane biofuels in *S. cerevisiae* (Ling et al., 2013). When exposed to alkanes, plasma membrane efflux pumps Snq2p and Pdr5p were significantly induced in *S. cerevisiae*, suggesting that they may play a role in alkane export and tolerance. Indeed, overexpression of the two endogenous efflux pumps (Ling et al., 2013), as well as heterologous expression of *Y. lipolytica* ABC2 and ABC3 transporters (Chen et al., 2013), were able to significantly increase tolerance against decane and undecane through maintaining lower intracellular alkane levels. In another transcriptome response study, RNA-seq analysis of FFA-exporting *S. elongatus* 7942 mutants found increased expression of membrane associated channels such as ABC transporters and porins (Ruffing, 2013), further implying that these complexes may be involved in the secretion of FFAs to alleviate intracellular FFA toxicity. These observations, taken together, demonstrated that expression of ABC transporters could actively pump out next-generation biofuels through transporter engineering, paving the way for improving biofuel production and recovery.

A straightforward approach to engineer microalgae to secrete biofuels is to introduce ABC transporters known to export fatty acids, such as the recently described plasma membrane-localized ABC transporters ABCG11 and ABCG12 from *A. thaliana* (Bird et al., 2007; McFarlane et al., 2010). While the exact mechanisms are not yet known, these transporters were shown to be important for exporting cuticular wax (long chain fatty acids), as knock-out mutants produced a 50% reduction in extracellular waxes and accumulated large amounts of intracellular lipids, indicating that fatty acid transport was impaired by the loss of the ABC transporter (Bird et al., 2007). ABCG11 exports long chain FAs of 16 to 18C in length (Bird et al., 2007), similar to the FA profile of microalgae (Davidi et al., 2012), raising a possibility that ABCG11 could export FAs in the latter as well. It is worth noting that cyanobacteria have already been engineered to secrete FFAs by overexpressing an *E. coli* TE (Liu et al., 2011b) and/or knockout of an acyl-ACP synthetase (AAS) (Kaczmarzyk and Fulda, 2010; Liu et al., 2011b; Ruffing and Jones, 2012). Since these genes are not directly involved in the active transport of FFAs across the cell membrane, it is likely that any manipulation that enables the buildup of intracellular FFAs could result in the fast free diffusion (passive "flip-flop") of FFAs through the phospholipid bilayer (Black and DiRusso, 2003; Tarling et al., 2013). In addition to their ability to secrete endogenous FFAs, knockout mutants of AAS are characterized by the inability to utilize exogenous FFAs, which suggest a role for AAS in recycling the released FFAs (Kaczmarzyk and Fulda, 2010). Membrane porin knockout mutants in *S.*

elongatus 7942 also displayed enhanced extracellular FFAs, suggesting that these porins may actually contribute to FFA uptake rather than export (Ruffing, 2013). Thus, blocking the re-uptake of extracellular FFAs could work in concert with FFA export as a strategy for the net secretion of FFAs.

While secretion of FFAs may be easily established in prokaryotes, it may prove to be more complicated for eukaryotic microalgae due to the presence of thick cell walls (Popper and Tuohy, 2010) and that they possess unique metabolic attributes such as the conversion of FAs into TAGs. For instance, overexpression of TEs in *P. tricornutum* resulted in fatty acid accumulation, but unlike observations in cyanobacteria, no significant secretion was detected as the bulk of FAs (75-90%) were incorporated into TAGs which are too large to be secreted by simple diffusion (Radakovits et al., 2011). As such, future strategies that focus on the secretion of biofuels from microalgae might have to include inhibiting the TAG synthesis pathway. *Botrycoccus braunii*, a green colonial microalga known for its ability to secrete hydrocarbons spontaneously, accumulates only 2 – 6% of lipids as TAGs (Metzger and Largeau, 2005). In addition, its capability to produce up to 63% total lipids was achieved through storage of most lipids in the extracellular space (Largeau et al., 1980a; Largeau et al., 1980b). This is in contrast to other microalgae which store lipids as lipid droplets in the cytoplasm. Thus, understanding how different microorganisms produce and secrete lipids would enable the adoption of potential strategies to promote FA secretion. Identifying secretion signals unique to endogenous ABC transporters could be

useful in engineering MLDP or TAG molecules for secretion (Chung et al., 2009; Park et al., 2012). Currently, how ABC transporters recognize and mediate substrate translocation is unclear, but future insights into the structure, function and substrate recognition by ABC transporters (Gao et al., 2012; Hohl et al., 2012; Srinivasan et al., 2014) might allow for the design of ABC transporters tailored for the specific efflux of FAs or TAGs.

1.7 Potential environmental impacts of microalgae production

While genetically engineered microalgae hold great promise for commercial production of fuels and feedstocks, they also pose possible risks to the health of ecosystems if they escape from bioreactors or open ponds. For example, a leak from the contained microalgae production facility could result in algal blooms in nearby water bodies, especially when nutrient sources are available. Due to their high surface area-to-volume ratio, microalgae have the potential to absorb large amounts of nutrients across their surface, enhancing their growth (Usher et al., 2014), thus making them highly adaptive to their environment. Sudden explosive growth of algae in natural environments is facilitated nutrient availability. Singapore, in particular, experiences high rainfall during the monsoon seasons (Northeast and Southwest monsoons) which causes surface runoffs from terrestrial inputs (Leong et al., 2015). Under favourable environmental conditions (e.g. high nitrogen concentrations), algal biomass could accumulate and form algal blooms which have in the past resulted in the deaths of up to 600 tonnes of fish from local fish farms (Leong et al., 2015). In addition,

contamination by genetically engineered microalgae that are resistant to viruses may provide a competitive advantage to growth in the local environment, allowing for dense growth without dying which could result in devastating effects to native biodiversity. Before novel strains are introduced as feedstocks for industrial use, key biosafety issues should be addressed by formal environmental risk assessments to properly guide the sustainable development of microalgal biofuels. The cost and benefits of investing in microalgae biofuel production should also be assessed to ensure the benefits outweigh the economic and environmental costs. Hence, the balance between economic and environmental viability while minimizing negative environmental impacts would be key factors in promoting the feasibility of microalgal biofuel production in Singapore.

1.8 Project objectives and hypotheses

The primary objective of this project is to enhance lipid productivity in microalgae through identification of the genetic determinants which correspond with increased lipid production (**Fig. 1.2**). The organism of study is *Dunaliella tertiolecta*, a motile, halotolerant microalga that can be grown in high salinity (up to 4M NaCl) which could exclude contaminating species and not compete for freshwater sources. In addition, it possesses high growth rates in a wide range of pH, temperature and light, and do not have a cell wall, making cell lysis much less energy intensive.

Firstly, in order to identify the major enzymes associated with increased lipid synthesis in *D. tertiolecta*, the cells will be subjected to nitrogen depletion

which is known to stimulate lipid accumulation. Analysis of carbon allocation and the expression profile of genes related to lipid synthesis will be evaluated. As *D. tertiolecta* is a non-model organism with no sequenced genome, next-generation RNA sequencing would be employed to derive its transcriptome signatures, followed by mapping of its putative sequences to an annotated database of the closely related model microalga species *Chlamydomonas reinhardtii*. The findings from this study would potentially reveal the transcriptomic influence behind storage reserve allocation in *D. tertiolecta* and provides valuable insights into the possible manipulation of genes for engineering microorganisms to synthesize products of interest. After the lipid synthesis genes are identified, specific full-length coding sequences would have to be obtained by Rapid Amplification of cDNA ends (RACE) and engineered into *D. tertiolecta*. Should transformation in *D. tertiolecta* prove to be unsuccessful, we will attempt to use the model microalga *C. reinhardtii* to test our concepts. It is hypothesized that the overexpression of genes which contribute to substrate supply for fatty acid (FA) synthesis would increase lipid production.

The second aim of this project is to introduce an active transport protein known to secrete FAs into model species of cyanobacteria and microalgae due to their ease of transformation (**Fig. 1.4**). Inducing secretion of FAs might be difficult if the cells have low basal levels of lipids. Thus, inhibition of competing pathways (e.g. β-oxidation of FAs) would be used to increase intracellular FAs. Gene deletions and foreign gene insertions can be achieved via homologous

recombination in prokaryotic cyanobacteria, allowing for precise relationships between genes and lipid production/secretion to be studied. The findings from this project would provide valuable insights into the use of genetic strategies to promote FA secretion, and contribute to lowering the costs of biofuel production.

Chapter 2 Lipid accumulation and expression profile of genes contributing to fatty acid synthesis in *Dunaliella tertiolecta* during nitrogen depletion

2.1 Introduction

2.1.1 Scientific significance

A major bottleneck in cost-efficient biofuel production from microalgae is the dilemma between biomass productivity and lipid accumulation. Photosynthetic microalgae can accumulate large amounts of energy-rich lipids, predominantly TAGs, under stressful culture conditions such as nitrogen depletion (Radakovits et al., 2010). This ability enables the microalgae to survive adverse environmental changes as the energy deposits can be easily mobilized when growth conditions are restored (Yu et al., 2011). However, the accumulation of lipids under such circumstances comes at the expense of cellular growth and biomass productivity. For biotechnological applications where large-scale production of lipids is desired, utilizing an approach involving nitrogen depletion is unfavourable as the culture will suffer from low biomass production which negatively impacts overall lipid productivity. Therefore, it is essential to obtain an ideal strain which has a high growth rate while also possessing high lipid production.

Because growth and lipid synthesis pathways essentially compete for photosynthetic assimilate, overexpression of genes that increase FA or TAG synthesis alone is likely to reduce microalgae growth rate because their processes channel carbon away from the pathways supporting cellular growth, such as glycolysis and the TCA cycle (Liu and Benning, 2013; Shtaida et al., 2015). Increasing the activity of lipid synthesis pathways may instead "pull" carbon away from those which support cellular growth. For instance, overexpression of FA synthesis genes such as ACCase could result in reduced growth because carbon required for FA synthesis is tapped from acetyl-CoA, the key two-carbon metabolite shared between the TCA cycle and FA synthesis. As both of these pathways compete for acetyl-CoA, it is not surprising that overexpression of genes involved in FA synthesis produced only modest increases in lipid content (Courchesne et al., 2009). Increasing evidence suggest that the "pushing" of substrates to lipid synthesis pathways might be more important than increasing the activity of the pathways themselves. Recent transcriptomic studies on carbon fixation in the diatom *Phaeodactylum tricornutum* (Valenzuela et al., 2012; Yang et al., 2013) found that the build-up of precursors such as acetyl-CoA and NADPH may provide a more significant contribution to TAG accumulation than the activity of ACCase itself. In addition, the supply of carbon substrates in the plastids were found to be the major contributing factor for oleagenicity in oil palms as transcript levels of enzymes contributing to plastidial carbon metabolism were more than 50-fold higher compared to date palm, a closely-related species

that accumulate almost exclusively sugars rather than oil (Bourgis et al., 2011). In contrast, enzymes involved in TAG synthesis were unchanged in oil palm and date palm. These studies suggest that substrate availability may be a critical bottleneck in increased production of FAs. Hence, increasing the availability of precursors for both primary metabolism and FA synthesis could be a viable approach to simultaneously improve the yield of lipids and biomass in microalgae.

2.1.2 Aims and objectives

We hypothesize that substrate availability is a critical bottleneck in balancing growth and FA production. To improve lipid productivity (i.e. increased biomass productivity and lipid content) in microalgae, we propose to identify and overexpress rate-limiting enzymes which could increase the intracellular pool of substrates required for FA synthesis, namely acetyl-CoA and NADPH. Enzymes contributing to the supply of acetyl-CoA include pyruvate dehydrogenase complex **(PDC)** and ATP:citrate lyase **(ACL)**, while those that provide for NADPH include malic enzyme **(ME)** and glucose 6-phosphate dehydrogenase **(G6PDH)**. For robust comparison, we also studied two enzymes directly involved in the FA and TAG synthesis pathways, malonyl CoA-ACP transacylase **(MCAT)** and diacylglycerol acyltransferase **(DGAT)**, to provide an objective contrast to our hypothesis. Fatty acyl-ACP thioesterase **(TE)**, which relieves the negative feedback inhibition of ACCase by hydrolysis of accumulated

acyl-ACPs into free FAs, is also analyzed. Finally, we included β oxidation enzymes acyl-CoA dehydrogenase **(ACD)** and acyl-CoA oxidase **(ACOX)**, which are responsible for the breakdown of FAs in the mitochondria and peroxisome respectively(Winkler et al., 1988), as they could be promising targets for microRNA silencing.

In this study, we seek to sequence and profile the expression of genes contributing to the generation of acetyl-CoA and NADPH during increased lipid production in the halotolerant, green microalga *Dunaliella tertiolecta*. The objective is to identify key *D. tertiolecta* genes that are correlated with lipid accumulation. Subsequently, these genes would be transformed in the microalga to improve lipid productivity. *D. tertiolecta* was selected as the organism of choice as it can be grown in waters of high salinity (up to 4M NaCl) such as saltwater, wastewater or brackish water (Tang et al., 2011) which could exclude contaminating species and would not compete with freshwater sources. Secondly, it is an ideal species for biofuel production because it can maintain high growth rates in a wide range of pH, temperature and light, and contain relatively high lipid content (Gouveia and Oliveira, 2009; Bouchard et al., 2013; Georgianna et al., 2013). Unlike most microalgae, *D. tertiolecta* is a motile species possessing flagella and do not have a cell wall, making cell lysis much less energy intensive while auto-flocculation drastically reduces energy required for harvesting (de Boer et al., 2012). As it is a non-model organism, a drawback of using *D. tertiolecta* is that its genome is not sequenced and efficient transformation

methods are lacking. Thus, Rapid Amplification of cDNA ends (RACE) was used to obtain the cDNA sequences of the enzymes required for this study. In order to stimulate increased lipid synthesis in *D. tertiolecta*, the cells will be subjected to nitrogen depletion which is known to stimulate lipid accumulation (Radakovits et al., 2010). Gene expression of the various candidate enzymes will be determined and analyzed for correlations with increased lipid content during its growth phases. Neutral lipids will be measured using the Nile Red staining assay and fluorescence microscopy will be performed for visualization purposes.

Aims: To identify genes associated with increased storage product accumulation in *D. tertiolecta*, particularly genes which encode for enzymes responsible for providing substrates for fatty acid synthesis.

Hypothesis: Genes which contribute acetyl-CoA or NADPH are upregulated upon nitrogen depletion, a condition known to halt cell division but increase storage product accumulation in microalgae. In contrast, the expression of genes directly involved in the synthesis of storage products (e.g. fatty acid synthesis genes) will remain unchanged.

2.1.3 Rationale for gene subunit and isoform selection in *D. tertiolecta*

Our hypothesis for improving lipid productivity is based on increasing the supply of substrates for general cell metabolism and FA synthesis (i.e. acetyl-CoA and NADPH). However, because membranes are impermeable to NADPH and

CoA derivatives (Fatland et al., 2002; Antonenkov and Hiltunen, 2006), acetyl-CoA and NADPH are generated in distinct metabolic pools within the organelles. Therefore, the enzymes responsible for generating these substrates may have isoforms that are localized in different subcellular compartments: plastids, mitochondria, peroxisomes, and the cytosol. For example, PDC can be found in the plastids and mitochondria (Johnson and Alric, 2013), while ME has 6 isoforms differentially localized in the cytosol, mitochondria and plastids (Terashima et al., 2011). Although the primary source of acetyl-CoA and NADPH for FA synthesis is still unknown, FA synthesis in microalgae is generally accepted to occur within the chloroplast (Radakovits et al., 2010), indicating that acetyl-CoA and NADPH produced within the chloroplast would be most suited for use in FA synthesis. Hence, whenever possible, we chose to select for plastidial isoforms of the enzymes.

Pyruvate dehydrogenase (plastidial) E1β subunit (DtPDH). PDC is a multi-enzyme complex consisting of 3 subunits (Li et al., 2014): Pyruvate dehydrogenase (E1), dihydrolipoyl transacetylase (E2) and Dihydrolipoyl dehydrogenase (E3). Complicating efforts in metabolic engineering of microalgae are the distinct metabolic processes that occur within algal organelles and the numerous enzyme isoforms present. We chose to study the plastidial pyruvate dehydrogenase E1 beta (E1β) subunit (hereafter PDH) – which catalyzes the first step of conversion from pyruvate to acetyl-CoA – as its mRNA levels was previously found to correlate strongly with lipid formation in developing seeds of

Arabidopsis (Ke et al., 2000) and showed increased expression under N-depleted conditions in the diatom *Phaeodactylum tricornutum* (Yang et al., 2014). Specifically, 67% of total cellular PDC activity was found to be in the plastids of the oleaginous oilseed rape (Kang and Rawsthorne, 1994), while transcript levels of plastidial PDH were 2- to 6-fold higher than mitochondrial PDH during lipid accumulation in *Nannochloropsis* (Li et al., 2014), suggesting that the plastid may be the major site for acetyl-CoA formation. Moreover, plastidial pyruvate kinase activity was discovered to be crucial for seed oil accumulation (Andre et al., 2007), suggesting a preferred plastid route to convert carbon from photosynthate into FAs.

ATP:citrate lyase subunit A (DtACLA). ACL is a cytosolic enzyme that cleaves citrate to form acetyl-CoA and oxaloacetate, and has often been proposed to be a major rate-limiting enzyme for oleaginicity (Ratledge, 2004; Kosa and Ragauskas, 2011). ACL activity is correlated with lipid accumulation (Ratledge et al., 1997) and its mRNA levels coincide with peak cytosolic ACCase expression (Fatland et al., 2002). Two species of microalgae had demonstrated ACL activity comparable to those in oleaginous heterotrophs (Bellou and Aggelis, 2012), indicating that microalgae may possess ACL to enable the utilization of citrate as a carbon source for acetyl-CoA production. Negative regulation of ACL subunit A (ACLA) reduced cuticular wax (long-chain FAs) synthesis in epidermal cells of *Arabidopsis* (Go et al., 2014), leading to the notion that increased acetyl-CoA supply in the cytosol may be to support the synthesis and elongation of long-chain

FAs. Thus, we chose to derive the sequence of DtACLA in order to determine if the expression of ACL contributes to increased FA synthesis in *D. tertiolecta*. ACLA is one of two subunits of ACL (the other being ACLB) and it consists of an ATP-binding domain and a portion of the N-terminal CoA lyase domain.

Malic enzyme (DtMME). Several isoforms of ME exist with distinct localization in the mitochondria, cytosol and plastid (Wheeler et al., 2005; Vongsangnak et al., 2012), possibly carrying out different functions. In oleaginous heterotrophic species, cytosolic ME is proposed to form a lipogenic metabolon with ACL and ACCase, where it supports FA synthesis by continuous NADP reduction (Kosa and Ragauskas, 2011). While the use of cytosolic ME may only be effective when fatty acid synthesis occurs in the cytosol (Zhang et al., 2007; Meng et al., 2011), overexpression of mitochondrial ME did not result in any significant changes in lipid content (Zhang et al., 2013). Plastidial ME, on the other hand, was found to increase over 7-fold in transcript levels during N-depletion in *P. tricornutum* (Yang et al., 2013), suggesting that it could provide for essential reducing power for FA synthesis in photoautotrophic cells. In the model microalga *C. reinhardtii* whose genome have been sequenced, six isoforms of ME exist (denoted MME): CrMME1 is predicted mitochondrial, CrMME2 and CrMME3 are predicted cytosolic while CrMME6 localization is unknown. CrMME4 and CrMME5 were found to be plastidial, but are associated with anaerobic metabolism and not with FA synthesis (Dubini et al., 2009; Terashima et al., 2011). A comparison of ME catalytic activities in *Arabidopsis* revealed that

isoform AtME2 had the highest catalytic efficiency for forward malate decarboxylation into pyruvate (Wheeler et al., 2008) and is responsible for the majority of ME activity in leaves (Wheeler et al., 2005). A BLAST search with AtME2 (NP_196728.1) against the *Chlorophyta* database showed that CrMME6 (XP_001696415.1) and CrMME2 (XP_001692778.1) had the closest homology. Further BLAST searches with an ME isoform (ABM45933.1) from the fungus *Mucor circinelloides*, which improved lipid content by up to 2.5-fold (Zhang et al., 2007; Li et al., 2013), also showed homologies with CrMME6 and CrMME2. Therefore, we decided to sequence for DtMME2 and DtMME6 to examine their relationship with lipid accumulation in *D. tertiolecta*.

2.2 Materials and Methods

2.2.1 Microalgae Strain and Culture Conditions

The *Dunaliella tertiolecta* strain (UTEX LB 999) was obtained from the University of Texas at Austin (UTEX) and maintained in sterile ATCC-1174 DA medium under nitrogen-replete condition of 5 mM KNO_3 (American Type Culture Collection at Manassas, Virginia) containing 0.5 M NaCl (**Table S1**). The cells were grown in 50-mL batch cultures on a rotary shaker at 25^{o}C and illuminated with 30 µmol photons m^2/s under a photoperiod of 14h Light/10h Dark, with or without 5% CO_2 aeration. Cell densities were determined using an automated cell counter (TC20^{TM} automated cell counter, Biorad Laboratories). Prior to counting, *D. tertiolecta* cells were fixed with 2% paraformaldehyde.

Optical density measurements (OD_{680}) were conducted with an UV spectrophotometer (Genesys 10S UV-VIS, ThermoFisher Scientific). Biomass was determined by dry cell weight (DCW) (g/mL) measurement and combined with cell density (cells/mL) to get dcw per cell (g/cell). Ten-milliliter (10 mL) of cells were collected by filtration on pre-weighed Advantec GB-140 filter paper (0.4 µm pore size; diameter 47 mm), and washed with isotonic 0.5 M ammonium formate (40 mL) to remove salts without causing the cells to burst. Cells captured on filter paper discs were dried in oven at 95^{o}C until the weight was constant. Work conducted throughout the study is based on biological triplicates unless otherwise stated.

2.2.2 Nitrogen Depletion and Cultivation

D. tertiolecta subjected to nitrogen depletion (N-depletion) were grown in nitrogen-limited media (ATCC-1174 DA medium containing 0.5 mM KNO_3, equivalent to 10% of original KNO_3 concentration; K substituted with KCl) (**Table S1)**. N-depletion was achieved by harvesting exponentially growing cells (cell density approximately 3 x 10^6 cells/mL) and twice washing them with fresh ATCC medium containing 10% KNO_3. All experimental cultures began at an OD_{680} of 0.1 for standardization. Nitrate concentration was determined using a UV spectrophotometric method measuring the difference between OD_{220} and OD_{275}, and converted with a standard curve (**Fig. S1**). Cells were harvested at regular time intervals corresponding to exponential, late-exponential and

stationary phases for RNA extraction, neutral lipid analysis, fluorescence microscopy, and biomass measurements. Experiments were conducted as independent biological triplicates.

2.2.3 Determination of physiological parameters (Total Organic Carbon, acetyl-CoA and NADPH, starch, glycerol, chlorophyll, photosynthetic yield)

Intracellular total organic carbon (TOC) content was measured using an automated High Temperature Combustion TOC Analyzer (LOTIX; Teledyne Tekmar), installed with a Non-Dispersive Infrared Detector. Cell densities of 3 x 10^7 cells were harvested, spun down and washed with 1 mL of 0.08M NaCl, reconstituted in ultrapure water to a final volume of 20 mL, and transferred to the TOC analyzer for analysis.

Acetyl-CoA and NADPH levels were determined with the Acetyl-CoA Assay Kit (MAK039; Sigma-Aldrich) and NADP/NADPH Quantification Kit (MAK038; Sigma-Aldrich) respectively, following the manufacturers' protocol. Before the assay, cells were extracted by resuspension in the provided buffers and broken by 3 freeze-thaw cycles in liquid nitrogen. Cell supernatants were then deproteinized by filtering through a 10 kDa cut-off spin filter (Amicon Ultra 0.5 mL centrifugal filter; Z677108; Sigma-Aldrich) before use in the assay.

Starch content was measured using the Starch Assay Kit (STA20; Sigma-Aldrich), performed according to the manufacturer's instructions. Glycerol

content was measured using the Free Glycerol Determination Kit (FG0100; Sigma-Aldrich) as previously reported by Chow *et al*(Chow et al., 2013). Harvested cells were centrifuged (10,000 g for 10 mins, 4^{o}C) and the cell pellet and supernatant were separated for measurement of intracellular and extracellular glycerol respectively. For intracellular glycerol, the cell pellet was washed with equivalent volume of 0.5M NaCl and centrifuged again to remove remaining extracellular glycerol. The cell pellet was then resuspended in 200 µL of ultrapure water, vortexed and boiled for 15 mins. Subsequently, the samples were centrifuged to remove cell debris, and the supernatant collected for intracellular glycerol analysis.

Photosynthetic yields (maximum efficiency of photosystem II; F_v/F_m) were evaluated using chlorophyll fluorescence measured with AquaPen-C fluorometer (AP-C 100/USB; Photon Systems Instruments). Cells were dark-adapted for 5 mins before using the fluorometer to measure F_v/F_m values according to the user's manual.

For chlorophyll measurements, cells were centrifuged (10,000 g for 10 mins, 4^{o}C), supernatant were removed, and the cell pellet resuspended in 0.5 mL DMSO and vortexed for 1 min until the pellet disintegrated. An equivalent volume of 90% acetone was added and mixed well, followed by centrifugation to remove cell debris. The supernatant (extraction volume of 800 µL) was used for measuring absorbances at 630 nm, 647 nm, 664 nm, 665 nm, and 750 nm using a UV spectrophotometer. Correction of pheopigments was done by adding 40 µL of

1M HCl to To the mixture and incubating at room temperature for 90 secs. Absorbances were measured again at 665 nm and 750 nm. Chlorophyll amounts were calculated according to trichromatic equations(Jeffrey and Humphrey, 1975) and the monochromatic equation for pheopigment correction(LORENZEN, 1967).

Trichromatic equations:

Chlorophyll *a* (μg/mL) = $[11.85\times(OD_{664} - OD_{750}) - 1.54\times(OD_{647} - OD_{750}) - 0.08\times(OD_{630}-OD_{750})] \times (V_e/L\times V_s)$

Chlorophyll *b* (μg/mL) = $[-5.43\times(OD_{664} - OD_{750}) + 21.03\times(OD_{647} - OD_{750}) – 2.66\times(OD_{630}-OD_{750})] \times (V_e/L\times V_s)$

Monochromatic equation for pheopigment correction:

Corrected chlorophyll *a* (μg/mL) = $11.4\times K\times[(OD665o - OD750o) - (OD665a - OD750a)] \times (V_e/L\times V_s)$

where

OD665o, OD750o = Absorbances before acidification with HCl

OD665a, OD750a = Absorbances after acidification with HCl

L = Light path of the cuvette (cm)

V_e = Extraction volume (mL)

V_s = Sample volume which was harvested (mL)

R = maximum absorbance ratio of OD665o/OD665a in the absence of pheopigments = 1.7

$$K = R/(R - 1) = 2.43$$

Total chlorophyll (μg/mL) = Chlorophyll *b* (μg/mL) + Corrected chlorophyll *a* (μg/mL)

2.2.4 Neutral Lipid Quantification

A modified Nile Red staining method (Yao et al., 2015) was used to quantify intracellular TAGs. Briefly, cells were harvested by centrifugation (3000 *g* for 10 min at 4^{o}C), supernatant was removed and the pellet resuspended in fresh 0.5M ATCC-1174 DA media to an OD_{680} of 0.3. Triolein was used as a standard for determining neutral lipid concentrations by Nile Red (**Fig. S10**). Two hundred microliters of triolein standards (40, 20, 10, 5, 2.5, 0 μg/mL) and cell suspensions were loaded as technical triplicates onto a 96-well black, clear bottom plate (CLS3603; Sigma-Aldrich). Prior to staining, Nile red stock is diluted in acetone to obtain a working solution (25 μg/mL), and 2 μL of the Nile red working solution is added to each well of sample and standard, followed by a 5 min incubation in the dark. Fluorescence of each sample was detected using a microplate reader (Infinite M200 PRO, Tecan) at excitation and emission wavelengths of 524 nm and 586 nm. Fluorescence imaging of Nile Red-stained

cells was performed with an automated fluorescence microscope (Olympus BX63). Acquisition and processing of data was done using the cellSens software.

2.2.5 Total Lipid Analysis by Gas Chromatography-Mass Spectrometry

To analyze the accumulation of total lipids, cells were harvested, snap-frozen in liquid nitrogen and stored at -80^{o}C until analysis. Frozen culture samples were lyophilized by freeze-drying and lipids were extracted by hexane using direct transesterification (Lee et al., 2014) as it was reported to be a convenient and accurate method for analyzing total fatty acids (Cavonius et al., 2014). Biomass quantities of between 5 and 10 mg of biomass were weighed into glass 55-mL PYREX culture tubes with polytetrafluoroethylene (PTFE)-lined phenolic caps (25 mm diameter × 150 mm height, PYREX #9826-25, Corning). To each sample, 0.2 mL of chloroform-methanol (2:1, *v*/*v*) was added and mixed by vortexing, followed by simultaneous transesterification of lipids with 0.3 mL of 1.25M methanolic HCl and vortexed to mix. An internal standard (100 µg Methyl tridecanoate, C13-Fatty Acid Methyl Ester, C13-FAME; Cat. no. 91558, Sigma-Aldrich) was included to correct for the loss of FAME during the reaction, and to correct for subsequent incomplete extraction of hexane (Laurens et al., 2012). The culture tube was then incubated in a 50^{o}C waterbath overnight. After 24 hours, 1 mL of hexane was added and mixed by vortex, and incubated at room temperature for 1 hour. The upper organic phase containing FAMEs was removed using a glass pipette, filtered through a 0.22-µm PTFE syringe filter (Agilent

Technologies), and collected in a 250-µL glass vial insert (Part no. 5181-1270, Agilent Technologies). FAME extracts were injected into a GC system (Model 7890B, Agilent Technologies) equipped with an Agilent Agilent HP-5ms Ultra Inert column (30m x 250µm x 0.25µm) (Cat. no. 19091S-433UI, Agilent Technologies) interfaced with a mass spectrometric detector (Model 5977A, Agilent Technologies). Injection volume was set at 1 µL with a 5:1 split ratio at a GC inlet temperature of 250^{o}C. Helium was used as the carrier gas in a fixed flow of 1 mL/min throughout. Temperature program is as follows: initial oven temperature of 70^{o}C held for 3 mins, ramp to 130^{o}C at 20^{o}C/min, 178^{o}C at 4^{o}C/min, 190^{o}C at 1^{o}C/min, and 290^{o}C at 10^{o}C/min. The total run time was 40 minutes. Shifting of retention times (RTs) were eliminated by comparing the RTs of each FA compound to the C13-FAME internal standard. Analysis was performed using the MassHunter WorkStation Qualitative Analysis B.07.00 software (Agilent Technologies) and compounds were identified with the NIST mass spectral library (National Institute of Standards and Technology, Data Version: NIST 14).

2.2.6 Preparation of cDNA Libraries for Transcriptome-sequencing

Total RNA of N-replete and N-deplete cells on day 3 and day 5 were used for RNA-seq as they correspond to late-exponential and stationary phases of cells grown under N-deplete conditions, compared to N-replete cells which are in exponential phase. RNA integrity was assessed on an Agilent 2100 Bioanalyzer

(Agilent Technologies) using the RNA 6000 Nano Kit (Cat. no. 5067-1511; Agilent Technologies). Construction of cDNA was performed with approximately 2 μg of RNA using a TruSeq Stranded Total RNA LT Sample Prep Kit (Illumina) following the manufacturer's procedures (first and second strand cDNA synthesis, 3' end adenylation, adapter ligation, DNA fragment enrichment of ~300 bp in length). Ribo-Zero rRNA Removal Kit for Plant (Illumina) was used to reduce ribosomal RNA amount in each sample. The quality of constructed cDNA libraries and size of DNA fragments were validated on the Bioanalyzer with Agilent DNA 1000 kit (Cat. no. 5067-1505; Agilent Technologies), before being quantified by qPCR with the KAPA Library Quantification Kit for Illumina platforms (Cat. no. KK4824; Kapa Biosystems).

2.2.7 RNA-Seq and Differential Gene Expression Analysis

The cDNA libraries were normalized to 10 nM, pooled in equal volumes, and sequenced for 2 x 300-bp runs (paired-end) using Illumina MiSeq Sequencer (Illumina). A set of four cDNA libraries were sequenced per run in order to generate sufficient reads for each sample. FASTQ datasets generated from Illumina Miseq were uploaded into a Partek® Flow® web server (version 4.0, Partek Inc.). To ensure quality, the raw data were trimmed from both ends with the following criteria: Phred-equivalent quality score of more than 20, minimum read length of 25, quality encoding = autodetect. The filtered reads were aligned with STAR aligner (version 2.3.1j; default parameters) (Dobin et al., 2013) to an

assembled *D. tertiolecta* transcriptome database previously created by our colleagues (Yao et al., 2015). Data aligned to the transcriptome from STAR were used to test for differential expression of genes between N-replete and N-deplete samples. This was performed at transcript level with the Gene-specific analysis (GSA) approach from Partek® Flow® (Poisson model was selected) and normalized to RPKM (Reads Per Kilobase per Million mapped reads) values. Genes were considered to be significantly differentially expressed if their expression values had at least a fold change greater than ± 2, a false discovery rate (FDR)-corrected p value of ≤ 0.05 (Benjamini-Hochberg step-up correction), and the read coverage at either of the culture conditions were ≥ 10. The RNA-seq raw data were deposited in the Sequence Read Archive database (http://www.ncbi.nlm.nih.gov/Traces/sra/) under the accession numbers SRR4011621, SRR4011622, SRR4011623, SRR4011624, SRR4011625, SRR4011626, SRR4011627, and SRR4011628.

2.2.8 Functional Annotation and Biological Interpretation of RNA-seq data

Functional annotation of cDNA reads was performed with the Partek® Genomics Suite® (PGS) software (version 6.6, Partek Inc.). The GSA file containing filtered genes and their associated information was imported into PGS and merged with the assembled *D. tertiolecta* transcriptome annotation file according to the name of *D. tertiolecta* contigs. The annotated data was subsequently used to perform Gene Ontology (GO) enrichment with a modified *C. reinhardtii* GO annotation

file (Yao et al., 2015) downloaded from JGI website (http://jgi.doe.gov/). Representative pathways were discovered by mapping the gene names to the *C. reinhardtii* Kyoto Encyclopedia of Genes and Genomes (KEGG) database (http://www.genome.jp/) using the pathway analysis tool. Both GO enrichment and KEGG pathway analyses were conducted using the Fisher's Exact test; the analysis was restricted to pathways with more than 2 genes, and results were filtered by enrichment p-value of less than 0.05.

2.2.9 Cloning full length cDNAs from *D. tertiolecta* using RACE

Rapid Amplification of cDNA ends (RACE) was performed on total RNA using the SMARTer^{TM} RACE cDNA amplification kit (Clontech). Gene specific RACE primers were designed by looking for conserved nucleotide regions between the gene sequences of *C. reinhardtii* and *D. tertiolecta*. For example, primers used for RACE of DtPDH were designed by comparing with a plastidial form of PDH E1β subunit from *C. reinhardtii* (NCBI RefSeq: XP_001693114.1). *C. reinhardtii* mRNA sequences were obtained from NCBI and subjected to a BLAST on the Sequence Read Archive (SRA) database (http://www.ncbi.nlm.nih.gov/sra) of *D. tertiolecta* under the accession number SRX029446 (Rismani-Yazdi et al., 2011). Overlapping sequences conserved between *C. reinhardtii* and *D. tertiolecta* were then identified and used to design the RACE primers (**Table S2**). When unspecific bands were observed from the initial PCR, nested PCR was done using internal primers to achieve higher target

specificity. Open reading frames (ORFs) were identified using ORF Finder (http://www.ncbi.nlm.nih.gov/gorf/) and the full length coding sequences were confirmed using a high fidelity Taq polymerase (Platinum Taq DNA polymerase, High Fidelity; Invitrogen). The full length sequences of the RACE sequenced genes can be found in the **Appendix section**.

2.2.10 Analysis of the putative genes and their subcellular localization

Nucleotide and amino acid sequence homology to the Chlorophyta phylum were determined by searching on the NCBI GenBank database with nucleotide query (blastn) and translated query against protein (blastx) (www.ncbi.nlm.nih.gov/BLAST/). To obtain inferred amino acid sequences, ORF sequences were submitted to EMBOSS Transeq (http://www.ebi.ac.uk/Tools/st/emboss_transeq/). Multiple sequence alignment of full-length protein sequences was performed using Clustal Omega (https://www.ebi.ac.uk/Tools/msa/clustalo/). The subcellular localization of the proteins and chloroplast transit peptide sequences were predicted by widely used protein subcellular localization programs, including TargetP (http://www.cbs.dtu.dk/services/TargetP/), ChloroP (http://www.cbs.dtu.dk/services/ChloroP/), and PSORT II (http://psort.hgc.jp/form2.html) (**Table S3**).

2.2.11 Real-time PCR for gene expression

Total RNA was isolated with the RNeasy Plant Mini Kit (Cat. no. 74904; Qiagen) according to the manufacturer's instructions, and reverse transcribed to cDNA using random hexamers with SuperScript® II Reverse Transcriptase (Cat. no. 18064014; ThermoFisher Scientific). Real-time PCR was performed on a Bio-Rad CFX96 Real-Time PCR detection system (Biorad) with Maxima SYBR Green/ROX qPCR Master Mix (Cat. no. K0222; ThermoFisher Scientific). Reaction mixtures composed of 10 μL of SYBR Green Master Mix, 0.4 μL of each primer pair, 2 μL of DNA template (or distilled water as the no-template control), and 7.2 μL of autoclaved distilled water. PCR cycling conditions were as follows: 50^{o}C for 2 min, 95^{o}C for 10 min, followed by 40 amplification cycles at 95^{o}C for 15s and 60^{o}C for 1 min. Results are based on triplicate technical experiments performed with three independent biological cultures (n = 3). Relative fold differences were calculated using the Comparative C_T ($\Delta\Delta C_T$) method using DtTubulin as an internal control to normalize gene expression as it is constitutively expressed (Lin et al., 2013). The qPCR primers were designed using an online tool (Genscript Real-time PCR Primer Design) and are listed in **Table S2**. Results are based on triplicate technical experiments performed with three independent biological cultures (n = 3). Relative fold differences were calculated using the Comparative C_T ($\Delta\Delta C_T$) method using DtTubulin as an internal control to normalize gene expression as it is constitutively expressed (Lin et al., 2013). The qPCR primers were designed using an online tool (Genscript

Real-time PCR Primer Design) and are listed in **Table S2**. When using a primer pair for the first time, PCR samples were subjected to agarose gel electrophoresis to ensure amplification of a single product corresponding to the expected size. For each run, the integrity of the PCR products were checked by observing gene-specific single peaks in the melt-curve profile.

2.2.12 Statistical analysis

All data were expressed as means ± standard deviation (SD). For gene expression experiments, the fold change for each gene was expressed as the mean ± SD of each independent biological replicate normalized to housekeeping gene DtTubulin expression values. Statistical analyses were performed using Student's *t* test. A p-value <0.05 was considered statistically significant.

2.3 Results

2.3.1 Physiological response of *D. tertiolecta* under Nitrogen depletion

In the *Dunaliella* genus which dominates list of top strains for carbohydrate production, *D. tertiolecta* is one of the most researched species due to its ease of culture, tolerance to varied environmental conditions, fast growth rate, high accumulation of storage compounds per dry weight (protein, starch, lipids), and overall biomass productivity (Nikookar et al., 2005; Slocombe et al., 2015), making it an attractive microalgal feedstock for commercial mass cultivation(Hosseini Tafreshi and Shariati, 2009). *D. tertiolecta* strain UTEX LB

999 was grown in ATCC-1174 DA medium with an initial nitrate concentration of 5 mM and 0.5 mM for N-replete and N-deplete cultures respectively. From day 1 to 15, cell density for N-replete cultures increased from 0.75 x 10^6 to 14.4 x 10^6 cells/mL, before dropping to 13.88 x 10^6 cells/mL (**Fig. 2.1a**), suggesting that cell division had ceased. On the other hand, N-deplete cultures peaked at day 8, at 4.28 x 10^6 cells/mL. The nitrate concentrations in the culture medium was depleted after 3 days for N-deplete cells, and 9 days for N-replete cells (**Fig. 2.1a**), but cell growth continued for N-replete cells, likely driven by intracellular nitrogen stores, which remain at steady levels despite the lack of extracellular nitrate in the media (Lv et al., 2013). For the purpose of this study, cells were harvested for metabolite analyses at days 3, 5, 8, 12, and 17 to capture the passage through exponential and stationary growth phases.

Although cell division has slowed for N-deplete cells from the fourth day onwards, the increase in dry weight (**Fig. 2.1d**) was largely due to the accumulation of storage compounds such as starch and glycerol, as the cells continue to accumulate organic carbon (**Fig. 2.1b, c**). Over the course of the experiment, N-depletion also led to reduced total chlorophyll content (**Fig. 2.1e**) and photosynthetic yield (F_v/F_m) (**Fig. 2.1f**). Although there was a decrease in chlorophyll content for both N-replete and N-deplete cultures on day 3 – possibly due to the cells acclimatizing to a new culture state – N-replete cultures subsequently recovered chlorophyll levels to the original state (i.e. Day 0) during the exponential growth phase, while those of N-deplete cultures continue to fall

(**Fig. 2.1e**). The health of photosystem II as determined by F_v/F_m, held steady at around 0.68 – 0.74 for N-replete cultures. On the other hand, N-deplete cultures experience a drop in photosynthetic yield from 0.59 to 0.41, indicative of cell stress and possible damage to photosystem II (**Fig. 2.1f**).

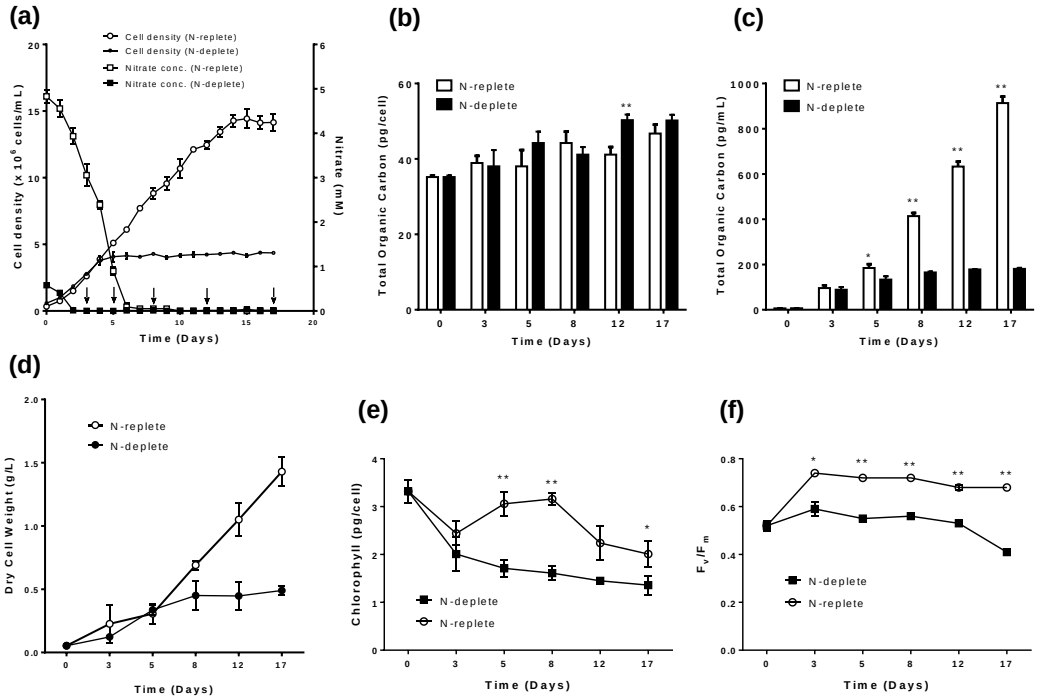

Figure 2.1 Physiological parameters of *D. tertiolecta* under nitrogen depletion. *D. tertiolecta* was cultured in 50-mL batch cultures supplemented with 5% CO_2. Cell growth and media nitrogen concentration (a) was measured every day. Total organic carbon (b, c) and dry cell weight (d), chlorophyll (e) and photosynthetic yield (f) were measured at different time points (Day 0, 3, 5, 8, 12, 17) to illustrate the different phases of growth. Error bars represent standard deviations from three independent biological replicates. Asterisks indicate statistically significant differences between N-replete and N-deplete samples after two-tailed t-tests (* p value ≤ 0.05; ** p value ≤ 0.01).

2.3.2 Accumulation pattern of storage compounds upon N-depletion

Lipid, starch and glycerol synthesis pathways share common carbon precursors fed from the glycolytic pathway, but the regulation of carbon allocation into these routes is not well understood (Johnson and Alric, 2013; Subramanian et al., 2013). Under the favorable condition where nitrogen is available, N-replete *D. tertiolecta* maintained basal levels of starch (7-8 pg/cell)

during the first 5 days of cultivation; consequently, when nitrogen is depleted, it increasing to 19 pg/cell on day 8 (**Fig. 2.2a**). In contrast, N-deplete cultures had starch rapidly accumulated on the third day (27 pg/cell), and the starch content of the latter remained higher during the entire process. Interestingly, starch was accumulated much earlier and in greater absolute amounts compared to lipids (neutral lipids and total lipids) (**Fig. 2.2b, c**). Notably, despite a large increase in neutral lipids (**Fig. 2.2b, 2.3c**), N-depletion did not result in a corresponding increase in total lipids (**Fig. 2.2c**). On the contrary, it led to a cessation in its production (5.8% in N-deplete vs. 9.5% in N-replete on Day 17). Intracellular glycerol was relatively constant for both cultures throughout the experiment (**Fig. 2.2d**), with only extracellular glycerol showing marked increase, especially by N-deplete cells (**Fig. 2.2e**). This is consistent with findings in current literature implicating the continued release of glycerol by *D. tertiolecta* into the culture medium ((Chow et al., 2013; Chow et al., 2015)). The amount of extracellular glycerol produced was able to reach higher quantities as it is not restricted by cell volume, enabling it to deliver microgram levels per cell not achievable with intracellular glycerol, starch or lipids.

When presented on a percentage dry cell weight (DCW) basis, similar trends were observed with subtle differences. Starch content of N-deplete cells peaked sharply on day 3 (28% DCW) compared to N-replete cells where it moderately increased until the media is deprived of nitrogen on day 8 (25% DCW) (**Fig. 2.2f**). Intracellular glycerol accounted for 9-14% of DCW in N-

replete cells and N-deplete cells. However, in the latter stages (Day 8-17), intracellular glycerol representation in N-deplete cells dropped to 2-3% DCW as the DCW increased while intracellular glycerol content remained the same. Total lipid production was greatly attenuated in N-deplete cultures, accounting for 5.8% DCW on day 17, which is 39% less than the N-replete culture (**Fig. 2.2f**). There were minimal changes to the fatty acid (FA) composition between either cultures; C18:3 is the most abundant FA in *D. tertiolecta*, making up to 66% of its profile (**Fig. 2.3a, b**). The proportion of C16:0, however, appears to increase over time particularly for cells experiencing N-depletion, while those of C18:2 and C18:3 levels declined.

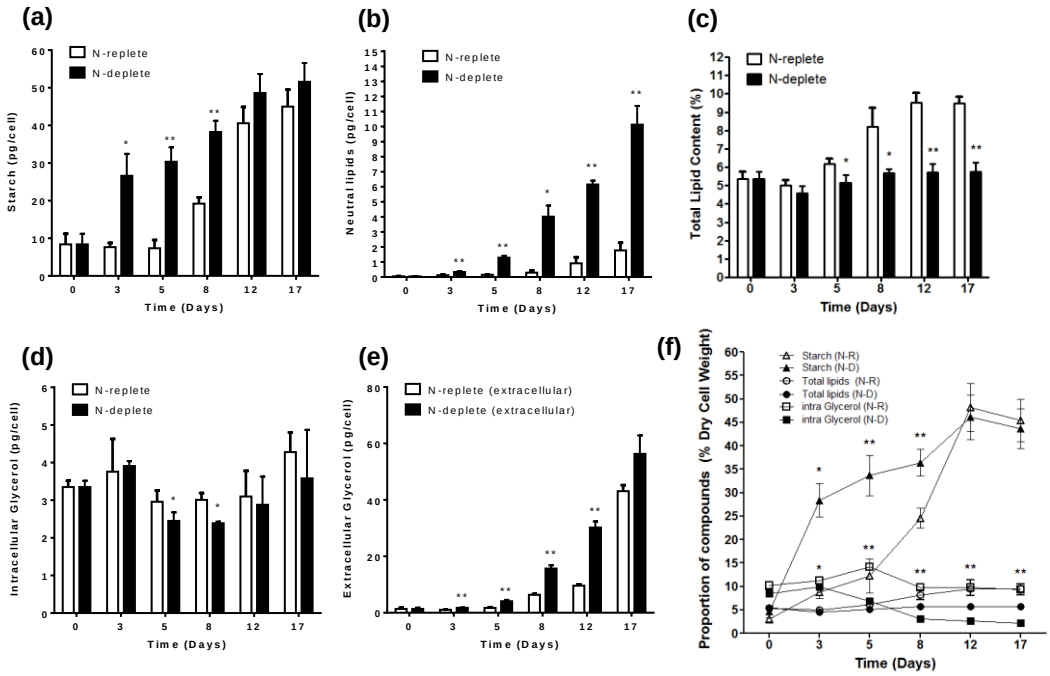

Figure 2.2 Effects of nitrogen depletion on storage product accumulation in *D. tertiolecta*. The starch (a), neutral lipids (b), total lipids (c), intracellular glycerol (d) and extracellular glycerol (e) content in *D. tertiolecta* cells under nitrogen-replete and nitrogen-deplete conditions in different phases of cell growth. Proportion of starch, total lipids and intracellular glycerol are presented as a percentage of dry cell weight (f). Error bars represent standard deviations from three independent biological replicates. Asterisks indicate statistically significant differences between N-replete and N-deplete samples after two-tailed t-tests (* p value ≤ 0.05; ** p value ≤ 0.01).

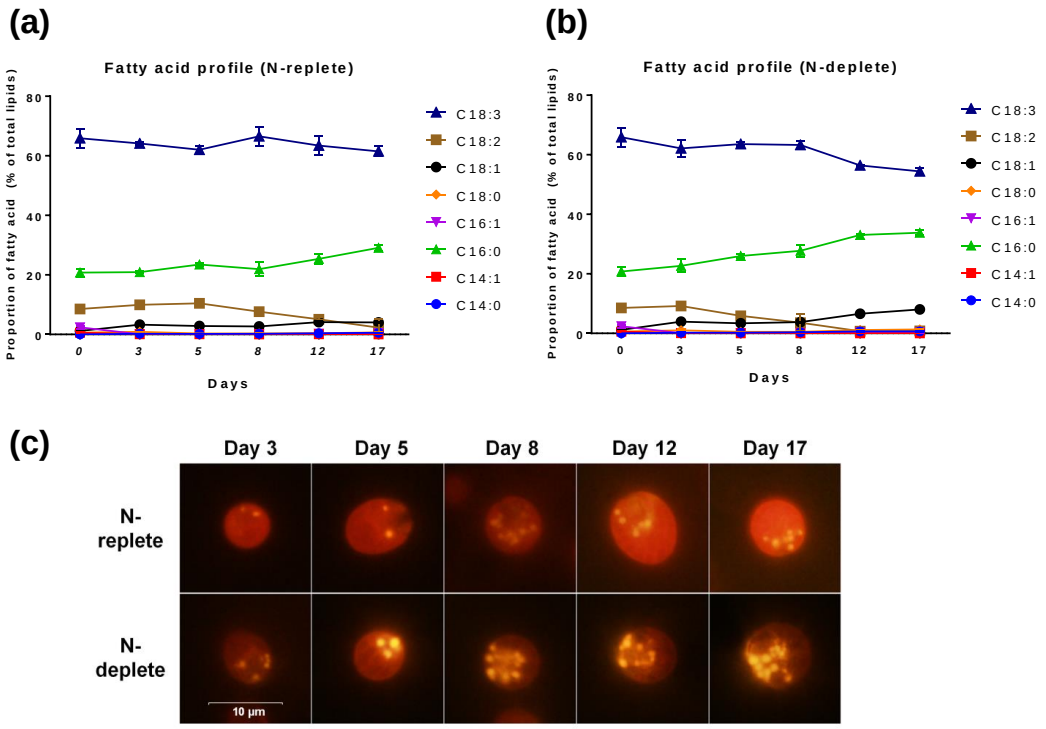

Figure 2.3 Fatty acid profiles and detection of neutral lipids by Nile red staining of *D. tertiolecta* lipids. Proportion of the major types of fatty acids (A, B) are expressed as percentage (%) of total lipids. After staining with the nonpolar lipid fluorophore Nile red, cells were examined by fluorescence microscopy which showed the formation of lipid droplets corresponding with the state of nitrogen depletion (C). Yellow fluorescence reflects the staining of neutral lipids, which form lipid droplets. Red fluorescence corresponds to background chlorophyll auto-fluorescence.

2.3.3 Analysis of gene expression by transcriptomics

The growth of *D. tertiolecta* in either cultures presented two distinctive phases: Exponential and Stationary (**Fig. 1A**). To assess the transcriptional regulation of selective carbon partitioning, we carried out transcriptome analyses at 2 times points representing N-deplete exponential phase (N-replete vs. N-deplete; both in Day 3 exponential phase) and stationary phase (N-replete exponential vs. N-deplete Day 5 stationary phase). Gene expression was expressed as fold change relative to N-replete samples. Out of all the annotated genes for Day 3 (D3) and Day 5 (D5) samples, we filtered for significantly expressed genes using a False discovery rate (FDR)-corrected p-value ≤ 0.05. This translated to 3,962 and 1,234 significantly expressed genes for D3 and D5, accounting respectively for ~17% and 6% of all genes annotated (**Table S4**). Among this filtered set of genes, 96% (D3) and 89% (D5) of genes were over/under-expressed ($\leq$ -2x or $\geq$ 2x fold-change) in N-deplete samples relative to N-replete samples.

2.3.4 Functional annotation and enrichment of differentially expressed genes

Gene Ontology (GO) enrichment of the differentially expressed genes showed that in D3, upregulated genes form the majority of categories while in D5 most genes were downregulated (**Fig. S2, S3**). Nitrogen compound metabolic process was upregulated in both D3 and D5, an indication that the cells were increasing capacity for utilizing nitrogen in response to the nutrient's depletion.

The top 10 most highly expressed or repressed genes were related to nitrogen-scavenging or photosynthesis (**Table S5**). For instance, THB1, a truncated hemoglobin highly expressed in the presence of nitric oxide (Sanz-Luque et al., 2015), was repressed by almost 300-fold. Likewise, three subunits of the urea active transporter were upregulated between 52- and 72-fold, representing one of the many enzymes whose expression are known to increase to harvest nitrogen from nitrogen-containing compounds such as ammonium, nitrate, nitrite, urea, purines, pyrimidines and amino acids(Park et al., 2015). In D3, the upregulated genes frequently represented those involved in central carbon metabolism (CCM) (Noor et al., 2010), which includes the pathways of TCA cycle (75% enriched), glycolysis (28.6% enriched), and the oxidative pentose phosphate pathway (OPPP) (enrichment of glucose-6-phosphate dehydrogenase activity) (**Fig. S2**). Moreover, mitochondrial electron transport and enzymatic activity on NADH or NADPH (85-88%) were significantly upregulated, as well as pyruvate kinase activity (62.5%) and malate dehydrogenase activity (75%), while those of photosynthesis (17%) were slightly downregulated (**Fig. S2**). As the cells progress to stationary phase on D5, the most obvious difference was the enrichment for multiple downregulated categories in photosynthesis: Chlorophyll biosynthetic process (75%), photosynthesis (56.5%), photosystem I (50%), photosynthesis, light harvesting (41.7%) (**Fig. S3**). Nevertheless, TCA cycle (37.5%) and glycolysis (14.3%) continue to be upregulated, albeit to a lesser degree. Surprisingly, FA biosynthesis (46.1%) and acetyl-CoA carboxylase activity

(66.7%) were downregulated in N-replete samples, suggesting a repression of *de novo* FA synthesis. Likewise, KEGG pathway analysis reflect enrichments in carbon metabolism, TCA cycle, and pyruvate metabolism for both D3 and D5, while only D5 had significant enrichments in glycolysis and photosynthesis (**Fig. S4**).

2.3.5 Coordinated expression of central carbon metabolism genes for storage compound synthesis

Photosynthetic components and antenna proteins were severely affected in N-deplete cells, as evidenced by the global downregulation of genes encoding for light-harvesting complexes, photosystem, and RuBisCO activase, an enzyme catalyzing the activation of RuBisCO (**Fig. 2.4, S8, S9**). Nonetheless, carbon continued to be assimilated as seen from the upregulation of three isoforms of gamma carbonic anhydrase (CAG1, CAG2, CAG3) in D3 (**Supplementary dataset**), which would provide a source of bicarbonate from CO_2 assimilation. Pyruvate phosphate dikinase (PPD2) was upregulated by 23-fold on D3 and 4-fold on D5. PPD2 is used in the C4 carbon-concentrating mechanism pathway, where it converts pyruvate to PEP, which then reacts with bicarbonate to produce oxaloacetate (**Fig. 2.4**).

The CCM pathways were notably active during N-depletion. Glycolysis breaks down glucose to form pyruvate and acetyl-CoA. Phosphofructokinase (PFK2), pyruvate kinase (PYK1,2) and the E2 subunit of pyruvate dehydrogenase

complex (DLA1; dihydrolipoamide acetyltransferase) were upregulated, forming pyruvate and acetyl-CoA which feeds into the TCA cycle. Similarly, genes in the TCA cycle were simultaneously upregulated; transcripts of citrate synthase (CIS1), aconitase (ACH1), isocitrate dehydrogenase (IDH2), oxoglutarate dehydrogenase (OGD1), succinate dehydrogenase (SDH2), fumarate hydratase (FUM1) and malate dehydrogenase (MDH3) were greatly enhanced on both D3 and D5 N-deplete samples (**Fig. 2.4, S5, S6**). Interestingly, a triose phosphate/phosphoenolpyruvate translocator (TPT1) was dramatically upregulated 29- and 24-fold on D3 and D5. TPT1 could export dihydroxyacetone phosphate (DHAP) out of the chloroplast for use in glycerol synthesis as the expression of glycerol-3-phosphate dehydrogenase (GPDH) was also increased. Particularly, genes participating in starch metabolism were upregulated, including ADP-glucose pyrophosphorylase (STA1), starch synthase (SSS1) and UDP-glucose pyrophosphorylase (UGP1) and starch branching enzyme (SBE2), which together coordinate the synthesis of starch from glucose-1-phosphate (**Fig. 2.4, S7**).

ATP:citrate lyase (ACLB1) and NADP-malic enzyme (MME2) were overexpressed, which would supply the cell with acetyl-CoA and NADPH respectively. In addition, glucose-6-phosphate dehydrogenase (G6PDH), a provider of reducing power from the OPPP, was also upregulated. Surprisingly, genes involved in the FA synthesis pathway were largely unchanged except for some downregulation; expression levels of malonyl-CoA-acyl carrier protein

transacylase (MCAT) and acetyl-CoA carboxylase (ACCase) subunits were depressed.

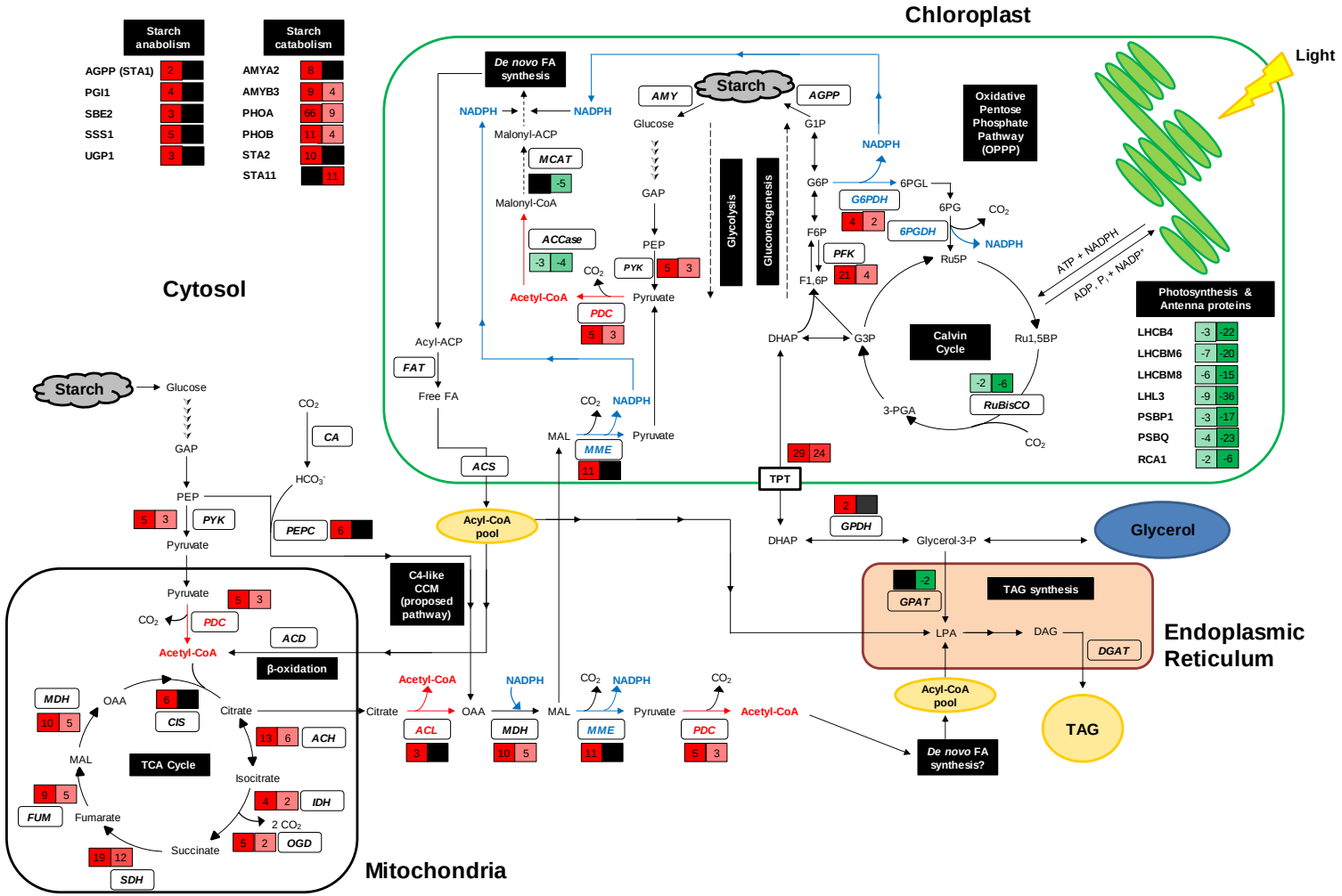

Figure 2.4 Proposed scheme of transcriptome changes to the central carbon metabolism in *D. tertiolecta* upon nitrogen depletion. Arrows represent potential carbon fluxes. Enzymes are in bold italics. Blue arrows represent reducing power (NADPH) and red arrows represent acetyl-CoA. Black boxes denote pathway names. A recently proposed C4-like carbon-concentrating mechanism (CCM) in microalgae (Radakovits et al., 2012) is shown to depict

an alternative route for carbon assimilation. Neutral lipid droplets found in microalgae consist mostly of triacylglycerols (TAGs), formed by combining FAs and glycerol. *Legend:* ACCase, acetyl-CoA carboxylase; ACD, acyl-CoA dehydrogenase; ACL, ATP-citrate lyase; ACS, acyl-CoA synthetase; AGPP, ADP-glucose pyrophosphorylase; AMY, amylase; CA, carbonic anhydrase; DGAT, diacylglycerol acyltransferase; DHAP, dihydroxyacetone phosphate; F1,6P, fructose 1,6-bisphosphate; F6P, fructose 6-phosphate; FAT, fatty acyl-acyl carrier protein (ACP) thioesterase; G1P, glucose 1-phosphate; G6P, glucose 6-phosphate; G6PDH: G6P dehydrogenase, GAP, glyceraldehyde 3-phosphate; GPAT, glycerol-3-phosphate acyltransferase; GPDH, glycerol-3-phosphate dehydrogenase; MAL, malate; MDH, malate dehydrogenase; MME: NADP-malic enzyme; OAA, oxaloacetate; PDC, pyruvate dehydrogenase complex; PEP, phosphoenolpyruvate; PEPC, PEP carboxylase; PK, pyruvate kinase; Ru5P, ribulose 5-phosphate; Ru1,5BP, ribulose 1,5-bisphosphate; RuBisCO, Ru1,5BP carboxylase/oxygenase; TPT, triose phosphate translocator; 3-PGA, 3-phosphoglycerate; 6PGDH, 6-phosphogluconate dehydrogenase. Please refer to *Supplementary Information* for abbreviations of genes involved in starch synthesis and photosynthesis and antenna proteins.

2.3.6 Comparing the N-depletion response in *D. tertiolecta* and other oleaginous and non-oleaginous microorganisms

To evaluate the differences in storage product accumulation between oleaginous and non-oleaginous microalgae during N-depletion, we compared the published physiological and transcriptomic data of three widely studied oleaginous species: *Nannochloropsis oceanica* (Li et al., 2014; Goncalves et al., 2016a), *Chlamydomonas reinhardtii* (Siaut et al., 2011; Cakmak et al., 2012; Davey et al., 2014), and *Chlorella vulgaris* (Ikaran et al., 2015) **(Fig. 2.5, Table 2.1**). *D. tertiolecta* accumulates very low amounts of TAGs in N-replete and N-deplete conditions (0.2% and 1% DCW respectively), but stores a large amount of starch, thus making it a high starch and low TAG accumulator (**Fig. 2.5, Table S6**). Interestingly, although *N. oceanica* – a marine microalga alike *D. tertiolecta* – stores the same amount of TAGs under N-replete conditions, it rapidly accumulates TAGs under N-deplete conditions (up to 40% DCW); it however lacks starch as a storage compound (Vieler et al., 2012a; Dong et al., 2013). *C. reinhardtii* and *C. vulgaris*, both heterotrophically grown microalgae, accumulates high amounts of starch and TAGs during N-depletion.

Analysis of the expression of key genes in the FA, TAG and starch synthesis pathways showed that upon N-depletion, the oleaginous microalga *N. oceanica* and moderate TAG accumulator *C. vulgaris* experienced downregulation in the FA synthesis pathway, a pattern similar to that in the low TAG-accumulating *D. tertiolecta* from this study **(Table 2.1, S7**). In contrast, *C.*

reinhardtii had moderate overexpression of its FA synthesis genes. TAG synthesis genes had variable changes in each microalga: In *D. tertiolecta* GPAT was downregulated while LPAAT was upregulated, *N. oceanica* and *C. reinhardtii* genes were mostly unchanged, while *C. vulgaris* genes were upregulated. Noticeably, *D. tertiolecta* has most of its starch synthesis genes upregulated, suggesting a coordinated push towards starch accumulation during N-depletion.

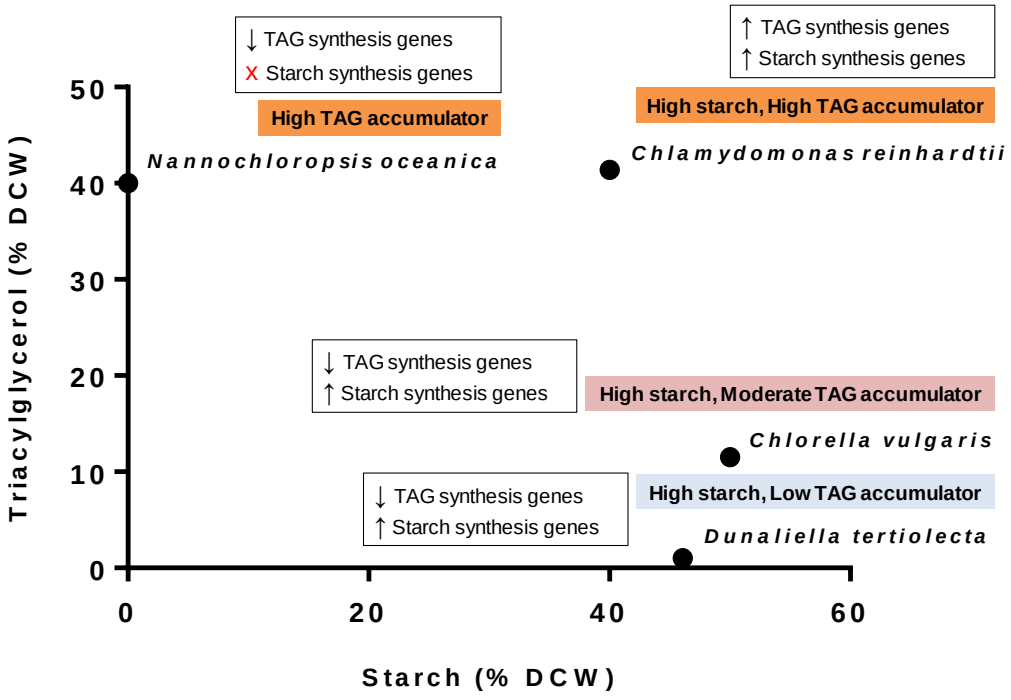

Figure 2.5 Differences in starch and TAG contents in oleaginous and non-oleaginous microalgae upon nitrogen depletion. Refer to Supplementary Information Table S4 and S5 for more information on the composition of storage compounds and gene expression in N-replete and N-deplete conditions.

Table 2.1 Comparison of representative genes involved in fatty acid, triacylglycerol and starch synthesis in oleaginous and non-oleaginous microalgae. Red bars: Gene expression up-regulated, Green bars: Gene expression down-regulated, Grey bars: Gene expression unchanged, Yellow bars: Gene not identified in transcriptome analysis. For more information regarding fold change, please refer to Supplementary Information Table S5.

		Microalgae species			
Pathway	**Genes**	***Dunaliella tertiolecta***	***Nannochloropsis oceanica***(Dong et al., 2013)	***Chlamydomonas reinhardtii*** (Sato et al., 2014; Valledor et al., 2014; Gargouri et al., 2015; Park et al., 2015)	***Chlorella vulgaris***(Fan et al., 2015)
FA synthesis	***ACCase****				
	MCAT				
	KAS I				
TAG synthesis	***GPAT***				
	LPAAT				
	DGAT				
	PDAT				
Starch synthesis	***STA1***		Gene not present		
	UGP1				
	SSS1		Gene not present		
	SBE2		Gene not present		

*ACCase denotes the *Acetyl-CoA biotin carboxyl carrier subunit* as it was the most reported gene among the literature.

2.3.7 Expression patterns for Acetyl-CoA and NADPH-generating genes

Acetyl-CoA and NADPH are essential substrates for FA synthesis. In order to affirm the upregulation of genes which contribute to the production for acetyl-CoA and NADPH, we used Rapid Amplification of cDNA ends (RACE) to derive the coding sequence of genes and conducted a real-time PCR analysis for validation. Malic enzyme (ME) and G6PDH) were chosen to be sequenced as the NADPH-generating genes, while pyruvate dehydrogenase (PDH) and ATP:citrate lyase (ACL) were chosen as the acetyl-CoA generating genes. There are 6 known isoforms of malic enzyme in the model green alga *C. reinhardtii* (Dubini et al., 2009; Terashima et al., 2011). We chose to sequence for the malic enzyme (ME) isoform MME2 (predicted to be cytosolic) and MME6 (predicted to be plastidial) which showed BLASTp homologies with known MEs in *Arabidopsis thaliana* (Wheeler et al., 2005; Wheeler et al., 2008) and *Mucor circinelloides* (Zhang et al., 2007; Li et al., 2013) known to be associated with increased lipid synthesis. The plastidial pyruvate dehydrogenase E1 beta (E1β) subunit – which catalyzes the first step of conversion from pyruvate to acetyl-CoA – was chosen to be sequenced as its mRNA levels was previously found to correlate strongly with lipid formation in developing seeds of *Arabidopsis* (Ke et al., 2000) and showed increased expression under N-depleted conditions in the diatom *Phaeodactylum tricornutum* (Yang et al., 2014). Negative regulation of ACL subunit A (ACLA) reduced long-chain FA synthesis in epidermal cells of *Arabidopsis* (Go et al., 2014), leading to the notion that increased acetyl-CoA supply might be needed to

support the synthesis of FAs. We chose to investigate the expression of ACLA in contrast to ACLB which was shown to increase in our transcriptome data.

The expression levels of the gene coding for MME2 and G6PDH showed similar patterns throughout the experiment. At the onset of N-depletion, the cells increase their expression of MME2 and G6PDH significantly by 8- and 4-fold (**Fig. 2.6b**), but the difference in expression levels relative to N-replete cells decreased with time. In contrast, the expression of MME6 remained relatively unchanged. The increase in gene expression of MME2 and G6PDH was correlated with the NADPH levels in N-deplete cells. On day 3, N-deplete cells experienced a 125% increase in NADPH levels, which is maintained till day 5. However, on day 8 onwards as the gene expression decreases, the NADPH levels correspondingly dropped to almost the same levels as the N-replete cells (**Fig. 2.6b**). On the other hand, acetyl-CoA and its associated genes showed a different trend. Although acetyl-CoA levels were 3 times higher in the N-deplete cells during the exponential phase (D3), PDH and ACLA did not have significant changes in expression (**Fig. 2.6a**). Unexpectedly, PDH E1β expression only began to increase from day 8, correlating with the corresponding drop in acetyl-CoA levels. The expression of β-oxidation genes acyl-CoA dehydrogenase (ACD) and acyl-CoA oxidase (ACOX) were measured to determine if β-oxidation could contribute to acetyl-CoA availability from degradation of membrane lipids. ACOX increased sharply by 4-fold at the onset of stationary phase at day 5 and day 8 before decreasing slightly to 3-fold (**Fig. 2.6c**). Thioesterase expression was

similarly most pronounced in the stationary phase, increasing from 3- to 4-fold on day 5 and day 8 respectively.

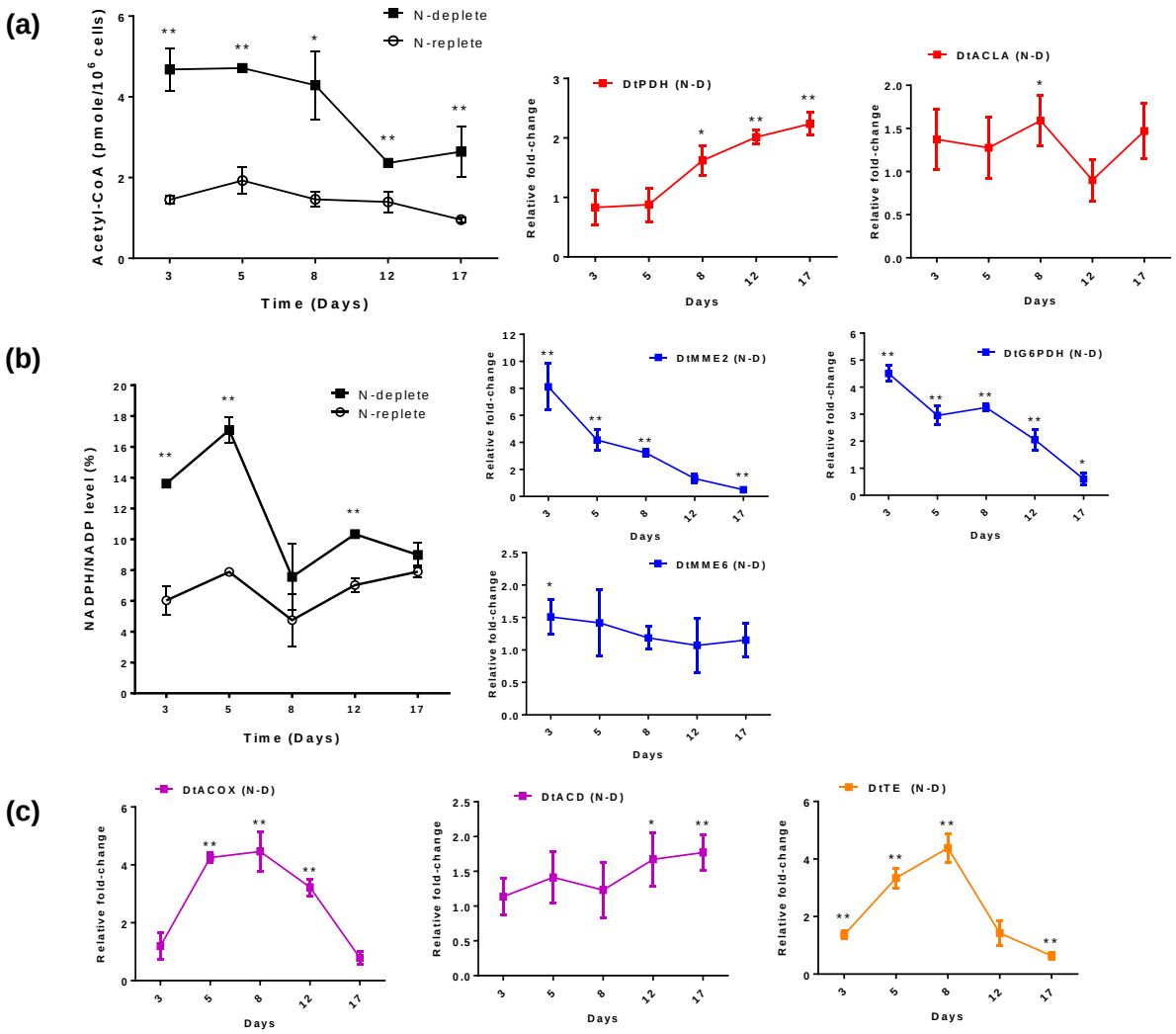

Figure 2.6 Acetyl-CoA and NADPH production, and expression levels of target genes in *D. tertiolecta* during N-depletion. The acetyl-CoA (a) and NADPH (b) levels and the accompanying genes which may contribute to their production. Expression of β-oxidation genes acyl-CoA dehydrogenase (ACD) and acyl-CoA oxidase (ACOX), as well as fatty acyl-ACP thioesterase (TE) were also measured to determine their possible regulation during N-depletion (c). Error bars represent standard deviations from three independent biological replicates. Asterisks indicate statistically significant differences between N-replete and N-deplete samples after two-tailed t-tests (* p value ≤ 0.05; ** p value ≤ 0.01).

2.4 Discussion

In microalgae, TAGs and starch are the two primary energy storage products and both synthesis pathways share common carbon precursors. It has been reported that oleaginous microalgae are able to accumulate large amounts of TAGs (up to 60% of dry weight) under N-depletion (Siaut et al., 2011; Cakmak et al., 2012; Vieler et al., 2012a; Davey et al., 2014; Ikaran et al., 2015). Although these studies show that N-depletion enabled oleaginous cells to channel carbon to TAGs, little attention has been paid to non-oleaginous species which prefer alternative carbon stores such as starch and glycerol, and the transcriptomic basis governing these carbon fluxes. In this study, we tracked the storage product accumulation and global gene expression profile of the halophilic, high-starch accumulating microalga *D. tertiolecta* upon N-depletion, and compared its preference of storage products with other oleaginous microalgae. A coordinated upregulation of genes involved in central carbon metabolism was identified in exponentially growing cells, suggesting that the genetic response to N-depletion occurs prior to the cessation of cell growth (i.e. stationary phase). Surprisingly, the transcriptome profile of *D. tertiolecta* – specifically the upregulation of CCM genes contributing to the supply of acetyl-CoA and NADPH – were vastly similar to oleaginous microalgae including *N. oceanica* (Li et al., 2014) and *C. reinhardtii* (López García de Lomana et al., 2015). The increased in transcript levels of TCA cycle genes and genes contributing to reducing power such as

G6PDH and ME were correspondingly observed in heterotrophic fungi such as *Mortierella alpina* (Chen et al., 2015a) and *M. circinelloides* (Zhang et al., 2007; Li et al., 2013) to be critical determinants of lipid synthesis.

Nitrogen is a key component for the synthesis of chlorophyll and essential proteins of the photosystem (e.g. LHCII apoprotein), thus the restriction of nitrogen supply could hinder both structural and physiological components of photosynthesis (Young and Beardall, 2003). The observed drop in chlorophyll content and decreased PSII quantum yield (**Fig. 1E, F**) coincides with previous reports that demonstrated the degradation of chlorophyll and carotenoids in *D. tertiolecta* upon nitrogen starvation (Geider et al., 1998; Young and Beardall, 2003; Kim et al., 2013). Corresponding downregulation of most light harvesting complex genes (**Fig. S8, S9**) suggest that N-depletion triggered a response of the cell to reorganize its photosynthetic apparatus. Multiple studies of nutrient limitation in microalgae point to the degradation of thylakoid membranes in favour of the *de novo* synthesis of TAGs where intracellular membrane remodeling substantially contribute to neutral lipid accumulation(Simionato et al., 2013; Urzica et al., 2013; Yang et al., 2013; Martin et al., 2014). Our present study shows that *D. tertiolecta* is able to accumulate up to six times more neutral lipids under N-deplete conditions (**Fig. 2B**), but concurrently experienced a substantial decrease in total lipid content relative to N-replete samples (9.5% of DCW in N-replete vs. 5.8% of DCW in N-deplete) (**Fig. 2C**). This is similar to other researchers who observe similar declines in total fatty acid content in *D.*

tertiolecta under N-depletion (7.5% of DCW in N-sufficient vs 5.9% of DCW in N-deficient) (Shin et al., 2015). The parallel increase in neutral lipids could be explained by a dramatic shift in intracellular processes, from the catabolic degradation of thylakoid membranes (which contribute to total lipids) to the anabolic reactions of storage compound accumulation (neutral lipids and starch content). This notion is supported by a recent report which showed that when cultured under N-depleted conditions, *D. tertiolecta* had significant decreases in the lipid classes of diacylglyceryltrimethylhomoserine (DGTS) and digalactosyldiacylglycerol (DGDG), a main component of chloroplast membranes (Kim et al., 2013). This suggests the occurrence of a major remodeling of lipid membranes during nitrogen starvation in *D. tertiolecta*, a response akin to other microalgae (Simionato et al., 2013; Urzica et al., 2013; Yang et al., 2013; Martin et al., 2014).

Glycolytic genes that shunt carbon precursors to *de novo* FA synthesis, including phosphofructokinase, pyruvate kinase and pyruvate dehydrogenase complex (PDC), are upregulated in *N. oceanica* and *C. reinhardtii* under N-depleted conditions correlating with TAG accumulation up to 40% DCW, despite a downregulation of the genes directly involved in TAG and FA synthesis (Li et al., 2014; Shtaida et al., 2015). This transcriptome response is unexpectedly similar to *D. tertiolecta* in this study (**Fig. 2.4**), which accumulates more starch (46% DCW) than lipids (**Fig. 2.2f, 2.5**). Even more striking is the similarity in the overexpression of genes involved in the TCA cycle in the mitochondria (**Fig. 2.4**),

which is also greatly enhanced in *N. oceanica* and was attributed to the utilization of carbon skeletons derived from membrane lipids to produce energy for TAG or its precursors (Li et al., 2014). As *Nannochloropsis* cells lack starch synthesis genes consistent with the absence of pyrenoid starch (Vieler et al., 2012b; Dong et al., 2013; Scholz et al., 2014), it may be logical the excess carbon and energy derived from the breakdown of membrane lipids are channeled to TAGs. However, in *D. tertiolecta* the response was to channel more carbon to starch instead of TAGs, as can be seen from the synchronized upregulation of genes in gluconeogenesis and starch synthesis genes (**Table S5**). Thus, the increased activity of CCM pathways and genes contributing to the generation of acetyl-CoA and NADPH may merely be a general response of microalgae cells to N-depletion rather than a determinant of oleaginicity. Indeed, it has been previously proposed that the CCM could play varied roles upon N-depletion; the pathways could be involved in providing carbon skeletons, for nitrogen reassimilation, or for channeling excess carbon into FA synthesis (Hockin et al., 2012). Noting that most TCA cycle enzymes are bidirectional, Sweetlove *et al* (Sweetlove et al., 2010) proposed that the TCA cycle could catalyze reverse reactions and be highly adaptable to changing conditions of the cell. Hence, the TCA cycle may act as a central hub, balancing between demands for specific carbon skeletons for anabolic processes, and the energetic needs of the cell in absence of photosynthetic activity as they produce reducing equivalents for ATP synthesis.

The preference to store carbon as starch may stem from the fact that it is energetically more favourable to make than TAGs, and is the preferential reserve which is rapidly mobilized during switch from N-deplete to N-replete conditions (Siaut et al., 2011). On a per carbon basis, a 55-carbon TAG molecule requires 6.25 ATP and 2.93 NADPH, while 55 carbon units of starch requires 4.16 ATP and 2 NADPH (Subramanian et al., 2013); TAG synthesis require 50% more ATP and 45% more NADPH per carbon to make. While TAGs return more ATP than sugars during metabolism, the energy recovered is less than the energy invested in its synthesis (Johnson and Alric, 2013; Subramanian et al., 2013), chiefly due to the carbon lost during the conversion of pyruvate to acetyl-CoA by PDC. Much of this begs the question: Why do some microalgae prefer to store more TAGs and others prefer to store predominantly starch, while some are able to store moderately equal amounts of both? One possible explanation is that as lipids require more ATP and reducing power than starch for production, photoheterotrophically grown cells such as *C. reinhardtii* and *C. vulgaris* (**Table S4**) can generate more substrates needed for FA synthesis due to their ability to assimilate organic carbon sources on top of inorganic carbon fixation from photosynthesis. For instance, acetate can be directly converted into acetyl-CoA from acetyl-CoA synthetase (ACS), and incorporate immediately into the TCA cycle or used in FA synthesis by *C. reinhardtii* (Johnson and Alric, 2013). Likewise, *Chlorella* grown in acetate medium use ACS to directly incorporate acetate into acetyl-CoA, by-passing the PDC route for acetyl-CoA production and

enabling a high rate of lipid synthesis under N-depletion (Avidan and Pick, 2015). Furthermore, glucose-fed *Chlorella* cultures generate more reducing power in the dark than photoautotrophically cultured *Chlorella* in the light, thus the former accumulates more lipids and less starch (Chen et al., 2015b). This explanation does not extend to *Nannochloropsis* however, due to its inability to synthesize starch (Vieler et al., 2012b; Dong et al., 2013; Scholz et al., 2014). Rather, it stores small amounts of carbohydrates (5-17%) while channeling majority of carbon to TAGs during N-depletion.

Microalgae of the genus *Dunaliella* dominate the ranks of top carbohydrate producers, and *D. tertiolecta* – with the ability to accumulate up to 63% DCW in carbohydrates – leads the list (Slocombe et al., 2015). In this study, we show that *D. tertiolecta* rapidly accumulates starch in response to N-depletion, suggesting that *D. tertiolecta* cells tend to favor starch over TAGs as an efficient strategy for chemical energy accumulation (**Fig. 2.2a, 2.2f)**. As an obligate photoautotroph that cannot use dissolved organic compounds (Segovia et al., 2003; Hosseini Tafreshi and Shariati, 2009), efficient energy storage and utilization is of paramount importance, especially since photosynthesis is inefficient with less than 8% conversion of solar energy chemical energy (Subramanian et al., 2013). Notably, starch reserves provide the energy required in the dark for DNA replication and general cell metabolism (Bišová and Zachleder, 2014). This is in line with the increase in gene expression of starch-degrading enzymes in *D. tertiolecta* during N-depletion (**Fig. 2.4, Fig. S7**), when

photosynthesis is compromised. *D. tertiolecta* also specifically degrade starch in high salinity stress conditions to yield DHAP which can be used to produce glycerol (Liska et al., 2004), making starch a more suitable storage compound as the cells can respond to both nutrient deficiency and salinity stress, conditions which could fluctuate greatly in their natural environments (Oren, 2014). In light of these observations, it is reasonable to assume that carbon would be channeled to TAG production once starch synthesis is blocked. However, this notion was refuted as there was no increase in oil among three starchless *C. reinhardtii* mutants examined (Siaut et al., 2011), suggesting that blocking starch synthesis does not result in oil accumulation. Preference of starch and TAG accumulation in microalgae may instead stem from natural evolutionary patterns and exposure to different carbon sources.

D. tertiolecta was previously reported to accumulate and release glycerol into the external medium, and that the process was not affected by nutrient starvation or cell death (Chow et al., 2015). In this study, we show that under N-depletion increased amounts of glycerol were present in the extracellular medium (**Fig. 2.2e**), indicating that glycerol synthesis and export is a response to nutrient stress. This is supported by the marked upregulation of a triose phosphate translocator, which exports photosynthetically fixed carbon or carbon derived from starch breakdown from the chloroplast to the cytosol, where the enzyme GPDH converts into glycerol (**Fig. 2.4**). *D. tertiolecta* is known to uptake exogenous glycerol in response to stress (Lin et al., 2013), and as releasing

glycerol to the external medium provides the cells with an expansive carbon sink not restricted by cell size, the extracellular glycerol may serve as a readily utilizable carbon source for the cells in anticipation of improving nutrient environments (Chow et al., 2015).

Supply of substrates for FA synthesis – namely acetyl-CoA and NADPH – are proposed to be rate-limiting for lipid production in microalgae (Avidan et al., 2015; Shtaida et al., 2015). The production of acetyl-CoA have been attributed mainly to PDH and ACL in oleaginous fungi and microalgae (Hynes and Murray, 2010; Sharma and Chauhan, 2016), while NADPH is associated with G6PDH and ME (Chen et al., 2015a; Xue et al., 2015; Xue et al., 2016).

We found that in *D. tertiolecta*, the expression of the plastidial PDH E1β subunit was increased during neutral lipid accumulation in N-depletion, coinciding with the increase in acetyl-CoA levels (**Fig. 2.6a**). Expression of PDH was also observed in real-time PCR as well as the Next Generation Sequencing (NGS) experiments. On the other hand, even though the ACL transcripts were detected to be upregulated from NGS, the expression of ACL did not change in real-time PCR (**Fig. 2.6a**). Furthermore, as the *de novo* synthesis of FAs occur in the chloroplast (Goncalves et al., 2016b), the cell might be more dependent on acetyl-CoA supply at the site of FA synthesis (by plastidial PDH) than acetyl-CoA production in the cytosol (by cytosolic ACL). The importance of PDH for FA synthesis is corroborated by a study on the antisense knockdown of PDH kinase (PDK), which deactivates the PDC, in *P. tricornutum* by Ma *et al.* (Ma et

al., 2014). The researchers found that by reducing transcript abundance and enzymatic activity of PDK, the neutral lipid content in the cells increased by 82%, suggesting that acetyl-CoA synthesis by PDH may contribute to higher lipid production. The increase in acetyl-CoA during N-depletion may not be entirely attributed to PDH, however, as the acetyl-CoA levels were already elevated before PDH was upregulated (**Fig. 2.6a**). Acetyl-CoA can also be produced from lipid degradation and turnover from β-oxidation, and the expression of ACOX was upregulated from real-time PCR analyses (**Fig. 2.6c**), indicating that the breakdown of lipids during N-depletion might be a source of acetyl-CoA. The increase accumulation of neutral lipids (i.e. TAGs) with no corresponding increase in total lipids (**Fig. 2.2b, c**) suggest a rechanneling of existing total lipids to storage TAGs. The increased expression of ACOX might contribute to the degradation of membrane lipids, thus providing for acetyl-CoA for use in CCM pathways.

Transcript levels of TE were increased during N-depletion in *D. tertiolecta*, from both the NGS and real-time PCR results. This finding is similar to previous reports in *Haematococcus pluvialis* (Lei et al., 2012) and *Neochloris oleoabundans* (Rismani-Yazdi et al., 2012) which showed increased TE expression under nitrogen limitation conditions. The upregulation of TE is associated with increased FA synthesis in cyanobacteria, *E. coli* and *P. tricornutum* as it reduces the negative feedback inhibition of acyl-ACPs that partially controls the rate of FA production (Gong et al., 2011; Liu et al., 2011b).

Although TE is also suggested to be positively correlated with monounsaturated and polyunsaturated FAs in *H. pluvialis* (Lei et al., 2012), we do not see similar trends here in *D. tertiolecta*.

The expression of NADPH-producing genes showed a slightly different trend to the genes involved in acetyl-CoA production. Despite NGS results suggesting that ME was upregulated, it does not provide information on the exact isoform and cellular localization of the enzyme due to the short sequence (~300 bp) obtained from the analysis. Thus, we used RACE to obtain the full-length sequences of two isoforms (MME2 and MME6) which shared the closest homology to the plant AtME2 that is responsible for majority of the forward malate decarboxylation into pyruvate (described in Section 2.1.3). MME2, a predicted cytosolic isoform (**Table S3**), has significantly increased upregulation during early N-depletion. On the other hand, the expression of the mitochondrial isoform MME6 did not change (**Fig. 2.6b**). ME catalyzes the irreversible decarboxylation of malate to pyruvate, yielding NADPH from $NADP^+$, thus providing essential reducing power for FA synthesis. ME was previously found to be upregulated in *P. tricornutum* following nitrogen depletion (Yang et al., 2013), and subsequent overexpression of PtME in mutant strains increased neutral lipids by 2.5-fold (Xue et al., 2015). Recently, PtME was overexpressed in the green microalga *Chlorella pyrenoidosa*, enabling the cells to increase neutral lipids by 3.2-fold and 4.6-fold under N-replete and N-deplete conditions respectively (Xue et al., 2016). It is worth noting that the PtME used in those studies were identified

to target to mitochondria (Xue et al., 2015), while MME2 in our study is predicted to be cytosolic. In heterotrophic fungal cells, MME2 is part of a shuttle that utilizes malate from the mitochondria for FA synthesis in the cytosol (Zhang et al., 2007). How the production of NADPH by ME in the mitochondria or cytosol could influence lipid synthesis and accumulation in the chloroplast of green alga still not understood.

G6PDH, the rate-limiting enzyme in the OPPP, also showed the same trend as MME2 in *D. tertiolecta*, with the most significant upregulation occurring particularly in the early days of N-depletion (**Fig. 2.6b)**. G6PDH was established as a critical NADPH producer responding to lipogenesis in oleaginous fungi; the response was not present in non-oleaginous fungi (Chen et al., 2015a). Likewise, a comparison between 2 strains of *M. circinelloides* found that a high lipid-producing strain that could accumulate up to 36% lipids exhibited 46% greater G6PDH activity than a low lipid-producing strain that can only accumulate less than 15% lipids (Tang et al., 2015). Further G6PDH knockdown experiments in *M. alpina* showed 40% lower NADPH/NADP levels in the mutants, resulting in decreased total FA production. At the same time, knockdown of ME did not decrease FA production, suggesting that the OPPP might play a more significant role during lipogenesis (Chen et al., 2015a). The similarity in MME2 and G6PDH expression patterns in *D. tertiolecta* suggest that both might have an equal role in provision of NADPH in the cell. However, further experiments, preferably

involving knockdown or overexpression transformants, have to be done to determine their significance in FA synthesis.

2.5 Conclusion

The present study identifies the unique transcriptome signatures of *D. tertiolecta*, a high starch-accumulating microalga in response to N-depletion. In particular, its coordinated upregulation of genes involved in starch synthesis could be attributed to its preference to store starch over TAGs. However, *D. tertiolecta* also shares similar upregulation of CCM genes as the oleaginous microalga *N. oceanica*, where CCM pathways were suggested to provide substrates for FA and TAG synthesis during N-depletion. The perplexing similarities and differences in transcriptomic and metabolic responses of oleaginous and non-oleaginous microalgae thus demand a relook into the role of biochemical pathways governing the allocation of carbon and energy in the cell. Addressing these issues would advance our understanding of starch and lipid synthesis in microalgae as well as facilitate the genetic engineering of microorganisms designed to accumulate either storage product of interest.

It appears that the genes which show most correlation with neutral lipid accumulation during nitrogen depleted conditions in *D. tertiolecta* are malic enzyme isoform 2 (MME2), glucose 6-phosphate dehydrogenase (G6PDH), plastidial pyruvate dehydrogenase E1 beta (E1β) subunit (PDH), and fatty acyl-ACP thioesterase (TE). MME2 and G6PDH are enzymes which contribute to

NADPH production, PDH converts pyruvate to acetyl-CoA, and TE relieves the inhibitory feedback which acyl-ACPs have on FA synthesis by hydrolyzing the thioester bond on acyl-ACPs, producing free FAs. Overexpression experiments of these 4 genes (MME2, G6PDH, PDH, TE) and their accompanying metabolic analyses (e.g. NADPH and acetyl-CoA levels, neutral lipids and FA content) would be required to confirm their role in improving lipid productivity in microalgae. Thus, the findings from this study have paved the way for selective genetic engineering of this and other related microalgae for the overproduction of lipids.

Chapter 3 Overexpression of genes promoting lipid production in the model alga *Chlamydomonas reinhardtii*

3.1 Introduction

3.1.1 Scientific significance

Biofuel production from microalgae is rapidly becoming an area of intensive research as scientists look for sustainable solutions to generate renewable biofuels in the midst of declining fossil fuel reserves and emerging concerns over global warming (Stephens et al., 2010b; Wigmosta et al., 2011). After identifying the genes which correlates with neutral lipid accumulation in *D. tertiolecta* (from Chapter 2), we aim to overexpress these genes into a microalga to study its effects on improving lipid accumulation without sacrificing biomass.

As *D. tertiolecta* has proven to be traditionally difficult to transform (Walker et al., 2005; Zhang et al., 2015), we adopt the model microalga *Chlamydomonas reinhardtii* for the present study. We chose to investigate *C. reinhardtii* as it is one of the microalgal species which can be easily transformed with current transformation techniques (Berthold et al., 2002), and heterologous promoters have been developed for robust expression of transgenes in the nuclear and plastid genomes (Specht et al., 2010; Díaz-Santos et al., 2013). In addition, it presents the favourable properties of fast growth, a fully sequenced genome, and close relations to other green algae that allow for interspecies comparisons

(Morowvat et al., 2010; Ibáñez-Salazar et al., 2014; Scranton et al., 2015). The plausibility of cross-species gene expression have been previously demonstrated in microalgae; overexpression of *C. reinhardtii* sedoheptulose-1,7-bisphosphatase into *Dunaliella bardawil* enhanced photosynthesis and glycerol production in the latter (Fang et al., 2012), while the overexpression of malic enzyme from the diatom *Phaeodactylum tricornutum* into the green microalga *Chlorella pyrenoidosa* resulted in oil accumulation (Xue et al., 2016). Therefore, the aim of this study is to genetically engineer 4 genes from *D. tertiolecta* into *C. reinhardtii* to determine its effects on growth, neutral lipid, and total fatty acid (FA) content. The 4 genes selected are Malic enzyme isoform 2 (DtMME2), Glucose-6-phosphate dehydrogenase (DtG6PDH), Pyruvate dehydrogenase (plastidial) E1β subunit (DtPDH), Fatty acyl-ACP thioesterase (DtTE).

3.1.2 Background on genes selected for overexpression

Supply of NADPH and Acetyl-CoA: MME2, G6PDH, PDH. Malic enzyme (ME) catalyzes the irreversible decarboxylation of malate to pyruvate, producing NADPH which is needed for FA synthesis. Overexpression of ME is suggested to be one of the most promising targets for improving lipid synthesis in microorganisms (Liang and Jiang, 2013). Specifically, overexpression of ME was recently shown to improve neutral lipid accumulation in the microalgae *P. tricornutum* and *Chlorella pyrenoidosa* (Xue et al., 2015; Xue et al., 2016). Likewise, G6PDH, which produces NADPH through the oxidative pentose

phosphate pathway (OPPP), was observed to be upregulated in cells participating in lipid accumulation (Wu et al., 2015) and its knockdown reduces NADPH levels and lipid content by 40% (Chen et al., 2015a). From our results in Chapter 2, we found the expression levels of MME2 and G6PDH to be elevated in the early days of N-depletion (Day 3 and Day 5), correlating with the initial phase of neutral lipid accumulation, suggesting that availability of reducing power could be the key rate-limiting step to improving FA synthesis. However, ME and G6PDH expression was reduced at the later phases, similar to other studies which show ME activity which disappeared by the end of lipid-accumulation phase (Zhang et al., 2007), inferring the possibility of a second bottleneck, suggested to be the generation of acetyl-CoA (Liang and Jiang, 2013).

PDH is the major chloroplastic acetyl-CoA producer in microalgae, with its transcript levels correlating with acetyl-CoA formation and triacylglycerol (TAG) accumulation (Avidan et al., 2015). However, transcript levels of PDH E1α were not rapidly induced in parallel with acetyl-CoA accumulation in the moderate-TAG accumulators *D. tertiolecta* and *C. reinhardtii* (Avidan et al., 2015), underlying the importance of PDH gene expression and acetyl-CoA levels in contributing to TAG accumulation in these microalgae. In our study from Chapter 2, we found that acetyl-CoA levels were increased in the early days of N-depletion in *D. tertiolecta* (Day 3 and 5), but PDH transcript levels did not increased correspondingly until Day 8 to Day 17. The increased acetyl-CoA may be contributed by degradation through β-oxidation of membrane lipids (e.g.

thylakoid membranes) arising from N-depletion. Hence, we seek to constitutively overexpress PDH in *C. reinhardtii* so that acetyl-CoA can be produced in excess during normal growth conditions, allowing for increased carbon substrate available for FA synthesis.

Relief of inhibition of FA synthesis: TE. A strategy to improve the productivity of lipid synthesis in microalgae is through modification of their fatty acid (FA) synthesis pathways. Rate-limiting enzymes of FA synthesis were potential targets for gene manipulation with the aim of improving overall lipid synthesis (Radakovits et al., 2010). Overexpression of the enzyme acetyl-CoA carboxylase (ACCase), believed to catalyze the important rate-limiting step in FA synthesis, have been performed in diatoms (Dunahay et al., 1995) and plants (Kindle, 1990; Roesler et al., 1997) but no increase in lipid content were observed. Increasing the expression of another enzyme in FA synthesis, 3-ketoacyl-acyl carrier protein synthase (KAS) III, was also not successful in improving lipid content in three species of plants (Dehesh et al., 2001). *De novo* FA synthesis and elongation occurs within an algal plastid by the action of ACCase and KAS, and ends with the production of 16 to 18C fatty acyl groups esterified to acyl carrier protein (ACP), a central protein that carries the growing FA chain for elongation (Chen and Smith, 2012). To finally off-load the cargo from the ACP, the cells utilize an acyl-ACP thioesterase (TE) to hydrolyze the mature FA chain from the ACP (Beld et al., 2014).

The buildup of fatty acyl-ACPs can regulate the rate of FA synthesis by feedback inhibition of ACCase (Davis and Cronan, 2001), KAS, and enoyl-ACP reductase activities (Heath and Rock, 1996a; Heath and Rock, 1996b). TEs can relieve this inhibition by hydrolyzing the acyl-ACP into free FAs, which are subsequently converted into acyl-CoA and released from the chloroplast to be incorporated into TAGs (Chen and Smith, 2012). Recently, the expression of endogenous TEs such as oleoyl-ACP hydrolase and acyl-ACP thioesterase A were found to be up-regulated in microalgae subjected to nitrogen limiting conditions (Miller et al., 2010; Rismani-Yazdi et al., 2012). In addition, expression of TE showed a linear relationship with FA synthesis in *Haematococcus pluvialis*, indicating that TE could be involved in a key rate-limiting step for FA synthesis (Lei et al., 2012). Based on this principle, increasing the activity of TEs appears to be a good strategy to promote the continuous production of FAs and channeling them to storage lipids rather than membrane lipids. Indeed, the overexpression of TEs has been shown to increase total FAs in *E. coli* (Lu et al., 2008), cyanobacteria (*Synechocystis* sp. PCC6803) (Liu et al., 2011b), and diatoms (*Phaeodactylum tricornutum*) by up to 72% (Gong et al., 2011). While plants develop specific TEs for FAs of different chain lengths and saturation, FatA and FatB (Salas and Ohlrogge, 2002), microalgae use one broad-specificity TE, termed FAT1 (Blatti et al., 2012), which could allow for cross-species expression of microalgal TEs to influence FA production and profile. Plant TEs have been heterologously engineered into a variety of species to effectively alter their oil

content (Liu et al., 2011b; Zhang et al., 2011b), but introducing plant TEs into *C. reinhardtii* did not alter the FA profile, suggesting that plant TEs may not functionally interact with CrACP to affect FA synthesis. Hence, we propose using *D. tertiolecta* TE to be overexpressed in *C. reinhardtii* to investigate its effects towards enhancing FA production without compromising growth.

3.1.3 Aims and objectives

Aims: To increase lipid productivity by investigating the role of enzymes providing substrates (MME2, G6PDH, PDH) for fatty acid synthesis in *C. reinhardtii*. In addition, TE would also be investigated for its effects in increasing FA content.

Hypothesis: Overexpression of genes encoding for enzymes that increase intracellular acetyl-CoA or NADPH, or overexpression of a gene which relieves inhibition of FA synthesis, will increase FA content without compromising growth.

3.2 Materials and Methods

3.2.1 Microalgae Strain and Culture Conditions

The *Chlamydomonas reinhardtii* strain used was CC-424 (cw15, arg2, sr-u-2-60, mt^-) obtained from the Chalmydomonas Resource Center. The cells were grown in 50-mL batch cultures with Tris-Acetate-Phosphate (TAP) medium on a

rotary shaker at 25^{o}C under continuous light (approximately 30 µmol photons m^{2}/s). Cell densities were determined using an automated cell counter (TC20^{TM} automated cell counter, Biorad Laboratories). Transformants were maintained in TAP medium containing 10 µg/mL hygromycin B.

3.2.2 Plasmid construction and transformation of *C. reinhardtii*

To construct plasmids overexpressing our genes-of-interest, the full-length coding region of the genes were amplified using forward and reverse primers listed in **Table S8**. The PCR products were digested with the respective restriction enzymes and ligated into a cassette containing the heterologous Cauliflower Mosaic Virus 35S (CaMV 35S) promoter for efficient transcriptional expression (Ruecker et al., 2008; Díaz-Santos et al., 2013). The CaMV 35S promoter and terminator flanked-gene fragments were then PCR amplified using a high fidelity Taq polymerase (Cat. no. 11304011, Thermo Scientific), and inserted into the PciI site of the hygromycin-resistance plasmid, pHyg3 (**Fig. S11**).

C. reinhardtii was transformed using the glass beads method (Kindle, 1990) with minor modifications. Cultures grown to an OD_{680} of between 0.5 to 0.6 (2–3 x 10^{6} cells/mL) in TAP media were harvested by centrifugation (3000 *g* for 10 min at 4^{o}C) and resuspended in 500 µL of fresh TAP medium to a cell density of approximately 1–2 x 10^{8} cells/mL. A 300 µL aliquot of the cell suspension was added to 1.5 mL sterile screw-cap tubes containing 0.3 g of acid-washed glass beads (425-600 µm diameter; Sigma-Aldrich), 100 µL 20%

polyethylene glycol (PEG-8000; Sigma-Aldrich) and 1 µg of linearized plasmid. After a 20-second vortex of the mixture at maximum speed, the cells were plated onto TAP medium agar plates containing 10 µg/mL hygromycin B as the selection marker. Colonies typically appearing within 7 – 10 days were picked and inoculated into liquid selective medium of TAP medium containing 10 µg/mL hygromycin B.

3.2.3 Screening of *C. reinhardtii* transformants

C. reinhardtii transformants selected on TAP medium supplemented with hygromycin (TAP-hyg) were genotyped using primers specific for the heterologous CaMV 35S promoter and terminator (**see Fig. 3.1 for representative figure**). Genomic DNA was extracted using phenol-chloroform-isoamyl alcohol (25:24:1) and used as template for genotyping PCR to confirm the existence of the transgene. Heterologous CaMV 35S primers (Table S8), which did not produce unspecific bands in wild-type *C. reinhardtii*, were used for amplification of target genes producing varied sizes depending on the length of the genes-of-interest. The PCR reaction, using 1 µg of template in a volume of 25 µL, was hot-started at 95^{o}C and cycled for 35 rounds of denaturation (95^{o}C for 30 sec), annealing (60^{o}C for 30 sec), and extension (72^{o}C for 2 min), followed by a final extension (72^{o}C for 10 min). The PCR products were run on a 2% agarose gel for approximately 1.5 hours at a current of 80 V.

3.2.4 Quantitative real-time PCR (qRT-PCR) analysis

Total RNA was isolated with the RNeasy Plant Mini Kit (Cat. no. 74904; Qiagen) according to the manufacturer's instructions, and reverse transcribed to cDNA using random hexamers with SuperScript® II Reverse Transcriptase (Cat. no. 18064014; ThermoFisher Scientific). Real-time PCR was performed on a Bio-Rad CFX96 Real-Time PCR detection system (Biorad) with Maxima SYBR Green/ROX qPCR Master Mix (Cat. no. K0222; ThermoFisher Scientific). Reaction mixtures composed of 10 μL of SYBR Green Master Mix, 0.4 μL of each primer pair, 2 μL of DNA template (or distilled water as the no-template control), and 7.2 μL of autoclaved distilled water. PCR cycling conditions were as follows: 50^{o}C for 2 min, 95^{o}C for 10 min, followed by 40 amplification cycles at 95^{o}C for 15s and 60^{o}C for 1 min. Results are based on triplicate technical experiments performed with three independent biological cultures (n = 3). Transcript levels were normalized to the endogenous reference gene G-protein β-subunit-like polypeptide (CBLP) as it is known to be constitutively expressed (Terauchi et al., 2009; Castruita et al., 2011; Pape et al., 2012); the transcript abundance of CBLP remained constant and did not change across the samples in this work. The qPCR primers were designed using an online tool (Genscript Real-time PCR Primer Design) and are listed in **Table S2**.

3.2.5 Measurement of enzymatic activities and substrate levels (NADPH, Acetyl-CoA)

ME and G6PDH activities were determined by spectrometric measurement of NADPH absorbance at 340 nm. Cells were resuspended in 250 mM Glycylglycine buffer (pH 7.4), lysed by 3 freeze-thaw cycles, and centrifuged at 10,000g for 10 mins at 4^{o}C. The supernatant was immediately harvested and used for enzyme activity measurement. The assays were conducted at 25^{o}C. One unit of enzyme activity (U) was defined as 1 nmol/L NADPH generated by 10^6 cells per minute under the reaction conditions.

PDH activity was determined with the PDH Activity Assay Kit (MAK183, Sigma-Aldrich), which uses a coupled enzyme reaction resulting in a colorimetric (450 nm) product proportional to enzymatic activity present. One unit of PDH is defined as the amount of enzyme that will generate 1 µmole NADH per minute at pH 7.5 at 37^{o}C. PDH activity (U) is reported as nmole/min/L.

TE activity was determined kinetically (420 nm) by monitoring the hydrolysis of para-nitrophenyl hexanoate for 10 mins at room temperature (Meier et al., 2008; Blatti et al., 2012). Cells were lysed and supernatant harvested similarly to the ME and G6PDH assays. The formation of the substrate (p-nitrophenoxide anion; λ_{max} = 420 nm; ε = 8570 M^{-1} cm^{-1}) was monitored on a microplate reader (Infinite M200 PRO, Tecan). Each 150-µL reaction contained 19.2 mM Tris-HCl (pH 7.0), 0.28 mM of substrate (para-nitrophenyl hexanoate) dissolved in acetonitrile (CH_3CN).

Acetyl-CoA and NADPH levels were determined with the Acetyl-CoA Assay Kit (MAK039; Sigma-Aldrich) and NADP/NADPH Quantification Kit (MAK038; Sigma-Aldrich) respectively, following the manufacturers' protocol. Before the assay, cells were extracted by resuspension in the provided buffers and broken by 3 freeze-thaw cycles in liquid nitrogen. Cell supernatants were then deproteinized by filtering through a 10 kDa cut-off spin filter (Amicon Ultra 0.5 mL centrifugal filter; Z677108; Sigma-Aldrich) before use in the assay.

3.2.6 Neutral Lipid Quantification and TE activity assay

A modified Nile Red staining method (Yao et al., 2015) was used to quantify intracellular TAGs. Briefly, cells were harvested by centrifugation (3000 *g* for 10 min at 4^{o}C), supernatant was removed and the pellet resuspended in fresh 0.5M ATCC-1174 DA media to an OD_{680} of 0.3. Triolein was used as a standard for determining neutral lipid concentrations by Nile Red (**Fig. S1**). Two hundred microliters of triolein standards (40, 20, 10, 5, 2.5, 0 µg/mL) and cell suspensions were loaded as technical triplicates onto a 96-well black, clear bottom plate (CLS3603; Sigma-Aldrich). Prior to staining, Nile red stock is diluted in acetone to obtain a working solution (25 µg/mL), and 2 µL of the Nile red working solution is added to each well of sample and standard, followed by a 5 min incubation in the dark. Fluorescence of each sample was detected using a microplate reader (Infinite M200 PRO, Tecan) at excitation and emission wavelengths of 524 nm and 586 nm.

3.2.7 Total Lipid Analysis by Gas Chromatography-Mass Spectrometry

To analyze the accumulation of total lipids, cells were harvested, snap-frozen in liquid nitrogen and stored at -80^{o}C until analysis. Frozen culture samples were lyophilized by freeze-drying and lipids were extracted by hexane using direct transesterification (Lee et al., 2014) as it was reported to be a convenient and accurate method for analyzing total lipids (Cavonius et al., 2014). Biomass quantities of between 5 and 10 mg of biomass were weighed into glass 55-mL PYREX culture tubes with polytetrafluoroethylene (PTFE)-lined phenolic caps (25 mm diameter × 150 mm height, PYREX #9826-25, Corning). To each sample, 0.2 mL of chloroform-methanol (2:1, *v*/*v*) was added and mixed by vortexing, followed by simultaneous transesterification of lipids with 0.3 mL of 1.25M methanolic HCl and vortexed to mix. An internal standard (100 µg Methyl tridecanoate, C13-Fatty Acid Methyl Ester, C13-FAME; Cat. no. 91558, Sigma-Aldrich) was included to correct for the loss of FAME during the reaction, and to correct for subsequent incomplete extraction of hexane (Laurens et al., 2012). The culture tube was then incubated in a 85^{o}C waterbath for 1 hour, and 1 mL of hexane was added, mixed by vortex, and incubated at room temperature for 1 hour. The upper organic phase containing FAMEs was removed using a glass pipette, filtered through a 0.22-µm PTFE syringe filter (Agilent Technologies), and collected in a 250-µL glass vial insert (Part no. 5181-1270, Agilent Technologies). FAME extracts were injected into a GC system (Model 7890B,

Agilent Technologies) equipped with an Agilent CP-Sil 88 column (100m x 250μm x 0.2μm) (Agilent Technologies) interfaced with a mass spectrometric detector (Model 5977A, Agilent Technologies). Injection volume was set at 1 μL with a 5:1 split ratio at a GC inlet temperature of 240^{o}C. Helium was used as the carrier gas in a fixed flow of 1 mL/min throughout. Temperature program is as follows: initial oven temperature of 80^{o}C, ramp to 220^{o}C at 4^{o}C/min and held for 5 mins, followed by ramping up to 240^{o}C at 4^{o}C/min and held for 10 mins. The total run time was 55 minutes**.** Shifting of retention times (RTs) were eliminated by comparing the RTs of each FA compound to the C13-FAME internal standard. Analysis was performed using the MassHunter WorkStation Qualitative Analysis B.07.00 software (Agilent Technologies) and compounds were identified with the NIST mass spectral library (National Institute of Standards and Technology, Data Version: NIST 14).

3.2.8 Statistical analysis

All data were expressed as means ± standard deviation (SD). For gene expression experiments, the fold change for each gene was expressed as the mean ± SD of each independent biological replicate normalized to housekeeping gene expression values. Statistical analyses were performed using Student's *t* test. A *p*-value <0.05 was considered statistically significant.

3.3 Results

3.3.1 Selection and characterization of *C. reinhardtii* mutants

C. reinhardtii cells that appear on TAP-hyg agar plates after 7 – 10 days were grown and screen for insertion by genotyping PCR (**see Fig. 3.1 for representative figure**). Two DtMME2 mutants, four DtG6PDH mutants, 7 DtPDH mutants, and 7 DtTE mutants (selected from TAP-hyg agar plates and confirmed from genotyping PCR) were cultured on TAP-only liquid media along with the wild-type till stationary phase and harvested for GC-MS quantification of total fatty acids. The best performing mutants (DtMME2 2, DtG6PDH 4, DtPDH 2, DtTE 7) found to demonstrate higher FA content relative to the wild-type were selected for further analyses (**Fig. 3.2**). The 4 selected *C. reinhardtii* mutants were again confirmed by PCR of genomic DNA using heterologous CaMV 35S primers, which do not produce unspecific bands in the wild-type *C. reinhardtii* genomic DNA samples. Bands of expected sizes were present in the transgenic lines (**Fig. 3.1**), but absent in the wild-type. The mutant cultures were grown with periodic subculturing for at least 3 months, and repeated genotyping PCR still showed the presence of the foreign gene in the samples, verifying its genetic stability.

Transcript levels of the respective genes were determined by qPCR (**Fig. 3.3**), which demonstrated the absence of the foreign mRNA in the wild-type strain. Although the various mutants displayed contrasting levels of transcription, they nevertheless showed transcription of the exogenous *D. tertiolecta* genes not

apparent in the wild-type sample. Except for the DtPDH mutant which did not exhibit higher PDH activity than the wild-type **(Fig. 3.4c)**, the mutants displayed higher enzymatic activities than the wild-type **(Fig. 3.4a – 3.4d).** Specifically, there was a 62% increase in ME activity in the DtMME2 mutant **(Fig. 3.4a)**, a 41% increase in G6PDH activity in the DtG6PDH mutant **(Fig. 3.4b)**, and a 92% increase in TE activity in the DtTE mutant **(Fig. 3.4d)**. Taken together, these observations showed that the introduction of the 35S-promoter plasmids into *C. reinhardtii* led to the respectively increased transcript abundance and, apart from the DtPDH mutant, increased enzymatic activity.

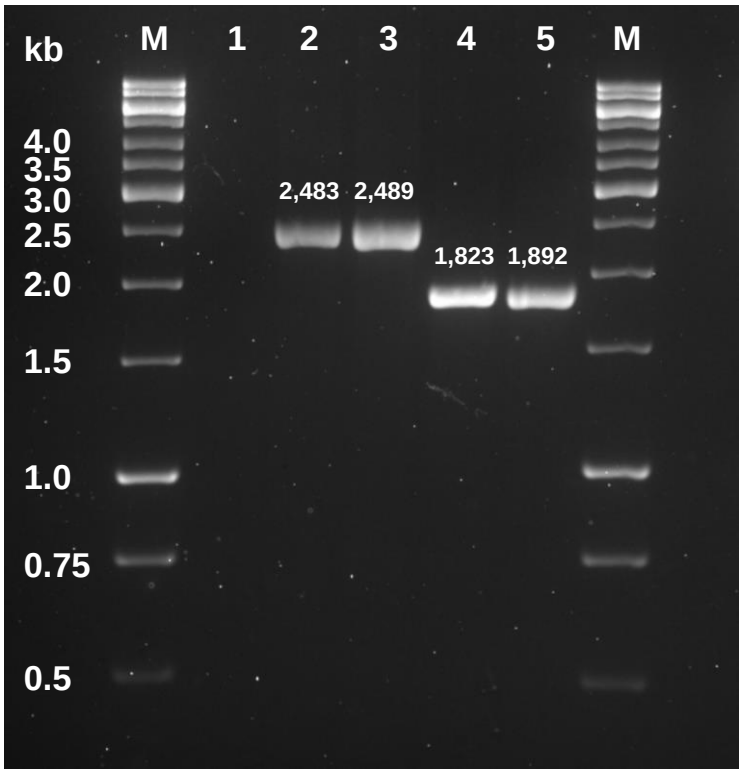

Figure 3.1 PCR identification of respective gene insertions in *C. reinhardtii*. Genomic DNA extracted from the *C. reinhardtii* mutants and wild-type were subjected to PCR using primers specific for the heterologous CaMV 35S promoter and terminator. Approximately 2.5-kb bands were observed in the DtMME2 (lane 2) and DtG6PDH (lane 3) mutants, 1.9-kb bands were present in the DtPDH (lane 4) and DtTE (lane 5) mutants, while no bands were produced from the wild-type (lane 1), indicating an insertion of 35S cassette in the genome. Expected band sizes are shown above each gene (2,483 bp for 35S-DtMME2, 2,489 bp for 35S-DtG6PDH, 1,823 bp for 35S-DtPDH, 1,892 bp for 35S-DtTE). Note: Predicted band sizes include the plasmid backbone sequences. Please refer to Figure S11 for plasmid maps corresponding to the respective genes, and Appendix for the exact nucleotide length for each individual gene.

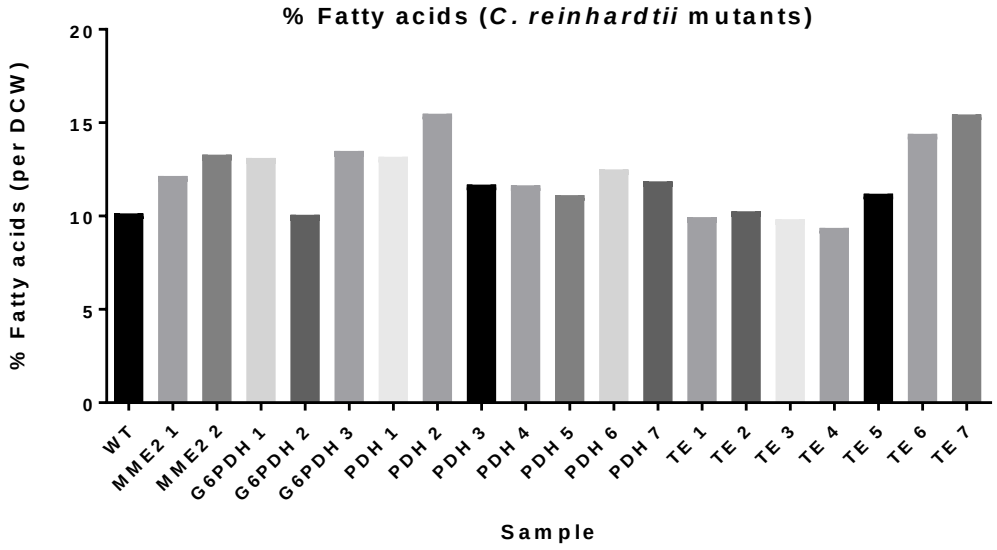

Figure 3.2 Rough screen of *C. reinhardtii* mutants based on phenotype. Two DtMME2 mutants, four DtG6PDH mutants, 7 DtPDH mutants, and 7 DtTE mutants (selected from TAP-hyg agar plates and confirmed from genotyping PCR) were cultured on TAP-only liquid media along with the wild-type till stationary phase and harvested for GC-MS quantification of total fatty acids. The best performing mutants (DtMME2 2, DtG6PDH 4, DtPDH 2, DtTE 7) were then selected for further analyses.

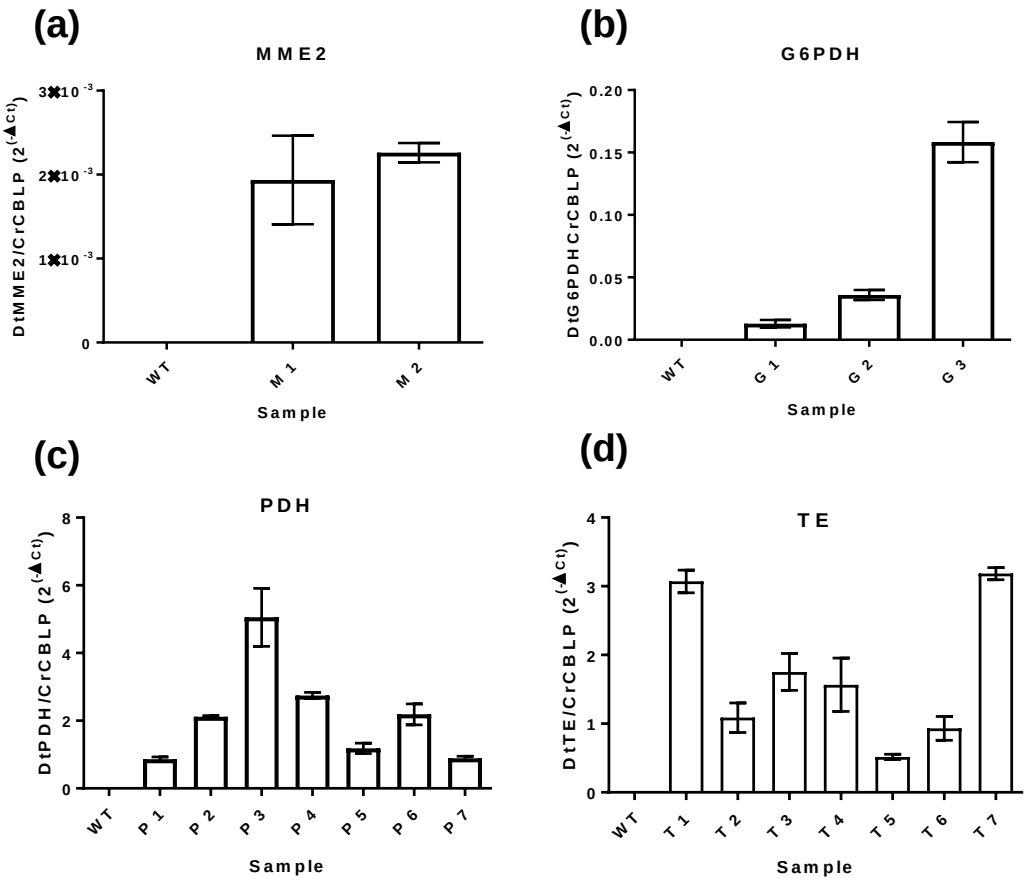

Figure 3.3 Gene expression for *C. reinhardtii* mutants measured by real-time PCR. Transcript levels were normalized to the endogenous reference gene G-protein β-subunit-like polypeptide (CBLP) as it is known to be constitutively expressed. Real-time PCR primers were designed on genetic regions to only recognize and replicate the genes from *D. tertiolecta* and not *C. reinhardtii*.

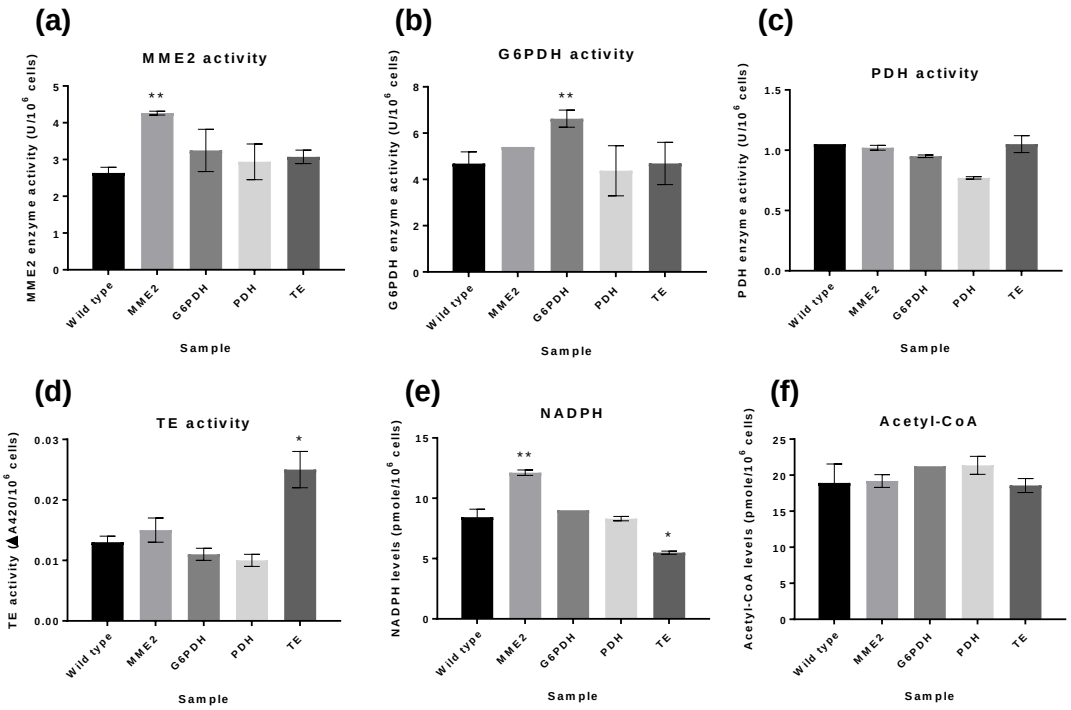

Figure 3.4 Enzyme activity assays and substrate levels in the 4 *C. reinhardtii* mutants. MME2 activity (a) and G6PDH activity (b) were determined by spectrometric measurement of NADPH absorbance at 340 nm, PDH activity (c) was measured using a commercial PDH activity assay kit, and TE activity (d) determined kinetically (420 nm) by monitoring the hydrolysis of para-nitrophenyl hexanoate. NADPH (e) and acetyl-CoA (f) levels were measured using their corresponding assay kits available commercially. Asterisks indicate statistically significant differences between mutant and wild-type samples after two-tailed t-tests (* p value ≤ 0.05; ** p value ≤ 0.01).

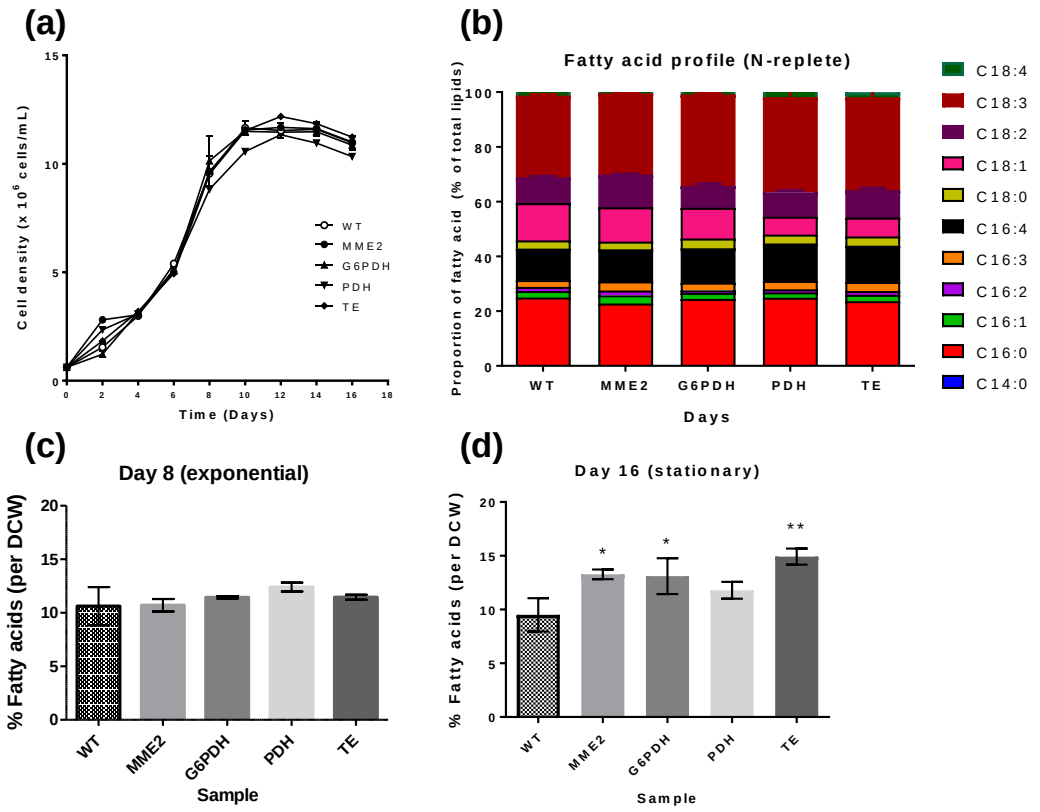

Figure 3.5 Growth curve, total fatty acid (FA) content, and FA profile of the 4 *C. reinhardtii* mutants. Cells were grown in TAP medium under constant illumination, reaching maximum cell density on Day 12 (a). FA profile of between the mutants and wild-type did not change significantly (b), except for a slight increase in C18:3 (and reduced C18:1) from the DtPDH and DtTE mutants. During the exponential growing phase, the mutants did not have significant increase in FA content relative to the wild-type (c), but in the stationary phase, their FA content increased (d) while those of wild-type remained the same. Asterisks indicate statistically significant differences between mutant and wild-type samples after two-tailed t-tests (* p value ≤ 0.05; ** p value ≤ 0.01).

3.3.2 Growth and lipid overproduction of *C. reinhardtii* mutants

To determine the biomass accumulation of the DtTE mutants, growth curves without hygromycin were measured. The cultures started from the same cell densities and sampled at equal intervals (**Fig. 3.5a**). Compared to the wild-

type, there was marginal growth compromise in the mutants; all cultures reached stationary phase at the same time (beginning from Day 8), with similar cell densities. Total lipids quantified in the stationary phase showed that the mutants DtMME2, DtG6PDH and DtTE had a higher lipids on a dry cell weight (DCW) basis than the exponential phase **(Fig. 3.5c, d)**. During the exponential phase (Day 8), all *C. reinhardtii* samples had between 10% lipids in DCW **(Fig. 3.5c)**. In the stationary phase, the lipid content of the wild-type and DtPDH mutant did not change, while those of DtMME2 and DtG6PDH increased slightly to 13% DCW, and DtTE had 15% lipids DCW, a 56% increase from the wild-type **(Fig. 3.5d)**.

As foreign thioesterases may differ in their chain-length specificity, FA profiles were further analyzed to check for any changes in lipid composition. Only minor differences in FA compositions were observed among the DtMME2 and DtG6PDH mutants relative to the wild-type (**Fig. 3.4b**). However, DtPDH and DtTE mutant strains exhibited a 50% reduction in C18:1, while demonstrating slightly higher levels of polyunsaturated C16:3, C16:4, C18:3, and C18:4.

3.4 Discussion

Lipid productivity, which is defined as the product of biomass productivity and lipid content, is touted as a key characteristic for the economic feasibility of industrial-scale biofuel production from microalgae (Griffiths and Harrison, 2009; Hempel et al., 2012; Moody et al., 2014). Producing lipids while also maintaining growth rates and increasing biomass is vital for algal biofuel

production on large economic scales. High biomass productivity increases yield per harvest volume while high lipid content decreases the cost of extraction per unit product (Griffiths and Harrison, 2009). Rapid growth rate also provides a competitive advantage over contaminating algal species in outdoor cultures, and requires less culture space due to a higher cell density per area. Thus, cost-effective lipid production ideally requires a microalga strain that is able to constitutively accumulate high amounts of lipids, regardless of environmental conditions that impede growth (Tan and Lee, 2016). In this study, we overexpressed 4 genes identified to correspond with lipid accumulation in *D. tertiolecta* into the model microalga *C. reinhardtii* to investigate the effects on lipid production without sacrificing growth. Our work here generated stable strains of *C. reinhardtii* overexpressing DtME, DtG6PDH, DtPDH and DtTE. Although all mutants did not show increases in lipid content during exponential phase, there were slight increases in lipid content in the stationary phase. However, the 4 mutants differ in their magnitude of increase in lipid content.

Acetyl-CoA is a key two-carbon metabolite central to a cell's anabolic and catabolic processes, which includes it as a substrate for FA synthesis (Tan and Lee, 2016). As FA synthesis primarily occurs in the plastid, the primary source of acetyl-CoA would theoretically come from glycolysis, where PDH converts pyruvate into acetyl-CoA. To this end, we produced a DtPDH-overexpressing mutant in *C. reinhardtii*. The DtPDH mutant however, did not exhibit any increase in acetyl-CoA levels and there was no change in lipid content relative to

wild-type. This is most likely due to the overexpression of only a single subunit (plastidial PDH E1β subunit) from *D. tertiolecta* which may not complement with the endogenous *C. reinhardtii* PDH complex which comprises 3 enzymes (Tan and Lee, 2016). Another strategy to increase the supply of acetyl-CoA may be to overexpress Acetyl-CoA synthetase (ACS), which converts acetate to acetyl-CoA. Since *C. reinhardtii* is able to grow mixotrophically on acetate, energy for FA synthesis need not come from photosynthesis alone. The overexpression of ACS in microalgae could allow it to better utilize exogenously supplied acetate for increased lipid production (Goodson et al., 2011; Ramanan et al., 2013). However, it should be noted that this would be counterproductive to the use of microalgae for inorganic CO_2 fixation, as an organic source (acetate) would have to be supplied. In addition, autotrophic microalgae species like *D. tertiolecta* and *Nannochloropsis* are unable to use acetate as a carbon source, thus overexpression of ACS would have limited potential for cross-species application.

Other than carbon supply from acetyl-CoA, production of FAs requires the provision of reducing power in the form of NADPH. Generation of NADPH for FA synthesis was mainly attributed to the metabolism of glucose-6-phosphate (G6P) and malate by G6PDH and ME respectively (Smith et al., 1992; Pleite et al., 2005). The mutants overexpressing NADPH-producing genes (DtMME2 and DtG6PDH) demonstrated increased enzymatic activities, but only the DtMME2 mutant had significantly higher NADPH levels. DtG6PDH mutant did not show any increase in NADPH levels despite an increase in its activity, suggesting that

the NADPH generated might have been immediately used for metabolic processes. Indeed, as G6PDH is localized in the chloroplast, the NADPH derived from the OPPP may be used up concurrently with Ribulose-5-phosphate for reductive anabolic processes such as nucleotide synthesis, which competes with FA synthesis for reducing equivalents (Johnson and Alric, 2013). In contrast, ME produces NADPH from the decarboxylation of malate to pyruvate, and relies on the availability of malate. Malate can be transported to the chloroplast via malate transporters (Kinoshita et al., 2011) and utilized by plastidial ME producing pyruvate and NADPH, which flows into FA synthesis. Moreover, the CO_2 produced by this reaction could be directly fixed by RuBisCO to increase photosynthetic capacity. Nevertheless, both DtMME2 and DtG6PDH mutants reflected modest (~30%) improvement in lipid content, suggesting that the NADPH produced from either source may only partially fulfill the demand for reducing power by FA synthesis (Schwender et al., 2003; Alonso et al., 2010), or that acetyl-CoA may have been the limiting factor.

Overexpression of DtTE induced the highest increase in lipid content among the four mutants (~56% increase in lipids relative to wild-type; up to 15% DCW). TE plays an important role in FA synthesis by hydrolyzing the thioester bond which links the ACP from the acyl-ACP, thus releasing free FAs which are subsequently converted into acyl-CoA and released from the chloroplast to be incorporated into TAGs (Chen and Smith, 2012). Reduced accumulation of acyl-ACPs relieves the negative feedback inhibition of ACCase (Davis and Cronan,

2001), KAS, and enoyl-ACP reductase activities (Heath and Rock, 1996a; Heath and Rock, 1996b), which allows for more efficient FA synthesis. Upregulation of TE transcripts were often observed to occur concurrent with the accumulation of TAGs stimulated under nitrogen starvation, when growth is halted (Miller et al., 2010; Lei et al., 2012; Rismani-Yazdi et al., 2012), prompting researchers to hypothesize that TE contributes to increase lipid production. Our findings that DtTE overexpression in *C. reinhardtii* leads to increase in total lipids coincides with a recent study, where overexpression of the endogenous PtTE in the diatom *P. tricornutum* enhanced its total FA content by 72%, but did not alter the FA composition (Gong et al., 2011), suggesting that it is possible to increase FA synthesis using TE. The introduction of DtTE is not expected to cause a major change in FA composition as the major FAs in *D. tertiolecta* and *C. reinhardtii* are very similar, with both microalgae producing majority C16:0 and C18:3 FAs (Tang et al., 2011). Interestingly, DtTE-expressing *C. reinhardtii* mutants accumulated more polyunsaturated FAs, especially that of C18:3, as the higher DtTE activity in the mutant strains may have conferred the preference for C18:3 hydrolysis (Tang et al., 2011).

The introduction of DtPDH or DtTE is not expected to cause a major change in FA composition as the major FAs in *D. tertiolecta* and *C. reinhardtii* are very similar, with both microalgae producing majority C16:0 and C18:3 FAs (Tang et al., 2011). Wild-type *C. reinhardtii* produces mostly C16:0 and C18:3 fatty acids, and only negligible amounts of C14:0 and C18:1 (James et al., 2011;

Blatti et al., 2012). Interestingly, DtTE-expressing *C. reinhardtii* transformants accumulated more polyunsaturated FAs, especially that of C16:3, C16:4, and C18:3, at the expense of C18:1 which was reduced in the transformants. This could be explained by the higher DtTE activity in the transformed strains, which may have conferred the preference for C18:3 hydrolysis. C18:3 are the main FA type in *D. tertiolecta*, accounting for up to 66% proportion of its FAs (Tang et al., 2011; Tan et al., 2016), while C18:1 only account for 4% of its FAs. Blatti et al. (Blatti et al., 2012) reported that overexpression of the endogenous CrTE in *C. reinhardtii* shifted the FA profile to produce increased levels of C14:0 and C18:1; they postulated that CrTE is more homologous to FatA TEs, which confers the preference for C18:1 FAs. As our introduction of DtTE exhibited a different response compared to CrTE in *C. reinhardtii*, we hypothesize that DtTE may have a preference for C18:3 over C18:1. Nevertheless, as both are microalgal TEs, they may be more homologous to FatA TEs (Voelker et al., 1992; Jones et al., 1995), which explains the preference for oleoyl-ACP substrates.

Microalgal TEs were suggested to evolve to specifically hydrolyze polyunsaturated FAs – which are not normally produced in higher plants – to confer flexibility, fluidity and selective permeability to its cellular membranes in unfavourable environments (Uttaro, 2006; Yu et al., 2011). Our phylogenetic analyses revealed that DtTE formed a separate clade along with other microalgal TEs, including CrTE, which are separate from the plant TEs (**Fig. 1**), suggesting that cross-species functionality could work better within the microalgal clade.

This was shown in recent studies where the *in vivo* introduction of plant TEs from *Umbellularia californica* and *Cuphea hookeriana* did not result in changes to the FA content in *C. reinhardtii*, as plant TEs do not functionally interact with acyl-ACPs from microalgae (Blatti et al., 2012; Beld et al., 2014). On the other hand, engineering algal TEs into *E. coli* were able to increase FA content in bacteria significantly (Gong et al., 2011; Radakovits et al., 2011), indicating that plant TEs may have further evolved to not recognize algal and bacteria acyl-ACPs.

Extracellular nitrate levels were reported to be depleted after 5 days of culture in *C. reinhardtii* (Kamalanathan et al., 2016), although it might take some time for the cell to adapt into a "N-depleted" state as intracellular nitrogen stores were shown to remain at stable levels even after nitrate depletion in the media (Lv et al., 2013). It has to be noted that despite overexpression of the four genes in *C. reinhardtii*, the increase in FAs was only observed in stationary phase and not during the exponential phase. Previous studies have shown that *C. reinhardtii* which were depleted of nitrogen in stationary phase had upregulated expression of PDH and TE (Miller et al., 2010; López García de Lomana et al., 2015), suggesting that overexpression of these genes could exert their effects on FA synthesis once the cell's metabolism has shifted to lipid accumulation phase. Indeed, overexpression of ME in *Chlorella pyrenoidosa* and *Phaeodactylum tricornutum* resulted in increased neutral lipid accumulation only during stationary phase, or under N-depleted conditions (Xue et al., 2015; Xue et al., 2016), suggesting that high cell divisions during exponential phase might have

discounted the effects on lipid accumulation, as intracellular substrates could have been channeled to growth. The results of this study do not indicate increased productivity in terms of improved FA content during growth, but may provide a platform for further studies into using the various genes-of-interest as a strategy to increase biofuel production from microalgae (Tan and Lee, 2017).

3.5 Conclusion

Individual genes participating in the supply of acetyl-CoA or NADPH are claimed by various studies to be rate-limiting for FA synthesis (Ratledge, 2004; Zhang et al., 2007; Lei et al., 2012). However, due to limited time in the current project, and the increased effort required to clone more than one gene into a plasmid (e.g. more RE sites need to be identified to insert genes), we decided to first pursue single gene transformation in *C. reinhardtii* and study its physiological effects (16 day growth, enzyme activity assays, GC-MS analyses of FAs). Nevertheless, it is likely that a multi-gene approach may be required to completely rewire an organism's ability to switch from non-oleaginous to oleaginous, without compromising growth. For example, the claim that NADPH provision by ME was a rate-limiting step in FA synthesis was previously backed by observations that ME overexpression in the fungus *Mucor circinelloides* led to a 2.5-fold increase in FAs (Zhang et al., 2007). This conclusion was challenged by another report revealing that it is actually leucine auxotrophy - which the previous authors used for selection - that decreased FA content by 2.5-fold, and that ME overexpression did not translate into higher lipid levels despite an increase in ME activity (Rodríguez-Frómeta et al., 2013). It was thus proposed

that the leucine metabolism pathway, by participating in the generation of acetyl-CoA substrates, may be critical for FA synthesis in *M. circinelloides*. A subsequent study showed that ME overexpression increased FA content by only 30% relative to control, despite a 2-fold increase in ME activity, suggesting that ME may not be the sole rate-limiting enzyme, but does play a role during FA synthesis in oleaginous fungi (Hao et al., 2014). Recently, a large-scale genomic engineering of *Y. lipolytica* involved the simultaneous overexpression of ACL and ME to increase acetyl-CoA and NADPH supply, while DGAT was also overexpressed to increase carbon flux towards TAG synthesis (Blazeck et al., 2014). In addition, these targets were multiplexed with deletions of genes which serve to reduce FA catabolism by inhibiting the peroxisomal β-oxidation pathway. Consequently, the cells became lipid saturated up to 90% biomass with lipid titres exceeding 25 g/L, which is a 60-fold improvement over the parental strain (Blazeck et al., 2014). Thus, increasing of FA synthesis in microorganisms may not be simply explained by overexpression of a single enzyme, but influenced by a combination of pathways spanning FA synthesis, TAG synthesis and central carbon metabolism, including production of FA precursors like acetyl-CoA and NADPH.

Chapter 4 Inducing fatty acid production and secretion in *Synechococcus elongatus* PCC 7942 and *Chlamydomonas reinhardtii*

4.1 Introduction

4.1.1 Scientific significance

Among the difficulties involved in commercial production of microalgae biofuels, cost-effective extraction of lipids remains a major bottleneck. Despite the routine demonstration of laboratory-scale technologies for microalgal lipid extraction such as organic solvent extraction and supercritical CO_2 extraction, there is yet to be a standard established for industrial-scale extraction (Halim et al., 2012). Furthermore, harvested microalgal cultures exists as dilute aqueous suspension and need to be dewatered and concentrated to reduce downstream processing costs (Halim et al., 2012). As these additional steps are costly and energy intensive, the use of microorganisms that secrete lipids into the culture media provide an interesting way to simplify extraction and reduce production costs.

Numerous hosts have been explored and engineered to overproduce and secrete free fatty acids (FFAs), particularly in prokaryotic systems like *E. coli* (Liu et al., 2012; Meng et al., 2013) and cyanobacteria (Liu et al., 2011b; Ruffing and Jones, 2012; Ruffing et al., 2013), but has also been proven to work in the eukaryote *Saccharomyces cerevisiae* (Michinaka et al., 2003; Leber et al., 2015).

Unlike triacylglycerols (TAGs), FFAs are not bound to another molecule, and are desired for their straightforward chemical conversion into a broad range of biochemical products, including alkanes, alkenes, fatty acid methyl esters, ethyl esters and fatty alcohols (Runguphan and Keasling, 2014; Yu et al., 2014). Overexpression of a truncated acyl-acyl carrier protein (ACP) thioesterase (TE) I (mutant protein called 'tesA) – that is missing the signal sequence peptide that directs the enzyme to the periplasm – redirects FA synthesis to FFA production and secretion in the culture medium (Cho and Cronan, 1995), and have been demonstrated to work in *E. coli*, *Synechocystis* sp. PCC 6803, and *Synechococcus elongatus* PCC 7942 (Liu et al., 2011b; Liu et al., 2012; Ruffing and Jones, 2012). The rate-limiting enzyme, acyl-CoA carboxylase (ACCase), suffers from negative feedback inhibition from the accumulation of fatty acyl-ACPs and thioesterases can relieve this inhibition (Jiang and Cronan, 1994; Davis and Cronan, 2001), thus facilitating the continuous overproduction of FFAs. Mutants deficient in acyl-CoA synthetases (ACS) – which catalyzes the esterification of FFAs into acyl-CoAs for β-oxidation – have also been characterized to overproduce and secrete FFAs out of cells in *E. coli*, *S. cerevisiae*, *Synechocystis* sp. PCC 6803, and *S. elongatus* PCC 7942 (Scharnewski et al., 2008; Liu et al., 2011b; Liu et al., 2012; Ruffing and Jones, 2012; Leber et al., 2015). Despite much evidence proving FFA secretion, all of the strategies have focused on pathways leading to FFA overproduction; the release of FFAs to the extracellular media appears to be

a convenient phenotype that these cells exhibit after accumulation of intracellular FFAs.

Fatty acid secretion from cells is an active area of research (Lane et al., 2016; Theodoulou et al., 2016) and reports suggest that FAs could be exported out of cells either through diffusion across a concentration gradient via "flip flop" (Black and DiRusso, 2003; Pohl et al., 2005) or through active transport by carrier proteins such as ATP binding cassette (ABC) transporters (Pohl et al., 2005; Bird, 2008; Moussatova et al., 2008) or Resistance-Nodulation-Cell division (RND) transporters in bacteria and cyanobacteria (Dunlop et al., 2011a). The disruption of ACS or the overexpression of TEs were linked with most secretion phenotypes, which led scientists to believe that overproduced intracellular FFAs perform fast free diffusion out of the cell by "flip-flopping" in the phospholipid bilayer (Hamilton, 2007); FFA export in such a manner is driven by diffusion by concentration gradient. However, there is also evidence showing that different cell types export exogenous FFAs at differing rates (Black and DiRusso, 2003), implying that efflux proteins are also involved in the process, especially when cells are known to export biofuels to alleviate product toxicity (Dunlop et al., 2011a; Ruffing and Jones, 2012; Lennen et al., 2013).

Microarray data sets identified a plasma membrane-localized ATP binding cassette (ABC) transporter named ABCG11 in *Arabidopsis thaliana* as required for cuticular lipid transport (Bird et al., 2007; McFarlane et al., 2010). Knock-out mutants produced a 50% reduction in extracellular waxes and accumulated large

amounts of intracellular lipids, indicating that fatty acid transport was impaired by the loss of ABCG11 (Bird et al., 2007). ABCG11 exports long chain FAs of 16 to 18C in length (Bird et al., 2007), similar to the FA profile of microalgae and cyanobacteria (Kaczmarzyk and Fulda, 2010; Tang et al., 2011; Davidi et al., 2012; Ruffing and Jones, 2012), raising a possibility that ABCG11 could export FAs in the latter as well. Furthermore, foreign bacterial ABC transporters transformed into *E. coli* were able induce secretion of hydrophobic carotenoids (Doshi et al., 2013), supporting the notion that plant ABC transporters could secrete hydrophobic FAs in eukaryotic microalgae. Despite ABCG11 being a plant gene, the high functional conservation among the ABCG gene family across biological kingdoms (Pohl et al., 2005) may allow its mechanism in microalgae. If demonstrated to work, ABCG11 could be tested as a lipid efflux system in various oleaginous species of cyanobacteria and microalgae to achieve high production of biofuels. The success of this system may also encourage the identification of other transporters in the ABC subfamilies for the export of co-products of high pharmacological or nutritional interest (Brennan and Owende, 2010).

β-oxidation is a major contributor to the loss of FAs in exponential and stationary growth phases as FAs are continuously broken down to generate acetyl-CoA, a central metabolite used as a building block by the TCA cycle (Quintana et al., 2011b). Acyl-CoA dehydrogenase (ACD) – the enzyme responsible for catalyzing the first step of β-oxidation (**Fig. 4.1**) – have been deleted to prevent FFA degradation in *E. coli* strains and shown to increase the yields of the desired

products (Steen et al., 2010; Choi and Lee, 2013; Janßen et al., 2014). While deletion of ACD may increase FA content by preventing degradation, another strategy of overproducing FAs is to increase carbon flux towards the FA synthesis pathway. Specifically, phosphoenolpyruvate synthase (ppsA) was found to be significantly downregulated in *S. elongatus* PCC 7942 mutants which were engineered to overproduce FFAs (Ruffing et al., 2013). The repression of ppsA prevents the energy-consuming phosphorylation of pyruvate to phosphoenolpyruvate (**Fig. 4.1**), permitting the one-directional carbon flow towards pyruvate and acetyl-CoA, thus increasing the amount of carbon substrates for FA synthesis.

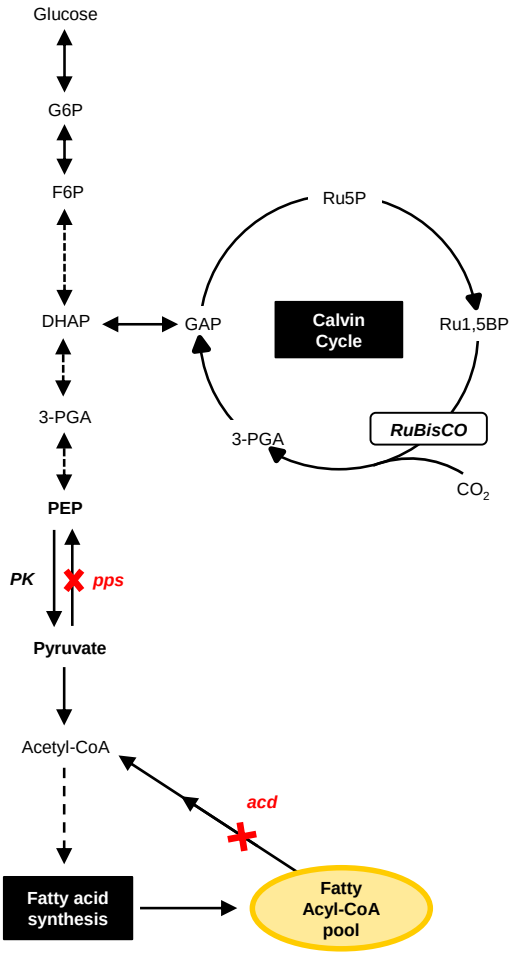

Figure 4.1 Carbon capture and conversion in central metabolic pathways of S. elongatus PCC 7942 directing carbon flux towards fatty acids. *Abbreviations:* acd, acyl-CoA dehydrogenase; DHAP, dihydroxyacetone phosphate; F6P, fructose 6-phosphate; GAP: Glyceraldehyde 3-phosphate; G6P, glucose 6-phosphate; Ru5P, ribulose 5-phosphate; Ru1,5BP carboxylase/oxygenase, RuBisCO, Ru1,5BP carboxylase/oxygenase; 3-PGA, 3-phosphoglycerate; PEP, phosphoenolpyruvate; PK, pyruvate kinase; pps, PEP synthase.

4.1.2 Rationale for transformation of *S. elongatus* 7942 and *C. reinhardtii*

To promote secretion of lipids from microalgae, we hypothesize that introducing a plant ABC transporter (i.e. ABCG11) required for lipid export would facilitate the secretion of FAs. If ABCG11 is necessary and sufficient for

the export of long chain FAs (16-18C), it's overexpression in the model cyanobacteria *S. elongatus* PCC 7942 and the model microalgae *C. reinhardtii* should be adequate to induce FA secretion into the culture medium. We concede that the expression of a eukaryotic gene in a bacterial system might not result in a fully functional protein. However, considering the presence and functional conservation of ABC systems in all organisms and the ability of bacterial ABC transporters to substitute mammalian drug transport (Pohl et al., 2005; Doshi et al., 2013), it would be logical to assume the cross-species translation potential of these transporters. The functional interchangeability among ABC transporters was exemplified by studies in which LmrA, a bacterial ABC exporter, was found to be capable to substituting the drug transport function of a multidrug-resistance P-glycoprotein in human cells (van Veen et al., 1998).

S. elongatus PCC 7942 was chosen as a model organism because cyanobacteria provides the ease of genetic manipulation via homologous recombination, and were shown to have the fastest growth rate and highest lipid productivity in exponentially growing cultures (Sheehan et al., 1998; Quintana et al., 2011b). The ability to use homologous recombination in *S. elongatus* allows for the precise targeting of specific genes, creating insertions, deletions, or replacement mutations in cyanobacterial chromosomes (Berla et al., 2013). In addition, *S. elongatus* PCC 7942 has a better FA productivity (8.4 nmol/L/day) than *Synechocystis* PCC 6803 (6.4 nmol/L/day), making it a better candidate for industrial applications (Kaczmarzyk and Fulda, 2010; Quintana et al., 2011b). *C.*

reinhardtii was selected for examining the effect of ABCG11 expression in an eukaryotic host. *C. reinhardtii* is a genetically well-characterized model microalgae whose genome is fully sequenced and extensive molecular transformation methods are well established for it (Doron et al., 2016). *C. reinhardtii* is able to grow photoautotrophically or mixotrophically on organic carbon sources, which enables it to divide relatively quickly, doubling every 5 to 8 hours (Rasala and Mayfield, 2011), allowing for rapid experimentation and testing of hypotheses.

Inducing secretion by overexpression of ABC transporters might prove to be difficult if the cells have low basal levels of lipids. Although cyanobacteria possess the highest biomass productivity, it showed low lipid contents per cell, reflecting the high metabolic cost of FA production (Francisco et al., 2010). Thus, inhibiting β-oxidation or increasing carbon substrate supply for FA synthesis would be used to increase the intracellular pool of FAs prior to the introduction of ABCG11. Gene deletion of ACD and ppsA will be achieved by homologous recombination in *S. elongatus* PCC 7942. Furthermore, codon optimization of ABCG11 for *S. elongatus* PCC 7942 may be required before transforming the gene into the host cells.

4.1.3 Aims and objectives

Aim 1: To increase lipid production in cyanobacteria by 1) preventing fatty acid degradation, or 2) increasing the provision of carbon substrates for fatty acid synthesis.

Hypothesis 1: Gene deletion of acyl-CoA dehydrogenase (ACD) and phosphoenolpyruvate synthase (ppsA) in *S. elongatus* PCC 7942 will increase intracellular fatty acid content.

Aim 2: To determine the potential of using *Arabidopsis* ATP binding cassette (ABC) transporter ABCG11 for active export of lipids in cyanobacteria and microalgae.

Hypothesis 2: Introducing *At*ABCG11 into the host cell will lead to the secretion of fatty acids into the culture medium in cyanobacteria and microalgae.

4.2 Materials and Methods

4.2.1 Cyanobacterial strains, media and growth conditions

Cultures of *Synechococcus elongatus* sp. PCC 7942 were grown at 30^{o}C in BG-11 medium (Stanier et al., 1979) under continuous illumination (50 µmol photons/m^2/s) in a shaking incubator (Certomat BS-1 Shaking Incubator, Sartorius Stedim Biotech) with shaking at 120 rpm. Growth was monitored by spectrophotometric measurement at OD_{730}. The standard curve relationship between culture optical density and cell density is used for conversion (**Fig. S12**).

For selection plating on solid media, BG-11 was supplemented with 1.5% (w/v) agar and 7 µg/mL kanamycin. Mutants were maintained in the presence of the antibiotic for selection. From solid BG-11 agar, *S. elongatus 7942* strains were inoculated into 2 mL of BG-11 media (supplemented 7 µg/mL kanamycin for the mutants), and grown under conditions stated previously. After 4-5 days of cultivation, cultures were transferred in 1000x dilutions to 20 mL of BG-11 media in a 125-mL flask, to serve as inoculum. Inoculum cultures were added to 50 mL of BG-11 media in 250-mL baffled flasks to an initial OD_{730} of 0.05. Samples were aerated with filter-sterilized air supplemented with 1% CO_2, and growth was monitored at 2-day intervals.

4.2.2 Generation of knockout mutants of *S. elongatus 7942* and introduction of ABCG11 in *S. elongatus* 7942 and *C. reinhardtii*

The acd and ppsA knockout mutants were created via homologous recombination by replacing the coding region with a cassette containing a kanamycin resistance gene (kan cassette). The plasmid was constructed first by cloning the kan gene into the multiple-cloning site of pGEM-T (Promega) using the primers listed in **Table S9**. KanR genes were derived from the plasmid pYUB870, generously provided by Thomas Dick (National University of Singapore). Next, 400-bp DNA fragments homologous to upstream and downstream of the open reading frame of ACD or ppsA were inserted into the regions flanking the kanR cassette. As single RE sites were used for cloning, the

correct orientation of the inserts was further evaluated with DNA sequencing. For construction of the strain which overexpress ABCG11 only (i.e. without gene knockout), the sequence for Neutral Site 2 (NS2) was used as the flanking regions for homologous combination (**Table S9**). The gene sequence for ABCG11 was obtained from NCBI RefSeq (Accession number NM_101647.5), codon optimized and synthesized from GenScript with a Ptrc promoter sequence (5' – GAGCTGTTGACAATTAATCATCCGGCTCGTATAATTTTAAAGAGGAGA AA – 3') artificially added before the start codon for strong transcription in *S. elongatus* 7942. The Ptrc-ABCG11 cassette was inserted into the plasmid, positioned beside the kanR cassette. Description of the strains and their corresponding genotype are presented in **Table 4.1**.

S. elongatus 7942 were transformed as described before (Clerico et al., 2007). Briefly, 15 mL of cells grown to an OD_{730} of 0.7 were harvested, washed with 10 mM NaCl and resuspended in 300 µL fresh BG-11 medium. Approximately 1 µg of recombinant plasmid DNA was added and the sample was incubated overnight at 30^{o}C with gentle agitation, away from light. The entire suspension was then plated on BG-11 agar plates containing 7 µg/mL kanamycin and incubated at 30^{o}C in constant light for a minimum of 5 days until single colonies appear.

For *C. reinhardtii* transformation, the pHyg3 plasmid was used (refer to Chapter 3 for details). First, ABCG11 inserted into a plasmid (pGreen) containing the endogenous CrRbcS2 (small subunit of ribulose bisphosphate carboxylase)

promoter. The CrRbcS2-ABCG11 fragment was then removed by PCR and inserted into the PciI site of the hygromycin-resistance plasmid, pHyg3 (**Fig. S13**). Transformation was performed according to Chapter 3, Section 3.2.2.

4.2.3 Genetic confirmation of mutants

For *S. elongatus* 7942, cells from a colony were harvested in 10 µL BG-11 media in a 200-µL PCR tube and subjected to three freeze-thaw cycles at -80^{o}C for 2 min, and then thawed in a 60^{o}C water bath. Freeze-thawed cell suspensions were used as 1-µL template in a 25-µL PCR reaction with corresponding primers specific for inserted segments or the deleted region (**Table S10**). For *C. reinhardtii*, the protocol for genotyping PCR follows that of Chapter 3 (Section 3.2.3) using ABCG11 and pHyg3 backbone specific primers.

4.2.4 Quantitative real-time PCR (qRT-PCR) analysis

RNA was extracted according to Chapter 2 (section 2.2.11). Constitutively expressed 16S rRNA (Billini et al., 2008; Pinto et al., 2012) was used as the reference gene when conducting real-time PCR for *S. elongatus* 7942. Real-time PCR primers used are listed on **Table S10**.

4.2.5 Total Lipid Analysis by Gas Chromatography-Mass Spectrometry

To analyze the accumulation of lipids, cells were harvested when they have reached early stationary phase with densities of about 3 x 10^8 cells/mL. Cell samples were immediately frozen in liquid nitrogen and stored at -80^{o}C until analysis. Frozen culture samples were lyophilized by freeze-drying and lipids were extracted by hexane using direct transesterification (Lee et al., 2014) as it was reported to be a convenient and accurate method for analyzing total fatty acids (Cavonius et al., 2014). Biomass quantities of between 5 and 10 mg of biomass were weighed into glass 55-mL PYREX culture tubes with polytetrafluoroethylene (PTFE)-lined phenolic caps (25 mm diameter × 150 mm height, PYREX #9826-25, Corning). To each sample, 0.2 mL of chloroform-methanol (2:1, *v*/*v*) was added and mixed by vortexing, followed by simultaneous transesterification of lipids with 0.3 mL of 1.25M methanolic HCl and vortexed to mix. An internal standard (100 μg methyl tridecanoate, C13-FAME; Product no. 91558, Sigma-Aldrich) was included to correct for the loss of FAME during the reaction, and to correct for subsequent incomplete extraction of hexane (Laurens et al., 2012). The culture tube was then incubated in a 50^{o}C waterbath overnight. After 24 hours, 1 mL of hexane was added and mixed by vortex, and incubated at room temperature for 1 hour. The upper organic phase was removed using a glass pipette and transferred to a new 2-mL screw-top amber glass vial (Part no. 5182-0716, Agilent Technologies) and dried with a stream of nitrogen gas for analysis by GC-MS. To detect secretion of FAs, 30 mL of culture supernatant (10 μg C13-

FAME added as internal standard) was acidified with 0.6 mL of 1M H_3PO_4 containing 0.6 g NaCl, and FAs were separated from the culture medium by 15 mL hexane, which is unable to release lipids from intact cells (Liu et al., 2011b).

Dried lipid extracts (fatty acid methyl esters; FAMEs) were re-dissolved in 200 µL of hexane, filtered through a 0.22-µm PTFE syringe filter (Agilent Technologies), and collected in a 250-µL glass vial insert (Part no. 5181-1270, Agilent Technologies). FAME extracts were injected into a GC system (Model 7890B, Agilent Technologies) equipped with an Agilent 19091S-433UI column (30m x 250µm x 0.25µm) interfaced with a mass spectrometric detector (Model 5977A, Agilent Technologies). Injection volume was set at 1 µL with a 5:1 split ratio at a GC inlet temperature of 250^{o}C. Helium was used as the carrier gas in a fixed flow of 1 mL/min throughout. Temperature program is as follows: initial oven temperature of 70^{o}C held for 3 mins, ramp to 130^{o}C at 20^{o}C/min, 178^{o}C at 4^{o}C/min, 190^{o}C at 1^{o}C/min, and 290^{o}C at 10^{o}C/min. The total run time was 40 minutes. Shifting of retention times (RTs) were eliminated by comparing the RTs of each FA compound to the C13-FAME internal standard. Analysis was performed using the MassHunter WorkStation Qualitative Analysis B.07.00 software (Agilent Technologies) and compounds were identified with the NIST mass spectral library (National Institute of Standards and Technology, Data Version: NIST 14).

4.2.6 Statistical analysis

All data were expressed as means ± standard deviation (SD). For gene expression experiments, the fold change for each gene was expressed as the mean ± SD of each independent biological replicate normalized to housekeeping gene expression values. Statistical analyses were performed using Student's *t* test. A *p*-value <0.05 was considered statistically significant.

4.3 Results

4.3.1 Molecular characterization of mutant strains by PCR and qPCR

In the final plasmid vector, an aminoglycoside phosphotransferase (kanR) cassette was inserted between 400-bp flanking regions of ACD, ppsA, or NS2 gene sequences, allowing for homologous recombination. Transformed cells surviving on kanamycin plates were selected and subjected to PCR screening with primers which would generate either bands corresponding to the size of the native genes (i.e. intact ACD, ppsA, or NS2), or the size of a kanR-sacB cassette which replaces it (**Table 4.1, Fig. 4.2**). For example, an expected 3.8-kb band was present in the mutant lines (**Fig. 4.2**), while a 2.5-kb band was present in the wild-type representing the size of an intact ppsA (Synpcc7942_0781); the 3.8-kb band represents the size of the kanR cassette which replaces the locus of the gene targeted for knockout. For mutants where the native gene locus is replaced by an ABCG11-kanR plasmid, the expected size of the band would be approximately 4.2-kb (**Fig. 4.2**).

Transcript abundance of ACD, ppsA, and ABCG11 were determined by qPCR. As shown in **Fig. 4.3a**, mutant strains aS and aA exhibited no observable transcription for the ACD gene, while the transcript levels of ppsA were correspondingly absent in pS and pA mutants (**Fig. 4.3b**). Moreover, when probed for the transcription of the exogenous ABCG11 gene, only mutants aA, pA, and nA showed detectable signals (**Fig. 4.3c**), suggesting that the mutation worked and ABCG11 transcripts were present.

Table 4.1 Description of the *S. elongatus* PCC 7942 strains used.

Name of mutant	**Genotype description**
WT	*Synechococcus elongatus* PCC 7942 wild type
aS	Acyl-CoA dehydrogenase (*Synpcc7942_1215*) deletion
aA	Acyl-CoA dehydrogenase (*Synpcc7942_1215*) deletion, ABCG11 overproduction
pS	Phosphoenolpyruvate synthase (*Synpcc7942_0781*) deletion
pA	Phosphoenolpyruvate synthase (*Synpcc7942_0781*) deletion, ABCG11 overproduction
nA	ABCG11 overproduction only

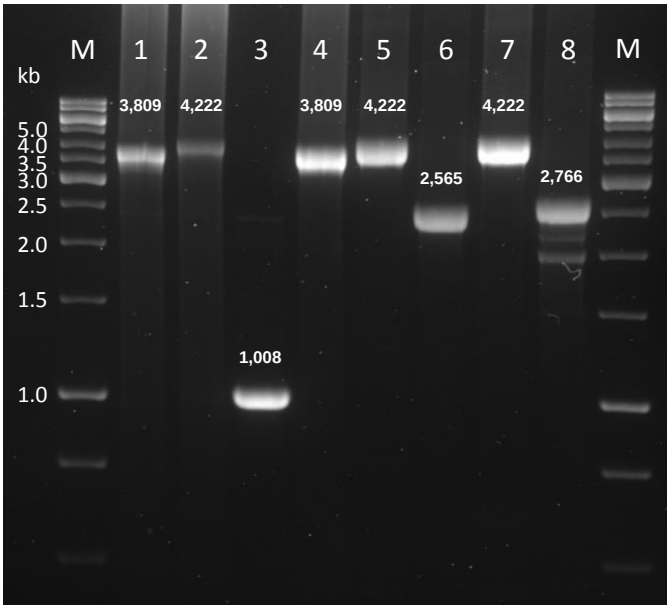

Figure 4.2 PCR identification of deletions and insertions in *S. elongatus* 7942. Genomic DNA extracted from the mutants and WT were subjected to PCR using primers listed in Table S10. Lane 1: DNA from aS (PCR with ACD primers); Lane 2: DNA from aA (PCR with ACD primers); Lane 3: DNA from WT (PCR with ACD primers); Lane 4: DNA from pS (PCR with ppsA primers); Lane 5: DNA from pA (PCR with ppsA primers); Lane 6: DNA from WT (PCR with ppsA primers); Lane 7: DNA from nA (PCR with NS2 primers); Lane 8: DNA from WT (PCR with NS2 primers). Expected band sizes are shown in the picture.

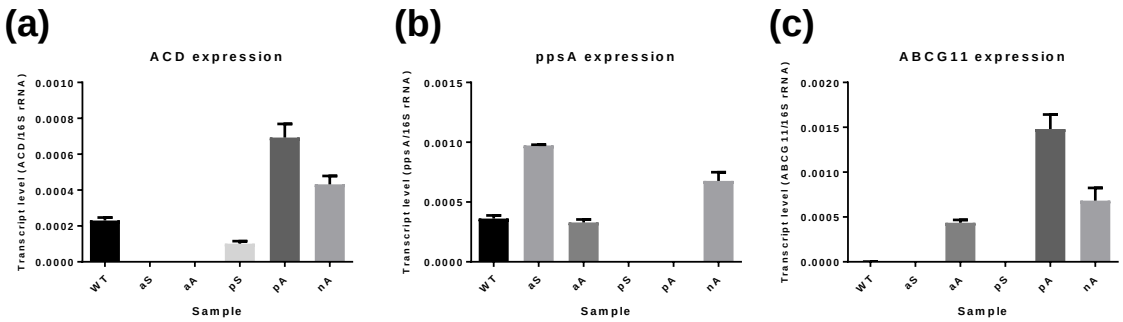

Figure 4.3 Gene expression for *S. elongatus* 7942 mutants by real-time PCR. Transcript levels were normalized to the endogenous reference 16S rRNA. ACD (a) and ppsA (b) expression is only present in the strains which did not have ACD and ppsA knockout, while ABCG11 is only expressed (c) in strains with the Ptrc-ABCG11 inserted by homologous recombination.

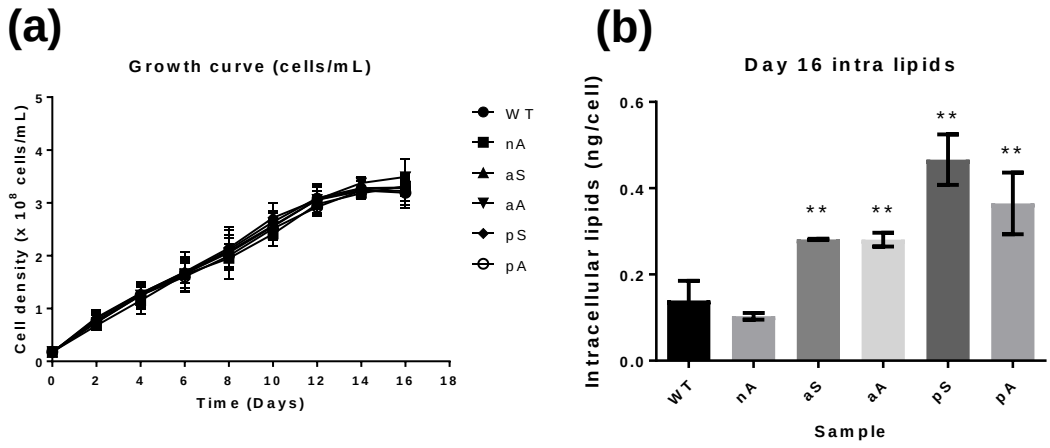

Figure 4.4 Growth curve and total fatty acid (FA) content of the *S. elongatus* 7942 mutants. Cells were grown in BG-11 medium under constant illumination, reaching maximum cell density on Day 16 (a). FA content were increased in the ACD and ppsA knockout mutants relative to the wild type, while the FA content of nA did not change (b). Asterisks indicate statistically significant differences between N-replete and N-deplete samples after two-tailed t-tests (* p value $\leq$ 0.05; ** p value $\leq$ 0.01).

Table 4.2 Fatty acid profile of the *S. elongatus* 7942 mutants.

FFA Type	Fatty acid weight percentage (%)					
	aS	*aA*	*pS*	*pA*	*nA*	WT
14:0	1.8 ± 0.1	0.0 ± 0.0	0.4 ± 0.5	0.0 ± 0.0	0.0 ± 0.0	0.9 ± 1.3
16:0	47.6 ± 1.8	52.1 ± 5.1	43.7 ± 4.0	45.4 ± 1.4	47.5 ± 0.5	42.6 ± 0.1
16:1	35.4 ± 2.3	31.9 ± 2.7	27.6 ± 4.9	32.8 ± 2.1	32.8 ± 0.6	31.4 ± 1.9
18:0	2.3 ± 1.2	1.8 ± 0.5	2.9 ± 1.0	2.2 ± 0.4	3.1 ± 0.9	2.3 ± 0.5
18:1	12.9 ± 2.8	14.2 ± 1.9	25.4 ± 7.4	19.6 ± 3.1	16.6 ± 2.0	22.9 ± 3.8
Total (%)	100	100	100	100	100	100

4.3.2 Intracellular and extracellular lipids in *S. elongatus* 7942 and *C. reinhardtii* mutants

To determine if the knockout mutation had any negative effects on growth, cells were grown in BG-11 medium without antibiotics, and the growth curves were followed. However, there was no difference in cell densities (**Fig. 4.4a**), suggesting that the mutation had no impact on growth. On the other hand, knocking out ACD and ppsA appeared to have improved the lipid accumulation in the mutants. Compared to the wild-type, ACD and ppsA mutants had an average 2-fold and 3-fold increase in lipids, respectively. There were also no observable difference in the FA profile between the strains (**Table 4.22**). The major fatty acids detected were C16:0 (comprising 42% to 52% of total lipids), C16:1 (28% to 35%), and C18:1 (13% to 25%) (**Fig. 4.5**), which is similar to the findings reported in the literature (Kaczmarzyk and Fulda, 2010; Ruffing and Jones, 2012).

To detect for extracellular lipids, we harvested the media at the same time cells were collected; upon centrifugation, cells were spun down and the

supernatant was harvested. The media supernatant was immediately separated and concentrated for lipids, with the addition of C13-FAME internal standard to ensure the method was technically sound. However, we did not find any detectable peaks representing FAs in the GC-MS chromatogram (**Fig. 4.5a – f**). To determine if ABCG11 would function differently in a eukaryotic system compared to a prokaryotic one, we transformed *C. reinhardtii* with ABCG11 (**Fig. 4.6a, b**). There was no change in intracellular lipids for the ABCG11 mutants (all samples had ~ 9% total lipids). In addition, no observable FA peaks were detected by GC-MS when the media was analyzed (**Fig. 4.6c, d**).

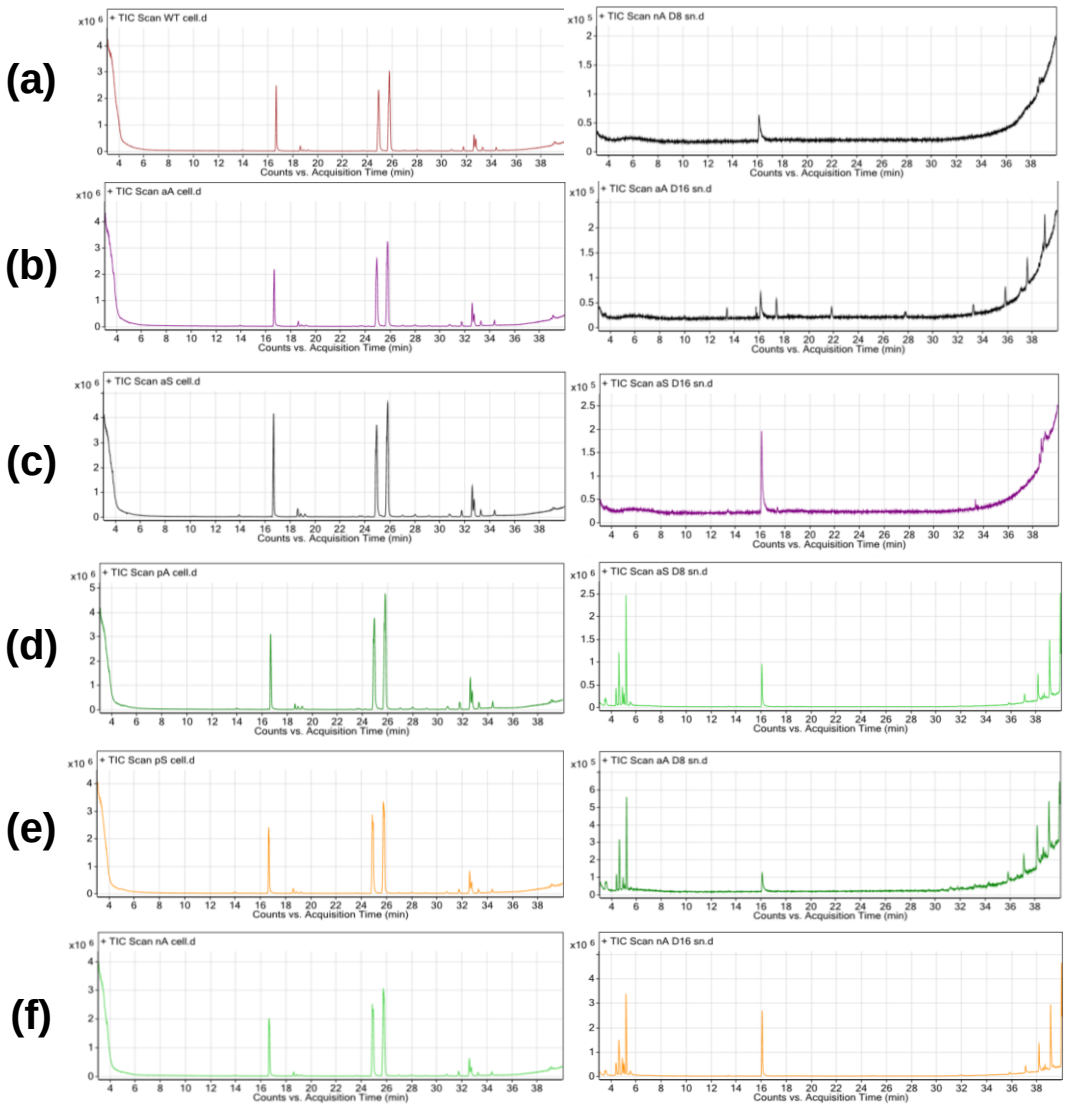

Figure 4.5 GC-MS chromatograms of intracellular (right) and extracellular (left) lipids in *S. elongatus* 7942 mutants. (a) Wild type; (b) aA; (c) aS; (d) pA; (e) pS; (f) nA. The internal standard (methyl tridecanoate, C13-FAME) is depicted by the peak at 16 mins. Major peaks for fatty acids C16:1 (Hexadecenoic acid) and C16:0 (Hexadecanoic acid) are shown in the images on the right.

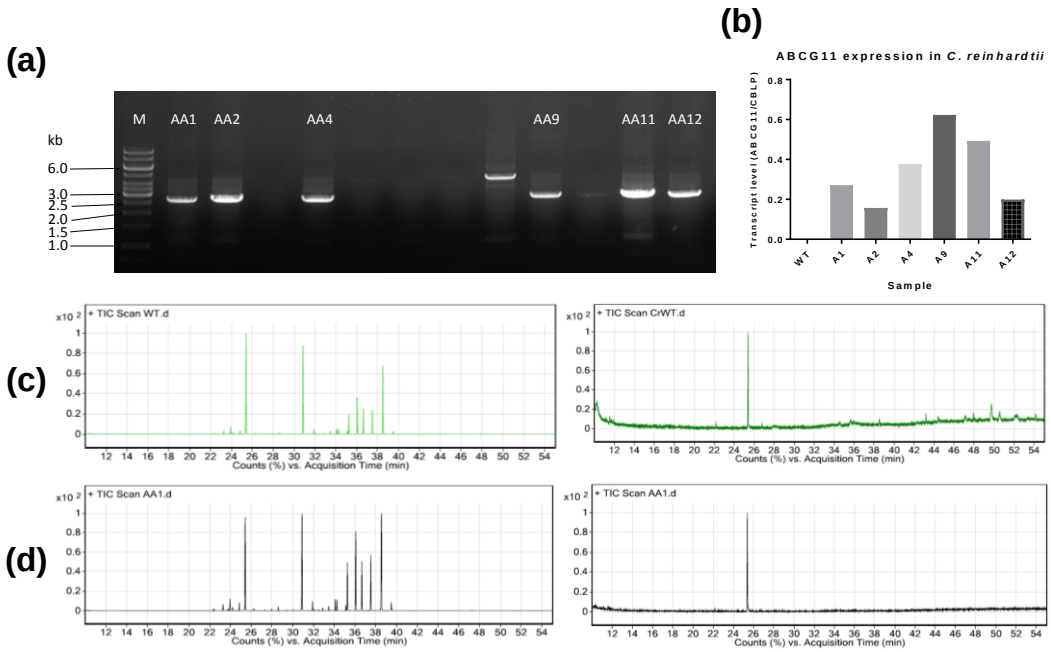

Figure 4.6 ABCG11 overexpression in *C. reinhardtii*. (a) Genotyping PCR identification of CrRbcS2-ABCG11 insertion in *C. reinhardtii* mutants (Expected size: 2,778-bp). Refer to Fig. S13 for plasmid map of CrRbcS2-ABCG11 in pHyg3 plasmid. (b) Expression of the heterologous plant ABCG11 in selected *C. reinhardtii* mutants. Only the mutants show expression of the foreign mRNA. Representative GC-MS analysis of the intracellular (right) and extracellular (left) lipids of wildtype (c) and AA1 (d) cells are presented (all 6 mutants displayed similar phenotype). The internal standard (methyl tridecanoate, C13-FAME) is depicted by the peak at 25 mins. Samples were harvested for analysis when cells were at stationary phase.

4.4 Discussion

Acyl-CoA dehydrogenase (ACD) deletion. Elimination of FA degradation pathways is a popular approach to improve FA accumulation (Beld et al., 2015). For example, enzymes which target the degradation of FAs, such as fatty acyl-CoA ligase, acyl-CoA synthetase (ACS), and acyl-CoA dehydrogenase (ACD), have all been previously knocked out in *E. coli* and *Synechocystis* sp. PCC6803 (Lu et al., 2008; Steen et al., 2010; Liu et al., 2011b). In our study, we

found that ACD deletion in *S. elongatus* PCC 7942 was able to increase FA accumulation by 2-fold, which yields 2.8 to 2.9 ng/cell FAs. However, this still translates only to 0.1 g/L of FAs, ten times less yield than theoretically possible in *E. coli* (Zhang et al., 2011a). Perhaps, in order to achieve high titers of FAs, other accompanying genes have to be sequentially introduced. For instance, a modified tesA gene encoding a truncated version of the endogenous *E. coli* thioesterase was overexpressed in parallel with ACD knockout (Steen et al., 2010). The thioesterase catalyzed the hydrolysis of acyl-ACP, releasing free FAs from the FA synthesis pathway, while ACD prevented the degradation of FAs. This resulted in the engineered *E. coli* strain yielding 1.2g/L of FAs after a 72 hour incubation, reaching 14% of the theoretical limit (Zhang et al., 2011a). Nevertheless, it has to be noted that genetic engineering of cyanobacteria for FA production might be more complicated than in *E. coli*, as minimal carbon from photosynthesis is directed towards biofuel production (Quintana et al., 2011b). Thus, combinatorial engineering might be needed to drive metabolic flux towards feeding the fatty acyl pool.

Phosphoenolpyruvate synthase (ppsA) deletion. Overexpression of ppsA in mutant *E. coli* leads to growth retardation (Patnaik et al., 1992), while deletions in ppsA and pyruvate kinase prevented growth on glucose or acetate alone, as carbon interchange between phosphoenolpyruvate (PEP) and pyruvate were blocked (Sabido et al., 2014). Interestingly, deletion of ppsA in this study did not negatively affect the growth of *S. elongatus* 7942, as only the reverse

reaction (pyruvate to PEP) was hindered. Synthesis of carbon and energy storage polysaccharides such as glycogen is unlikely to be affected by ppsA deletion as glycogen is mainly synthesized during light periods from assimilated CO_2 and later degraded via glycolysis for the TCA cycle (Quintana et al., 2011b; Saha et al., 2016). Overexpression of ppsA was found to increase levels of PEP for synthesis of commercial compounds of interests, including isoprenoids, lycopenes, and antifungal phenazines (Liao and Farmer, 2000; Jung et al., 2016; Liu et al., 2016). On the other hand, metabolically engineered *E. coli* cells containing deleterious mutations on ppsA were found to accumulate pyruvate under high glycolytic flux after being fed with glucose and acetate (Zhu et al., 2008). Indeed, deletion of ppsA increased pyruvate levels and improved the production of downstream products such as lactate (Zhou et al., 2011), indicating that ppsA inhibition could contribute to a carbon 'push' effect downstream of glycolysis. *S. elongatus* 7942 with knockout mutation in the gene encoding ADP-glucose pyrophosphorylase displayed similarly improved levels of pyruvate, as carbon flux was redirected to glycolysis from gluconeogenesis (Benson et al., 2016). While ppsA is essential for growth of *E. coli* when pyruvate is the only carbon source (McCormick and Jakeman, 2015), in photosynthetic organisms not reliant on organic carbon sources, deletion of ppsA has been suggested to be an important target for down-regulation to increase the pool of pyruvate, a fatty acid precursor (Smith et al., 2012). In this study, intracellular lipids were elevated by 2.6- to 3.3-fold in the ppsA mutants, with no significant changes in FA profile of

the mutants relative to the wild-type. This suggests that accumulated carbon that is flowed through to pyruvate may be pushed downstream contributing to increased carbon substrates for the synthesis of FAs.

ATP binding cassette transporter G 11 (ABCG11). Although ABCG11 was found to export extracellular FAs in *A. thaliana*, we did not find any secretion phenotype in *S. elongatus* 7942 or *C. reinhardtii*. There could be several possibilities to explain this outcome. Firstly, although genotyping PCR and real-time PCR showed genomic integration and mRNA transcription of the foreign gene, we were unable to prove translation was successful as we cannot identify a specific band for 6X histidine tagged to our gene-of-interests (**Fig. S14**) due to massive contamination by unspecific proteins. This problem is not new to the microalgae field as others have attempted and failed with 6X-his tag for *C. reinhardtii* (Derrien et al., 2012), with the authors ascribing the failure to the occurrence of poly-histidine stretches in hundreds of *Chlamydomonas* proteins. Secondly, if the protein was indeed translated, the localization of the ABCG11 protein was not known. In *A. thaliana*, ABCG11 is localized to the plasma membranes (McFarlane et al., 2010). However, its structure, function, and localization in unicellular cyanobacteria and microalgae is unknown, even as we seek to use codon optimized cDNA sequences for maximum translation potential. Because plant cells consist of a cell wall in addition to a plasma membrane, the interactions between ABCG11 and these structural components may affect its similar function in cell wall-less *S. elongatus* 7942 and *C. reinhardtii*. More

studies into the structure and function of ABCG11 should be conducted, and the relationships between related species elucidated, before its applications in microalgae can be validated (Hwang et al., 2016). Although it is able to homodimerize, ABCG11 is also known to form heterodimers with the ABCG12 transporter in order to export cuticular lipids in *A. thaliana* (McFarlane et al., 2010). Overexpression of ABCG11/12 in concert may be considered as an alternative strategy to facilitate the active secretion of FAs.

In addition to active export of FAs by ABC transporters, alternative strategies for FA secretion include passive diffusion or FA flip flopping across the plasma membrane (Pohl et al., 2005), which is possible through overproduction of intracellular FAs. This has been achieved in *E. coli* via the overexpression of tesA and deletion of ACS (Liu et al., 2012), but is still not reliably proven in *S. elongatus* 7942 or microalgae. As microalgae are eukaryotes which readily convert free FAs to TAGs, the strategy of FA secretion by passive diffusion may not hold much promise. However, FA secretion has been previously observed in *S. cerevisiae* mutants with disruptions in ACS genes, although it mainly stores lipids as TAGs (Michinaka et al., 2003; Leber et al., 2015), suggesting that ACS might be a useful target for FA overproduction leading to secretion in microalgae as well. ACS is responsible for the addition of coenzyme A to a free FA, tagging the resulting acyl-CoA to be used for TAG synthesis. Disruptions in the ACS gene would thus allow the accumulation of free FAs and possibly stimulate the passive diffusion of FAs out of the cell. Microorganisms are also known to

actively export FAs when it accumulates to toxic levels in the cells (Dunlop et al., 2011b). Recently, researchers have been identifying and testing various efflux pumps in *E. coli* (Dunlop et al., 2011a; Doshi et al., 2013; Lennen et al., 2013) which were able to pump out various fuel molecules including FAs, butanol and isopentanol. The approaches employed to identify such proteins primarily involved bioinformatics screening of sequenced genome libraries, followed by genetic deletion or overexpression of native or foreign prokaryotic transporters. A similar approach could be used in cyanobacteria or *C. reinhardtii* to establish novel export proteins which might trigger a secretion phenotype for FAs.

4.5 Conclusion

This study characterized the deletion of ACD and ppsA with FA synthesis in *S. elongatus* PCC 7942. Mutants of *S. elongatus* 7942 deficient in ACD and ppsA showed elevated levels of intracellular lipids while not impacting the capacity for growth. The results suggest that blocking the fatty acid degradation (e.g. β-oxidation) pathway or preventing the backward flow of pyruvate towards gluconeogenesis could lead to increased lipid accumulation in cyanobacteria. Although cyanobacteria offer a promising option as biofuel feedstock, its yield is far below that of other well studied hosts such as *E. coli* and *S. cerevisiae* to be used at an industrial production scale. Cyanobacteria suffer from several disadvantages compared to heterotrophic organisms. Firstly, photosynthetic efficiency is a limiting factor to carbon and energy capture (Subramanian et al.,

2013). Secondly, a high-efficiency expression system must be incorporated for cyanobacteria (Camsund and Lindblad, 2014). Thirdly, in order for energy production to be optimized for biofuels, pathway engineering is needed to redistribute the carbon flux from other storage compounds into FAs (Quintana et al., 2011b). Furthermore, as cyanobacteria are prokaryotes, it should be noted that the observations and conclusions from this study may not apply to eukaryotic microalgae as the latter possess more sophisticated lipid synthesis pathways which include TAG synthesis. Nevertheless, the findings from this project will provide useful strategies for the improved production of biofuels.

Chapter 5 Conclusion and future directions

Microalgae biofuels currently suffers from high capital and operating costs due to low yields and costly extraction methods. Two main bottlenecks in achieving improved yields and decreased costs are: **1)** achieving increased lipid accumulation without sacrificing biomass productivity, and **2)** reducing the costs incurred while extracting lipids from the cells. In this project, we aim to address these issues by first identifying the genes which may contribute to lipid accumulation in microalgae, and subsequently overexpressing these genes to study their impact on lipid productivity. In addition, we seek to induce fatty acid (FA) secretion in cyanobacteria and microalgae by introducing a plant ATP binding cassette (ABC) transporter that is known to secrete long chain FAs.

When the halotolerant microalga *Dunaliella tertiolecta* was subjected to nitrogen depletion (N-depletion), its growth was halted but the starch neutral lipid content per cell increased, suggesting an internal rechanneling of carbon towards starch and triacylglycerol (TAG) accumulation. However, apart from an increased expression of genes in the starch synthesis pathway, its transcriptome signatures are similar to those of *Chalmydomonas reinhardtii* and the oleaginous *Nannochloropsis oceanica*. Genes in the central carbon metabolism pathways, particularly those of the tricarboxylic acid cycle, were simultaneously upregulated, indicating a robust interchange of carbon skeletons for anabolic and catabolic processes. In contrast, fatty acid and triacylglycerol synthesis genes

were downregulated or unchanged. Moreover, the upregulated genes, which include malic enzyme (ME), glucose-6-phosphate dehydrogenase (G6PDH), pyruvate dehydrogenase (PDH), and fatty acyl-ACP thioesterase (TE), appeared to coincide with increased levels of substrates for FA synthesis, namely acetyl-CoA and NADPH. To further substantiate the observations from transcriptome sequencing, we cloned out the genes-of-interest individually for the first time from *D. tertiolecta*. Real-time PCR found that expression of the 4 genes were found to be concurrently upregulated with lipid accumulation in N-depleted conditions, supporting the results obtained from RNAseq. These results suggest that increasing the expression of genes involved in the supply of substrates may be more useful in influencing lipid content than the manipulating the genes in the FA or TAG synthesis pathway.

Despite our continuous efforts, *D. tertiolecta* has proven to be difficult to transform. During the period of this PhD project (2013 – 2016), we have tried different methods to transform *D. tertiolecta*: Electroporation, glass-beads abrasion, *Agrobacterium tumefaciens*-mediated transformation using variations in selective markers including bleomycin, norflurazon, glufosinate ammonium, and varying the concentration of selective markers and media compositions. Although recently scientists have claimed to have used homologous recombination in microalgae (Kilian et al., 2011), it remains to be seen if this could be a reliable and replicable technique for transformation. *D. tertiolecta* presents its own unique challenges as it is halophilic, and the salt concentrations in its media could have

inhibitory effects on the selectable markers, making it increasingly difficult for selection between mutants and wild-types. As genetic transformation in non-model *D. tertiolecta* was repeatedly unsuccessful, the 4 enzymes (DtME, DtG6PDH, DtPDH, DtTE) were overexpressed in the model microalga *C. reinhardtii* to investigate its effects on increasing lipid productivity. When DtME and DtG6PDH were overexpressed, the mutants saw a 30% increase in total lipid content, but overexpression of PDH did not result in changes in lipid levels, likely due to the fact that PDH exists as a part of a multi-protein complex and a foreign PDH subunit may be unable to integrate with the endogenous proteins. On the other hand, the mutant which overexpressed DtTE demonstrated the highest gain in lipid content (56%) without compromising growth, suggesting that relieving the negative feedback of FA synthesis caused by the accumulation of acyl-ACPs might be the rate-limiting step in microalgal lipid production.

The second bottleneck is the costly extraction of lipids from microalgae, where drying of harvested microalgae and extraction of lipids by cell lysis and separation accounts for 70 to 80% of the total cost of production. Here, we introduced a codon-optimized plant ABC protein, ABCG11, which is known to actively secrete FAs from plant cells, into the model cyanobacteria *Synechococcus elongatus* PCC 7942 and *C. reinhardtii*. We hypothesize that ABCG11 would be able to function similarly in cyanobacteria and microalgae as ABC are a well-conserved family of proteins. We were able to increase FA production in the cells from the deletion of genes from competing pathways such

as β-oxidation and glycolysis. Specifically, the knockout of acyl-CoA dehydrogenase (ACD) in *S. elongatus* 7942 led to a 2-fold increase in lipids, while the knockout of phosphoenolpyruvate synthase (ppsA) led to an average 3-fold increase in lipids. Despite the increase in intracellular lipids, we did not find evidence of FA secretion in the external culture media. Lipid secretion by introduction of an exporter protein might be limited by other factors such as protein structure, localization, and functionality specific to the host species. Possible future work could involve investigating the export mechanisms related to FA secretion, the genes involved and its portability to other organisms.

References

Alonso AP, Dale VL, Shachar-Hill Y (2010) Understanding fatty acid synthesis in developing maize embryos using metabolic flux analysis. Metab Eng **12**: 488–97

Alonso AP, Goffman FD, Ohlrogge JB, Shachar-Hill Y (2007) Carbon conversion efficiency and central metabolic fluxes in developing sunflower (Helianthus annuus L.) embryos. Plant J **52**: 296–308

Andre C, Froehlich JE, Moll MR, Benning C (2007) A heteromeric plastidic pyruvate kinase complex involved in seed oil biosynthesis in Arabidopsis. Plant Cell **19**: 2006–22

Antonenkov VD, Hiltunen JK (2006) Peroxisomal membrane permeability and solute transfer. Biochim Biophys Acta - Mol Cell Res **1763**: 1697–1706

Avidan O, Brandis A, Rogachev I, Pick U (2015) Enhanced acetyl-CoA production is associated with increased triglyceride accumulation in the green alga Chlorella desiccata. J Exp Bot **66**: 3725–35

Avidan O, Pick U (2015) Acetyl-CoA synthetase is activated as part of the PDH-bypass in the oleaginous green alga Chlorella desiccata. J Exp Bot **66**: 7287–98

Baud S, Lepiniec L (2010) Physiological and developmental regulation of seed oil production. Prog Lipid Res **49**: 235–49

Beld J, Blatti JL, Behnke C, Mendez M, Burkart MD (2014) Evolution of acyl-ACP-thioesterases and β-ketoacyl-ACP-synthases revealed by protein-protein interactions. J Appl Phycol **26**: 1619–1629

Beld J, Lee DJ, Burkart MD (2015) Fatty acid biosynthesis revisited: structure elucidation and metabolic engineering. Mol Biosyst **11**: 38–59

Bellou S, Aggelis G (2012) Biochemical activities in Chlorella sp. and Nannochloropsis salina during lipid and sugar synthesis in a lab-scale open pond simulating reactor. J Biotechnol **164**: 318–29

Benson PJ, Purcell-Meyerink D, Hocart CH, Truong TT, James GO, Rourke L, Djordjevic MA, Blackburn SI, Price GD (2016) Factors Altering Pyruvate Excretion in a Glycogen Storage Mutant of the Cyanobacterium, Synechococcus PCC7942. Front Microbiol **7**: 475

Berla BM, Saha R, Immethun CM, Maranas CD, Moon TS, Pakrasi HB (2013) Synthetic biology of cyanobacteria: unique challenges and opportunities. Front Microbiol **4**: 246

Berthold P, Schmitt R, Mages W (2002) An engineered Streptomyces hygroscopicus aph 7" gene mediates dominant resistance against hygromycin B in Chlamydomonas reinhardtii. Protist **153**: 401–12

Billini M, Stamatakis K, Sophianopoulou V (2008) Two members of a network of putative Na+/H+ antiporters are involved in salt and pH tolerance of the freshwater cyanobacterium Synechococcus elongatus. J Bacteriol **190**: 6318–29

Bird DA (2008) The role of ABC transporters in cuticular lipid secretion. Plant Sci **174**: 563–569

Bird D, Beisson F, Brigham A, Shin J, Greer S, Jetter R, Kunst L, Wu X, Yephremov A, Samuels L (2007) Characterization of Arabidopsis ABCG11/WBC11, an ATP binding cassette (ABC) transporter that is required for cuticular lipid secretion. Plant J **52**: 485–98

Bišová K, Zachleder V (2014) Cell-cycle regulation in green algae dividing by multiple fission. J Exp Bot **65**: 2585–602

Black PN, DiRusso CC (2003) Transmembrane movement of exogenous long-chain fatty acids: proteins, enzymes, and vectorial esterification. Microbiol Mol Biol Rev **67**: 454–72

Blatti JL, Beld J, Behnke CA, Mendez M, Mayfield SP, Burkart MD (2012) Manipulating fatty acid biosynthesis in microalgae for biofuel through protein-protein interactions. PLoS One **7**: e42949

Blazeck J, Hill A, Liu L, Knight R, Miller J, Pan A, Otoupal P, Alper HS (2014) Harnessing Yarrowia lipolytica lipogenesis to create a platform for lipid and biofuel production. Nat Commun **5**: 3131

de Boer K, Moheimani NR, Borowitzka MA, Bahri PA (2012) Extraction and conversion pathways for microalgae to biodiesel: a review focused on energy consumption. J Appl Phycol **24**: 1681–1698

Bouchard JN, García-Gómez C, Rosario Lorenzo M, Segovia M (2013) Differential effect of ultraviolet exposure (UVR) in the stress response of the Dinophycea Gymnodinium sp. and the Chlorophyta Dunaliella tertiolecta: mortality versus survival. Mar Biol **160**: 2547–2560

Bourgis F, Kilaru A, Cao X, Ngando-Ebongue G-F, Drira N, Ohlrogge JB, Arondel V (2011) Comparative transcriptome and metabolite analysis of oil palm and date palm mesocarp that differ dramatically in carbon partitioning. Proc Natl Acad Sci **108**: 12527–12532

Brennan L, Owende P (2010) Biofuels from microalgae—A review of technologies for production, processing, and extractions of biofuels and co-products. Renew Sustain Energy Rev **14**: 557–577

Cakmak T, Angun P, Demiray YE, Ozkan AD, Elibol Z, Tekinay T (2012) Differential effects of nitrogen and sulfur deprivation on growth and biodiesel feedstock production of Chlamydomonas reinhardtii. Biotechnol Bioeng **109**: 1947–57

Camsund D, Lindblad P (2014) Engineered transcriptional systems for cyanobacterial biotechnology. Front Bioeng Biotechnol **2**: 40

Castruita M, Casero D, Karpowicz SJ, Kropat J, Vieler A, Hsieh SI, Yan W, Cokus S, Loo JA, Benning C, et al (2011) Systems biology approach in Chlamydomonas reveals connections between copper nutrition and multiple metabolic steps. Plant Cell **23**: 1273–92

Cavonius LR, Carlsson NG, Undeland I (2014) Quantification of total fatty acids in microalgae: Comparison of extraction and transesterification methods. Anal Bioanal Chem **406**: 7313–7322

Chapman KD, Dyer JM, Mullen RT (2013) Commentary: why don't plant leaves get fat? Plant Sci **207**: 128–34

Chen B, Ling H, Chang MW (2013) Transporter engineering for improved tolerance against alkane biofuels in Saccharomyces cerevisiae. Biotechnol Biofuels **6**: 21

Chen H, Hao G, Wang L, Wang H, Gu Z, Liu L, Zhang H, Chen W, Chen YQ (2015a) Identification of a critical determinant that enables efficient fatty acid synthesis in oleaginous fungi. Sci Rep **5**: 11247

Chen JE, Smith AG (2012) A look at diacylglycerol acyltransferases (DGATs) in algae. J Biotechnol **162**: 28–39

Chen T, Liu J, Guo B, Ma X, Sun P, Liu B, Chen F (2015b) Light attenuates lipid accumulation while enhancing cell proliferation and starch synthesis in the glucose-fed oleaginous microalga Chlorella zofingiensis. Sci Rep **5**: 14936

Chitlaru E, Pick U (1991) Regulation of glycerol synthesis in response to osmotic changes in dunaliella. Plant Physiol **96**: 50–60

Cho H, Cronan JE (1995) Defective export of a periplasmic enzyme disrupts regulation of fatty acid synthesis. J Biol Chem **270**: 4216–9

Choi YJ, Lee SY (2013) Microbial production of short-chain alkanes. Nature **502**: 571–574

Chow Y, Tu WY, Wang D, Ng DHP, Lee YK (2015) The role of micronutrients and strategies for optimized continual glycerol production from carbon dioxide by Dunaliella tertiolecta. Biotechnol Bioeng **112**: 2163–71

Chow YYS, Goh SJM, Su Z, Ng DHP, Lim CY, Lim NYN, Lin H, Fang L,

Lee YK (2013) Continual production of glycerol from carbon dioxide by Dunaliella tertiolecta. Bioresour Technol **136**: 550–555

Chung C, You J, Kim K, Moon Y, Kim H, Ahn J, Andersen C, Angkawidjaja C, Kanaya S, Koronakis E, et al (2009) Export of recombinant proteins in Escherichia coli using ABC transporter with an attached lipase ABC transporter recognition domain (LARD). Microb Cell Fact **8**: 11

Clerico EM, Ditty JL, Golden SS (2007) Specialized techniques for site-directed mutagenesis in cyanobacteria. Methods Mol Biol **362**: 155–71

Courchesne NMD, Parisien A, Wang B, Lan CQ (2009) Enhancement of lipid production using biochemical, genetic and transcription factor engineering approaches. J Biotechnol **141**: 31–41

Davey MP, Horst I, Duong G-H, Tomsett E V, Litvinenko ACP, Howe CJ, Smith AG (2014) Triacylglyceride production and autophagous responses in Chlamydomonas reinhardtii depend on resource allocation and carbon source. Eukaryot Cell **13**: 392–400

Davidi L, Katz A, Pick U (2012) Characterization of major lipid droplet proteins from Dunaliella. Planta **236**: 19–33

Davis MS, Cronan JE (2001) Inhibition of Escherichia coli acetyl coenzyme A carboxylase by acyl-acyl carrier protein. J Bacteriol **183**: 1499–503

Dehesh K, Tai H, Edwards P, Byrne J, Jaworski JG (2001) Overexpression of 3-ketoacyl-acyl-carrier protein synthase IIIs in plants reduces the rate of lipid synthesis. Plant Physiol **125**: 1103–14

Delrue F, Li-Beisson Y, Setier P-A, Sahut C, Roubaud A, Froment A-K, Peltier G (2013) Comparison of various microalgae liquid biofuel production pathways based on energetic, economic and environmental criteria. Bioresour Technol **136**: 205–12

Delrue F, Setier P-A, Sahut C, Cournac L, Roubaud A, Peltier G, Froment A-K (2012) An economic, sustainability, and energetic model of biodiesel production from microalgae. Bioresour Technol **111**: 191–200

Derrien B, Majeran W, Effantin G, Ebenezer J, Friso G, van Wijk KJ, Steven AC, Maurizi MR, Vallon O (2012) The purification of the Chlamydomonas reinhardtii chloroplast ClpP complex: additional subunits and structural features. Plant Mol Biol **80**: 189–202

Desbois AP, Smith VJ (2010) Antibacterial free fatty acids: activities, mechanisms of action and biotechnological potential. Appl Microbiol Biotechnol **85**: 1629–42

Díaz-Santos E, de la Vega M, Vila M, Vigara J, León R (2013) Efficiency of different heterologous promoters in the unicellular microalga

Chlamydomonas reinhardtii. Biotechnol Prog **29**: 319–28

Dobin A, Davis CA, Schlesinger F, Drenkow J, Zaleski C, Jha S, Batut P, Chaisson M, Gingeras TR (2013) STAR: Ultrafast universal RNA-seq aligner. Bioinformatics **29**: 15–21

Dong H-P, Williams E, Wang D, Xie Z-X, Hsia R, Jenck A, Halden R, Li J, Chen F, Place AR (2013) Responses of Nannochloropsis oceanica IMET1 to Long-Term Nitrogen Starvation and Recovery. Plant Physiol **162**: 1110–26

Doron L, Segal N, Shapira M (2016) Transgene Expression in Microalgae—From Tools to Applications. Front Plant Sci **7**: 505

Doshi R, Nguyen T, Chang G (2013) Transporter-mediated biofuel secretion. Proc Natl Acad Sci **110**: 7642–7647

Dubini A, Mus F, Seibert M, Grossman AR, Posewitz MC (2009) Flexibility in anaerobic metabolism as revealed in a mutant of Chlamydomonas reinhardtii lacking hydrogenase activity. J Biol Chem **284**: 7201–13

Dunahay TG, Jarvis EE, Roessler PG (1995) GENETIC TRANSFORMATION OF THE DIATOMS CYCLOTELLA CRYPTICA AND NAVICULA SAPROPHILA1. J Phycol **31**: 1004–1012

Dunlop MJ, Dossani ZY, Szmidt HL, Chu HC, Lee TS, Keasling JD, Hadi MZ, Mukhopadhyay A (2011a) Engineering microbial biofuel tolerance and export using efflux pumps. Mol Syst Biol **7**: 487

Dunlop MJ, Fischer C, Klein-Marcuschamer D, Stephanopoulos G, Fortman J, Chhabra S, Mukhopadhyay A, Chou H, Lee T, Steen E, et al (2011b) Engineering microbes for tolerance to next-generation biofuels. Biotechnol Biofuels **4**: 32

Fan J, Andre C, Xu C (2011) A chloroplast pathway for the de novo biosynthesis of triacylglycerol in Chlamydomonas reinhardtii. FEBS Lett **585**: 1985–91

Fan J, Cui Y, Wan M, Wang W, Li Y (2014) Lipid accumulation and biosynthesis genes response of the oleaginous Chlorella pyrenoidosa under three nutrition stressors. Biotechnol Biofuels **7**: 17

Fan J, Ning K, Zeng X, Luo Y, Wang D, Hu J, Li J, Xu H, Huang J, Wan M, et al (2015) Genomic Foundation of Starch-to-Lipid Switch in Oleaginous Chlorella spp. Plant Physiol **169**: 2444–61

Fang L, Lin HX, Low CS, Wu MH, Chow Y, Lee YK (2012) Expression of the Chlamydomonas reinhardtii sedoheptulose-1,7-bisphosphatase in Dunaliella bardawil leads to enhanced photosynthesis and increased glycerol production. Plant Biotechnol J **10**: 1129–35

Fatland B, Anderson M, Nikolau BJ, Wurtele ES (2000) Molecular biology of cytosolic acetyl-CoA generation. Biochem Soc Trans **28**: 593–5

Fatland BL, Ke J, Anderson MD, Mentzen WI, Cui LW, Allred CC, Johnston JL, Nikolau BJ, Wurtele ES (2002) Molecular characterization of a heteromeric ATP-citrate lyase that generates cytosolic acetyl-coenzyme A in Arabidopsis. Plant Physiol **130**: 740–56

Feng P, Deng Z, Fan L, Hu Z (2012) Lipid accumulation and growth characteristics of Chlorella zofingiensis under different nitrate and phosphate concentrations. J Biosci Bioeng **114**: 405–10

Flügge U-I, Häusler RE, Ludewig F, Gierth M (2011) The role of transporters in supplying energy to plant plastids. J Exp Bot **62**: 2381–92

Francisco ÉC, Neves DB, Jacob-Lopes E, Franco TT (2010) Microalgae as feedstock for biodiesel production: Carbon dioxide sequestration, lipid production and biofuel quality. J Chem Technol Biotechnol **85**: 395–403

Franz AK, Danielewicz MA, Wong DM, Anderson LA, Boothe JR (2013) Phenotypic screening with oleaginous microalgae reveals modulators of lipid productivity. ACS Chem Biol **8**: 1053–62

Furumoto T, Yamaguchi T, Ohshima-Ichie Y, Nakamura M, Tsuchida-Iwata Y, Shimamura M, Ohnishi J, Hata S, Gowik U, Westhoff P, et al (2011) A plastidial sodium-dependent pyruvate transporter. Nature **476**: 472–5

Gao X, Gu H, Li G, Rye K-A, Zhang D-W (2012) Identification of an amino acid residue in ATP-binding cassette transport G1 critical for mediating cholesterol efflux. Biochim Biophys Acta **1821**: 552–9

Gardeström P, Igamberdiev AU, Raghavendra AS (2002) Mitochondrial Functions in the Light and Significance to Carbon-Nitrogen Interactions. Photosynth. Nitrogen Assim. Assoc. Carbon Respir. Metab. Kluwer Academic Publishers, Dordrecht, pp 151–172

Gargouri M, Park J-J, Holguin FO, Kim M-J, Wang H, Deshpande RR, Shachar-Hill Y, Hicks LM, Gang DR (2015) Identification of regulatory network hubs that control lipid metabolism in Chlamydomonas reinhardtii. J Exp Bot **66**: 4551–66

Geider R, Macintyre, Graziano L, McKay RM (1998) Responses of the photosynthetic apparatus of *Dunaliella tertiolecta* (Chlorophyceae) to nitrogen and phosphorus limitation. Eur J Phycol **33**: 315–332

Georgianna DR, Hannon MJ, Marcuschi M, Wu S, Botsch K, Lewis AJ, Hyun J, Mendez M, Mayfield SP (2013) Production of recombinant enzymes in the marine alga Dunaliella tertiolecta. Algal Res **2**: 2–9

Ghoshal D, Mach D, Agarwal M, Goyal A, Goyal A (2002) Osmoregulatory

isoform of dihydroxyacetone phosphate reductase from Dunaliella tertiolecta: purification and characterization. Protein Expr Purif **24**: 404–11

Go YS, Kim H, Kim HJ, Suh MC (2014) Arabidopsis Cuticular Wax Biosynthesis Is Negatively Regulated by the DEWAX Gene Encoding an AP2/ERF-Type Transcription Factor. Plant Cell **26**: 1666–1680

Goncalves EC, Koh J, Zhu N, Yoo M-J, Chen S, Matsuo T, Johnson J V, Rathinasabapathi B (2016a) Nitrogen starvation-induced accumulation of triacylglycerol in the green algae: evidence for a role for ROC40, a transcription factor involved in circadian rhythm. Plant J **85**: 743–57

Goncalves EC, Wilkie AC, Kirst M, Rathinasabapathi B (2016b) Metabolic regulation of triacylglycerol accumulation in the green algae: identification of potential targets for engineering to improve oil yield. Plant Biotechnol J **14**: 1649–1660

Gong Y, Guo X, Wan X, Liang Z, Jiang M (2011) Characterization of a novel thioesterase (PtTE) from Phaeodactylum tricornutum. J Basic Microbiol **51**: 666–72

Goodson C, Roth R, Wang ZT, Goodenough U (2011) Structural correlates of cytoplasmic and chloroplast lipid body synthesis in Chlamydomonas reinhardtii and stimulation of lipid body production with acetate boost. Eukaryot Cell **10**: 1592–606

Gopalakrishnan S, Baker J, Kristoffersen L, Betenbaugh MJ (2015) Redistribution of metabolic fluxes in Chlorella protothecoides by variation of media nitrogen concentration. Metab Eng Commun **2**: 124–131

Gouveia L, Oliveira AC (2009) Microalgae as a raw material for biofuels production. J Ind Microbiol Biotechnol **36**: 269–74

Griffiths MJ, Harrison STL (2009) Lipid productivity as a key characteristic for choosing algal species for biodiesel production. J Appl Phycol **21**: 493–507

Halim R, Danquah MK, Webley PA (2012) Extraction of oil from microalgae for biodiesel production: A review. Biotechnol Adv **30**: 709–32

Hamilton JA (2007) New insights into the roles of proteins and lipids in membrane transport of fatty acids. Prostaglandins Leukot Essent Fatty Acids **77**: 355–61

Hao G, Chen H, Wang L, Gu Z, Song Y, Zhang H, Chen W, Chen YQ (2014) Role of malic enzyme during fatty acid synthesis in the oleaginous fungus Mortierella alpina. Appl Environ Microbiol **80**: 2672–8

He Q, Qiao D, Bai L, Zhang Q, Yang W, Li Q, Cao Y (2007) Cloning and characterization of a plastidic glycerol 3-phosphate dehydrogenase cDNA from Dunaliella salina. J Plant Physiol **164**: 214–20

He Y, Meng X, Fan Q, Sun X, Xu Z, Song R (2009) Cloning and characterization of two novel chloroplastic glycerol-3-phosphate dehydrogenases from Dunaliella viridis. Plant Mol Biol **71**: 193–205

Heath RJ, Rock CO (1996a) Inhibition of beta-ketoacyl-acyl carrier protein synthase III (FabH) by acyl-acyl carrier protein in Escherichia coli. J Biol Chem **271**: 10996–1000

Heath RJ, Rock CO (1996b) Regulation of fatty acid elongation and initiation by acyl-acyl carrier protein in Escherichia coli. J Biol Chem **271**: 1833–6

Hempel N, Petrick I, Behrendt F (2012) Biomass productivity and productivity of fatty acids and amino acids of microalgae strains as key characteristics of suitability for biodiesel production. J Appl Phycol **24**: 1407–1418

Herrera-Valencia VA, Macario-González LA, Casais-Molina ML, Beltran-Aguilar AG, Peraza-Echeverría S (2012) In silico cloning and characterization of the glycerol-3-phosphate dehydrogenase (GPDH) gene family in the green microalga Chlamydomonas reinhardtii. Curr Microbiol **64**: 477–85

Higgins CF (1992) ABC transporters: from microorganisms to man. Annu Rev Cell Biol **8**: 67–113

Hockin NL, Mock T, Mulholland F, Kopriva S, Malin G (2012) The response of diatom central carbon metabolism to nitrogen starvation is different from that of green algae and higher plants. Plant Physiol **158**: 299–312

Hohl M, Briand C, Grütter MG, Seeger MA (2012) Crystal structure of a heterodimeric ABC transporter in its inward-facing conformation. Nat Struct Mol Biol **19**: 395–402

Hosseini Tafreshi A, Shariati M (2009) *Dunaliella* biotechnology: methods and applications. J Appl Microbiol **107**: 14–35

Howard TP, Middelhaufe S, Moore K, Edner C, Kolak DM, Taylor GN, Parker DA, Lee R, Smirnoff N, Aves SJ, et al (2013) Synthesis of customized petroleum-replica fuel molecules by targeted modification of free fatty acid pools in Escherichia coli. Proc Natl Acad Sci **110**: 7636–7641

Hu Q, Sommerfeld M, Jarvis E, Ghirardi M, Posewitz M, Seibert M, Darzins A (2008) Microalgal triacylglycerols as feedstocks for biofuel production: perspectives and advances. Plant J **54**: 621–39

Hutchings D, Rawsthorne S, Emes MJ (2005) Fatty acid synthesis and the oxidative pentose phosphate pathway in developing embryos of oilseed rape (Brassica napus L.). J Exp Bot **56**: 577–85

Hwang J-U, Song W-Y, Hong D, Ko D, Yamaoka Y, Jang S, Yim S, Lee E, Khare D, Kim K, et al (2016) Plant ABC Transporters Enable Many

Unique Aspects of a Terrestrial Plant's Lifestyle. Mol Plant **9**: 338–355

Hynes MJ, Murray SL (2010) ATP-citrate lyase is required for production of cytosolic acetyl coenzyme A and development in Aspergillus nidulans. Eukaryot Cell **9**: 1039–48

Ibáñez-Salazar A, Rosales-Mendoza S, Rocha-Uribe A, Ramírez-Alonso JI, Lara-Hernández I, Hernández-Torres A, Paz-Maldonado LMT, Silva-Ramírez AS, Bañuelos-Hernández B, Martínez-Salgado JL, et al (2014) Over-expression of Dof-type transcription factor increases lipid production in Chlamydomonas reinhardtii. J Biotechnol **184**: 27–38

Ikaran Z, Suárez-Alvarez S, Urreta I, Castañón S (2015) The effect of nitrogen limitation on the physiology and metabolism of chlorella vulgaris var L3. Algal Res **10**: 134–144

Imamura S, Kawase Y, Kobayashi I, Sone T, Era A, Miyagishima S-Y, Shimojima M, Ohta H, Tanaka K (2015) Target of rapamycin (TOR) plays a critical role in triacylglycerol accumulation in microalgae. Plant Mol Biol **89**: 309–18

Jako C, Kumar A, Wei Y, Zou J, Barton DL, Giblin EM, Covello PS, Taylor DC (2001) Seed-specific over-expression of an Arabidopsis cDNA encoding a diacylglycerol acyltransferase enhances seed oil content and seed weight. Plant Physiol **126**: 861–74

James GO, Hocart CH, Hillier W, Chen H, Kordbacheh F, Price GD, Djordjevic MA (2011) Fatty acid profiling of Chlamydomonas reinhardtii under nitrogen deprivation. Bioresour Technol **102**: 3343–3351

Janßen H, Steinbüchel A, Antoni D, Zverlov V, Schwarz W, Uthoff S, Bröker D, Steinbüchel A, Madhavan A, Srivastava A, et al (2014) Fatty acid synthesis in Escherichia coli and its applications towards the production of fatty acid based biofuels. Biotechnol Biofuels **7**: 7

Jeffrey SW, Humphrey GF (1975) New spectrophotometric equations for determining chlorophylls a, b, c1 and c2 in higher plants, algae and natural phytoplankton. Biochem Physiol Pflanz BPP

Jiang P, Cronan JE (1994) Inhibition of fatty acid synthesis in Escherichia coli in the absence of phospholipid synthesis and release of inhibition by thioesterase action. J Bacteriol **176**: 2814–21

Johnson PE, Fox SR, Hills MJ, Rawsthorne S (2000) Inhibition by long-chain acyl-CoAs of glucose 6-phosphate metabolism in plastids isolated from developing embryos of oilseed rape (Brassica napus L.). Biochem J **348 Pt 1**: 145–50

Johnson X, Alric J (2013) Central carbon metabolism and electron transport in

Chlamydomonas reinhardtii: metabolic constraints for carbon partitioning between oil and starch. Eukaryot Cell **12**: 776–93

Johnston ML, Luethy MH, Miernyk JA, Randall DD (1997) Cloning and molecular analyses of the Arabidopsis thaliana plastid pyruvate dehydrogenase subunits. Biochim Biophys Acta **1321**: 200–6

Jones A, Davies HM, Voelker TA (1995) Palmitoyl-Acyl Carrier Protein (ACP) Thioesterase and the Evolutionary Origin of Plant Acyl-ACP Thioesterases. PLANT CELL ONLINE **7**: 359–371

Jung J, Lim JH, Kim SY, Im D-K, Seok JY, Lee S-J V, Oh M-K, Jung GY (2016) Precise precursor rebalancing for isoprenoids production by fine control of gapA expression in Escherichia coli. Metab Eng. doi: 10.1016/j.ymben.2016.10.003

Kaczmarzyk D, Fulda M (2010) Fatty acid activation in cyanobacteria mediated by acyl-acyl carrier protein synthetase enables fatty acid recycling. Plant Physiol **152**: 1598–610

KaiXian Q, Borowitzka MA (1993) Light and nitrogen deficiency effects on the growth and composition ofPhaeodactylum tricornutum. Appl Biochem Biotechnol **38**: 93–103

Kamalanathan M, Pierangelini M, Shearman LA, Gleadow R, Beardall J (2016) Impacts of nitrogen and phosphorus starvation on the physiology of Chlamydomonas reinhardtii. J Appl Phycol **28**: 1509–1520

Kang F, Rawsthorne S (1994) Starch and fatty acid synthesis in plastids from developing embryos of oilseed rape (Brassica napus L.). Plant J **6**: 795–805

Kang F, Rawsthorne S (1996) Metabolism of glucose-6-phosphate and utilization of multiple metabolites for fatty acid synthesis by plastids from developing oilseed rape embryos. Planta **199**: 321–327

Ke J, Behal RH, Back SL, Nikolau BJ, Wurtele ES, Oliver DJ (2000) The role of pyruvate dehydrogenase and acetyl-coenzyme A synthetase in fatty acid synthesis in developing Arabidopsis seeds. Plant Physiol **123**: 497–508

Kilian O, Benemann CSE, Niyogi KK, Vick B (2011) High-efficiency homologous recombination in the oil-producing alga Nannochloropsis sp. Proc Natl Acad Sci U S A **108**: 21265–9

Kim S-H, Liu K-H, Lee S-Y, Hong S-J, Cho B-K, Lee H, Lee C-G, Choi H-K (2013) Effects of light intensity and nitrogen starvation on glycerolipid, glycerophospholipid, and carotenoid composition in Dunaliella tertiolecta culture. PLoS One **8**: e72415

Kindle KL (1990) High-frequency nuclear transformation of Chlamydomonas reinhardtii. Proc Natl Acad Sci U S A **87**: 1228–32

Kinoshita H, Nagasaki J, Yoshikawa N, Yamamoto A, Takito S, Kawasaki M, Sugiyama T, Miyake H, Weber APM, Taniguchi M (2011) The chloroplastic 2-oxoglutarate/malate transporter has dual function as the malate valve and in carbon/nitrogen metabolism. Plant J **65**: 15–26

Kosa M, Ragauskas AJ (2011) Lipids from heterotrophic microbes: advances in metabolism research. Trends Biotechnol **29**: 53–61

Kruger NJ, von Schaewen A (2003) The oxidative pentose phosphate pathway: structure and organisation. Curr Opin Plant Biol **6**: 236–46

Lane TS, Rempe CS, Davitt J, Staton ME, Peng Y, Soltis DE, Melkonian M, Deyholos M, Leebens-Mack JH, Chase M, et al (2016) Diversity of ABC transporter genes across the plant kingdom and their potential utility in biotechnology. BMC Biotechnol **16**: 47

Lardizabal K, Effertz R, Levering C, Mai J, Pedroso MC, Jury T, Aasen E, Gruys K, Bennett K (2008) Expression of Umbelopsis ramanniana DGAT2A in seed increases oil in soybean. Plant Physiol **148**: 89–96

Largeau C, Casadevall E, Berkaloff C (1980a) The biosynthesis of long-chain hydrocarbons in the green alga Botryococcus braunii. Phytochemistry **19**: 1081–1085

Largeau C, Casadevall E, Berkaloff C, Dhamelincourt P (1980b) Sites of accumulation and composition of hydrocarbons in Botryococcus braunii. Phytochemistry **19**: 1043–1051

Laurens LML, Quinn M, Van Wychen S, Templeton DW, Wolfrum EJ (2012) Accurate and reliable quantification of total microalgal fuel potential as fatty acid methyl esters by in situ transesterification. Anal Bioanal Chem **403**: 167–78

Leber C, Polson B, Fernandez-Moya R, Da Silva NA (2015) Overproduction and secretion of free fatty acids through disrupted neutral lipid recycle in Saccharomyces cerevisiae. Metab Eng **28**: 54–62

Lee SY, Kim SH, Hyun SH, Suh HW, Hong SJ, Cho BK, Lee CG, Lee H, Choi HK (2014) Fatty acids and global metabolites profiling of Dunaliella tertiolecta by shifting culture conditions to nitrate deficiency and high light at different growth phases. Process Biochem **49**: 996–1004

Lei A, Chen H, Shen G, Hu Z, Chen L, Wang J (2012) Expression of fatty acid synthesis genes and fatty acid accumulation in haematococcus pluvialis under different stressors. Biotechnol Biofuels **5**: 18

Lennen RM, Politz MG, Kruziki MA, Pfleger BF (2013) Identification of Transport Proteins Involved in Free Fatty Acid Efflux in Escherichia coli. J Bacteriol **195**: 135–144

Leong S, Yew C, Lay Peng L, Siew Moon C, Kok Wai Kit J, Teo Lay Ming S (2015) Three new records of dinoflagellates in Singapore's coastal waters, with observations on environmental conditions associated with microalgal growth in the Johor Straits.

Levitan O, Dinamarca J, Zelzion E, Lun DS, Guerra LT, Kim MK, Kim J, Van Mooy BAS, Bhattacharya D, Falkowski PG (2015) Remodeling of intermediate metabolism in the diatom Phaeodactylum tricornutum under nitrogen stress. Proc Natl Acad Sci U S A **112**: 412–7

Li J, Han D, Wang D, Ning K, Jia J, Wei L, Jing X, Huang S, Chen J, Li Y, et al (2014) Choreography of Transcriptomes and Lipidomes of Nannochloropsis Reveals the Mechanisms of Oil Synthesis in Microalgae. Plant Cell **26**: 1645–1665

Li Y, Han D, Hu G, Sommerfeld M, Hu Q (2010) Inhibition of starch synthesis results in overproduction of lipids in Chlamydomonas reinhardtii. Biotechnol Bioeng **107**: 258–68

Li Y, Han D, Sommerfeld M, Hu Q (2011) Photosynthetic carbon partitioning and lipid production in the oleaginous microalga Pseudochlorococcum sp. (Chlorophyceae) under nitrogen-limited conditions. Bioresour Technol **102**: 123–9

Li Z, Sun H, Mo X, Li X, Xu B, Tian P (2013) Overexpression of malic enzyme (ME) of Mucor circinelloides improved lipid accumulation in engineered Rhodotorula glutinis. Appl Microbiol Biotechnol **97**: 4927–36

Liang M-H, Jiang J-G (2013) Advancing oleaginous microorganisms to produce lipid via metabolic engineering technology. Prog Lipid Res **52**: 395–408

Liao JC, Farmer WR (2000) Improving lycopene production in Escherichia coli by engineering metabolic control. Nat Biotechnol **18**: 533–537

Lichtenthaler HK, Golz A (1995) Chemical Regulation of Acetyl-Coa Formation and De Novo Fatty Acid Biosynthesis in Plants. Plant Lipid Metab. Springer Netherlands, Dordrecht, pp 58–60

Lin H, Fang L, Low CS, Chow Y, Lee YK (2013) Occurrence of glycerol uptake in *Dunaliella tertiolecta* under hyperosmotic stress. FEBS J **280**: 1064–1072

Lin M, Oliver DJ (2008) The role of acetyl-coenzyme a synthetase in Arabidopsis. Plant Physiol **147**: 1822–9

Ling H, Chen B, Kang A, Lee J-M, Chang MW (2013) Transcriptome response to alkane biofuels in Saccharomyces cerevisiae: identification of efflux pumps involved in alkane tolerance. Biotechnol Biofuels **6**: 95

Linton KJ (2007) Structure and function of ABC transporters. Physiology

(Bethesda) **22**: 122–30

Liska AJ, Shevchenko A, Pick U, Katz A (2004) Enhanced photosynthesis and redox energy production contribute to salinity tolerance in Dunaliella as revealed by homology-based proteomics. Plant Physiol **136**: 2806–17

Liu B, Benning C (2013) Lipid metabolism in microalgae distinguishes itself. Curr Opin Biotechnol **24**: 300–9

Liu H, Yu C, Feng D, Cheng T, Meng X, Liu W, Zou H, Xian M, Li Q, Du W, et al (2012) Production of extracellular fatty acid using engineered Escherichia coli. Microb Cell Fact **11**: 41

Liu J, Huang J, Sun Z, Zhong Y, Jiang Y, Chen F (2011a) Differential lipid and fatty acid profiles of photoautotrophic and heterotrophic Chlorella zofingiensis: assessment of algal oils for biodiesel production. Bioresour Technol **102**: 106–10

Liu K, Hu H, Wang W, Zhang X (2016) Genetic engineering of Pseudomonas chlororaphis GP72 for the enhanced production of 2-Hydroxyphenazine. Microb Cell Fact **15**: 131

Liu X, Sheng J, Curtiss R (2011b) Fatty acid production in genetically modified cyanobacteria. Proc Natl Acad Sci U S A **108**: 6899–904

Lonien J, Schwender J (2009) Analysis of metabolic flux phenotypes for two Arabidopsis mutants with severe impairment in seed storage lipid synthesis. Plant Physiol **151**: 1617–34

López García de Lomana A, Schäuble S, Valenzuela J, Imam S, Carter W, Bilgin DD, Yohn CB, Turkarslan S, Reiss DJ, Orellana M V, et al (2015) Transcriptional program for nitrogen starvation-induced lipid accumulation in Chlamydomonas reinhardtii. Biotechnol Biofuels **8**: 207

LORENZEN CJ (1967) DETERMINATION OF CHLOROPHYLL AND PHEO-PIGMENTS: SPECTROPHOTOMETRIC EQUATIONS1. Limnol Oceanogr **12**: 343–346

Lu X, Vora H, Khosla C (2008) Overproduction of free fatty acids in E. coli: implications for biodiesel production. Metab Eng **10**: 333–9

Lv H, Qu G, Qi X, Lu L, Tian C, Ma Y (2013) Transcriptome analysis of Chlamydomonas reinhardtii during the process of lipid accumulation. Genomics **101**: 229–237

Ma Y-H, Wang X, Niu Y-F, Yang Z-K, Zhang M-H, Wang Z-M, Yang W-D, Liu J-S, Li H-Y (2014) Antisense knockdown of pyruvate dehydrogenase kinase promotes the neutral lipid accumulation in the diatom Phaeodactylum tricornutum. Microb Cell Fact **13**: 100

Malcata FX (2011) Microalgae and biofuels: A promising partnership? Trends Biotechnol **29**: 542–549

Martin GJO, Hill DRA, Olmstead ILD, Bergamin A, Shears MJ, Dias DA, Kentish SE, Scales PJ, Botté CY, Callahan DL (2014) Lipid profile remodeling in response to nitrogen deprivation in the microalgae Chlorella sp. (Trebouxiophyceae) and Nannochloropsis sp. (Eustigmatophyceae). PLoS One **9**: e103389

McCormick NE, Jakeman DL (2015) On the mechanism of phosphoenolpyruvate synthetase (PEPs) and its inhibition by sodium fluoride: potential magnesium and aluminum fluoride complexes of phosphoryl transfer. Biochem Cell Biol **93**: 236–40

McFarlane HE, Shin JJH, Bird DA, Samuels AL (2010) Arabidopsis ABCG transporters, which are required for export of diverse cuticular lipids, dimerize in different combinations. Plant Cell **22**: 3066–75

Meier JL, Barrows-Yano T, Foley TL, Wike CL, Burkart MD (2008) The unusual macrocycle forming thioesterase of mycolactone. Mol Biosyst **4**: 663–71

Meng X, Shang H, Zheng Y, Zhang Z (2013) Free fatty acid secretion by an engineered strain of Escherichia coli. Biotechnol Lett **35**: 2099–103

Meng X, Yang J, Cao Y, Li L, Jiang X, Xu X, Liu W, Xian M, Zhang Y (2011) Increasing fatty acid production in E. coli by simulating the lipid accumulation of oleaginous microorganisms. J Ind Microbiol Biotechnol **38**: 919–25

Mercer P, Armenta RE (2011) Developments in oil extraction from microalgae. Eur J Lipid Sci Technol **113**: 539–547

Metzger P, Largeau C (2005) Botryococcus braunii: a rich source for hydrocarbons and related ether lipids. Appl Microbiol Biotechnol **66**: 486–96

Michinaka Y, Shimauchi T, Aki T, Nakajima T, Kawamoto S, Shigeta S, Suzuki O, Ono K (2003) Extracellular secretion of free fatty acids by disruption of a fatty acyl-CoA synthetase gene in Saccharomyces cerevisiae. J Biosci Bioeng **95**: 435–40

Miller R, Wu G, Deshpande RR, Vieler A, Gärtner K, Li X, Moellering ER, Zäuner S, Cornish AJ, Liu B, et al (2010) Changes in transcript abundance in Chlamydomonas reinhardtii following nitrogen deprivation predict diversion of metabolism. Plant Physiol **154**: 1737–52

Moellering ER, Benning C (2010) RNA interference silencing of a major lipid droplet protein affects lipid droplet size in Chlamydomonas reinhardtii. Eukaryot Cell **9**: 97–106

Molina Grima E, Belarbi E-H, Acién Fernández F., Robles Medina A, Chisti Y (2003) Recovery of microalgal biomass and metabolites: process options and economics. Biotechnol Adv **20**: 491–515

Møller SG (2005) Plastids. Blackwell

Moody JW, McGinty CM, Quinn JC (2014) Global evaluation of biofuel potential from microalgae. Proc Natl Acad Sci U S A **111**: 8691–6

Morowvat MH, Rasoul-Amini S, Ghasemi Y (2010) Chlamydomonas as a "new" organism for biodiesel production. Bioresour Technol. doi: 10.1016/j.biortech.2009.11.032

Moussatova A, Kandt C, O'Mara ML, Tieleman DP (2008) ATP-binding cassette transporters in Escherichia coli. Biochim Biophys Acta - Biomembr **1778**: 1757–1771

Nagle N, Lemke P (1990) Production of methyl ester fuel from microalgae. Appl Biochem Biotechnol **24**–**25**: 355–361

Nguyen HM, Baudet M, Cuiné S, Adriano J-M, Barthe D, Billon E, Bruley C, Beisson F, Peltier G, Ferro M, et al (2011) Proteomic profiling of oil bodies isolated from the unicellular green microalga Chlamydomonas reinhardtii: with focus on proteins involved in lipid metabolism. Proteomics **11**: 4266–73

Nikookar K, Moradshahi A, Hosseini L (2005) Physiological responses of Dunaliella salina and Dunaliella tertiolecta to copper toxicity. Biomol Eng **22**: 141–146

Nishida I (2004) Plastid Metabolic Pathways for Fatty Acid Metabolism. Mol. Biol. Biotechnol. Plant Organelles. Springer Netherlands, Dordrecht, pp 543–564

Noor E, Eden E, Milo R, Alon U, Alberty RA, Alon U, Andrews KJ, Hegeman GD, Beg QK, Vazquez A, et al (2010) Central carbon metabolism as a minimal biochemical walk between precursors for biomass and energy. Mol Cell **39**: 809–20

Oren A (2014) The ecology of Dunaliella in high-salt environments. J Biol Res (Thessalonikē, Greece) **21**: 23

Pape M, Lambertz C, Happe T, Hemschemeier A (2012) Differential expression of the Chlamydomonas [FeFe]-hydrogenase-encoding HYDA1 gene is regulated by the copper response regulator1. Plant Physiol **159**: 1700–12

Park J-J, Wang H, Gargouri M, Deshpande RR, Skepper JN, Holguin FO, Juergens MT, Shachar-Hill Y, Hicks LM, Gang DR (2015) The response of Chlamydomonas reinhardtii to nitrogen deprivation: a systems biology

analysis. Plant J **81**: 611–24

Park Y, Moon Y, Ryoo J, Kim N, Cho H, Ahn J, Delepelaire P, Delepelaire P, Dinh T, Paulsen I, et al (2012) Identification of the minimal region in lipase ABC transporter recognition domain of Pseudomonas fluorescens for secretion and fluorescence of green fluorescent protein. Microb Cell Fact **11**: 60

Patnaik R, Roof WD, Young RF, Liao JC (1992) Stimulation of glucose catabolism in Escherichia coli by a potential futile cycle. J Bacteriol **174**: 7527–32

Pinto F, Pacheco CC, Ferreira D, Moradas-Ferreira P, Tamagnini P (2012) Selection of suitable reference genes for RT-qPCR analyses in cyanobacteria. PLoS One **7**: e34983

Pleite R, Pike MJ, Garcés R, Martínez-Force E, Rawsthorne S (2005) The sources of carbon and reducing power for fatty acid synthesis in the heterotrophic plastids of developing sunflower (Helianthus annuus L.) embryos. J Exp Bot **56**: 1297–303

Pohl A, Devaux PF, Herrmann A (2005) Function of prokaryotic and eukaryotic ABC proteins in lipid transport. Biochim Biophys Acta **1733**: 29–52

Popper ZA, Tuohy MG (2010) Beyond the green: understanding the evolutionary puzzle of plant and algal cell walls. Plant Physiol **153**: 373–83

Quintana N, Van der Kooy F, Van de Rhee MD, Voshol GP, Verpoorte R (2011a) Renewable energy from Cyanobacteria: energy production optimization by metabolic pathway engineering. Appl Microbiol Biotechnol **91**: 471–90

Quintana N, Van der Kooy F, Van de Rhee MD, Voshol GP, Verpoorte R (2011b) Renewable energy from Cyanobacteria: energy production optimization by metabolic pathway engineering. Appl Microbiol Biotechnol **91**: 471–90

Radakovits R, Eduafo PM, Posewitz MC (2011) Genetic engineering of fatty acid chain length in Phaeodactylum tricornutum. Metab Eng **13**: 89–95

Radakovits R, Jinkerson RE, Darzins A, Posewitz MC (2010) Genetic engineering of algae for enhanced biofuel production. Eukaryot Cell **9**: 486–501

Radakovits R, Jinkerson RE, Fuerstenberg SI, Tae H, Settlage RE, Boore JL, Posewitz MC (2012) Draft genome sequence and genetic transformation of the oleaginous alga Nannochloropis gaditana. Nat Commun **3**: 686

Ramachandra T V., Mahapatra DM, B K, Gordon R (2009) Milking Diatoms for Sustainable Energy: Biochemical Engineering versus Gasoline-Secreting

Diatom Solar Panels. Ind Eng Chem Res **48**: 8769–8788

Ramanan R, Kim B-H, Cho D-H, Ko S-R, Oh H-M, Kim H-S (2013) Lipid droplet synthesis is limited by acetate availability in starchless mutant of Chlamydomonas reinhardtii. FEBS Lett **587**: 370–7

Rangasamy D, Ratledge C (2000) Genetic enhancement of fatty acid synthesis by targeting rat liver ATP:citrate lyase into plastids of tobacco. Plant Physiol **122**: 1231–8

Rasala BA, Mayfield SP (2011) The microalga Chlamydomonas reinhardtii as a platform for the production of human protein therapeutics. Bioeng Bugs **2**: 50–4

Ratledge C (2004) Fatty acid biosynthesis in microorganisms being used for Single Cell Oil production. Biochimie **86**: 807–15

Ratledge C, Bowater MD, Taylor PN (1997) Correlation of ATP/citrate lyase activity with lipid accumulation in developing seeds of Brassica napus L. Lipids **32**: 7–12

Recht L, Töpfer N, Batushansky A, Sikron N, Gibon Y, Fait A, Nikoloski Z, Boussiba S, Zarka A (2014) Metabolite profiling and integrative modeling reveal metabolic constraints for carbon partitioning under nitrogen starvation in the green algae Haematococcus pluvialis. J Biol Chem **289**: 30387–403

Recht L, Zarka A, Boussiba S (2012) Patterns of carbohydrate and fatty acid changes under nitrogen starvation in the microalgae Haematococcus pluvialis and Nannochloropsis sp. Appl Microbiol Biotechnol **94**: 1495–503

Rismani-Yazdi H, Haznedaroglu BZ, Bibby K, Peccia J (2011) Transcriptome sequencing and annotation of the microalgae Dunaliella tertiolecta: pathway description and gene discovery for production of next-generation biofuels. BMC Genomics **12**: 148

Rismani-Yazdi H, Haznedaroglu BZ, Hsin C, Peccia J (2012) Transcriptomic analysis of the oleaginous microalga Neochloris oleoabundans reveals metabolic insights into triacylglyceride accumulation. Biotechnol Biofuels **5**: 74

Rodríguez-Frómeta RA, Gutiérrez A, Torres-Martínez S, Garre V (2013) Malic enzyme activity is not the only bottleneck for lipid accumulation in the oleaginous fungus Mucor circinelloides. Appl Microbiol Biotechnol **97**: 3063–72

Roesler K, Shintani D, Savage L, Boddupalli S, Ohlrogge J (1997) Targeting of the Arabidopsis homomeric acetyl-coenzyme A carboxylase to plastids of rapeseeds. Plant Physiol **113**: 75–81

Ruecker O, Zillner K, Groebner-Ferreira R, Heitzer M (2008) Gaussia-

luciferase as a sensitive reporter gene for monitoring promoter activity in the nucleus of the green alga Chlamydomonas reinhardtii. Mol Genet Genomics **280**: 153–162

Ruffing AM (2013) RNA-Seq analysis and targeted mutagenesis for improved free fatty acid production in an engineered cyanobacterium. Biotechnol Biofuels **6**: 113

Ruffing AM, Jones HDT (2012) Physiological effects of free fatty acid production in genetically engineered Synechococcus elongatus PCC 7942. Biotechnol Bioeng **109**: 2190–9

Ruffing AM, Ohlrogge J, Jaworski J, Kaczmarzyk D, Fulda M, Michinaka Y, Shimauchi T, Aki T, Nakajima T, Kawamoto S, et al (2013) RNA-Seq analysis and targeted mutagenesis for improved free fatty acid production in an engineered cyanobacterium. Biotechnol Biofuels **6**: 113

Runguphan W, Keasling JD (2014) Metabolic engineering of Saccharomyces cerevisiae for production of fatty acid-derived biofuels and chemicals. Metab Eng **21**: 103–13

La Russa M, Bogen C, Uhmeyer A, Doebbe A, Filippone E, Kruse O, Mussgnug JH (2012) Functional analysis of three type-2 DGAT homologue genes for triacylglycerol production in the green microalga Chlamydomonas reinhardtii. J Biotechnol **162**: 13–20

Rylott EL, Rogers CA, Gilday AD, Edgell T, Larson TR, Graham IA (2003) Arabidopsis mutants in short- and medium-chain acyl-CoA oxidase activities accumulate acyl-CoAs and reveal that fatty acid beta-oxidation is essential for embryo development. J Biol Chem **278**: 21370–7

Sabido A, Sigala JC, Hernández-Chávez G, Flores N, Gosset G, Bolívar F (2014) Physiological and transcriptional characterization of Escherichia coli strains lacking interconversion of phosphoenolpyruvate and pyruvate when glucose and acetate are coutilized. Biotechnol Bioeng **111**: 1150–60

Saha R, Liu D, Hoynes-O'Connor A, Liberton M, Yu J, Bhattacharyya-Pakrasi M, Balassy A, Zhang F, Moon TS, Maranas CD, et al (2016) Diurnal Regulation of Cellular Processes in the Cyanobacterium Synechocystis sp. Strain PCC 6803: Insights from Transcriptomic, Fluxomic, and Physiological Analyses. MBio **7**: e00464-16

Salas JJ, Ohlrogge JB (2002) Characterization of substrate specificity of plant FatA and FatB acyl-ACP thioesterases. Arch Biochem Biophys **403**: 25–34

Sanz-Luque E, Ocaña-Calahorro F, de Montaigu A, Chamizo-Ampudia A, Llamas Á, Galván A, Fernández E (2015) THB1, a truncated hemoglobin, modulates nitric oxide levels and nitrate reductase activity. Plant J **81**: 467–79

Sato A, Matsumura R, Hoshino N, Tsuzuki M, Sato N (2014) Responsibility of regulatory gene expression and repressed protein synthesis for triacylglycerol accumulation on sulfur-starvation in Chlamydomonas reinhardtii. Front Plant Sci **5**: 444

Scharnewski M, Pongdontri P, Mora G, Hoppert M, Fulda M (2008) Mutants of Saccharomyces cerevisiae deficient in acyl-CoA synthetases secrete fatty acids due to interrupted fatty acid recycling. FEBS J **275**: 2765–78

Scholz MJ, Weiss TL, Jinkerson RE, Jing J, Roth R, Goodenough U, Posewitz MC, Gerken HG (2014) Ultrastructure and composition of the Nannochloropsis gaditana cell wall. Eukaryot Cell **13**: 1450–64

Schwender J, Ohlrogge JB, Shachar-Hill Y (2003) A flux model of glycolysis and the oxidative pentosephosphate pathway in developing Brassica napus embryos. J Biol Chem **278**: 29442–53

Scranton MA, Ostrand JT, Fields FJ, Mayfield SP (2015) *Chlamydomonas* as a model for biofuels and bio-products production. Plant J **82**: 523–531

Segovia M, Haramaty L, Berges JA, Falkowski PG (2003) Cell death in the unicellular chlorophyte Dunaliella tertiolecta. A hypothesis on the evolution of apoptosis in higher plants and metazoans. Plant Physiol **132**: 99–105

Sharma T, Chauhan RS (2016) Comparative transcriptomics reveals molecular components associated with differential lipid accumulation between microalgal sp., Scenedesmus dimorphus and Scenedesmus quadricauda. Algal Res **19**: 109–122

Sheehan J, Dunahay T, Benemann J, Roessler P (1998) Look Back at the U.S. Department of Energy's Aquatic Species Program: Biodiesel from Algae; Close-Out Report. doi: 10.2172/15003040

Shin H, Hong SJ, Kim H, Yoo C, Lee H, Choi HK, Lee CG, Cho BK (2015) Elucidation of the growth delimitation of Dunaliella tertiolecta under nitrogen stress by integrating transcriptome and peptidome analysis. Bioresour Technol **194**: 57–66

Shtaida N, Khozin-Goldberg I, Boussiba S (2015) The role of pyruvate hub enzymes in supplying carbon precursors for fatty acid synthesis in photosynthetic microalgae. Photosynth Res **125**: 407–22

Shtaida N, Khozin-Goldberg I, Solovchenko A, Chekanov K, Didi-Cohen S, Leu S, Cohen Z, Boussiba S (2014) Downregulation of a putative plastid PDC E1α subunit impairs photosynthetic activity and triacylglycerol accumulation in nitrogen-starved photoautotrophic Chlamydomonas reinhardtii. J Exp Bot **65**: 6563–76

Sialve B, Bernet N, Bernard O (2009) Anaerobic digestion of microalgae as a

necessary step to make microalgal biodiesel sustainable. Biotechnol Adv **27**: 409–416

Siaut M, Cuiné S, Cagnon C, Fessler B, Nguyen M, Carrier P, Beyly A, Beisson F, Triantaphylidès C, Li-Beisson Y, et al (2011) Oil accumulation in the model green alga Chlamydomonas reinhardtii: characterization, variability between common laboratory strains and relationship with starch reserves. BMC Biotechnol **11**: 7

Simionato D, Block MA, La Rocca N, Jouhet J, Maréchal E, Finazzi G, Morosinotto T (2013) The response of Nannochloropsis gaditana to nitrogen starvation includes de novo biosynthesis of triacylglycerols, a decrease of chloroplast galactolipids, and reorganization of the photosynthetic apparatus. Eukaryot Cell **12**: 665–76

Singh J, Gu S (2010) Commercialization potential of microalgae for biofuels production. Renew Sustain Energy Rev **14**: 2596–2610

Slocombe SP, Zhang Q, Ross M, Anderson A, Thomas NJ, Lapresa Á, Rad-Menéndez C, Campbell CN, Black KD, Stanley MS, et al (2015) Unlocking nature's treasure-chest: screening for oleaginous algae. Sci Rep **5**: 9844

Smith RG, Gauthier DA, Dennis DT, Turpin DH (1992) Malate- and pyruvate-dependent Fatty Acid synthesis in leucoplasts from developing castor endosperm. Plant Physiol **98**: 1233–8

Smith SR, Abbriano RM, Hildebrand M (2012) Comparative analysis of diatom genomes reveals substantial differences in the organization of carbon partitioning pathways. Algal Res **1**: 2–16

Spalding MH (2009) The CO2-Concentrating Mechanism and Carbon Assimilation. Chlamydomonas Sourceb. Elsevier, pp 257–301

Specht E, Miyake-Stoner S, Mayfield S (2010) Micro-algae come of age as a platform for recombinant protein production. Biotechnol Lett **32**: 1373–83

Srinivasan V, Pierik AJ, Lill R (2014) Crystal structures of nucleotide-free and glutathione-bound mitochondrial ABC transporter Atm1. Science **343**: 1137–40

Stal LJ, Moezelaar R (2006) Fermentation in cyanobacteria1. FEMS Microbiol Rev **21**: 179–211

Stanier RY, Deruelles J, Rippka R, Herdman M, Waterbury JB (1979) Generic Assignments, Strain Histories and Properties of Pure Cultures of Cyanobacteria. Microbiology **111**: 1–61

Steen EJ, Kang Y, Bokinsky G, Hu Z, Schirmer A, McClure A, del Cardayre SB, Keasling JD (2010) Microbial production of fatty-acid-derived fuels and

chemicals from plant biomass. Nature **463**: 559–562

Stephens E, Ross IL, King Z, Mussgnug JH, Kruse O, Posten C, Borowitzka MA, Hankamer B (2010a) An economic and technical evaluation of microalgal biofuels. Nat Biotechnol **28**: 126–8

Stephens E, Ross IL, Mussgnug JH, Wagner LD, Borowitzka MA, Posten C, Kruse O, Hankamer B (2010b) Future prospects of microalgal biofuel production systems. Trends Plant Sci **15**: 554–64

Subramanian S, Barry AN, Pieris S, Sayre RT (2013) Comparative energetics and kinetics of autotrophic lipid and starch metabolism in chlorophytic microalgae: implications for biomass and biofuel production. Biotechnol Biofuels **6**: 150

Sun Z, Chen Y-F, Du J (2016) Elevated CO2 improves lipid accumulation by increasing carbon metabolism in Chlorella sorokiniana. Plant Biotechnol J **14**: 557–66

Sweetlove LJ, Beard KFM, Nunes-Nesi A, Fernie AR, Ratcliffe RG, Siedow JN, Day DA, Lancien M, al. et, Plaxton WC, et al (2010) Not just a circle: flux modes in the plant TCA cycle. Trends Plant Sci **15**: 462–70

Tan KWM, Lee YK (2016) The dilemma for lipid productivity in green microalgae: importance of substrate provision in improving oil yield without sacrificing growth. Biotechnol Biofuels **9**: 255

Tan KWM, Lee YK (2017) Expression of the heterologous Dunaliella tertiolecta fatty acyl-ACP thioesterase leads to increased lipid production in Chlamydomonas reinhardtii. J Biotechnol **247**: 60–67

Tan KWM, Lin H, Shen H, Lee YK (2016) Nitrogen-induced metabolic changes and molecular determinants of carbon allocation in Dunaliella tertiolecta. Sci Rep **6**: 37235

Tang H, Abunasser N, Garcia MED, Chen M, Simon Ng KY, Salley SO (2011) Potential of microalgae oil from Dunaliella tertiolecta as a feedstock for biodiesel. Appl Energy **88**: 3324–3330

Tang X, Chen H, Chen YQ, Chen W, Garre V, Song Y, Ratledge C (2015) Comparison of Biochemical Activities between High and Low Lipid-Producing Strains of Mucor circinelloides: An Explanation for the High Oleaginicity of Strain WJ11. PLoS One **10**: e0128396

Tang X, Feng H, Chen WN (2013) Metabolic engineering for enhanced fatty acids synthesis in Saccharomyces cerevisiae. Metab Eng **16**: 95–102

Tarling EJ, de Aguiar Vallim TQ, Edwards PA (2013) Role of ABC transporters in lipid transport and human disease. Trends Endocrinol Metab **24**: 342–50

Terashima M, Specht M, Hippler M (2011) The chloroplast proteome: a survey from the Chlamydomonas reinhardtii perspective with a focus on distinctive features. Curr Genet **57**: 151–68

Terauchi AM, Lu S-F, Zaffagnini M, Tappa S, Hirasawa M, Tripathy JN, Knaff DB, Farmer PJ, Lemaire SD, Hase T, et al (2009) Pattern of expression and substrate specificity of chloroplast ferredoxins from Chlamydomonas reinhardtii. J Biol Chem **284**: 25867–78

Theodoulou FL, Carrier DJ, Schaedler TA, Baldwin SA, Baker A (2016) How to move an amphipathic molecule across a lipid bilayer: different mechanisms for different ABC transporters? Biochem Soc Trans **44**: 774–82

Torella JP, Ford TJ, Kim SN, Chen AM, Way JC, Silver PA (2013) Tailored fatty acid synthesis via dynamic control of fatty acid elongation. Proc Natl Acad Sci U S A **110**: 11290–5

Trentacoste EM, Shrestha RP, Smith SR, Glé C, Hartmann AC, Hildebrand M, Gerwick WH (2013) Metabolic engineering of lipid catabolism increases microalgal lipid accumulation without compromising growth. Proc Natl Acad Sci U S A **110**: 19748–53

Urzica EI, Vieler A, Hong-Hermesdorf A, Page MD, Casero D, Gallaher SD, Kropat J, Pellegrini M, Benning C, Merchant SS (2013) Remodeling of membrane lipids in iron-starved Chlamydomonas. J Biol Chem **288**: 30246–58

Usher PK, Ross AB, Camargo-Valero MA, Tomlin AS, Gale WF (2014) An overview of the potential environmental impacts of large-scale microalgae cultivation. Biofuels **5**: 331–349

Uttaro AD (2006) Biosynthesis of polyunsaturated fatty acids in lower eukaryotes. IUBMB Life **58**: 563–71

Valenzuela J, Mazurie A, Carlson RP, Gerlach R, Cooksey KE, Peyton BM, Fields MW (2012) Potential role of multiple carbon fixation pathways during lipid accumulation in Phaeodactylum tricornutum. Biotechnol Biofuels **5**: 40

Valledor L, Furuhashi T, Recuenco-Muñoz L, Wienkoop S, Weckwerth W (2014) System-level network analysis of nitrogen starvation and recovery in Chlamydomonas reinhardtii reveals potential new targets for increased lipid accumulation. Biotechnol Biofuels **7**: 171

van Veen HW, Callaghan R, Soceneantu L, Sardini A, Konings WN, Higgins CF (1998) A bacterial antibiotic-resistance gene that complements the human multidrug-resistance P-glycoprotein gene. Nature **391**: 291–5

Verrier PJ, Bird D, Burla B, Dassa E, Forestier C, Geisler M, Klein M,

Kolukisaoglu U, Lee Y, Martinoia E, et al (2008) Plant ABC proteins--a unified nomenclature and updated inventory. Trends Plant Sci **13**: 151–9

Vieler A, Wu G, Tsai C-H, Bullard B, Cornish AJ, Harvey C, Reca I-B, Thornburg C, Achawanantakun R, Buehl CJ, et al (2012a) Genome, Functional Gene Annotation, and Nuclear Transformation of the Heterokont Oleaginous Alga Nannochloropsis oceanica CCMP1779. PLoS Genet **8**: e1003064

Vieler A, Wu G, Tsai C-H, Bullard B, Cornish AJ, Harvey C, Reca I-B, Thornburg C, Achawanantakun R, Buehl CJ, et al (2012b) Genome, functional gene annotation, and nuclear transformation of the heterokont oleaginous alga Nannochloropsis oceanica CCMP1779. PLoS Genet **8**: e1003064

Vigeolas H, Waldeck P, Zank T, Geigenberger P (2007) Increasing seed oil content in oil-seed rape (Brassica napus L.) by over-expression of a yeast glycerol-3-phosphate dehydrogenase under the control of a seed-specific promoter. Plant Biotechnol J **5**: 431–41

Voelker TA, Davies HM (1994) Alteration of the specificity and regulation of fatty acid synthesis of Escherichia coli by expression of a plant medium-chain acyl-acyl carrier protein thioesterase. J Bacteriol **176**: 7320–7

Voelker T, Worrell A, Anderson L, Bleibaum J, Fan C, Hawkins D, Radke S, Davies H, Radke S, Davies H, et al (1992) Fatty acid biosynthesis redirected to medium chains in transgenic oilseed plants. Science (80-) **257**: 72–74

Vongsangnak W, Zhang Y, Chen W, Ratledge C, Song Y (2012) Annotation and analysis of malic enzyme genes encoding for multiple isoforms in the fungus Mucor circinelloides CBS 277.49. Biotechnol Lett **34**: 941–7

Wakao S, Andre C, Benning C (2008) Functional analyses of cytosolic glucose-6-phosphate dehydrogenases and their contribution to seed oil accumulation in Arabidopsis. Plant Physiol **146**: 277–88

Walker TL, Becker DK, Dale JL, Collet C (2005) Towards the development of a nuclear transformation system for Dunaliella tertiolecta. J Appl Phycol **17**: 363–368

Wheeler MCG, Arias CL, Tronconi MA, Maurino VG, Andreo CS, Drincovitch MF (2008) Arabidopsis thaliana NADP-malic enzyme isoforms: high degree of identity but clearly distinct properties. Plant Mol Biol **67**: 231–42

Wheeler MCG, Tronconi MA, Drincovich MF, Andreo CS, Flügge U-I, Maurino VG (2005) A comprehensive analysis of the NADP-malic enzyme gene family of Arabidopsis. Plant Physiol **139**: 39–51

Wigmosta MS, Coleman AM, Skaggs RJ, Huesemann MH, Lane LJ (2011) National microalgae biofuel production potential and resource demand. Water Resour Res **47**: n/a-n/a

Winkler U, Säftel W, Stabenau H (1988) β-Oxidation of fatty acids in algae: Localization of thiolase and acyl-CoA oxidizing enzymes in three different organisms. Planta **175**: 91–8

Wu S, Huang A, Zhang B, Huan L, Zhao P, Lin A, Wang G (2015) Enzyme activity highlights the importance of the oxidative pentose phosphate pathway in lipid accumulation and growth of Phaeodactylum tricornutum under CO2 concentration. Biotechnol Biofuels **8**: 78

Xiong W, Liu L, Wu C, Yang C, Wu Q (2010) 13C-tracer and gas chromatography-mass spectrometry analyses reveal metabolic flux distribution in the oleaginous microalga Chlorella protothecoides. Plant Physiol **154**: 1001–11

Xue J, Niu Y-F, Huang T, Yang W-D, Liu J-S, Li H-Y (2015) Genetic improvement of the microalga Phaeodactylum tricornutum for boosting neutral lipid accumulation. Metab Eng **27**: 1–9

Xue J, Wang L, Zhang L, Balamurugan S, Li D-W, Zeng H, Yang W-D, Liu J-S, Li H-Y (2016) The pivotal role of malic enzyme in enhancing oil accumulation in green microalga Chlorella pyrenoidosa. Microb Cell Fact **15**: 120

Yan J, Cheng R, Lin X, You S, Li K, Rong H, Ma Y (2013) Overexpression of acetyl-CoA synthetase increased the biomass and fatty acid proportion in microalga Schizochytrium. Appl Microbiol Biotechnol **97**: 1933–9

Yang C, Hua Q, Shimizu K (2000) Energetics and carbon metabolism during growth of microalgal cells under photoautotrophic, mixotrophic and cyclic light-autotrophic/dark-heterotrophic conditions. Biochem Eng J **6**: 87–102

Yang Z-K, Ma Y-H, Zheng J-W, Yang W-D, Liu J-S, Li H-Y (2014) Proteomics to reveal metabolic network shifts towards lipid accumulation following nitrogen deprivation in the diatom Phaeodactylum tricornutum. J Appl Phycol **26**: 73–82

Yang Z-K, Niu Y-F, Ma Y-H, Xue J, Zhang M-H, Yang W-D, Liu J-S, Lu S-H, Guan Y, Li H-Y (2013) Molecular and cellular mechanisms of neutral lipid accumulation in diatom following nitrogen deprivation. Biotechnol Biofuels **6**: 67

Yao L, Tan TW, Ng Y-K, Ban KHK, Shen H, Lin H, Lee YK (2015) RNA-Seq transcriptomic analysis with Bag2D software identifies key pathways enhancing lipid yield in a high lipid-producing mutant of the non-model green alga Dunaliella tertiolecta. Biotechnol Biofuels **8**: 191

Yao Y, Lu Y, Peng K-T, Huang T, Niu Y-F, Xie W-H, Yang W-D, Liu J-S, Li H-Y, Brennan L, et al (2014) Glycerol and neutral lipid production in the oleaginous marine diatom Phaeodactylum tricornutum promoted by overexpression of glycerol-3-phosphate dehydrogenase. Biotechnol Biofuels **7**: 110

Young EB, Beardall J (2003) PHOTOSYNTHETIC FUNCTION IN DUNALIELLA TERTIOLECTA (CHLOROPHYTA) DURING A NITROGEN STARVATION AND RECOVERY CYCLE. J Phycol **39**: 897–905

Yu A-Q, Pratomo Juwono NK, Leong SSJ, Chang MW (2014) Production of Fatty Acid-derived valuable chemicals in synthetic microbes. Front Bioeng Biotechnol **2**: 78

Yu W-L, Ansari W, Schoepp NG, Hannon MJ, Mayfield SP, Burkart MD (2011) Modifications of the metabolic pathways of lipid and triacylglycerol production in microalgae. Microb Cell Fact **10**: 91

Zhang F, Rodriguez S, Keasling JD (2011a) Metabolic engineering of microbial pathways for advanced biofuels production. Curr Opin Biotechnol **22**: 775–783

Zhang H, Zhang L, Chen H, Chen YQ, Chen W, Song Y, Ratledge C (2014) Enhanced lipid accumulation in the yeast Yarrowia lipolytica by over-expression of ATP:citrate lyase from Mus musculus. J Biotechnol **192 Pt A**: 78–84

Zhang H, Zhang L, Chen H, Chen YQ, Ratledge C, Song Y, Chen W (2013) Regulatory properties of malic enzyme in the oleaginous yeast, Yarrowia lipolytica, and its non-involvement in lipid accumulation. Biotechnol Lett **35**: 2091–8

Zhang JY, Jeon H, Sim SJ, Lee Y, Jin E (2015) Homologous sense and antisense expression of a gene in Dunaliella tertiolecta. Planta **242**: 1051–1058

Zhang X, Li M, Agrawal A, San K-Y (2011b) Efficient free fatty acid production in Escherichia coli using plant acyl-ACP thioesterases. Metab Eng **13**: 713–22

Zhang Y, Adams IP, Ratledge C (2007) Malic enzyme: the controlling activity for lipid production? Overexpression of malic enzyme in Mucor circinelloides leads to a 2.5-fold increase in lipid accumulation. Microbiology **153**: 2013–25

Zhou L, Zuo Z-R, Chen X-Z, Niu D-D, Tian K-M, Prior BA, Shen W, Shi G-Y, Singh S, Wang Z-X (2011) Evaluation of genetic manipulation strategies on D-lactate production by Escherichia coli. Curr Microbiol **62**: 981–9

Zhu Y, Eiteman MA, Altman R, Altman E (2008) High glycolytic flux improves pyruvate production by a metabolically engineered Escherichia coli strain. Appl Environ Microbiol **74**: 6649–55

Supplementary Information

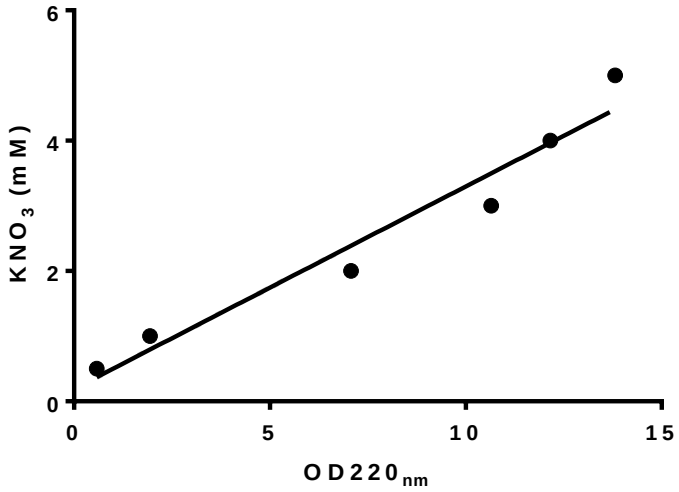

Figure S1. Standard curve for nitrate concentration in ATCC media-1174 DA media. Media samples collected in a quartz cuvette were measured at OD_{220nm} and OD_{275nm} with a UV spectrophotometer. The values of OD_{275nm} were subtracted from OD_{220nm} to correct the value.

Table S1. Media composition for ATCC-1174 DA medium. Compounds in bold are variable depending on type of media used for N-depletion experiments.

Compound	Quantity	Remarks
NaCl	29.22 g	For 0.5M NaCl.
Tris-HCl (pH 7.5)	6.024 g	
$NaHCO_3$	1.68 g	
KNO_3	0.505 g	For 10% KNO_3 media, KNO_3 was reduced to 0.0505 g (50.5 µg)
$MgSO_4.7H_2O$	1.232 g	
$CaCl_2$	0.033 g	
KH_2PO_4	0.014 g	
$FeCl_3$	50.0 mL	$FeCl_3$ (0.32 mg) + EDTA (5.84 mg) + Distilled Water (50 mL)
H_3BO_3	6.0 mg	
$MnCl_2.4H_2O$	99.0 µg	
$ZnCl_2$	14.0 µg	
$CoCl_2.6H_2O$	4.76 µg	
$CuCl_2.2H_2O$	34.0 ng	
Distilled water	1.0 L	
KCl		For 10% KNO_3 (N depletion) media only. KNO_3 was substituted with KCl for N depletion..

Table S2. Primers used in the N-depletion study. ACD: Acyl-CoA dehydrogenase; ACLA: ATP:citrate lyase subunit A; G6PDH: Glucose-6-phosphate dehydrogenase (plastidial); MME2: Malic enzyme isoform 2; MME6: Malic enzyme isoform 6; PDH: Pyruvate dehydrogenase (plastidial) E1β subunit; TE: Fatty acyl-ACP thioesterase.

Primer name	Sequence (5' to 3')
DtACD RACE F1	GTGTAATGTAGAAGGGTCTCTCCC
DtACD RACE R1	GGGAGAGACCCTTCTACATTACAC
DtACD RACE F2	CAAGATGGCAAGCCTCCAACCATA
DtACD RACE R2	TATGGTTGGAGGCTTGCCATCTTG
DtACOX RACE F1	GCTGCGACCCAACGCGGTGGC
DtACOX RACE R1	GCCACCGCGTTGGGTCGCAGC
DtACOX RACE F2	ACAGTGCTCTGGGCCGCCAGG
DtACOX RACE R2	CCTGGCGGCCCAGAGCACTGT
DtACLA RACE F1	GTGTGGCTGATGGTTGCTGGC
DtACLA RACE R1	GCCAGCAACCATCAGCCACAC
DtACLA RACE F2	AATCTACACGGACACAGTGGGAG
DtACLA RACE R2	CTCCCACTGTGTCCGTGTAGATT
DtMME2 RACE F1	GACATCCAGGGTACTGCCGCA
DtMME2 RACE R1	TGCGGCAGTACCCTGGATGTC
DtMME2 RACE F2	ATGAATGAGGCACGCAAGACC
DtMME2 RACE R2	GGTCTTGCGTGCCTCATTCAT
DtMME6 RACE F1	TACATGCAGAGTCTGCAGGAG
DtMME6 RACE R1	CTCCTGCAGACTCTGCATGTA
DtMME6 RACE F2	CGCGTGTTCCGCATCCTCAAG
DtMME6 RACE R2	CTTGAGGATGCGGAACACGCG
DtPDH-E1β RACE F1	TTCGAGCACGTGCTGCTGTACAA
DtPDH-E1β RACE R1	TTGTACAGCAGCACGTGCTCGAA
DtPDH-E1β RACE F2	GTGGAGGAGTGCATGAAGACCG
DtPDH-E1β RACE R2	CGGTCTTCATGCACTCCTCCAC
DtTE RACE F1	CCAGCACGTGGGTCACCATCAA
DtTE RACE R1	TTGATGGTGACCCACGTGCTGG
DtTE RACE F2	TTGACATGAATGGCCACATCAACAA
DtTE RACE R2	TTGTTGATGTGGCCATTCATGTCAA
DtACD real-time F1	CTGATCATCGACGCTGCTAT
DtACD real-time R1	AACTTTGCAATCGTGGTCAG
DtACLA real-time F1	ACTGAGCAGCATCAAAGTGG
DtACLA real-time R1	CATCGACATCAAGGAACACC
DtACOX real-time F1	GCAAGGACAAGATTCAACGA
DtACOX real-time R1	CCAGATACCAAACGATGCAC
DtG6PDH real-time F1	GCCATCCGTAATGAGAAGGT
DtG6PDH real-time R1	TATTGGCCCAGTGTGACATC
DtMME2 real-time F1	CGATGACATCCAGGGTACTG
DtMME2 real-time R1	ATCTGCTTTCCTGCTCGATT

Primer name	Sequence (5’ to 3’)
DtMME6 real-time F1	CTTACAAGCTGCCCTTCACA
DtMME6 real-time R1	TACTAGCACCGTTTGGCTTG
DtPDH-E1β real-time F1	AGTGATGCAGGCAGTAGCAG
DtPDH-E1β real-time R1	CTTCAAGCTGATGAGGTCCA
DtTE real-time F1	GGGACATGGTCACAGTTGAG
DtTE real-time F2	GGTGGCAGAACCATACTCCT
DtTubulin real-time F1	CAGATGTGGGATGCCAAGAACA
DtTubulin real-time R1	GTTCAGCATCTGCTCATCCACC

Table S3. Characterization of the genes and putative proteins. Full-length mRNA refers to the size of the cDNA fragment amplified and includes the 5' and 3' untranslated regions. Percentage protein identity and conserved domains were determined by subjecting the protein sequences to a NCBI BlastP homology-based search in the *Chlorophyta* database. The information in brackets refers to the respective accession number on the NCBI Conserved Domain Database and Refseq database. Cellular localizations of the enzymes were determined using ChloroP and TargetP and only served to be predictive. *Db*, *Dunaliella bioculata*; *Cr*, *Chlamydomonas reinhardtii*.

Parameters	**DtACD**	**DtACLA**	**DtACOX**	**DtG6PDH**
Full-length mRNA (bp)	3,099	1,784	2,645	3,217
Open reading frame (bp)	2,526	1,281	2,112	1,773
Putative protein size (aa)	841	426	703	590
Conserved domains(s)	Acyl-CoA dehydrogenase (PLN02876)	ATP citrate (pro-S)-lyase (PLN02235)	Acyl-coenzyme A oxidase (PLN02443)	Glucose-6-phosphate 1-dehydrogenase (PLN02333)
% protein identity	59% to *Cr*ACD (XP_001695945.1)	65% to *Cr*ACLA (XP_001700900.1)	63% to CrACOX (XP_001699193.1)	100% to *Db*G6PDH (CAB52685.1)
Predicted localization	Mitochondria	Cytosol	Unknown (probably peroxisomes)	Chloroplast
Parameters	**DtMME2**	**DtMME6**	**DtPDH**	**DtTE**
Full-length mRNA (bp)	2,395	2,961	2,427	2,198
Open reading frame (bp)	1,659	1,347	1,107	1,176
Putative protein size (aa)	552	448	368	391
Conserved domains(s)	NADP-dependent malic enzyme (PLN03129)	NADP-dependent malic enzyme (PLN03129)	Pyruvate dehydrogenase E1 component beta subunit (CHL00144)	acyl-ACP thioesterase (PLN02370)
% protein identity	55% to *Cr*MME2 (XP_001692778.1)	73% to *Cr*MME6 (XP_001696415.1)	73% to *Cr*PDH E1β (XP_001693114.1)	56% to *Cr*TE (XP_001696619.1)
Predicted localization	Unknown (probably cytosol)	Unknown (probably mitochondria)	Chloroplast	Chloroplast

Table S4. Transcriptome assembly details of *D. tertiolecta* samples.

	Day 3	**Day 5**
Number of genes annotated (Total)	23,778	19,173
Number of significantly expressed genes (FDR-corrected p-value ≤ 0.05)	3,962	1,234
Number of genes over/under-expressed (≥2 or ≤ -2)	3,799	1,096
No. of significant GO enrichment categories (FDR-corrected p-value ≤ 0.05)	57	31
No. of significant KEGG pathway categories (FDR-corrected p-value ≤ 0.05)	11	17

Table S5. List of the top 10 most upregulated or downregulated genes in N-depleted *D. tertiolecta* cells.

Day	KEGG ID	Gene/Protein name	Fold change	GO/KEGG Function
3	CHLREDRAFT_127387	COX19 (cytochrome c oxidase assembly protein)	58,363.7	
3	CHLREDRAFT_152591	HMOX2 (heme oxygenase)	52,488.1	Porphyrin and chlorophyll metabolism
3	CHLREDRAFT_154732	Adenine nucleotide alpha hydrolases-like superfamily protein	-46,367.6	
3	CHLREDRAFT_182662	RPB11 (DNA-directed RNA polymerase II)	-32,666.6	Transcription of DNA to mRNA
3	CHLREDRAFT_162635	FAP109 (Flagellar associated protein)	36,278.6	
3	CHLREDRAFT_107200	RING/U-box superfamily protein	32,693.9	Ubiquitin protein ligase activity
3	CHLREDRAFT_192192	hypothetical protein	31,387.3	
3	CHLREDRAFT_116571	CPA2 (N-carbamoylputrescine amidase)	29,614.5	Arginine and proline metabolism
3	CHLREDRAFT_191334	FAP114 (Flagellar associated protein)	28,521.0	
3	CHLREDRAFT_17065	ANK14	23,938.9	
5	CHLREDRAFT_140618	GAP1a (glyceraldehyde 3-phosphate dehydrogenase)	1,284.0	Glycolysis / Gluconeogenesis
5	CHLREDRAFT_184156	FOX1 (multicopper ferroxidase)	-561.8	Porphyrin and chlorophyll metabolism
5	CHLREDRAFT_81856	THB1 (Putative truncated hemoglobin)	-298.4	Regulates nitrogen assimilation pathway
5	CHLREDRAFT_196484	PHO1 (alkaline phosphatase)	-150.3	Protein dephosphorylation
5	CHLREDRAFT_170417	DUR3C (urea active transporter)	72.6	urea transmembrane transporter activity
5	CHLREDRAFT_196479	DUR3A (urea active transporter)	65.0	urea transmembrane transporter activity
5	CHLREDRAFT_154212	DUR3B (urea active transporter)	52.0	urea transmembrane transporter activity
5	CHLREDRAFT_187840	hypothetical protein	-43.3	
5	CHLREDRAFT_195162	Light-harvesting complex II chlorophyll a-b binding protein M3	-43.2	Photosynthesis - antenna proteins
5	CHLREDRAFT_185309	Lhc-like protein Lhl3	-36.1	

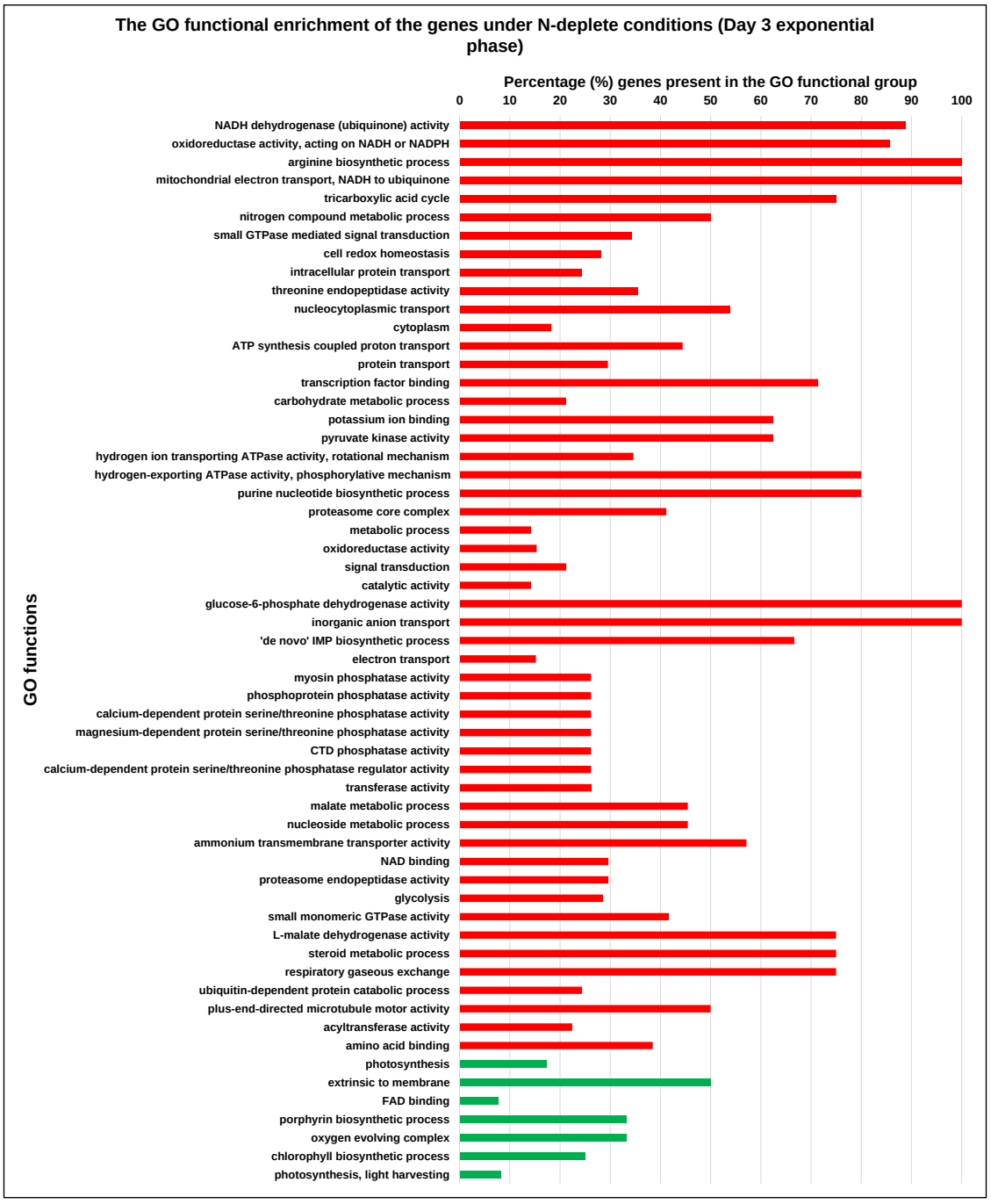

Figure S2. GO functional enrichment of up-regulated and down-regulated genes under N-deplete conditions on Day 3 exponential phase. Red and green bars indicate up- (≥ 2) and down- (≤ -2) regulation respectively. All data were filtered according to a FDR-corrected p value of ≤ 0.05.

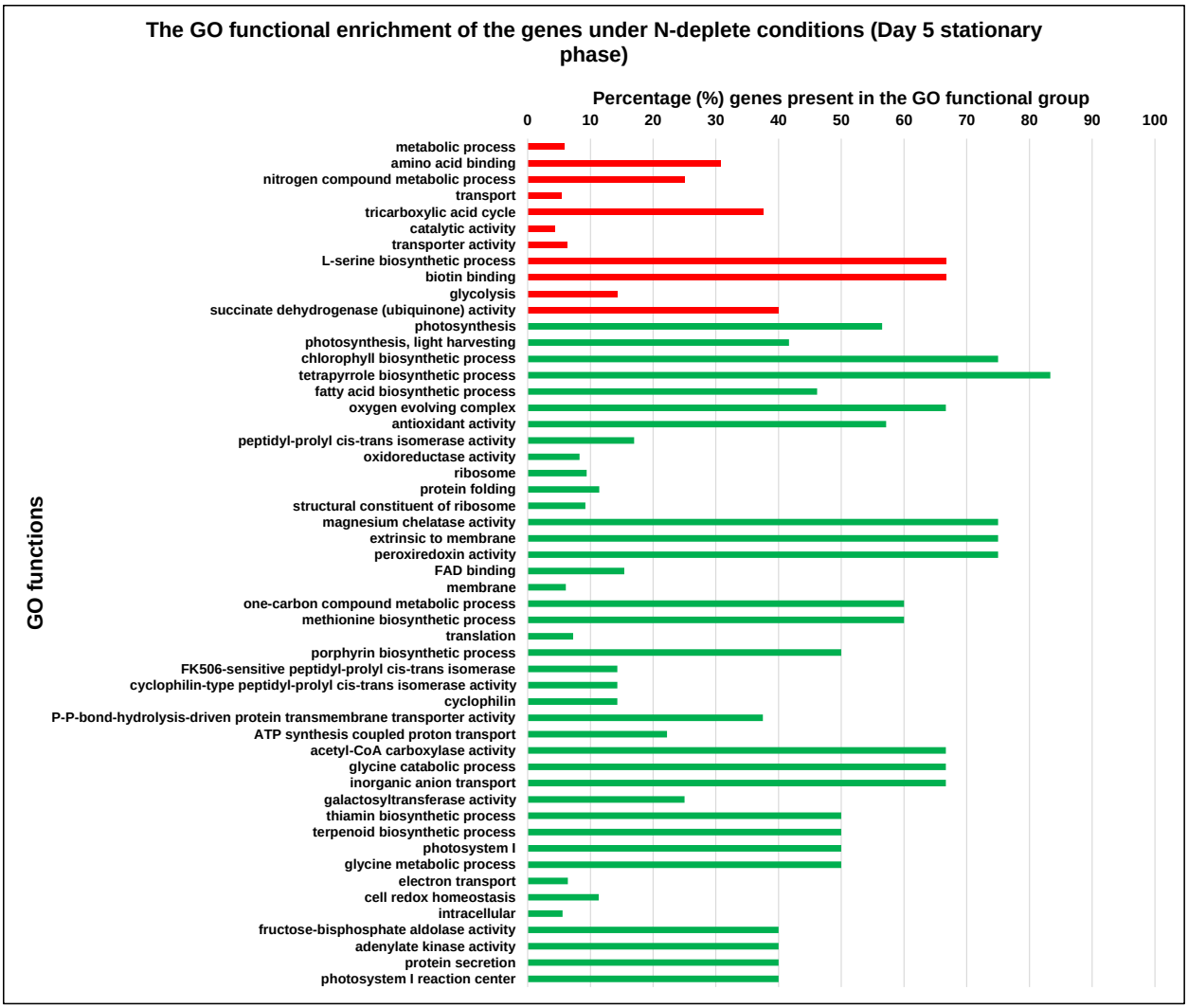

Figure S3. GO functional enrichment of up-regulated and down-regulated genes under N-deplete conditions on Day 5 stationary phase. Red and green bars indicate up- ($\geq$ 2) and down- ($\leq$ -2) regulation respectively. All data were filtered according to a FDR-corrected p value of ≤ 0.05.

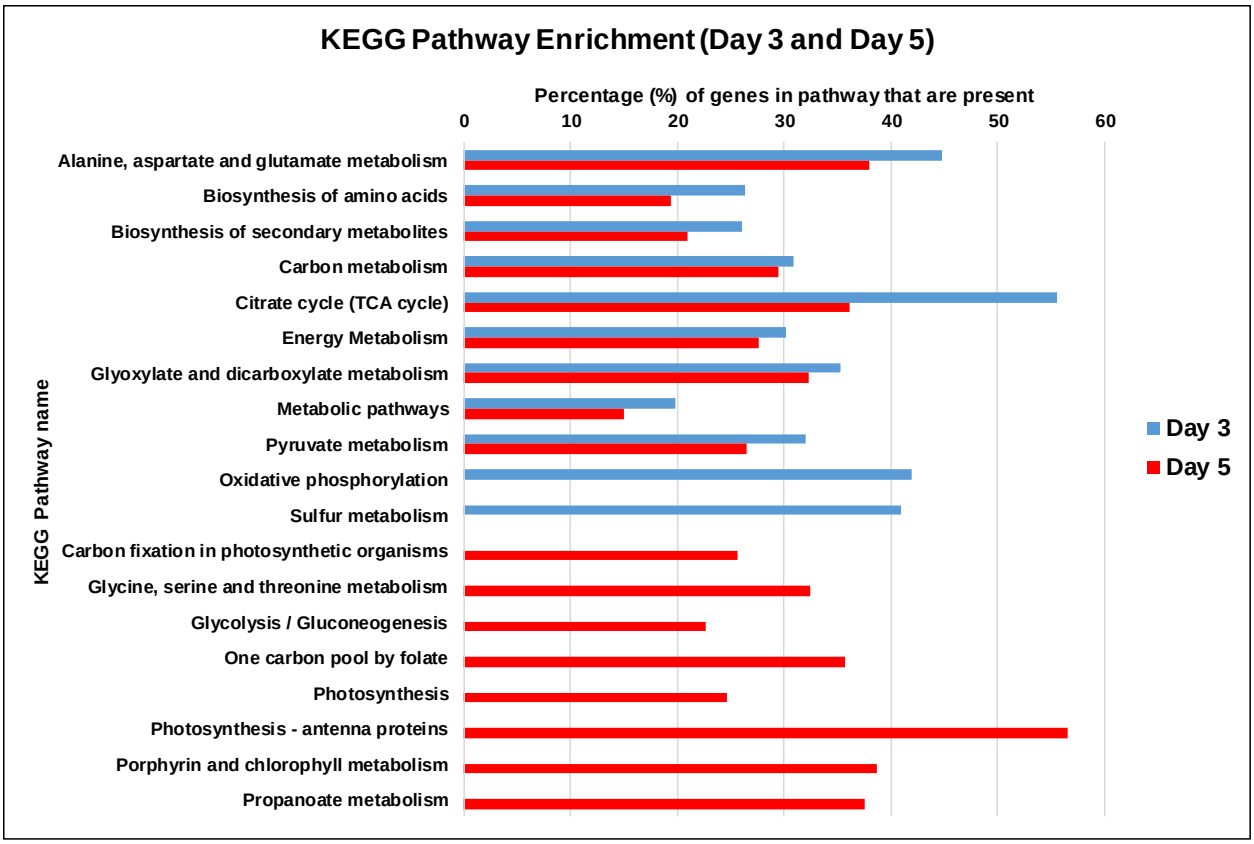

Figure S4. KEGG pathway enrichment of genes under N-deplete conditions on Day 3 (exponential phase) and Day (5 stationary phase). Blue bars represent the Day 3 samples and red bars represent the Day 5 samples. All data were filtered according to a FDR-corrected p value of ≤ 0.05.

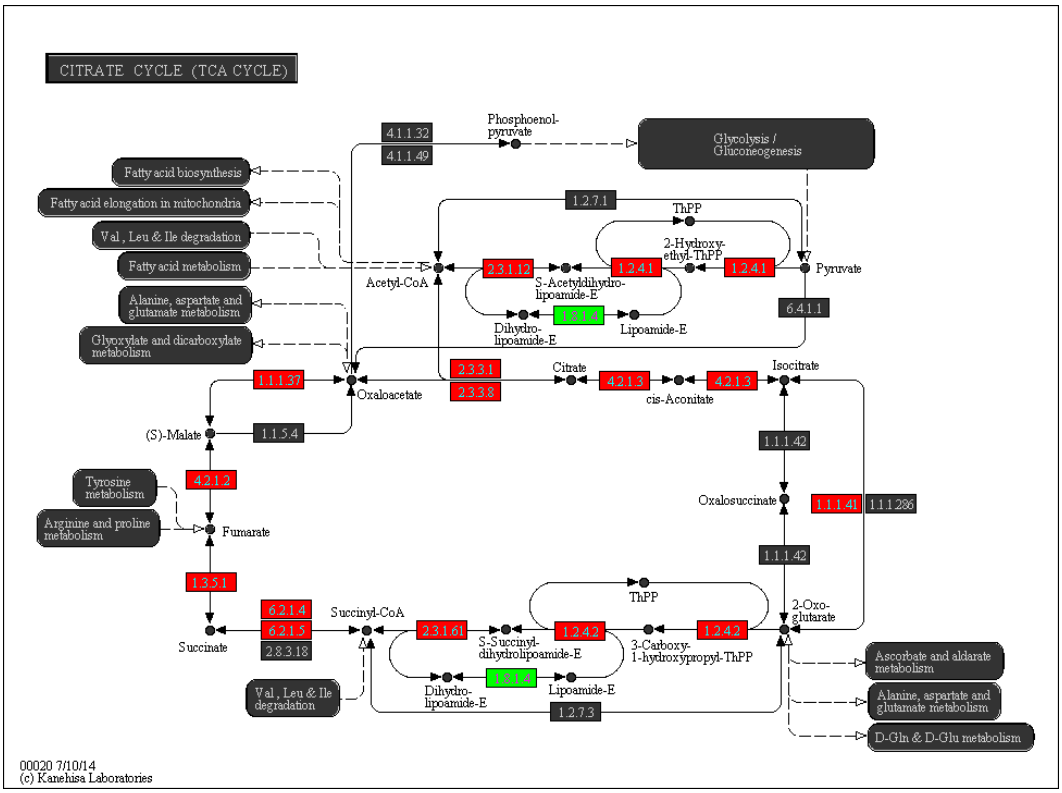

Figure S5. KEGG pathway analysis of TCA cycle (Day 3 exponential phase). Red and green highlighted bars indicate up- ($\geq$ 2) and down- ($\leq$ -2) regulation respectively. EC 2.3.1.12: PDH E2 component (Dihydrolipoamide acetyltransferase), EC 1.2.4.1: PDH2 (Pyruvate dehydrogenase E1 beta subunit), EC 1.8.1.4: PDH (Dihydrolipoamide dehydrogenase), EC 2.3.3.1/8: ACLB1 (ATP citrate lyase, subunit B), EC 4.2.1.3: ACH (Aconitase), EC 1.1.1.41: IDH (Isocitrate dehydrogenase), EC 1.2.4.2: OGD (Oxoglutarate dehydrogenase), EC 2.3.1.61: OGD2 (Dihydrolipoamide succinyltransferase), EC 6.2.1.4: SCLA (Succinyl coenzyme A synthetase subunit A), EC 6.2.1.5: SCLB (Succinyl coenzyme A synthetase subunit B), EC 1.3.5.1: SDH (Succinate dehydrogenase), EC 4.2.1.2: FUM (Fumarate hydratase), EC 1.1.1.37: MDH (Malate dehydrogenase).

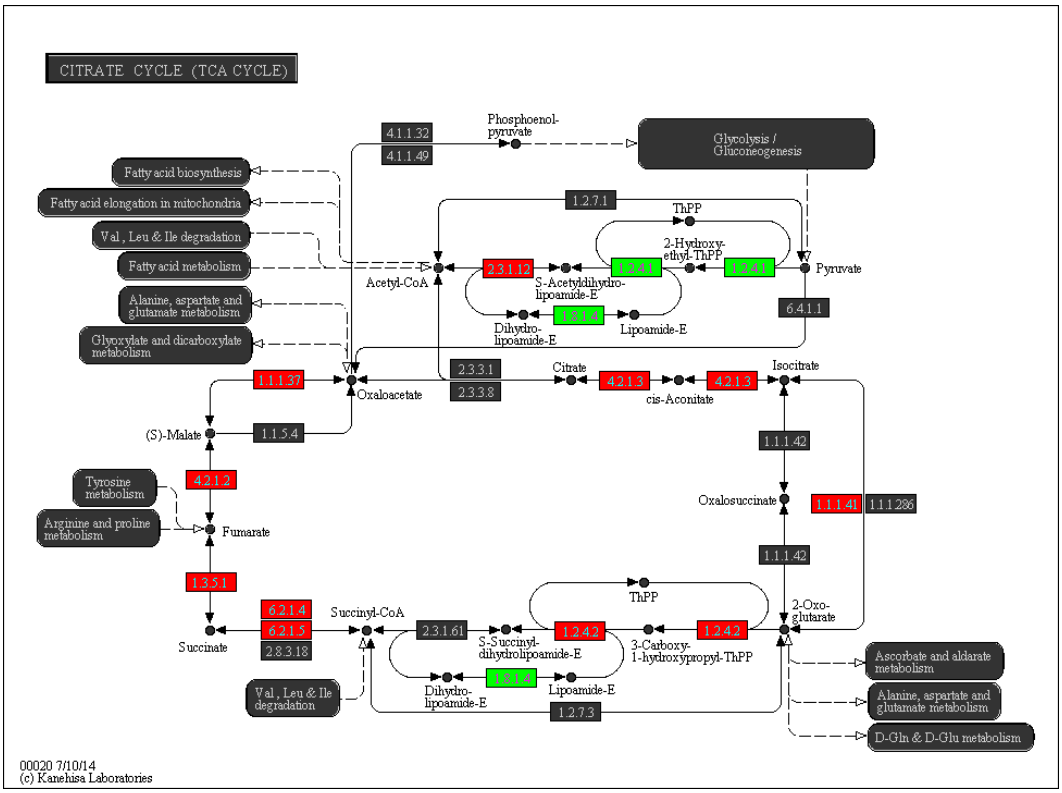

Figure S6. KEGG pathway analysis of TCA cycle (Day 5 stationary phase). Red and green highlighted bars indicate up- ($\geq$ 2) and down- ($\leq$ -2) regulation respectively. EC 2.3.1.12: PDH E2 component (Dihydrolipoamide acetyltransferase), EC 1.2.4.1: PDH2 (Pyruvate dehydrogenase E1 beta subunit), EC 1.8.1.4: PDH (Dihydrolipoamide dehydrogenase), EC 2.3.3.1/8: ACLB1 (ATP citrate lyase, subunit B), EC 4.2.1.3: ACH (Aconitase), EC 1.1.1.41: IDH (Isocitrate dehydrogenase), EC 1.2.4.2: OGD (Oxoglutarate dehydrogenase), EC 2.3.1.61: OGD2 (Dihydrolipoamide succinyltransferase), EC 6.2.1.4: SCLA (Succinyl coenzyme A synthetase subunit A), EC 6.2.1.5: SCLB (Succinyl coenzyme A synthetase subunit B), EC 1.3.5.1: SDH (Succinate dehydrogenase), EC 4.2.1.2: FUM (Fumarate hydratase), EC 1.1.1.37: MDH (Malate dehydrogenase).

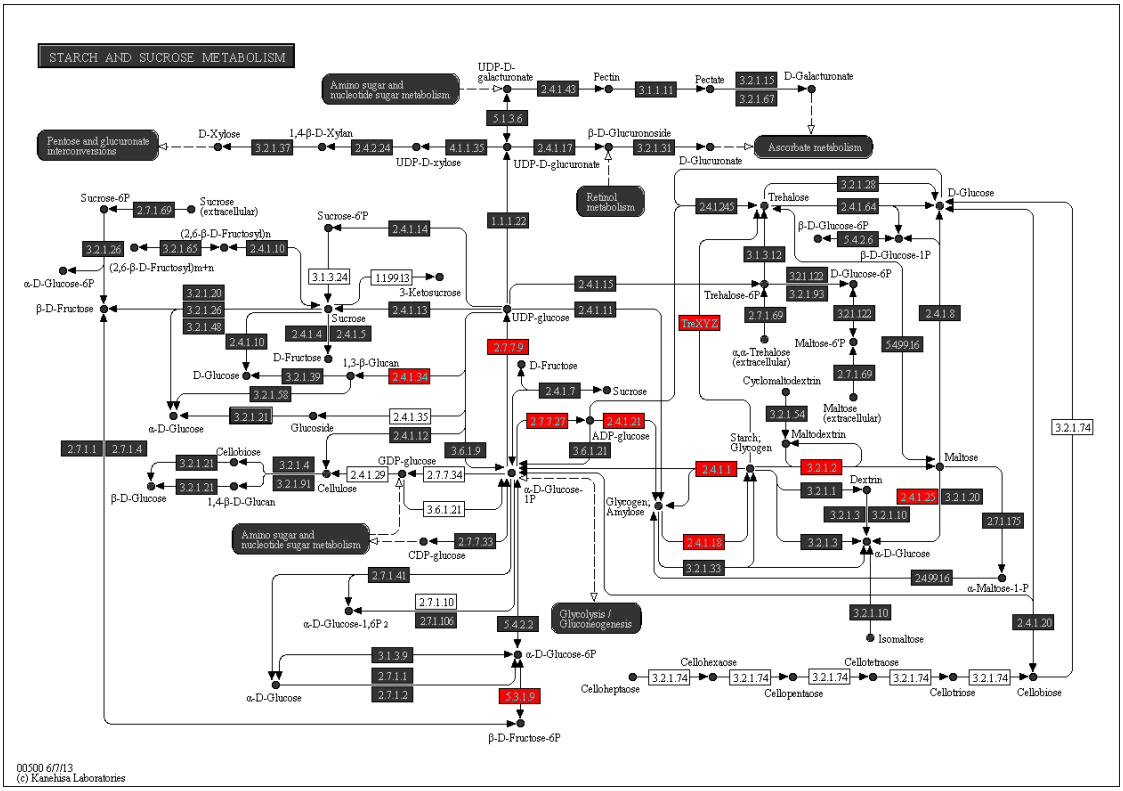

Figure S7. KEGG pathway analysis of Starch and sucrose metabolism (Day 3 exponential phase). Red highlighted bars indicate up- (≥ 2) and down- (≤ -2) regulation respectively. EC 2.4.1.34: STA2 (granule-bound starch synthase I; 1,3-beta-glucan synthase), EC 5.3.1.9: PGI1 (glucose-6-phosphate isomerase), EC 2.7.7.9: UGP1 (UDP-glucose pyrophosphorylase; UTP—glucose-1-phosphate uridylyltransferase), EC 2.7.7.27: STA1/AGPP (Glucose-1-phosphate adenylyltransferase; ADP-glucose pyrophosphorylase), EC 2.4.1.21: SSS (Starch synthase), EC 2.4.1.18: SBE (Starch branching enzyme), EC 2.4.1.1: PHOA/B (Starch phosphorylase), EC 3.2.1.2: AMYB3 (Beta-amylase), EC 2.4.1.25: STA11 (4-alpha-glucanotransferase).

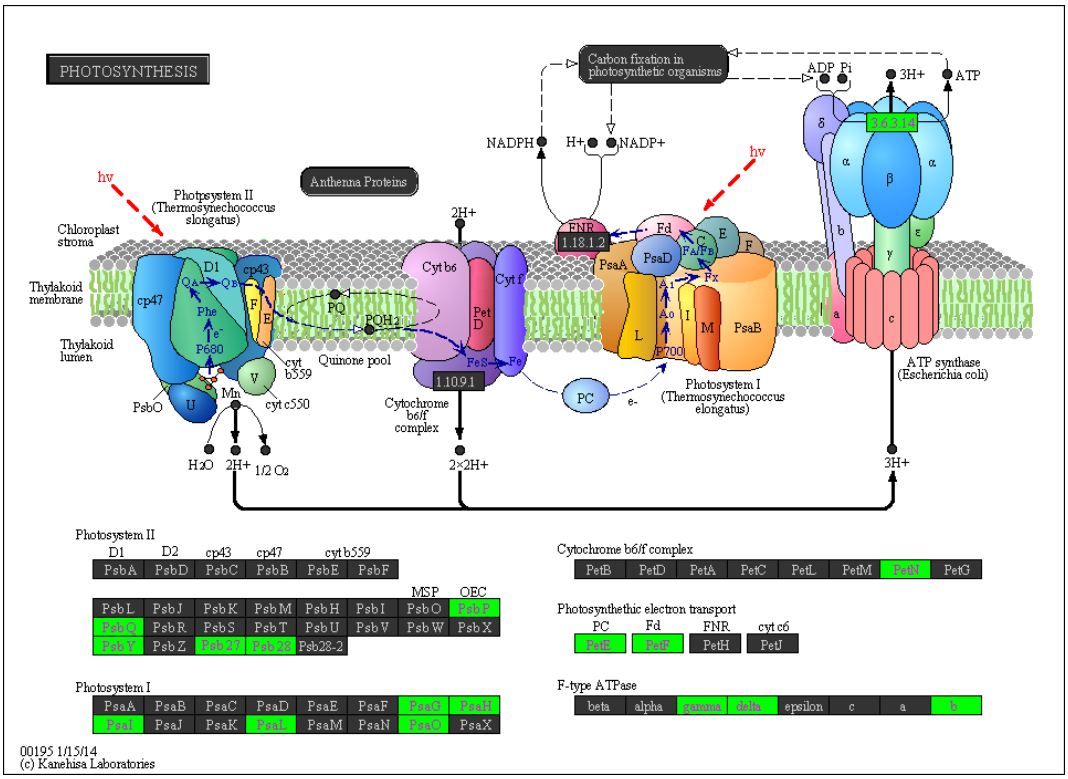

Figure S8. KEGG pathway analysis of Photosynthesis (Day 5 stationary phase). Red and green highlighted bars indicate up- (≥ 2) and down- (≤ -2) regulation respectively. PsbP: Photosystem II (PSII) reaction center PsbP family protein (Oxygen-evolving enhancer protein 2), PsbQ: PSII subunit Q-2 (Oxygen-evolving enhancer protein 3), PsbY: PSII Ycf32-related subunit, Psb27/28: PSII assembly proteins, PsaG: Photosystem I (PSI) reaction center subunit G, PsaH: PSI subunit H, PsaI: PSI subunit I, PsaL: PSI subunit L, PsaO: PSI subunit O, PetN: Cytochrome b6-f complex subunit VIII, Cytochrome b6-f complex subunit petN, PetE: Plastocyanin, PetF: 2Fe-2S ferredoxin-like superfamily protein

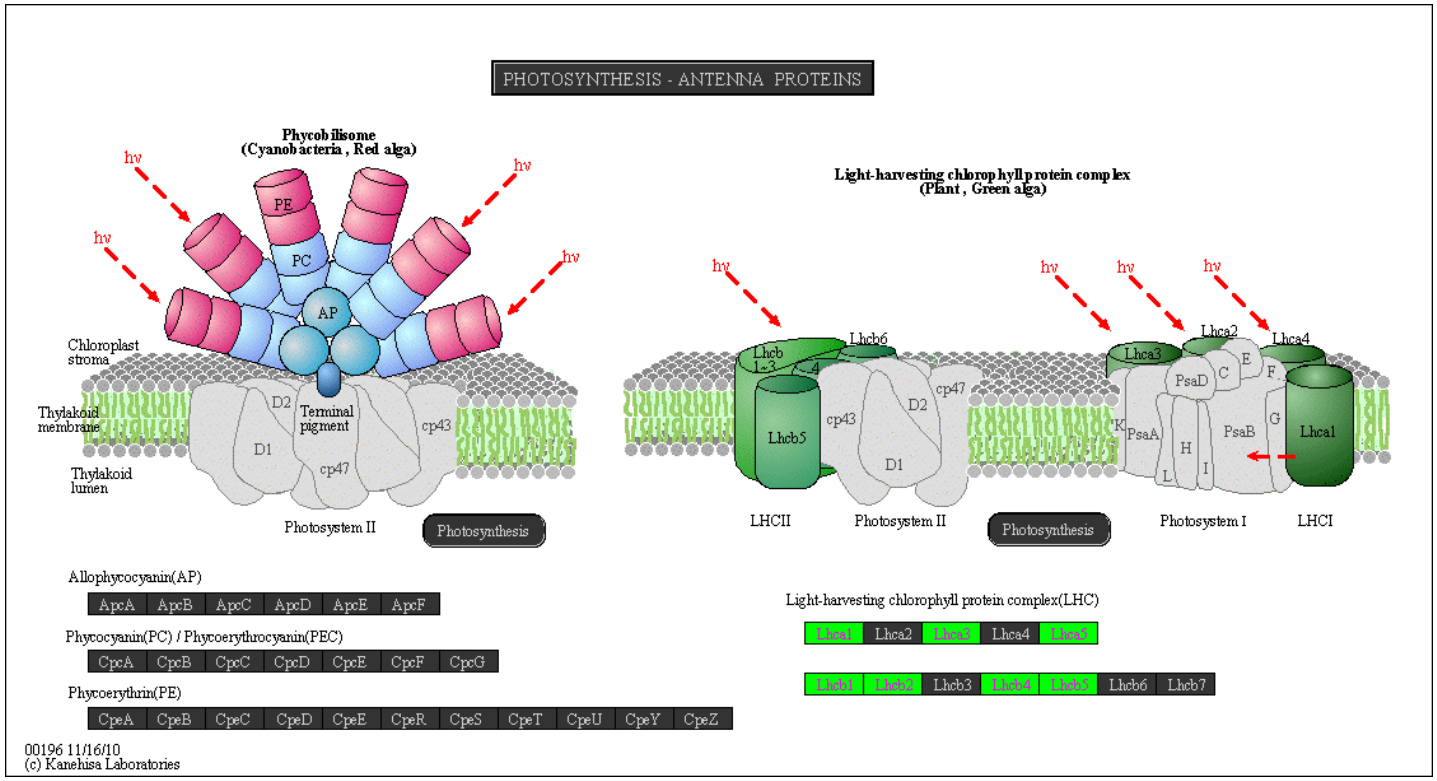

Figure S9. KEGG pathway analysis of Photosynthesis – Antenna proteins (Day 5 stationary phase). Red and green highlighted bars indicate up- (≥ 2) and down- (≤ -2) regulation respectively. LHCA1: Photosystem I light harvesting complex (LHC) gene 1, LHCA3: Photosystem I LHC gene 3, LHCA5: Photosystem I LHC gene 5, LHCB1: LHC II chlorophyll a/b binding protein 1, LHCB2: LHC II chlorophyll a/b binding protein 2, LHCB4: LHC II chlorophyll a/b binding protein 4, LHCB5: LHC II chlorophyll a/b binding protein 5.

Table S6. Comparison of TAG and starch accumulation in oleaginous and non-oleaginous microalgae.

		% TAGs (per DCW)		% Starch (per DCW)			
Species	**Carbon source**	**N-replete**	**N-deplete**	**N-replete**	**N-deplete**	**Type of cell**	**Reference(s)**
Dunaliella tertiolecta	Inorganic (CO_2)	0.2%	1%	12.3%	46.1%	High starch; Low TAG	**This Study**
Nannochloropsis oceanica	Inorganic (CO_2)	0.2%	40%	NIL	NIL	High TAG	(Li et al., 2014; Goncalves et al., 2016a)
Chlamydomonas reinhardtii	Organic (Acetate)	14.2%	41.4%	11%	40%	High starch; High TAG	(Siaut et al., 2011; Cakmak et al., 2012; Davey et al., 2014)
Chlorella vulgaris	Organic (Glucose/acetate glutamate/ lactate)	3.4%	11.5%	23%	50%	High starch; Moderate TAG	(Ikaran et al., 2015)

Table S7. Comparison of FA, TAG and starch synthesis genes in oleaginous and non-oleaginous microalgae.

		Microalgae species			
Pathway	**Genes**	***Dunaliella tertiolecta***	***Nannochloropsis oceanica*** (Dong et al., 2013)	***Chlamydomonas reinhardtii*** (Sato et al., 2014; Valledor et al., 2014; Gargouri et al., 2015; Park et al., 2015)	***Chlorella vulgaris*** (Fan et al., 2015)
FA synthesis	***ACCase****	-3.4	-2.6	1.7	-3.0
	MCAT	-4.7	-1.6	1.3	-3.9
	KAS I	-3.6	-1.6	4.1	-4
TAG synthesis	***GPAT***	-2.4	0.9		
	LPAAT	3.4	7 isoforms (2 up-, 3 down-, 2 unchanged)	1	2.1
	DGAT		13 isoforms (6 up-, 3 down-, 4 unchanged)	1.7	2.1
	PDAT		1.5	1.4	
Starch synthesis	***STA1***	2.4		0.5	2.0
	UGP1	2.6	-3.0		
	SSS1	4.6		1.0	1.6
	SBE2	2.3		0.8	

*ACCase denotes the *Acetyl-CoA biotin carboxyl carrier subunit* as it was the most reported gene among the literature.

Table S8. Primers used in the *C. reinhardtii* study. CBLP: Chlamydomonas beta subunit-like polypeptide; G6PDH: Glucose-6-phosphate dehydrogenase (plastidial); MME2: Malic enzyme isoform 2; PDH: Pyruvate dehydrogenase (plastidial) E1β subunit; TE: Fatty acyl-ACP thioesterase. Restriction enzyme sites in the primers are underlined. Bold italics denote the 6x his tag sequence that was added in the primer.

Plasmid construction primer sequence (5' to 3')	**Description**
5' - AATTCTCGAGATGGGCACGGCCAGGCAAATG - 3'	Forward primer for cloning DtMME2 into 35S Promoter/Terminator cassette
5' - AATTGGATCCTCA***GTGGTGATGGTGATGATG***CAGCCTG CTACTGCGGTG - 3'	Reverse primer for cloning DtMME2 into 35S Promoter/Terminator cassette
5' - AATTGATATCATGTTGGGTGGAAGGCAGTTG - 3'	Forward primer for cloning DtG6PDH into 35S Promoter/Terminator cassette
5' - AATTGGATCCTCA***GTGGTGATGGTGATGATG***GATCTCA TCCTCCGTCAA - 3'	Reverse primer for cloning DtG6PDH into 35S Promoter/Terminator cassette
5' - AATTCTCGAGATGCTGGCCCAGAAGCAGATG - 3'	Forward primer for cloning DtPDH into 35S Promoter/Terminator cassette
5' - AATTGATATCTTA***GTGGTGATGGTGATGATG***AGCTGCC AGTGCCATTCT - 3'	Reverse primer for cloning DtPDH into 35S Promoter/Terminator cassette
5' - AATTCTCGAGATGCAGCAGGTCACTTGGAGC - 3'	Forward primer for cloning DtTE into 35S Promoter/Terminator cassette
5' - AATTGGATCCTCA***GTGGTGATGGTGATGATG***AACTCCC ACAGGCCTCCA - 3'	Reverse primer for cloning DtTE into 35S Promoter/Terminator cassette
5' - CTTACATGTGTACCCCTACTCCAAAAATGT - 3'	Forward primer for cloning out gene with 35S Promoter/Terminator cassette to insert into pHyg3
5' - GAAACATGTGATCTGGATTTTAGTACTGGA - 3'	Reverse primer for cloning out gene with 35S Promoter/Terminator cassette to insert into pHyg3
Genotyping primer sequence (5' to 3')	**Description**
5' - CTTACATGTGTACCCCTACTCCAAAAATGT - 3'	Forward primer to confirm the presence of 35S Promoter/Terminator cassette in genome
5' - GAAACATGTGATCTGGATTTTAGTACTGGA - 3'	Reverse primer to confirm the presence of 35S Promoter/Terminator cassette in genome
Real-time primer sequence (5' to 3')	**Description**
5' - AGGTGCCCTACTGCGTGT - 3'	CrCBLP real-time F1
5' - ATCTGGCCGTCGGTGTAG - 3'	CrCBLP real-time F1

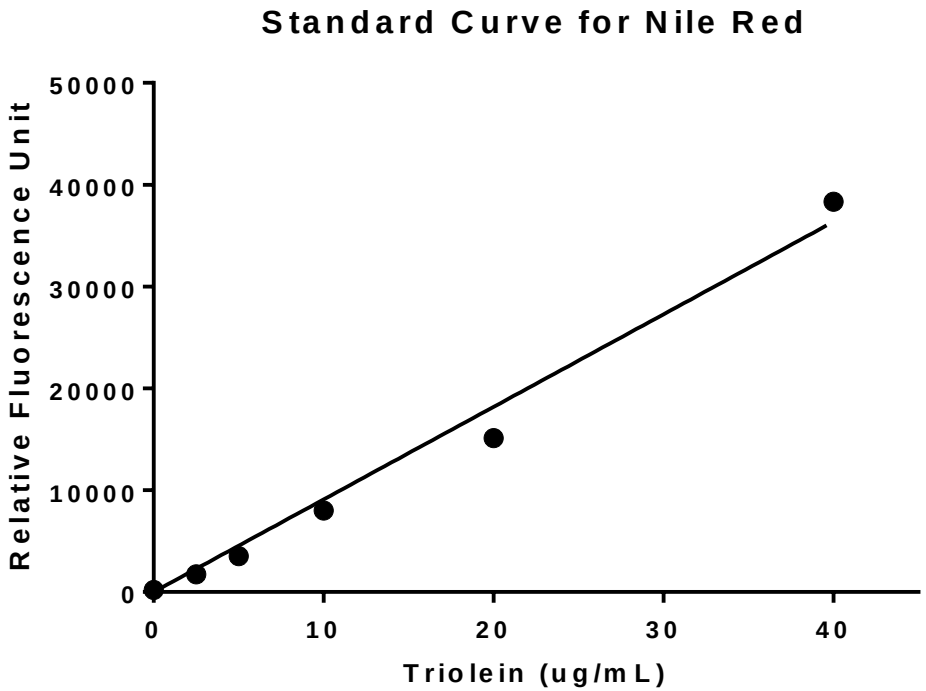

Figure S10. Standard curve for determining neutral lipid concentration. Two hundred microliters of triolein standards (40, 20, 10, 5, 2.5, 0 µg/mL) were loaded as technical triplicates onto a 96-well black, clear bottom plate. Prior to staining, Nile red stock is diluted in acetone to obtain a working solution (25 µg/mL), and 2 µL of the Nile red working solution is added to each well of standard, followed by a 5 min incubation in the dark. Fluorescence of each sample was detected using a microplate reader at excitation and emission wavelengths of 524 nm and 586 nm.

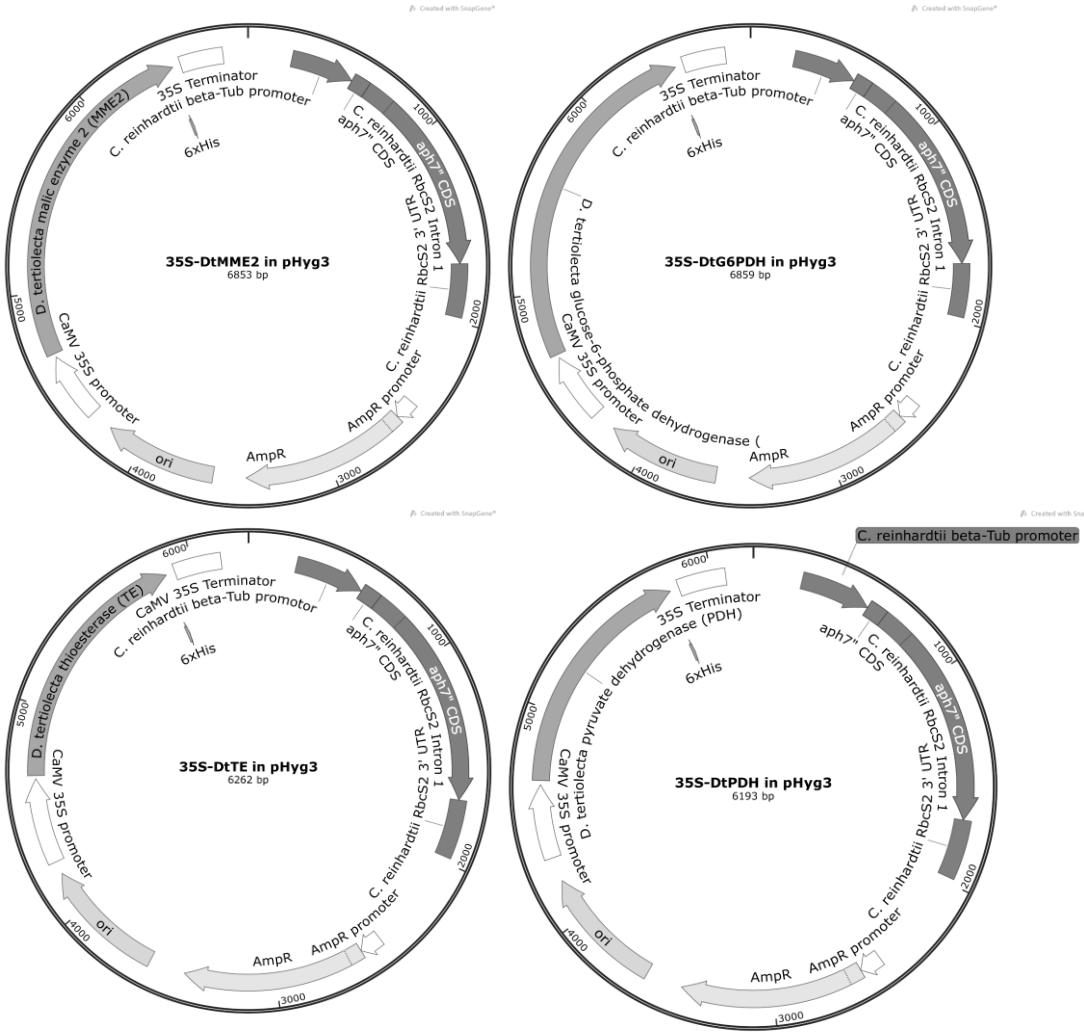

Figure S11. Plasmid map for *C. reinhardtii* transformation. Schematic diagram of transformation vectors which contain the gene-of-interests (DtMME2, DtG6PDH, DtPDH, DtTE) flanked with the Cauliflower Mosaic Virus 35S

(CaMV 35S) promoter and terminator. The plasmid backbone contains an ampicillin resistance cassette and the positively selectable marker aph7" (*Streptomyces hygroscopicus* aminoglycoside phosphotransferase gene). Genes-of-interest were first inserted into a plasmid (pGreen) containing the CaMV 35S promoter using the primers described in Table S8. The 35S-gene sequence was then amplified out with PCR and inserted into the PciI site of plasmid pHyg3, which contains the *S. hygroscopicus* aph7" gene conferring resistance against hygromycin B in *C. reinhardtii*. The aph7" gene is driven by the *C. reinhardtii* beta-Tubulin promoter and terminated with CrRbcS2 3' UTR terminator.

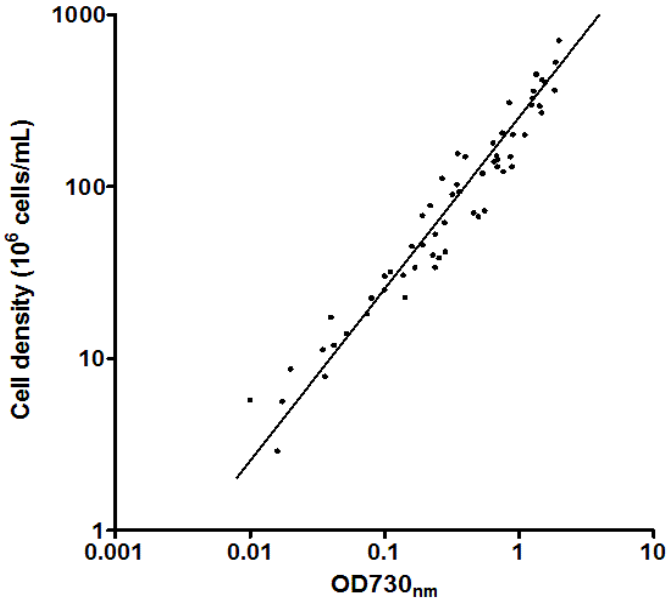

Figure S12. Standard curve for *S. elongatus* PCC 7942 cell density and optical density.

Table S9. Primers used in transforming *S. elongatus* PCC 7942. Restriction enzyme sites are underlined.

Primers	Description
5' - CTTGGGCCCATGGCTCCTCGATTCGACCTG - 3'	Forward primer for cloning the 400-bp region upstream of Acyl-CoA dehydrogenase (Synpcc7942_1215)
5’ - CTCGGGCCCTGTGATCCTTATGCCAACTGG - 3’	Reverse primer for cloning the 400-bp region upstream of Acyl-CoA dehydrogenase (Synpcc7942_1215)
5' - TTGAGCTCCTTGGTGACCATCCTGCCCGC - 3'	Forward primer for cloning the 400-bp region downstream of Acyl-CoA dehydrogenase (Synpcc7942_1215)
5' - TTGAGCTCCTAGCCAGCGATCGCGCTTAG - 3'	Reverse primer for cloning the 400-bp region downstream of Acyl-CoA dehydrogenase (Synpcc7942_1215)
5’ - TTGGGCCCATGACGCTCACCCGCTTCCAG - 3’	Forward primer for cloning the 400-bp region upstream of Phosphoenolpyruvate synthase (Synpcc7942_0781)
5' - TTGGGCCCCGGGGGTGGGTTCATAGCGAT - 3'	Reverse primer for cloning the 400-bp region upstream of Phosphoenolpyruvate synthase (Synpcc7942_0781)
5’ - TTGAGCTCCAACGTGATCTGTGCCGATGC - 3’	Forward primer for cloning the 400-bp region downstream of Phosphoenolpyruvate synthase (Synpcc7942_0781)
5’ - TTGAGCTCTCATCTGCGCTGTCGATCCTG - 3’	Reverse primer for cloning the 400-bp region downstream of Phosphoenolpyruvate synthase (Synpcc7942_0781)
5’ - CTTGGGCCCCGCTTTGGGACTTGGAACGGT - 3’	Forward primer for cloning the 400-bp region upstream of Neutral Site 2 (NS2)
5’ - CTCGGGCCCTGCGTTTGACCTCATCGCCCA - 3’	Reverse primer for cloning the 400-bp region upstream of Neutral Site 2 (NS2)
5' - TTGAGCTCGGTGTAGCCCGTCACGGGTAA - 3'	Forward primer for cloning the 400-bp region downstream of Neutral Site 2 (NS2)
5’ - TTGAGCTCGTAAGCGGGCCACGGCAGC - 3’	Reverse primer for cloning the 400-bp region downstream of Neutral Site 2 (NS2)
5’ – CTGCAGGAGCTGTTGACAATT – 3’	Forward primer for removal of the codon-optimized Ptrc-ABCG11 from Genscript provided plasmid
5’ – GTCGACTTACCAGCGGCGGGC – 3’	Reverse primer for removal of the codon-optimized Ptrc-ABCG11 from Genscript provided plasmid
5’ - GTACTTCTGCAGGGATCGCCTGAATCGCCCCAT - 3’	Forward primer for removal of aminoglycoside phosphotransferase (kanR) cassette from pGreenII 0000
5’ - CGACTCCCGCGGGAAGATCCTTTGATCTTTTCTACG - 3’	Reverse primer for removal of aminoglycoside phosphotransferase (kanR) cassette from pGreenII 0000
5’ - TTGTCGACGAAAAGAAACAGATAGATTTT - 3’	Forward primer for removal of sacB cassette from pYUB870
5' - GAGTCGACTTATTTGTTAACTGTTAATTGTCC - 3'	Reverse primer for removal of sacB cassette from pYUB870

Restriction enzyme sites are underlined.

Table S10. Primers used for molecular characterization of mutant strains by genotyping PCR and real-time PCR.

Primers	Description
Genotyping PCR Primers	
5' - CTTGGGCCCATGGCTCCTCGATTCGACCTG - 3'	Forward primer to confirm replacement of ACD region with kan-sacB (3,809-bp), or ABCG11 (4,222-bp)
5' - TTGAGCTCCTAGCCAGCGATCGCGCTTAG - 3'	Reverse primer to confirm replacement of ACD region with kan-sacB (3,809-bp), or ABCG11 (4,222-bp)
5’ - TTGGGCCCATGACGCTCACCCGCTTCCAG - 3’	Forward primer to confirm replacement of ppsA region with kan-sacB (3,809-bp), or ABCG11 (4,222-bp)
5’ - TTGAGCTCTCATCTGCGCTGTCGATCCTG - 3’	Reverse primer to confirm replacement of ppsA region with kan-sacB (3,809-bp), or ABCG11 (4,222-bp)
5’ - CGACTCCCGCGGGAAGATCCTTTGATCTTTTCTACG - 3’	Forward primer to confirm replacement of NS2 region with ABCG11 (4,222-bp)
5’ – GTCGACTTACCAGCGGCGGGC – 3’	Reverse primer to confirm replacement of NS2 region with ABCG11 (4,222-bp)
Real-time PCR Primers	
5' - TTTCTGAGCAAGCATCAACC - 3'	Forward primer for ACD (137 bp amplicon size)
5' - ACGATGTGATCCTTATGCCA - 3'	Reverse primer for ACD (137 bp amplicon size)
5' - GGTCTACGACGAAGGTGGAT - 3'	Forward primer for ppsA (106 bp amplicon size)
5' - ATCGTCACTGATTGCAAAGC - 3'	Reverse primer for ppsA (106 bp amplicon size)
5' - GTTTATCTCGGGCACCATTT - 3'	Forward primer for ABCG11 (97 bp amplicon size)
5' - GGTGACACTGGCGTACAAAC - 3'	Reverse primer for ABCG11 (97 bp amplicon size)
5' - GTCAGCTCGTGTCGTGAGAT - 3'	Forward primer for 16S rRNA (85 bp amplicon size)
5' - GAGTGCCCAACTGAATGATG - 3'	Reverse primer for 16S rRNA (85 bp amplicon size)

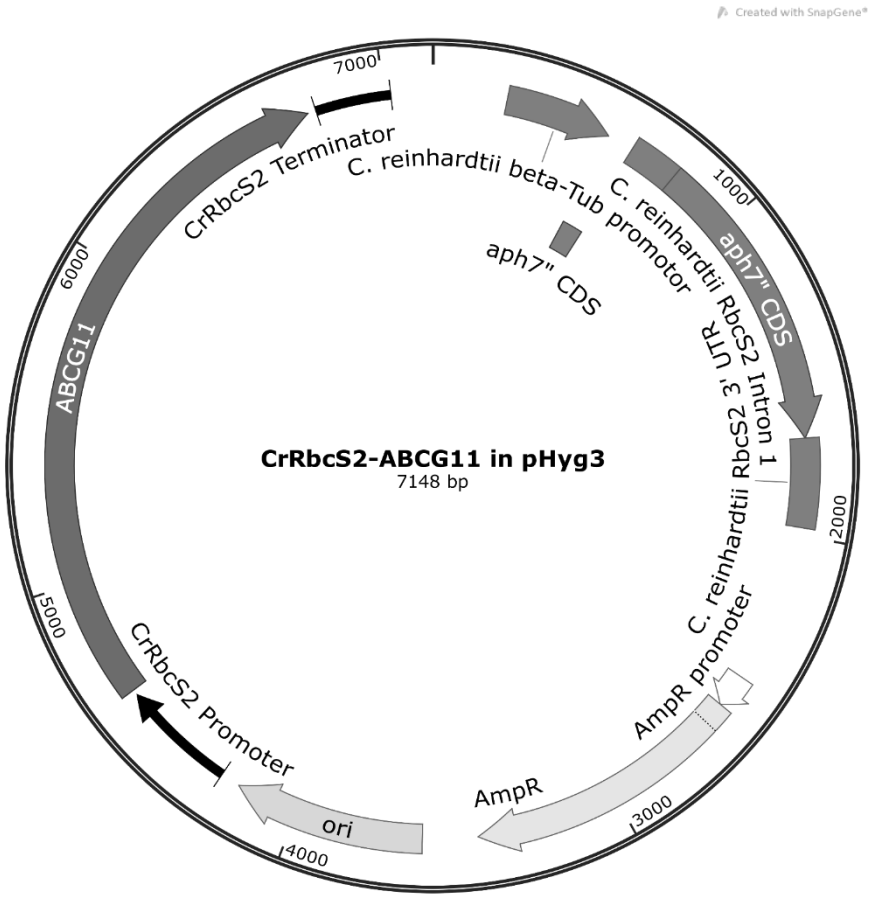

Figure S13. Plasmid map for ABCG11 transformation in *C. reinhardtii*. Schematic diagram of transformation vectors which contain ABCG11 flanked with the CrRbcS2 (small subunit of ribulose bisphosphate carboxylase) endogenous promoter. The plasmid backbone contains an ampicillin resistance cassette and the positively selectable marker aph7" (*Streptomyces hygroscopicus* aminoglycoside phosphotransferase gene). ABCG11 sequence were first inserted into a plasmid (pGreen) containing the CrRbcS2 promoter. The CrRbcS2-ABCG11 gene sequence was then amplified out with PCR and inserted into the PciI site of plasmid pHyg3, which contains the *S. hygroscopicus* aph7" gene conferring resistance against hygromycin B in *C. reinhardtii*. The aph7" gene is driven by the *C. reinhardtii* beta-Tubulin promoter and terminated with CrRbcS2 3' UTR terminator.

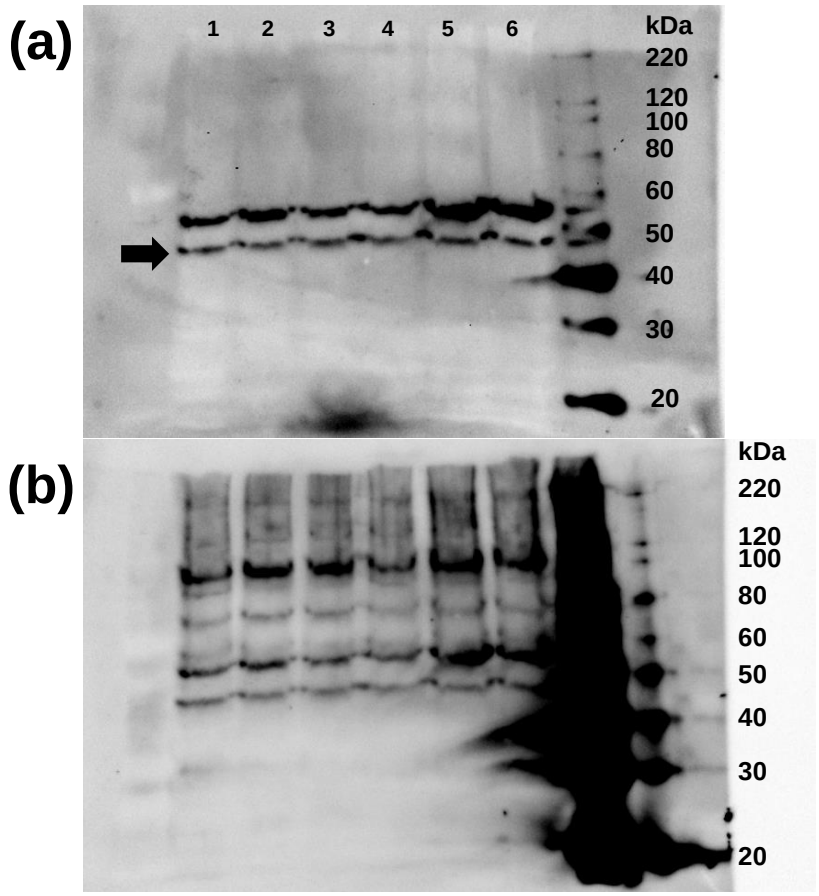

Figure S14. Western blot analysis for proteins in *C. reinhardtii*. (a) Samples probed with Anti-Actin antibody. *Expected size:* 42 kDa. (b) Samples probed with Anti-6X His tag antibody. *Legend:* 1: Wild type *C. reinhardtii*, 2: DtMME2 mutant (*expected size*: 91.9 kDa), 3: DtG6PDH mutant (*expected size*: 92.1 kDa), 4: DtPDH mutant (*expected size*: 67.5 kDa), 5: DtTE mutant (*expected size*: 70 kDa), 6: ABCG11 mutant. *Methods:* Cells were harvested at exponential phase and resuspended in 1 mL of lysis buffer (1 M Tris-HCl pH 7.2, 0.5 M EDTA, 4 M NaCl, 10% SDS) with protease and phosphatase inhibitors. The cell suspension was then lyzed by sonication for 15 mins in ice-cold water, and centrifuged at maximum speed for 10 mins at 4^{o}C. The supernatant containing proteins was harvested stored at -80^{o}C. Protein concentration was measured by the bicinchoninic acid (BCA) protein assay kit (QuantiPro BCA Assay Kit, Sigma; Cat. No. QPBCA). Two hundred micrograms of total protein was separated on 10% SDS-polyacrylamide gels (Biorad Mini-PROTEAN) and blotted on PVDF membranes. Even loading and effective transfer was verified on the membranes by staining with Ponceau S, then completely destained and blocked with 5% (w/v) nonfat dry milk in PBST (0.1% Tween-20 in 1X PBS) for 1 hr, followed by probing with the respective primary antibodies overnight at 4^{o}C (anti-Actin, Abcam Cat. No. ab14128, 1:200; Anti-6X His tag, Abcam Cat. No. ab18184, 1:1000). Membranes were washed three times with PBST prior to secondary antibody probe (anti-Mouse IgG, 1:10000, Pierce Cat. No. 31430) for 1 hr at room temperature. The bands were visualized with enhance chemiluminescence (Pierce Cat. No. 32106), exposed on a Biorad ChemiDoc™ MP System.

Appendix

CaMV 35S promoter sequence (404 bp)

GTACCCCTACTCCAAAAATGTCAAAGATACAGTCTCAGAAGACCAAA
GGGCTATTGAGACTTTTCAACAAAGGGTAATTTCGGGAAACCTCCTCG
GATTCCATTGCCCAGCTATCTGTCACTTCATCGAAAGGACAGTAGAAA
AGGAAGGTGGCTCCTACAAATGCCATCATTGCGATAAAGGAAAGGCT
ATCATTCAAGATGCCTCTGCCGACAGTGGTCCCAAAGATGGACCCCCA
CCCACGAGGAGCATCGTGGAAAAAGAAGACGTTCCAACCACGTCTTC
AAAGCAAGTGGATTGATGTGACATCTCCACTGACGTAAGGGATGACG
CACAATCCCACTATCCTTCGCAAGACCCTTCCTCTATATAAGGAAGTT
CATTTCATTTGGAGAGGACAGCCC

CaMV 35S terminator sequence (225 bp)

GGTACGCTGAAATCACCAGTCTCTCTCTACAAATCTATCTCTCTCTATT
TTCTCCATAAATAATGTGTGAGTAGTTTCCCGATAAGGGAAATTAGGG
TTCTTATAGGGTTTCGCTCATGTGTTGAGCATATAAGAAACCCTTAGTA
TGTATTTGTATTTGTAAAATACTTCTATCAATAAAATTTCTAATTCCTA
AAACCAAAATCCAGTACTAAAATCCAGATC

DtMME2 sequence (1,767 bp)

ATGGGCACGGCCAGGCAAATGGCCCACAACTTGGAGGAGCAACACAC
CCTAGGGCAGGACCAGGCCTTGGCCCGCTTGAATGCTATTCCATCAGA
CATTGAGAAGTACATGTGGCTCAGACTGCTCCTAGAAGAAAAACCTAG
TGAATATTACAGGCTTCTCACCAGTCAGACAGAGCGAGTGCTGCCTTT
TATTTACACACCAACTGTTGGGGAGGCCTGCACTCGCTACTTTGAGCT
CAAACAGCGTCCTCAGGAGCCTCGGCTGCGCCCTAAAGGCCTGTTTCT
GAGTTTGGAGGACAGAGGGAGAATTTTGGAGAAGCTGCGTTCCTGGC
CCCAGCAGAACGTGAAGGTGATAGTAGTGACTGATGGAGAGCGAATC
CTTGGGCTGGGTGACTTGGGTGCTGGAGGCATGGGTATCAGCGAAGGC
AAGATCACGCTTTACACGATAGCAGCAGGCGTGGACCCCAGTGTGTGC
CTGCCGGTGTGCCTTGATATGGGCACCAACAACAAGAGGCTGCTCAAT
GACCCAATGACCCAGTACCAAGGTTTGAAGCGGGAGCGCGCCACTGG
TGCAGAGTTTGACTCGTTTATGGCTGAGTTCATGGATGCACTCAGCCA
ATGGCAGCCCCACGTGCTTGTGCAGTACGAGGATTTTGGCAACACCAA
TGCCTTCAGGCTGCTTGAAAAGTACCGTGCCAGCCACTGCACTTTCAA
CGATGACATCCAGGGTACTGCCGCAATCACTCTCGCAGCGATTCTTGC
AGCCCTGCGTGCCGTTGAATTTGATAAAGGCAACAGTGGTATTAATCG
AGCAGGAAAGCAGATCGATTCGGATGAGGCGCTTGGATCGGGTCAGC
TGCTGGCAGGCAAGCAGGTGCTGTTCCTGGGTGCTGGAGAGGCGGGC

ACAGGCATCGGGGAGCTCATTGCTTACTGCGTGCACAGGCGCACAGG
CTGCAGCATGAATGAGGCACGCAAGACCTGCCACTTTGTGGACTCAAA
AGGCCTGGTTTGCGCCTCCCGCATGCCCGACCTGCAACACCACAAGCA
GGCGTTTGCCCACGACACGCCCTACTGCAAGACTTTGTTGGAGGCTGT
GCGCTTGCTGAAGCCAGTGGCCATCATCGGCGTGTCCACCATAGCTGG
AAGCTTCAATGAGGAGGTCCTGCGCGAAATGGCTGCCATCAACCACC
GCCCCATCATCTTCCCTCTGTCCAATCCAACCACCAAGTCAGAGTGCA
CCTTTGAGGAAGCTTTCAAGCACACGGAAGGGCGTGTGCTGTTTGCCT
CAGGCTCACCCTTTGACCCCATCTTCGTCCCATCACAGTCCTCAGGCA
ATGCAAGCCAGCCCGCTCTTGCAGGTGACGGCATCCTGATGCGGCCAG
CGCAGGCCAACAATGCGTACGTGTTCCCCGCGCTGGGCCATGCAGCAG
TGTTGGCACGCTGCAGCAGCATCTCAGACGAAGCATTCTTGACCGCCG
CAGAGGCTTTGGCAGCCATGGCCGACCCCAAGATGGTGTTGCGTGAGG
GTGCGTTGTTCCCTCCCTTTTCCAAGATCAAGGATACCAGTAGCCATGT
CATGGCCCACGTGATGGCATGCATGGTGCGCGAAGGCCGGGGATTGC
GTCCTGAGGGAGTGGCTGTGCAGCAGGGGCCTGCTAAGGCCAGCGAC
TTCTTGCCACACTGCCTGGCGCACATGTGGCTGGGTCCTGGAGAAAAA
GCCCCAGAGGCAGCCGTTGAACTCTCCCACCGCAGTAGCAGGCTG**TG**
A

DtG6PDH sequence (1,773 bp)

ATGTTGGGTGGAAGGCAGTTGGGTATGGACAAGCTGTCCCGGAAGCT
GTCCGGTGCTCAACCTGTTGCGAACTACTCGCGTCGCCCGATTTCGCG
CCCATTTCGCGCAGCGCCTGTTCCTCGAGTCGCGCAGAATTCCCAAGA
TGCTGTGACCCAGAATGGCAGCGGGACAAGCGAGGCACCCACCTCCT
GGCAGAACCCAGCACTCAAGAAGGCCATCCCCACTGTGGTTTCTCTCT
CAGATGAGGCTGCAGCCATGGCAGCTGATGACTGGAGCCAATCTAGCT
TGTCGGTTGTTGTGGTGGGCGCCAGCGGCGACCTGGCCAAGAAGAAA
ATTTTTCCTGCACTTTTTGCCCTTTTCTATGAGGGCCTGCTGCCACCGG
ACTTCCAGCTCTTTGGATATGCACGCAGCAAGATGACTGATGAGGAGT
TCCGAGACCTCATCGGCAACACCCTGACGTGCCGCATTGATGCCAGGT
CCCGCTGCGAAGACTCCCAGGCCGCCTTCTTGTCGCGCTGCTTCTACTG
CCCAGGCCAGTATGATGCCCCTGAGGGCTATGCCAACTTGGACAAGA
AGTGCAAGGAGCAGGAGGCCCTGACTGGCAAGATGGTAGCCAACCGC
ATGTTCTTCCTGTCCATCCCTCCCAACGTGTTTGTGCAAGCAGCAGGCG
GCGCAGCCGACAACTGCTCTTCTCCCACCGGCTGGACGCGCGTCATTG
TGGAGAAGCCCTTTGGCAGGGACAGCGCCAGCAGTGCTGAGCTTGGC
AGGGGTCTGGCCAGGCATTTGACAGAGGACCAGATCTACCGTATTGAC
CACTACCTGGGGAAGGAGCTGATTGAGAACCTGACAGTGCTGCGCTTT
TCAAACCTTGTGTTTGAGCCCTTGTGGAGCAGGCAGTACATCCGCAAT
GTGCAGGTGATCTTCTCAGAAGACTTTGGCACTGAAGGCCGCGGAGGC
TACTTCGACCGGTACGGCATCATCCGCGATGTCATGCAGAACCACTTG
CTCCAGATTGTGGCATTGTTCGCCATGGAGCCACCGGTGTCCCTGGAT
GGAGAGGCCATCCGTAATGAGAAGGTCAAGGTCCTGCAGTCTATGTCT

CAAGTGGCGCTGGAGGATGTCACACTGGGCCAATACCGCGGCAGGTC
TGGCGCTGGCCGTTCCGGTGGTGCTGATTTGCCTGGCTACCTGGATGA
TGCAACAGTGCCCAAGGGCTCCCTGTGCCCCACCTTTGCTGCCATTGC
GCTGCACATCAACAATGCACGCTGGGATGGTGTGCCATTCCTGCTCAA
GGCTGGCAAGGCGCTGCACACGCGCGGCGCTGAGATCCGTGTGCAGT
TCAGGCATGTGCCCGGCAACATTTTCAAGCACAAAGTGGGCCCCAACA
TCGACATGACCACCAACGAGCTTGTGATCCGCATTCAGCCGCGGGAGT
CCATCTACCTCAAGATCAACAACAAGGTCCCTGGCTTGGGCATGCGCC
TGGATACCACCAAGCTGGACCTGGTGTACAACGACGCATACTCCAAG
GAGTTGCCAGATGCGTATGAGCGCCTCCTGTTGGATGTGGTGAACGGC
GATAAGCGCTTGTTCATCCGCGATGATGAGCTGGAGCAGGCCTGGAAC
ATCTTTACCCCAGTGCTGCATGAGATCGAGCGCAGAAAGGTGGCACCT
GAGCTGTACCCCTACGGCAGCAGAGGCCCTGTGGGGGCACACTACTTG
GCTGCCAAGTACAACGTGCGCTGGGGAGACTTGACGGAGGATGAGAT
C**TGA**

DtPDH E1β subunit sequence (1,107 bp)

ATGCTGGCCCAGAAGCAGATGCGGGGGCTGGTGAAGGGTGCAGCCGC
GGGCGCAGTACCCCGCCCTGCCCGGCTGGCCGCTCCAGCACGCAGCA
GGGTGGCAGTGCAGGCCAAGAGGGAGTGCTTCATGTGGGAGGCCCTG
CGTGAGGCCGTGGATGAGGAGATGGAGAGGGATCCAGCTGTGTGCCT
GATGGGCGAGGACGTCGGCCACTACGGAGGCTGCTACAAGGTCTCCC
TGGGTCTGCACAAGAAGTTCGGGGACCTGCGCGTCCTTGACACGCCCA
TCTGCGAGAACAGCTTCATGGGCATGGGCATCGGCGCTGCAATGACCG
GCCTGCGGCCCATCATTGAGGGCATGAACATGGGCTTCCTGCTGCTAG
CCTTCAACCAGATCTCCAACAATGCTGGCATGCTGCACTACACTTCTG
GGGGCCAGTACAAGACGCCCGTGGTCATTCGCGGACCTGGAGGCGTG
GGCAAGCAGCTGGGCGCAGAGCACTCACAGCGCTTGGAGTCCTACTTC
CAATCAACCCCTGGAGTGCAGCTGGTGGCATGCTCCACTGTGCACAAC
TCCAAAGCCCTCCTGAAAGCGGCAATCCGCAGTGATAACCCTGTAGTA
TTTTTCGAGCACGTGCTGCTGTACAACGTCAAGGGCGAGGTCGGAGGC
CGGGATGAAGTGCAGTGCCTGGAAAAGGCGGAGGTCGTGAGGGAGGG
CACAGACATCTCCATCTTCACATACAGCCGCATGCGCTATGTAGTGAT
GCAGGCAGTAGCAGAGCTTGAGAAGAAGGGCTACAACCCGGAGGTGG
TGGACCTCATCAGCTTGAAGCCTTTTGACATGGGCACCATCGCGGCCT
CTGTCAGGAAGACACGCAGGGTGCTCATTGTGGAGGAGTGCATGAAG
ACCGGGGGCATCGGCGCCTCCCTGTCAGCTGTCATCTCAGAGTCCCTG
TTTGATGAGCTAGACCACCAGGTGCTGCGCCTGAGCTCGCAAGATGTG
CCCACCGCATATGCATACGAGCTGGAGGCTGCTACCATTGTGCAGCCA
AGCCAAGTGGTGGAGATGGTCGAGTCAGCTGTTGGACCCAGAATGGC
ACTGGCAGCT**TAA**

DtTE sequence (1,176 bp)

ATGCAGCAGGTCACTTGGAGCGCTGGCTGCGGTACAAGCCCTGGGCT
CTCATCAGTGCAGCAGGGGTTTCCGCGTCAAAGAATACGCACCAGTAG
GAGACAGGGAAGGCGTCCCCTGCCCTCCTTATGCCCCACTTTGTCCTA
TGAAGAGCCCTCCGTTGAGTTTGTGTGCCGAGCATCACAGCAGGCCGC
AGCGGTGCAGCAGGACGAGGGGCAGCAGCAGGAGGGCAACGGTCGT
GGGACGACTCAAGAGCTCGTGTCCATTGTGCAGTTCCACCCCCTGCAG
CCCGCTCAGTTCTCGGAAGACAGGCTATCCTTTTCAGAGCAGCACCGC
ATCAGAGGCTACGAGGTGGACGCCAACCAGCGCACGACCATTGTGAC
AATTGCCGACTTGTTGCAGGAGATAGCTGGAAACCATGCAGTTGGGAT
GTGGGGGCGGACAGACACTGGCTTTGCGAATTTGCCGAGTGTGAAGG
ACCTCATCTTTGTCATGTCAAGGCTGCAGATTAAGATGCACCAGTACC
CCAGATGGGGGGGACATGGTCACAGTTGAGACCTATTTCTCTGCAGATG
GCCGCCTGGCAGCACGTCGGGACTGGCGCATCAGGAATGCCTTGACTG
GGGAGGAGTATGGTTCTGCCACCAGCACGTGGGTCACCATCAATGCAG
CCACCCGCAAGCTGACCAGGCTGCCAGAGGACCTCAGGAACTTCTTCC
TCAGGCTCTCACCACAACAACCAAGGCATGCTATTCACCCAGAAGAG
ACAAAGAAAAAGCTGCCGGACATTGATGAACAGAAGCAGCAGTATGA
GGGCCCAAAGCAAATTGCACGCCGCAGCGATGTTGACATGAATGGCC
ACATCAACAATGTTACGTATTTGGCTTGGGCGCTGGAGACAATGCCCA
ACGATATCTATGAGAGCCACCGTGTATGTGAGGTAGAAATTGATTTTA
AGGCCGAGTGCCAGGCTGGCAATATCATTGAGTCCCTCTGCCATCCAT
TGGGCCTGGAAAGCTCCACCTCCGCTGCCAGCAGTAGCAATGGCAGC
AGCAATGGTAATGGCACAAACGCTGCAGACACTTTGCCCACCTTCCTG
CACTCCCTGCGGCGCTGTGACGACAGTGGTTGCTACGAGCTGGTGCGG
TGCAGGACCAAGTGGAGGCCTGTGGGAGTT**TGA**

DtACD sequence (2,526 bp)

ATGCAGTCAGCAACAAGTAACGGGGTGGGACTGAATGTAAGCAGCTT
GCAAGAGTATCTACAAAGACAGCTACCCACACTGTTCACCACTCAGCT
TGGAGGCACCCAGCGCCAGCCTCCAGGCCTCCATGTCCGCCAGTTCAG
CCATGGGCAGAGCAACCCCACGTTCCTGATCACGCTCATGGGAACCGA
TGACAAATTTGTGCTGAGGAAGAAGCCTGCTGGCCGCATTCTGGCCTC
TGCCCATGCTGTGGAGCGAGAGTATGCAGTGCTTGACGCTCTTTCCAA
GCACCACTCTGGAGTGCCTGTGCCTCGGCCCCTGTTGCTCTGCAATGA
CAAATCCGTGATTGGCACCCCCTTTTACCTCATGGAGTTCATTGAGGGT
GCTGTGTATGTGGACCCCAACATGCCTGAGGCGGCACCGGACACCAG
GCGAGATGTGTACCAGCAGATGGTGAGGTGCTTGGCCGCACTGCACA
ACGCACCTGTGCGGGAGCTGGGGCTGCAGAACTTTGGAGACCCACAG
GGCTACTGCGCGCGGCGGCTTAAGCGCTGGACCCAGCAGTACAACGC
CAGTGTGGCTGAGCCGATGCCTGAGGTGCTGCGGCTTGTAGAGTGGCT
CAAGGACCACGTTCCGCCTGAGGACCTAAACCCTGAGAGGCCTAGCA
TCTGCCATGGAGACTTCCGCTTGGATAACCTGATGTTTGCACCTAGTGC
GTCTGGCAGGCCTGTGCTGCATGCTGTGCTGGACTGGGAGCTGTCCAC
TGTGGGCAACCGCTGGGCGGACGTGGCTTACAACTGCTTACCCTACCA

CCTGCCGCGCGCGGGCATCCTCCAATGCTTGAACATGCCCCTGGCACC
TGGCATCCCTACGGAGCAGGAGTACGTGCAAACGTATTGTGAGGCAG
CAGGCTGCATGCCCCCCTCCCCCACCGCATGGTCCTTCTACATGGCCTT
GTCATTGTTCCGGCTTCTGGCCATTCTGGCTGGCGTCCAGGCACGCGC
AAAGCAGGGCAACGCCTCCTCTGCTCGTGCAGCCATGCTTGCTTCCGA
CGCAGTGCTGCAAGCGCTGGCAGAGGCTGCATTCCGTGCTGCAGGCCT
ACAAGACCCAACCAGCAGCAGCAGCAGCAGCAGCAGCAATGGCGTGC
CACAGCCTAAACTTGCCCCACCATCTTACAGCACCAGCATCGCTGTTG
CACCCCAACCCACTGCTGCTAACGCAACACATGGTGGCCAGGGTGTGC
AGGGAGGGAGTGACGTGGTGGGATTGCCCAGCGCGCGCGTGCAGGAG
CTGCGTGCGCGCGTGCTGGCATTTGTGGAGGAGCATGTGTTGCCTGCA
GAGGAGGTCCTGGAGGCGCATGCATGCGGTGCAGATCGCTGGACCAT
CCACCCTCGTATGGAGGAAATGAAGGCGATGGCCAAGGCAGCAGGGC
TGTGGAATTTGTGGCTGCCTGGCTCTTTGGCCGCCACCATCCAGCACAT
GCGAGATGCATGCAGCAATAGCGTGGAGCGCGATGTCTTGCTGGGGG
CGGGGTTGAACAACCTGGAGTACGCTCACGTGTGTGAAGTCATGGGCA
GGAGCGTCTGGGCCCCTGAGGTCTTCAACTGCGGTGCCCCAGACACCG
GGAACATGGAGGTGCTGGCCAAGTATGCAAGCCGCGAGCAGCAGCAG
CGCTGGTTGCTACCCCTGCTGCAAGGCCACATCCGCTCCTGCTTTGCCA
TGACTGAAAAGCTGGTAGCCTCTTCGGACGCCACCAACATACAGTCCA
GCATCCGGCGTGAGGGGGACAGCTATGTGCTGAATGGTGTGAAATGG
TGGACCAGTGGGGCCTGCGACCCACGCTGTGCTGTGGCCATCTTCATG
GGCAAAACAGACCCGACAGCACCCATGCACTTGCAGCAGTCCATGGT
ACTGGTGCCTATGGACACACCAGGGGTGCAAATTTTGCGCCCCCTGCT
GGTGTTCGGCTACGATGATGCTCCACATGGCCATGCAGAGGTGGCCTT
CAAGAACGTGCGAGTACCTGCTAGCAACATCATTCTGGGTGAGGGCCG
TGGGTTTGAGATTGCGCAAGGGCGGTTGGGCCCTGGCCGCTTGCACCA
CTGCATGCGCCTCATCGGCATGGCGGAGCGTGCCATCGCCACCATGAC
GCAGCGTTCCTTGCAGCGCCACGTGTTTGGGGGGAAGCTGGCCAGGCA
GGGTGCCTTCCAGGCCAGCCTGGCAAACTGCCGCATCCAGCTAGATGC
TGCACGCCTTATGGTCCTTGCAGCTGCCCCCCACCTAGACCGCTCTGG
CAACAAGGCAGCGCGGGGCACCATTGCAGCGGCTAAGGTGGTGGCAC
CAAATGCAGCGCAGCTGATCATCGACGCTGCTATTCAAGCGCACGGG
GGGGCAGGCGTCAGCCAGGACACTGTGTTGGCCCGGCTGTGGACTGCT
GCACGCACGCTGCGCATTGCAGACGGCCCTGATGAAGTGCACCTGACC
ACGATTGCAAAGTTGGAGATTGCGCGAGCCTCCAAATTG**TGA**

DtACL subunit A (ACLA) sequence (1,281 bp)

ATGGCTCGCAAGAAGGTCAGGGAGTACGATGCCAAGCGCATCCTGAA
GGCCCGATTTGAGGGCGTTATTGGGAAGACTCTGCCAATCCAAGTGGC
CCAGGTTACAAGTTCAACTGATTACAAGGATCTGTTGCAGCAGCATCC
GTGGCTGGGAAGTAGCAAGCTGGTTGTAAAACCAGACATGCTTTTTGG
ACAGCGTGGCAAGCATGACCTCGTCGGCCTGAACCTTTCATGGAGTCA
GGCGGAGGCATTTGTAAAAGAGCGCATTGGCAAGACAGTGACAGTAA

ACGAGTGTACAGGGCCGGTGACCACCTTCATTGTGGAGCCCTTCATGC
CTCATAAAGAGGAGATGTACATGTGCATCCAGAGCAACCGGCTTGACT
ACGAGGTGTCTTTTTCTGCCATGGGAGGAGTGTCCATTGAGGAGCACT
GGGACCAACTGAGCAGCATCAAAGTGGATGCCACAGCGCAGGACCTG
TCAAGTGAGGCCGTGGCTCCTCTCACCGCAAAGCTCCCCCTCGAAACC
CGTGGAAGGGTAGGCGACTTCATCAGGGCCATGTTTAAGGTGTTCCTT
GATGTCGATGCAACGCTCATTGAGATGAATCCTTTCACCTTTGACCTCA
CCGGCGAGCCCTTCCCCTTGGACATTAGGATGGAGCTTGATGACACAG
CGCAATTCCGCAGTGGTTCCAAGTGGTGCGGTGCAGAGTTCCCGCTAC
CCTTCGGGCGCACTCTGGCTCCAGCCGAGGAGCATGTTCAAAGCATGG
ACGAAACCACAGGGGCCTCTCTGAAGTTCACCGTGCTCAATCCAAAGG
GCCGCGTGTGGCTGATGGTTGCTGGCGGAGGTGCCAGTGTAATCTACA
CGGACACAGTGGGAGATCTCGGCTTTGCACAGGAGCTGGGAAATTAT
GGGGAATACAGCGGCGCCCCAAACACTAACGAGACTTACCAGTATGC
ACGCACTGTGCTCTCTTGTGCCACTGCAAACTCAGATGGGCGGGCGCG
TGCTCTGCTCATTGGAGGGGGCATTGCCAACTTCACCAATGTTGCGGC
TACCTTCCAAGGTATCATCAAGGCCTTGCGGGAGTCGTCTGAGGCTTT
GATAGCAGCCAAGGTGTTTACATTTGTGCGTCGAGGGGGACCTAACTA
CCTTGAGGGGCTGGACATGATGAGAGCACTGGGCTCCGAGATTGGCGT
TCCGATTGAGGTGTACGGCCCAGAGTCATCCATGACAGGCATCTGCGC
CAATGCCATCGAGCGGATCAAGGCCGACAAGTAC**TGA**

DtACOX sequence (2,112 bp)

ATGAGCATGTCGCAACGCGTGGACAGTCGGACAAGAGACCTGGTGGA
CAAGAGTACGCGACAGATTCTGAAAGCCTCCATCTCGCCTCAAGATGA
CATAATTGCTGAGCGGAGCCGTGCAACCTTTGACGCCCTCCAGATGTG
CTATGCCTTAAATGGCGGCAAGGACAAGATTCAACGAAGAGCACAGC
TCGTAGAGGCACTGAAGCGGACCTCATGGGGGAACAAGGAACGCCGG
CATTTCATGACCAGGGAGGAGGAGTACGTGGAAGCTCTGCGTGCATCG
TTTGGTATCTGGGAGAAGATGAAGCAGGAGAAAATGAGCCTCGAGGA
TGGCGTCACCATGCGCTCTTTGGTGGACTTCCCTGGTGGCCTCGAGCTG
CACATTGGGATGTTTATCCCAAGCATCCTGTCCCAGGGCACCCCCGAG
CAGCAGCAGCACTGGCTGCCGCTGTGCTACGACCTGTCAATCATCGGC
ACGTATGCACAGACCGAGCTGGGCCACGGCACGTTTGTGCGCGGCCTG
GAGACAACCGCCACATACGACAAGACGACGCAGGAATTCGTGCTGCA
CTCTCCAACCCTGACCTCCACGAAATGGTGGCCCGGTGGCCTGGGCAA
GACTGCCACCCATGCCGTGGTCATGGCACGCCTGTTTATTGACGGCAA
GGACTACGGACCTCATGCATTTGTGGTTCAAGTCCGAAGCCTGCAGGA
CCACCTGCCGCTGCCTGGCATCTGCGTGGGGGACATCGGCCCCAAGTT
TGGCTATGGGGGCGTGGACAATGGGTACCTTGCCATGGACCACCTGCG
CATCTCACGTGAGAGCATGCTGATGCGGTACTCCAAGGTGCTGCCGGA
CGGAACATATGTGCCTCCCCCACCCTCCAACGCCAAGGCATCATACGC
AACCATGGTGTACGTGCGCGCGGACATCGTGAAAAACGCGGGGTCGG
TGCTGGCCAAGGCTGTCACCATCGCCACGCGCTATGCTGCTGTGCGCA

GGCAGACAGCCCCATCACCTGGCCAGCCTGAAACACAGGTGCTGGAC
TACCAGAACACCTCGCACACGCTGCTGCCGCTCGTGGCGGCTGCGTAC
GCAGTGCACTTCATGGGGGAGACCATCATGGGCATGTACAAGCGATTC
GACAAGGACAGGGAGCGCGGAGAGTTCAGCAGCCTGCCGGAGCTGCA
TGCGCTGTCCTCAGGCTGCAAGGCGCTGTGCACATGGATTACCGCAGA
CGGCATCGAGTCCTGCCGCCGCACCTGTGGCGGCCACGGCTACAGCAA
GCTGCCAGGGCTGCCCACGTTGTTCCAGAACTATGTGCAGAATGTGAC
GTGGGAGGGCGACAACAACGTGCTGTGCCTGCAGACGGCCCGCTACC
TGCTGAAGGCGCTGGTGGGGGTGCAGAGGGGACAGCAGGCCACCGGC
AGCGCCTCCTACCTCAACCACGCAGCCGCAGAGCTGCACGCCAAGAG
CGCCGTCCAGGGCGCGTCTGGCTGGAATGCGCACGCCCTACAGTCTGC
CATGCGCCACTGTGCCACCCGCCTGGCTGCCTCCGCCACCGCCATGCT
GCAGTCTGCATCCAGATCTGCTGCCGGTGCCTCCAGCAGGGCTGCTGG
AGGCCTGGTGTTTGAGGGGCCTGCATGGAACAACTCCACTGTGGCCAT
GATCAAGCTCACTCGTGCGCACTGCATGGCCGAGCTCCACAGCAACAT
GCTGTCCAGCATCACAGCCCTGCACAGCTCCGGCAAGGTCGGCGGGC
GTGAGCTGGCGGTCCTGCAGCAGCTGGCATCGCTGTTTGCCTTGACGC
ACATTGAGGCTCACATGGGTGACTACCTGGAGGATGGCTACTTCACAG
GTGCCCAAGCCGCATCCATCCGCCAGCGACAGAACGCCCTGCTCCTTG
AGCTGCGACCCAACGCGGTGGCATTGGTGGATGCGTTTGGCATCGAGG
ACTACGTGCTGAACAGTGCTCTGGGCCGCCAGGACGGGGATGTGTACA
CAGCGCTGCTGGACATGGCACAGGGCTCACCCCTGAACAGCTCCCAG
GAGGGACCTGCTTGGCATACCGTGCTCAAGCCAGTCATGGTTAAGCAC
AGCAAGATG**TAA**

DtMME6 sequence (1,347 bp)

ATGGGCATCCTCCACCGTGCTGCCGCAGAGGTCAACTTGTTTCAGCAA
TGCAGGGGGCTGGTTTTTGCCCTGGAGAGCAGTGCCAAATGGTGGGGA
TCGCTTGAACGGCACAAGGATGCCAGCAGCAGAAGGGCATATGCTCC
AGGACCGATCAAGCCCAAACAGCTCCACACGGACGATGATGAGGACA
GCGATGATGGCAGGCCCACCACGCCTTGGATCCGGCAAGTCATTTCTG
GAGTTGACCTCATGCGGCACCCAAAGTACAACAAAGGGCTGGCATTCT
CTGACAGCGAGAGGGACAGGCTGTACTTGCGTGGCCTGCTTCCGCCAG
TGATTTTGTCCCAAGAGGTGCAGCTGGAGCGTACCATGCTCAACCTGC
GCACAAAGTCCTCTGACCTGGACAAGTACACGTACATGCAGAGCCTGC
AGGAGCGCAATGAGCGGCTATTCTTCCGTGTTCTAGTGGAGCATTTTG
AGGAGCTGAAACCTGTGATGAGCGACGCTACAGTGCGCGAAGCATGC
AGGCGGTATGGGCTCATGTTCAAGAGCGTGCCCCGTGCACTTTTCATA
ACCTTGGAAGACCGGGGGCGCGTGTTCCGCATCCTCAAGAACTGGCCA
GAACGCAATGTTCAGATGGTGGCCTTCACAGATGGCGAGAAAACTGCT
GGGGATGTGGGCGTGCAAGCCGTGGGAGTGCCCATCAGCAAGCTATC
GCTGTACAGTGCTTGCGGTGGCATCAACCCTGCAGGCTGCTTGCCCGT
GGTTATCGACTCTGGTACTGACAATGAGGAGCTGCTCAAAAGCCCCTT
CTATGTGGGCATGAGGCACAGGCGCGTCCGGGGGGACGCCTACTATG

AATTACTAGATGAGTTCCTGACCGCTGTCCGCCAACGCTATGGCAACA
CCACCTTCCTGCACTTTGAGGACATGGCTCATGACAACGCCTCCAAGC
TGCTCAACATGTACCGCACCGAGTTCCCCTGCTACAATGATGACATGT
CTGGGAGTGCCGCCACGGTCTTAGCAGGCATCTTGGCAGCGCTGCCCA
AGATCGGAGGGCGGCTGGGTGACCATGTGTACATGTTCTCAGGCGAG
AGTGCGATGGCTTCCTGCATTGCTGAGTTGCTCGCCACCGCAATCGCG
CAGCAAACAAACCAGACGGTGCTTGCTGCGCGGAAGCGCATTTGGTTT
GTAGACAACGGGGGCCTTGTCACTCGTGAGCGTGGGGACACCGCGAC
CTTGGAGCCTTACAAGCTGCCCTTCACACACAGTGGCCCTGCAGCCGG
GGACTTGCTGACGGCCGTGAAAGAGATCAAGCCAAACGGTGCTAGTA
GGCTTGGA**TAA**

List of publications/submitted manuscripts

Tan KWM, Lee YK. 2016. The dilemma for lipid productivity in microalgae: importance of substrate provision in improving oil yield without sacrificing growth. ***Biotechnology for Biofuels***, 9: 255.

Tan KWM, Lin HX, Shen H, Lee YK. 2016. Nitrogen-induced metabolic changes and molecular determinants of carbon allocation in *Dunaliella tertiolecta*. ***Scientific Reports***, 6: 37235.

Tan KWM, Lee YK. 2016. Expression of the heterologous *Dunaliella tertiolecta* fatty acyl-ACP thioesterase leads to increased lipid production in *Chlamydomonas reinhardtii*. ***Journal of Biotechnology*** (Submitted).

Tan KWM, Lee YK. 2016. Genetic deletion of phosphoenolpyruvate synthase leads to increased lipid production in *Synechococcus elongatus* PCC 7942. ***FEMS Microbiology Letters*** (Submitted).